Microscopy at the Frontiers of Science

Conference 2023

mfs2023
INL | Braga, Portugal

Table of Contents

mfs2023
INL | Braga, Portugal

Dear Colleagues and Friends,

It is our pleasure to welcome you in person to the beautiful city of Braga in Northern Portugal and to the 2023 Edition of the Microscopy at the Frontiers of Science. The last time we all met in person was 2019 in Granada and in those four long years, many things have happened. We are very happy to be with you again in person!

In terms of the MFS2023 Program you will see an explosion of CryoEM Oral and Poster presentations that will showcase how this field has gown within the Iberian Peninsula since 2019. In this vain, our hosts - The International Iberian Nanotechnology Laboratory – received the first CryoEM in Portugal in this last year and we invite you to take a tour of this new facility.

It is also very exciting to combine this meeting with the satellite meeting for the MultEMplex COST Innovators Grant meeting and we hope you will take advantage of this unique opportunity to attend the talks of scientists trying to innovate a new grid for CryoCLEM.

Over these three days, the MFS program is full of exciting research done by young scientists, some of whom have received the SPMicros and SME Thesis Awards. Our sincere congratulations to the award recipients. We would also like to welcome all students and technicians who are presenting their research for the first time. It is intimidating to present at a big meeting, but please remember you are within a supportive community and we wish you success in your presentations.

Lastly and very importantly we would like to take a moment to thank our corporate sponsors. Without your help and enthusiasm this meeting would not be the success it will be. We thank you for supporting our PhD awards, our social events and being part of the microscopy community within the Iberian Peninsula. We are very glad to have you here with us!

We wish you all a fabulous MFS2023! Thank you for joining and sharing your science!

On behalf of the SPMicros and the SME Boards,

Erin Tranfield (President of SPMicros)

Juan de Dios Alché (President of SME)

KEYNOTE SPEAKERS

APPLICATIONS OF SUB-SAMPLING AND INPAINTING FOR HIGH RESOLUTION, IN-SITU AND ULTRAFAST TEM/STEM

Nigel D. Browning[1,2], Alex W. Robinson[1], Daniel Nicholls[1], Jack Wells[3], Zoe Broad[1], Amirafshar Moshtaghpour[1,4], Angus Kirkland[4,5], B. Layla Mehdi[1]

1 - School of Engineering, University of Liverpool, Liverpool, L69 3GH, UK; 2 - Sivananthan Laboratories, 590 Territorial Drive, Bolingbrook, IL 60440, USA; 3 - Distributed Algorithms Centre for Doctoral Training, University of Liverpool, Liverpool, L69 3GH, UK; 4- Rosalind Franklin Institute, Harwell Science and Innovation Campus, Didcot, OX11 0QS, UK; 5 - Department of Materials, University of Oxford, Oxford, OX2 6NN, UK

Abstract

For many imaging and microanalysis experiments in high-resolution/in-situ/operando scanning transmission electron microscopy (STEM), the resolution and precision of the final result is primarily determined by the tolerance of the sample to the applied electron beam dose. If the dose is not controlled, the stability of structures and the kinetics of dynamic observations can be dramatically changed by the beam, leading to a different structure and/or chemistry than would be expected from an ex-situ experiment under similar reaction conditions. Recent results at the University of Liverpool (UoL) have shown that the optimal solution for dose control in any form of scanning/transmission electron microscopy is to form the image from discrete locations of a small electron beam separated by as far as possible in space and time. Instead of forming the image with an extended beam (as with TEM) or from a regular raster pattern (as in conventional STEM) this condition is satisfied ideally by moving the STEM probe over the area of the image using large jumps between the acquisition pixels. This form of STEM imaging presents numerous challenges to the stability of the microscope, but these stability issues can be routinely overcome using either a form of random walk scanning, a calibrated random scanning or a mixture of conventional scanning and rapid beam blanking. The larger than standard jumps between pixel acquisition locations in this methodology creates problems with image interpretation, as the gaps between locations of acquisition are missing information. Fortunately, we can use Inpainting to retrieve the missing information and form a full image. Here I will discuss the methodology of Inpainting, with particular reference to the speed/efficiency of the reconstruction method and the potential for real-time imaging. In addition, the use of simulations to provide a starting point for image interpretation and the use of deep learning approaches to allow the microscope to adapt its own imaging conditions, will be demonstrated. Finally, the integration of these methods into the hardware design for both the new JEOL 300kV AI-STEM at the UoL and the Relativistic Ultrafast Electron Diffraction and Imaging (RUEDI) UK national facility will also be discussed.

THE LONG AND WINDING ROAD TO IN SITU STRUCTURAL BIOLOGY WITH CRYO-ET

J.M. Plitzko[1], S. Klumpe[1], C.J.O. Kaiser[1], O. Schioetz[1]

1 - CryoEM Technology, Max-Planck-Institute of Biochemistry, Martinsried, Germany

Abstract

In situ structural biology, as we know it today, is the study of molecular machines at their original setting, i.e., inside the cell in which they reside. Cryo-electron tomography has provided the first insights into molecular details of various cell types. However, the route has been long and winding with many technical and methodological advances that have made this possible. Yet, along with the progress, challenges remain, and a key step still is sample preparation, especially for larger cells and tissues.

This lecture will take us to the beginnings of tomography, from the early days of contemplation to today's technical achievements and the latest methodology that is still evolving. Historical and theoretical aspects are not unimportant, but the view from the practitioner's perspective is maybe the most appealing and avoids glossiness in the structures and slides presented. It is worth noting that with some cutting-edge technologies, less than a handful of scientists have even been able to perform in situ cryo-ET at all. However, with the advent of new, streamlined, and simplified instruments and practices in recent years, that handful has grown to several dozen, and their numbers continue to grow.

We will showcase our latest workflow for in situ structural biology, from correlated light microscopy, integrated approaches, to lamellar milling of cells (on-the-grid) and of course tissues or whole organisms (lift-out) - and give you an up-close look at large-scale production of lamellae and tomograms. With regard to the latter, a perspective on revisiting visual proteomics will be given in light of having "1001+" tomograms readily at hand.

THE FINE ART OF OPTIMISING SAMPLE PREPARATION WORKFLOWS FOR BIOLOGICAL ELECTRON MICROSCOPY

Errin Johnson, PhD

Electron Microscopy Facility, Sir William Dunn School of Pathology, the University of Oxford, Oxford UK

Abstract

Alongside cryo-EM, the field of biological EM has undergone its own revolution in recent years, with the emergence of new volume EM and correlative approaches that are providing exciting new insights into biological systems with unprecedented precision across a range of scales. As for traditional EM, high quality sample preparation is at the core of these techniques. However, there is no one-size-fits-all approach for preparing biological samples for a given application and this is particularly true for volume EM and correlative microscopy, which have additional requirements for sample preservation and contrast. Furthermore, the sample itself may also complicate the process, for example the presence of a cell wall can significantly hinder reagent penetration. As such, it can often be a lengthy and challenging process to establish a novel protocol, or to optimise an existing one, for a new type of sample and/or EM technique.

In this talk I will highlight a number of different workflows that we have developed at the Dunn School EM Facility for preparing a range of biological samples, including mammalian cells, bacteria, yeast, fatty tissue and plant leaves, across a variety of standard and advanced EM techniques, such as Serial Block Face SEM and correlative light and electron microscopy. I will detail the approaches we have taken to achieve successful results, whilst also providing examples of failed preparations/dead-ends and how these have informed subsequent efforts. The value of mining historical EM literature to improve modern day sample preparation protocols will also be discussed, as will the importance of engaging with the wider biological EM community to benefit from the huge amount of knowledge and experience in the field.

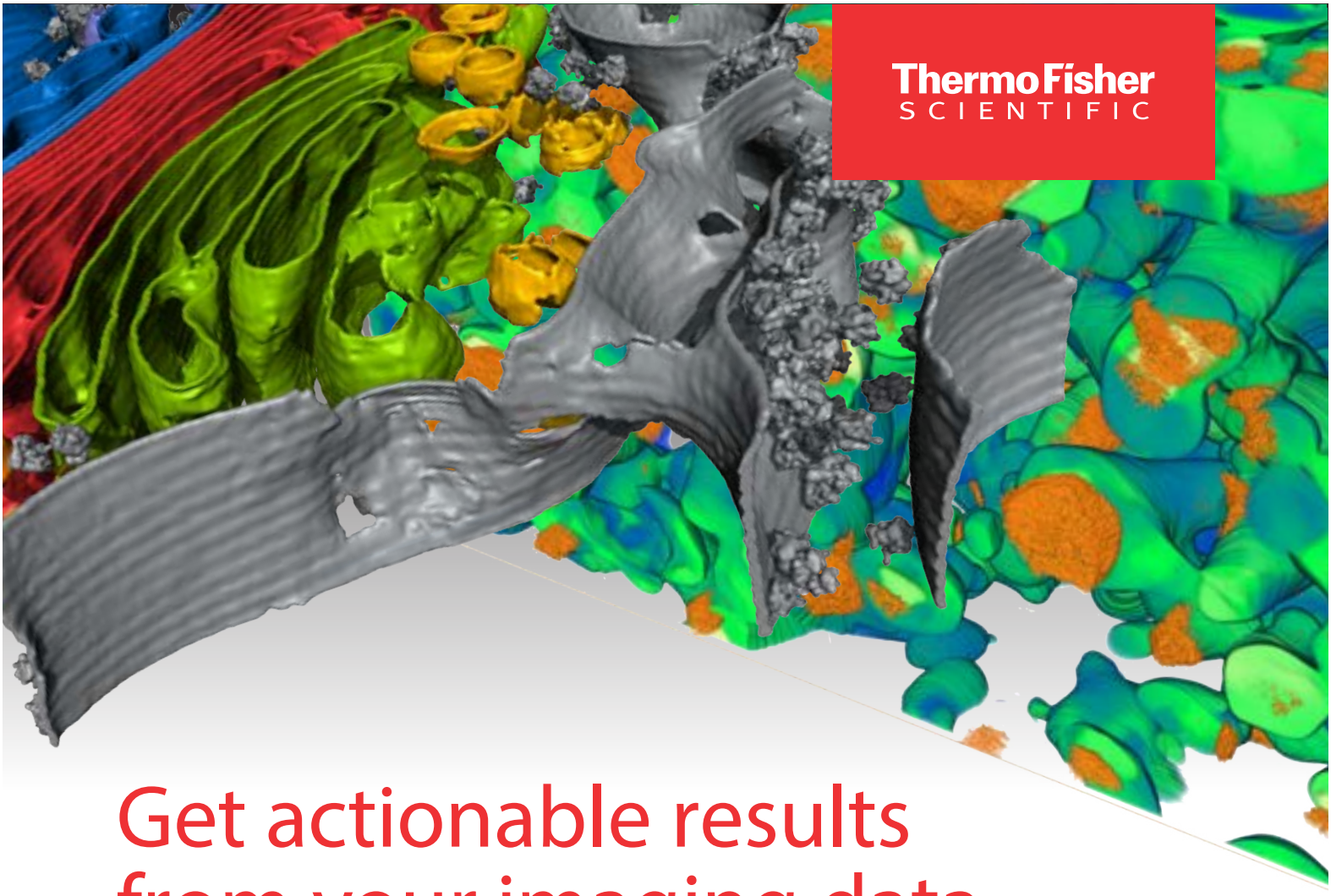

ThermoFisher SCIENTIFIC

Get actionable results from your imaging data

When you power your electron microscopy workflow with Thermo Scientific™ Amira™ and Avizo™ Software, you can:

- Take advantage of AI-driven image analysis tools
- Identify and understand structures, properties, and performance
- Extract valuable information from your data

Learn more at thermofisher.com/amira-avizo

thermo scientific

SPMicros and SME
2021-2022 PhD THESIS AWARDS

A ROBUST STUDY ON THE ATAXIN-3 FIBRILLIZATION PATHWAY FOR THE DISCOVERY OF NEW INHIBITORY COMPOUNDS

Francisco Figueiredo (Austria)[1]

1 - Institute Science and Technology Austria

Abstract

Machado-Joseph Disease (MJD) is linked to a gene mutation that causes an expansion in the Ataxin-3 protein. This leads to protein self-aggregation and triggers MJD. During my PhD, I have developed and published an experimental protocol that outlines the most important steps to study the aggregation of Ataxin-3 in vitro. This protocol was also used to perform high- throughput screening of a commercial chemical library of compounds that could inhibit Ataxin- 3 aggregation. The compounds with the best in vitro results were selected for in vivo analysis for their anti-aggregation properties in a C. elegans model of MJD. These findings prompted another publication, whereby I and my collaborators show the potential usages of dopaminergic compounds for the therapeutic use for MJD. Two provisional patents were filled for the Ataxin-3 aggregation inhibitors presented in both in vitro and in vivo studies. In addition, I optimized a new negative staining technique for studying Ataxin-3 aggregates using transmission electron microscopy. This was a crucial step, because it allowed me to gain access to cryo-electron microscopy facilities, to explore the structural and morphological characteristics of Ataxin-3 aggregates. The cryo-EM studies were performed at Prof. Sarah Butcher laboratory at the University of Helsinki (Finland), supported by an EMBO Scientific Exchange Grant.

Note of appreciation:
This award was supported by ThermoFisher Scientific.

DEVELOPMENT & IMPLEMENTATION OF AN ELECTRON DIFFRACTION APPROACH IN A TEM FOR CRYSTAL STRUCTURE ANALYSIS

Sergi Plana Ruiz (Spain)[1,2]

1 – LENS, MIND/IN2UB, Departament d'Enginyeria Electrònica i Biomèdica, Universitat de Barcelona, Martí i Franquès 1, 08028 Barcelona, Catalonia (Spain). 2 – Institut für Angewandte Geowissenschaften, Technische Universität Darmstadt, Petersenstrasse 23, 64287 Darmstadt, Germany.

Abstract

The use of electron diffraction to crystallographically characterize all kinds of materials has gained some attention in recent years due to, first, the wide availability of fast and sensitive detectors, and second, the appearance of commercial electron diffractometers. During this last decade, a large number of structural analyses from different compounds have been already carried out with the help of 3D electron diffraction data that were not possible with the current X-ray methods. In this context, the use of a transmission electron microscope as an electron nano-diffractometer has proved to be advantageous when diffraction data from single nanocrystals are required, for instance, in phase mixtures. Individual phases do not have to be purely synthesized; thus the risk of structural change is avoided. This work presents the development and implementation of a novel and universal routine for the accurate and reliable acquisition of electron diffraction data in a TEM. The potential of this new data collection strategy to solve various crystallographic problems is illustrated using three known materials. In addition, two unknown crystal structures from commercial products are fully determined and refined based solely on electron diffraction data: an organic dye of low symmetry and an incommensurate modulated structure of a major constituent of cement. In particular, the precise knowledge of the different crystal structures in cement clinkers enables the exact phase analysis of these industrial phase mixtures directly from the manufacturing process, and paves the way for its CO_2 emissions reduction.

Note of appreciation:
This award was supported by ThermoFisher Scientific.

NEW METHODS FOR THE STUDY OF PRIMARY CILIARY DYSKINESIA

Dr. Andreia Pinto (Portugal)[1]

1 – NOVA School of Science and Technology, NOVA medical school, Royal Brompton Hospital

Abstract

Cilia and flagella are cellular protrusions found in eucaryotic cells, highly conserved between species and found in almost every cell type. Motile cilia are known for their motility properties and are involved in propelling and moving fluids. Primary ciliary dyskinesia (PCD) is an inherited autosomal-recessive disorder of motile cilia that results in several clinical manifestations. The estimated prevalence of PCD is ~1 per 10,000 births, but it is more prevalent in populations where consanguinity is common, it is currently associated with mutations in more than 40 genes. To diagnose PCD it involves a combination of tests, in particular, electron microscopy (EM) that is essential for determining the type of ciliary ultrastructural defect. The focus of this work was motile cilia ultrastructure and how the differences in cilia can be identified and classified, through the development of tools and guidelines to make the quantification and analysis of cilia more reliable and informative. The differential diagnosis of PCD is complex but crucial, and the development of new potential targeted treatments is essential. For better investigating the molecular mechanisms underlying PCD, it has been modelled in several organisms like mice, frogs and Zebrafish (ZF). ZF is a teleost vertebrate used in many areas of research, and a well-known animal model. ZF embryos develop quickly and allow unique advantages for research studies owing to their transparency during larval stages. ZF has many ciliated organs and presents primary cilia as well as motile cilia together with homologs for all the disease causing genes. The use of mutant zebrafish has been contributing to the better understanding of PCD molecular aetiology. Here, is investigated whether zebrafish cilia are ultrastructurally suitable for the study of PCD and concluded that the motile cilia of zebrafish resemble the cilia in the human airway in healthy conditions and in PCD.

Acknowledgments

NOVA technological school
NOVA medical school
Royal Brompton Hospital London

Keywords: Primary Ciliary Dyskinesia (PCD), zebrafish, motile cilia, electron Microscopy (EM), diagnosis

Note of appreciation:
This award was supported by Izasa Scientific.

STRUCTURE OF TWO STABLE, COMPLEX CAPSIDS: ENTERIC AND FOWL ADENOVIRUSES

Marta Pérez-Illana (Portugal)[1,2]; Marta Martínez (Spain)[1]; Anna Schachnner (Austria)[3]; Gabriela N. Condezo (Spain)[1]; Mercedes Hernando-Pérez (Spain)[1,4]; Casandra Mangroo (Canada)[5]; Martha Brown (Canada)[5]; Michael Hess (Austria)[3]; Roberto Marabini (Spain)[6]; Carmen San Martín (Spain)[1]

1 - Department of Macromolecular Structures. Centro Nacional de Biotecnología, Madrid, Spain; 2 - Present address: Instituto de Tecnologia Química e Biológica. Universidade Nova de Lisboa, Oeiras, Portugal; 3 - Department for Farm Animals and Veterinary Public Health. University of Veterinary Medicine, Vienna, Austria; 4 - Present address: Departamento de Física de Materiales.Universidad Autónoma de Madrid, Madrid, Spain; 5 - Department of Molecular Genetics. University of Toronto, Ontario, Canada; 6 - Escuela Politécnica Superior. Universidad Autónoma de Madrid, Madrid, Spain

Abstract

Adenoviruses have a non-enveloped icosahedral capsid with a pseudo T=25 geometry. They are relatively large— with a diameter of 900 Å, enclosing a dsDNA genome in the range of 25-49 kbp (depending on the adenovirus genus) accompanied by virus encoded “histone-like” proteins. Adenoviruses infect a broad range of vertebrate hosts and are traditionally studied due to their pathogenicity in immunocompromised human individuals and in certain animal species. In particular human enteric adenoviruses are of interest because they constitute one of the main causes of viral gastroenteritis in the world and must withstand the harsh conditions found in the gut. This requirement suggests that capsid stability must be different from that of other adenoviruses. On the other hand, the use of non-human adenoviruses has been proposed as alternative vectors in terms of evading the pre-existing immune response against human adenovirus-based vectors.

In this thesis we have assessed the thermal stability of an enteric human adenovirus (HAdV-F41) and a fowl adenovirus (FAdV-C4). HAdV-F41 and notably FAdV-C4, are more thermostable than the prototype respiratory adenovirus HAdV-C5. We have determined the structure of HAdV-F41 at 4 Å resolution [1] and of FAdV-C4 at 3.3 Å [2] by single particle averaging cryo-electron microscopy. We have compared the structures with those of other adenoviruses with respiratory (HAdV-C5) and ocular (HAdV-D26) tropisms, as well as adenoviruses infecting lizards (LAdV-2) and cows (BAdV-3). Overall, major coat proteins reveal conservation among adenoviruses, although the organization of surface-exposed loop regions is substantially divergent in HAdV-F41 and FAdV-C4 from the prototype HAdV-C5. Unexpectedly, the organization of the external cementing protein (IX) in HAdV-F41 is unique compared to all previously characterized adenoviruses. In FAdV-C4, internal minor capsid proteins (VIII and IIIa) show important rearranged domains, as compared to other adenovirus structures. Finally, we provide preliminary insights on the different organization of the nucleoproteic core of FAdVC4. Variance in the core organization among adenoviruses might play a role in determining the stability features. All this knowledge could inform on modifications to use HAdV-F41-based oral vaccines with a longer “shelf-life” than drugs relying on HAdV-C5. Design of highly stable vectors, with reduced immunogenic response, based on FAdVs would be also of interest.

Acknowledgments

M.P.-I. held a predoctoral contract from La Caixa Foundation (ID 100010434), under agreement LCF/BQ/SO16/52270032

References

[1] M. Pérez-Illana, M. Martínez, G.N. Condezo, M. Hernando-Pérez, C. Mangroo, M. Brown, R. Marabini, C. San Martín, Cryo-EM structure of enteric adenovirus HAdV-F41 highlights structural variations among human adenoviruses, Science Advances 7(9) (2021) eabd9421.
[2] M. Pérez-Illana, A. Schachnner, G.N. Condezo, M. Hernando-Pérez, M. Martínez, R. Marabini, M. Hess, C. San Martín, Aviadenovirus structure:A highly thermostable capsid in the absence of stabilizing proteins [manuscript under preparation].

Keywords: cryo-electron microscopy, enteric adenoviruses, fowl adenoviruses, virus structure, virus stability

Note of appreciation:
This award was supported by Tescan.

PHASE TRANSFORMATIONS AND MODELLING OF THERMAL STRESSES IN A CAST SUPER DUPLEX STAINLESS STEEL

Ricardo O. Sousa (Portugal)[1,3]; Pedro Lacerda (Portugal)[2]; P.J. Ferreira (Portugal)[4]; L.M.M. Ribeiro (Portugal)

1 - Department of Metallurgical and Materials Engineering, University of Porto, Porto, Portugal; 2 - FERESPE – Fundição de Aço e Ferro, Lda, V. N. Famalicão, Portugal; 3 - INEGI, Department of Metallurgical and Materials Engineering, University of Porto, Porto, Portugal; 4 - Mechanical Engineering Department and IDMEC, Instituto Superior Técnico, University of Lisbon, Av. Rovisco Pais, 1049-001 Lisboa, Portugal

Abstract

Metal casting is an old manufacturing process that involves the melting and solidification of an alloy to make a product with a simple or complex shape. Despite the fact that metal casting is one of the most economical routes to transform raw materials into finished metal products, it is also one of the most challenging manufacturing processes. In the past, to control the quality of final products a trial-and-error approach was typical. Nowadays, the traditional methods of manufacturing have been replaced by advanced production systems capable of managing the small batch production of complex products and short lead times. Furthermore, computation is currently an essential tool because it displays new methods of modelling and simulation to optimize the design and manufacturing processes. In metal casting, there are several physical phenomena that affect the quality of the final products, such as solid-phase transformations of the material, heat transfer between the hot metal and the cold mold and thermal stresses generated during cooling. In this regard, for any current advanced production system, modelling plays an important role in describing quantitatively the relationships among the aforementioned physical phenomena. This methodology can be applied to solve complex problems associated with casting technology. In this context, the objective of the present work focused on creating a model that describes the main parameters affecting the formation of residual stresses in cast parts with complex geometries. In particular, this work centers on determining the solid-phase transformations occurring in 25Cr-7Ni-Mo-N super duplex stainless steel, as a function of temperature and cooling rate, 2) understanding the kinetics of formation of secondary phases and the distribution of phases across the thickness of the cast parts, and 3) creating numerical models to predict the residual stresses of 25Cr7Ni-Mo-N super duplex stainless steels parts. Through the development of numerical models, the effects of temperature distribution, mechanical constraints, and solid-phase transformations on the residual stresses of cast parts are effectively predicted. To understand the solid-phase transformations occurring in 25Cr-7Ni-Mo-N super duplex stainless steel, an initial study was made on the microstructural characterization of the as-cast components. Subsequently, the secondary phases formed at temperatures between 700 oC and 1000 oC were identified and their kinetics of formation were assessed. For this characterization, a combination of microscopy techniques was used: optical microscopy, scanning electron microscopy and transmission electron microscopy. With the characterization of solid-phase transformations, a sequentially coupled thermo-mechanical model was developed in AbaqusTM, using empirical descriptions of the thermos physical properties of the phases. The accuracy of the models was evaluated by measuring the residual stresses using the contour method. A close agreement between the predicted and measured residual stresses was achieved, showing the importance of defining the interfacial heat transfer coefficient, which strongly depends on the specific setup. In summary, this work greatly contributes to improve

the quality of cast super duplex stainless steel components. In addition, the methodology developed can be extrapolated to other materials and manufacturing processes. This work fosters future developments within the field of casting, in particular to predict the microstructure evolution along the thermal processing cycle.

Note of appreciation:
This award was supported by Zeiss.

MATERIAL SCIENCES/CATALAN INSTITUTE OF NANOSCIENCE AND NANOTECHNOLOGY (ICN2), BARCELONA, SPAIN

Ting Zhang (China)[1]; Jordi Arbiol (Spain)[2]

1 – Catalan Institute of Nanoscience and Nanotechnology (ICN2), Barcelona; 2 - Catalan Institute of Nanoscience and Nanotechnology (ICN2), Barcelona, Spain

Abstract

Electrochemical CO2 reduction reaction (eCO2RR) driven by renewable power is a promising way to convert CO2 to fuels and chemicals, which has been proposed as a sustainable process for the artificial carbon cycle.1 However, due to the innerness of CO2 molecules and competitive hydrogen evolution reaction (HER), the main challenges in the field eCO2RR are the high overpotential requirement that represents the unfavourable thermodynamics and low Faradaic efficiency (FE) for the target products.2 Therefore, searching for a high-efficient and cost-friendly electrocatalyst is sensible and necessary for practical applications. As a frontier in materials science, single-atom catalysts (SACs) with atomically dispersed active sites anchored on a specific solid support, have great potential of bridging the gap between homogenous and heterogenous catalysts, and thus emerged as an up-to-date frontier as electrocatalysts. Especially, benefiting from their simple and precise single metal-based active sites, their catalytic performance can be easily regulated, which help overcome the high activation barriers and the sluggish kinetics in eCO2RR, and therefore SACs have currently been widely used in eCO2RR and showed excellent selectivity and activity.3 Among all methods to prepare SACs, metal-organic frameworks (MOFs), because of their large specific surface area, rich pore structure, and uniformly dispersed active sites, have a great potential, which could form single active sites from the guest metal via spatial confinement effect.4 Thus, rational design of SACs derived from MOFs to fulfill the high FE and low overpotential is crucial for eCO2RR applications

Acknowledgments

Authors acknowledge funding from Generalitat de Catalunya 2017 SGR 327 and 2017 SGR 1246. T. Z. and J. A. acknowledge funding from the Spanish MINECO project NANOGEN (PID2020-116093RB-C43). ICN2 is supported by the Severo Ochoa program from Spanish MINECO (Grant No. SEV-2017-0706).

References

1. Zhao, K. & Quan, X. Carbon-Based Materials for Electrochemical Reduction of CO2 to C2+ Oxygenates: Recent Progress and Remaining Challenges. ACS Catal. 11, 2076–2097 (2021).
2. Jin, S., Hao, Z., Zhang, K., Yan, Z. & Chen, J. Advances and Challenges for the Electrochemical Reduction of CO2 to CO: From Fundamentals to Industrialization. Angew. Chem. Int. Ed. 60, 20627–20648 (2021).
3. Qu, Q., Ji, S., Chen, Y., Wang, D. & Li, Y. The atomic-level regulation of single-atom site catalysts for the electrochemical CO2 reduction reaction. Chem. Sci. 12, 4201–4215 (2021).
4. Zhou, D., Li, X., Shang, H., Qin, F. & Chen, W. Atomic regulation of metal–organic framework derived carbon-based single-atom catalysts for the electrochemical CO2 reduction reaction. J Mater Chem A 9, 23382–23418 (2021).

Keywords: MOFs, single atom catalysts, CO2 reduction reaction, electrocatalysis

Note of appreciation:
This award was supported by Zeiss.

RATIONAL DESIGN OF THE CATALYSTS MICROENVIRONMENT TO EFFECTIVELY BOOST THE CARBON DIOXIDE ELECTROCHEMICAL REDUCTION

Xu Han (China)[1]; Jordi Arbiol (Spain)[1]

1 – Catalan Institute of Nanoscience and Nanotechnology (ICN2), Spain

Abstract

Anthropogenic carbon dioxide (CO2) emission is anticipated to contribute to a projected global temperature rise of 1.5°C between the years 2030 and 2052. This escalation is associated with a range of environmental challenges, including but not limited to global warming, elevated sea levels, intensified weather events, and potential species endangerment. Although renewable energy and electrification have realized the decreasing CO2 emissions in some sectors, air transportation without electrified alternative and industries such as steel and cement requiring carbon oxidation in their operation must decrease carbon footprint through combining the implementation of renewable fuels and the conversion of CO2 conversion. Electrochemical conversion of CO2 powered by renewable energy to energy-dense fuels and commodity chemicals is considered as an elegant solution to achieve the carbon cycle. At least on a short to intermediate term renewable-powered electrochemical carbon dioxide reduction reaction (eCO2RR) to produce carbon monoxide (CO) provides a techno-economic feasible manner. In this dissertation we have conducted a series of studies around CO2-to-CO conversion. This conversion goes through two electrons and two protons transfer in solid-liquid-gas three-phase system. We will optimize different key steps of CO2-to-CO conversion by taking different strategies. The primary objective of this dissertation is to enhance specific reaction steps on catalysts, ultimately achieving heightened activity and selectivity in eCO2RR. The whole work includes three parts, focusing on improving adsorption of CO2 1 , the transformation of CO2 2 and desorption of CO3 respectively.

Acknowledgments

The authors acknowledge funding from Generalitat de Catalunya2021 SGR 01581 and 2021 SGR 00457. ICN2 is supported by the Severo Ochoa program fromSpanish MCIN/AEI (Grant no. CEX2021-001214-**S).**

References

1. *ACS Appl. Mater. Interfaces*. **2022**, *14*, 32157-32165.
2. *Small Struct.* **2023**, 2200388.
3. *Adv. Func. Mater.*, **2022**, *32,* 2111446.

Keywords: MOFs, Znic oxide, electrochemical CO2 reduction

Note of appreciation:
This award was supported by Zeiss.

LIFE SCIENCES

Biofilm Formation by ST17 and ST19 Strains of Streptococcus agalactiae

Inês Silvestre (Portugal)[1]; Maria José Borrego (Portugal)[2]; Luísa Jordão (Portugal)[3]

1 – Hospital de Santarém; 2 – Department of Infectious Diseases, National Institute of Health Doutor Ricardo Jorge; 3 – Department of Environmental Health, Research and Development Unit, National Institute of Health Doutor Ricardo Jorge.

Abstract

Bacterial biofilms are an important virulence factor with a vital role in evasion from the host immune system, colonization and infection. The aim of the present study was to evaluate in vitro the effects of three environmental factors (H+ , glucose and human plasma) in biofilm formation, by carrier and invasive S. agalactiae strains of ST17 and ST19 sequence types, including DNase producers and non-producers. Bacteria ability to assemble biofilms was classified based on crystal violet assay. Biofilm formation was also monitored by scanning electron microscopy. Depending on the growth medium used, each bacterial isolate could fit in different biofilm production categories. Our data showed that optimal conditions for S. agalactiae biofilm assembly were reached after 48 h incubation at pH 7.6 in the presence of glucose and inactivated human plasma. In the presence of inactivated human plasma, the biofilm biomass of ST19 strains experienced a higher increase than ST17 strains. The composition of the extracellular polymeric matrix of the three strongest biofilm producers (all from ST17) was accessed by enzymatic digestion of mature biofilms and proteins were shown to be the predominant component. The detailed identification of the extracellular protein components should contribute to the development of new therapeutic strategies to fight S. agalactiae infections. Acknowledgments The authors wish to thank Barbara Spellerberg for the kind gift of S. agalactiae strains from collection of the Institute of Medical Microbiology and Hygiene (IMMH), Ulm University, Germany. We are grateful to Joao Paulo Gomes and Alexandra Nunes (Instituto ~ Nacional de Saúde Doutor Ricardo Jorge, INSA, IP) for providing bN-acetylglucosaminidase enzyme and 96-well flat-bottomed polystyrene cell culture plates, respectively. We thank Rita Sobral (Nova School of Science and Technology, FCT/UNL) for the critical review of the manuscript and Hemovida® for IHP donation.

References

[1] Almeida A, Rosinski-Chupin I, Plainvert C, Douarre PE, Borrego MJ, Poyart C, et al. Parallel evolution of group B Streptococcus hypervirulent clonal complex 17 unveils new pathoadaptive mutations. mSystems 2017;2(5). e00074-17.

[2] Rosini R, Margarit I. Biofilm formation by Streptococcus agalactiae: influence of environmental conditions and implicated virulence factors. Front Cell Infect Microbiol 2015;5:6.

[3] Florindo C, Barroco CA, Silvestre I, Damião V, Gomes JP, Spellerberg B, et al. Capsular type, sequence type and microbial resistance factors impact on DNase activity of Streptococcus agalactiae strains from human and bovine origin. Eur J Microbiol Immunol 2018;8(4):149e54.

[4] Patras KA, Nizet V. Group B streptococcal maternal colonization and neonatal disease: molecular mechanisms and preventative approaches. Front Pediatr 2018;6:27.

[5] Shabayek S, Spellerberg B. Acid stress response mechanisms of group B streptococci. Front Cell Infect Microbiol 2017;7:395.

[6] Spellerberg B. Pathogenesis of neonatal Streptococcus agalactiae infections. Microb Infect 2000;2:1733e42.

[7] Bandeira M, Borges V, Gomes JP, Duarte A, Jordão L. Insights on Klebsiella pneumoniae biofilms assembled on different surfaces using phenotypic and genotypic approaches. Microorganisms 2017;5:16.
[8] Okshevsky M, Meyer RL. The role of extracellular DNA in the establishment, maintenance and perpetuation of bacterial biofilms. Crit Rev Microbiol 2015;41(3):341e52.
[9] Donelli G. Methods in Molecular Biology, vol. 1147. New York: Humana Press; 2014.
[10] Borges S, Silva J, Teixeira P. Survival and biofilm formation by Group B Streptococci in simulated vaginal fluid at different pHs. Antonie Leeuwenhoek 2012;101:677e82.
[11] Nijland R, Hall MJ, Burgess JG. Dispersal of biofilms by secreted, matrix degrading, bacterial DNase. PloS One 2010;5(12):e15668.
[12] Seper A, Fengler VH, Roier S, Wolinski H, Kohlwein SD, Bishop AL, et al. Extracellular nucleases and extracellular DNA play important roles in Vibrio cholerae biofilm formation. Mol Microbiol 2011;82(4):1015e37.
[13] Nie S, Lu X, Hu YW, Zheng L, Wang Q. Influence of environmental and genotypic factors on biofilm formation by clinical isolates of group B streptococci. Microb Pathog 2018;121:45e50.
[14] D'Urzo N, Martinelli M, Pezzicoli A, De Cesare V, Pinto V, Margarit I, et al. Acidic pH strongly enhances in vitro biofilm formation by a subset of hypervirulent ST-17 Streptococcus agalactiae strains. Appl Environ Microbiol 2014;80(7):2176e85.
[15] Ho YR, Li CM, Yu CH, Lin YJ, Wu CM, Harn IC, et al. The enhancement of biofilm formation in Group B streptococcal isolates at vaginal pH. Med Microbiol Immunol 2013;202(2):105e15.
[16] Konto-Ghiorghi Y, Mairey E, Mallet A, Dumenil G, Caliot E, Trieu-Cuot P, et al. Dual role for pilus in adherence to epithelial cells and biofilm formation in Streptococcus agalactiae. PLoS Pathog 2009;5(5):e1000422.
[17] Yang Q, Porter AJ, Zhang M, Harrington DJ, Black GW, Sutcliffe IC. The impact of pH and nutrient stress on the growth and survival of Streptococcus agalactiae. Antonie van Leeuwenhoek 2012;102(2):277e87.
[18] Kaur H, Kumar P, Ray P, Kaur J, Chakraborti A. Biofilm formation in clinical isolates of group B Streptococci from north India. Microb Pathog 2009;46(6):321e7.
[19] Lin FC, Whiting A, Adderson E, Takahashi S, Dunn DM, Weiss R, et al. Phylogenetic lineages of invasive and colonizing strains of serotype III group B streptococci from neonates: a multicenter prospective study. J Clin Microbiol 2006;44(4):1257e61.
[20] Martins ER, Pessanha MA, Ramirez M, Melo-Cristino J. And the Portuguese group for the study of streptococcal infections. Analysis of group B streptococcal isolates from infants and pregnant women in Portugal revealing two lineages with enhanced invasiveness. J Clin Microbiol 2007;45(10):3224e9.
[21] Parker RE, Laut C, Gaddy JA, Zadoks RN, Davies HD, Manning SD. Association between genotypic diversity and biofilm production in group B Streptococcus. BMC Microbiol 2016;16:86.
[22] Shabayek S, Spellerberg B. Group B streptococcal colonization, molecular characteristics, and epidemiology. Front Microbiol 2018;9:437.
[23] Xia FD, Mallet A, Caliot E, Gao C, Trieu-Cuot P, Dramsi S. Capsular polysaccharide of Group B Streptococcus mediates biofilm formation in the presence of human plasma. Microb Infect 2015;17(1):71e6.
[24] Florindo C, Damião V, Lima J, Nogueira I, Rocha I, Caetano P, et al. Accuracy of prenatal culture in predicting intrapartum group B Streptococcus colonization status. J Matern Fetal Neonatal Med 2014;27(6):640e2.
[25] Florindo C, Damião V, Silvestre I, Farinha C, Rodrigues F, Nogueira F, et al. Epidemiological surveillance of colonising group B Streptococcus epidemiology in the Lisbon and Tagus Valley regions, Portugal (2005 to 2012): emergence of a new epidemic type IV/clonal complex 17 clone. Euro Surveill 2014;19:23.

[26] Florindo C, Viegas S, Paulino A, Rodrigues E, Gomes JP, Borrego MJ. Molecular characterization and antimicrobial susceptibility profiles in Streptococcus agalactiae colonizing strains: association of erythromycin resistance with subtype III-1 genetic clone family. Clin Microbiol Infect 2010;16(9):1458e63.
[27] Fluegge K, Wons J, Spellerberg B, Swoboda S, Siedler A, Hufnagel M, et al. Genetic differences between invasive and noninvasive neonatal group B streptococcal isolates. Pediatr Infect Dis J 2011;30(11):1027e31.
[28] Fluegge K, Supper S, Siedler A, Berner R. Serotype distribution of invasive group B streptococcal isolates in infants: results from a nationwide active laboratory surveillance study over 2 years in Germany. Clin Infect Dis 2005;40(5):760e3.
[29] Fluegge K, Supper S, Siedler A, Berner R. Antibiotic susceptibility in neonatal invasive isolates of Streptococcus agalactiae in a 2-year nationwide surveillance study in Germany. Antimicrob Agents Chemother 2004;48(11):4444e6.
[30] Bandeira M, Carvalho PA, Duarte A, Jordão L. Exploring dangerous connections between Klebsiella pneumoniae biofilms and healthcare-associated infections. Pathogens 2014;3:720e31.
[31] Stepanovic S, Vukovic D, Hola V, Di Bonaventura G, Djukic S, Cirkovic I, et al. Quantification of biofilm in microtiter plates: overview of testing conditions and practical recommendations for assessment of biofilm production by Staphylococci. Apmis 2007;115(8):891e9.
[32] Charlebois A, Jacques M, Archambault M. Biofilm formation of Clostridium perfringens and its exposure to low-dose antimicrobials. Front Microbiol 2014;5:183.
[33] Al-Fattani MA, Douglas LJ. Biofilm matrix of Candida albicans and Candida tropicalis: chemical composition and role in drug resistance. J Med Microbiol 2006;55:999e1008.
[34] Alvim DCSS, Ferreira AFM, Leal MA, Oliveira LMA, Botelho AMN, Botelho ACN, et al. Biofilm production and distribution of pilus variants among Streptococcus agalactiae isolated from human and animal sources. Biofouling 2019;35:8.
[35] Azeredo J, Azevedo NF, Briandet R, Cerca N, Coenye T, Costa AR, et al. Critical review on biofilm methods. Critic Rev Microbiol 2017;43(3):313e51.
[36] Malone M, Goeres DM, Gosbell I, Vickery K, Jensen S, Stoodley P. Approaches to biofilm-associated infections: the need for standardized and relevant biofilm methods for clinical applications. Expert Rev Anti Infect Ther 2016;15(2): 147e56.
[37] Marks LR, Mashburn-Warren L, Federle MJ, Hakansson AP. Streptococcus pyogenes biofilm growth in vitro and in vivo and its role in colonization, virulence, and genetic exchange. J Infect Dis 2014;210(1):25e34.
[38] Ramstedt M, Ribeiro IAC, Bujdakova H, Mergulhão FJM, Jordão L, Thomsen P, et al. Evaluating efficacy of antimicrobial and antifouling materials for urinary tract medical devices: challenges and recommendations. Macromol Biosci 2019;19(5):e1800384.
[39] Rinaudo CD, Rosini R, Galeotti CL, Berti F, Necchi F, Reguzzi V, et al. Specific involvement of pilus type 2a in biofilm formation in group B Streptococcus. PloS One 2010;5(2):e9216.
[40] Tamura GS, Kuypers JM, Smith S, Raff H, Rubens CE. Adherence of group B Streptococci to cultured epithelial cells: roles of environmental factors and bacterial surface components. Infect Immun 1994;62(6):2450e8

Keywords: Streptococcus agalactiae, biofilms, extracellular polymeric substance matrix, DNases

DESIGNING AND TUNING FACILITY-BASED CRYOCLEM EXPERIMENTS ON AN EM FACILITY: A ROADMAP WITH CASE STUDIES AND A FRENCH TOUCH.

Stéphane Tachon (France)[1], Jan Groen (France)[1,2], Léa Swistak (France)[2], Margot Sahnine (France)[3], Jerzy Witwinowsky (France)[4], Anna Sartori-Rupp (France)[1]

1 – NanoImaging core facility, Institut Pasteur; 2 – Dynamics of host-pathogen interactions' group, Institut Pasteur; 3- Pathogenesis of vascular infection's group, Institut Pasteur; 4 – Evolutionary biology of the microbial cell, Institut Pasteur

Abstract

Carefully designing complex Fluorescence (FLM)/Electron microscopy (EM) experiments is a fundamental pre-requisite for the success of every project involving advanced imaging technologies. Collaborative projects run between research groups and imaging facilities in a research structure strongly rely on the infrastructure and expertise of the facilities. They are based on established imaging workflows developed to answer specific biological topics related to the main themes and objectives of the concerned research structure. In this presentation I will elaborate on how to design successful cryo-electron tomography (cryoTOMO) and in particular cryoCLEM imaging experiments, based on my long-term experience of working on an EM facility at Institut Pasteur Paris (IPP). IPP' research is focused on pathogen and host-pathogen interaction studies and offers advanced FLM and a recent cutting-edge cryoEM infrastructure, featuring dedicated systems upgraded to the latest standards, such as a Titan krios cryo-TEM, an Aquilos2 cryoFIB/SEM and a cryoFLM system. Within the Institute, we developed cryo-tomography (cryoTOMO)/cryoCLEM pipelines[1,2] for in situ cellular studies, accessible to the campus and to external users. These approaches are tailored to the study of isolated pathogens such as bacteria, viruses, fungi and of pathogen interacting with host cells, looking at different time points of infection and at the molecular players involved in the infectious process. These workflows are made of multiple interconnected steps that require specific optimisation and troubleshooting, starting from sample preparation on EM grids up to image acquisition in cryogenic conditions and image processing[3,4]. Using cryogenic tomography approaches on cellular samples has the great advantage of preserving and imaging the sample as close as possible to its native state, but it often comes at the expenses of speed and throughput. The results obtained provide generally a morphological characterisation of the sample coupled to quantification, while the high-resolution structural analysis remains more challenging and strongly structure-dependant[5]. Moreover, the critical aspects to be considered when designing a cryoTOMO/cryoCLEM experiments are availability of microscope time, the overall costs and timing, the available resources in terms of human expertise and established technologies and finally safety issues and protocols for inactivation of pathogens, compatible with the structural integrity of the samples[6]. I will showcase our roadmap for designing cryoTOMO/cryoCLEM experiments with several examples on model systems, representing some relevant applications to finalised and ongoing projects. I will conclude with some perspective on implementations of novel methodologies to extend our pipelines to higher spatial resolution and to more complex biological systems such as organoids and tissues.

Acknowledgments

We thank Jean-Marie Winter, Eduard Baquero-Salazar & Matthijn Vos at the NanoImaging core facility at Institut Pasteur, Paris, for the kind and expert support for developing tomography-based workflows. This work is supported by a grant from the Programme Fédérateur de Recherche (PFR6) SARS-CoV-2 & COVID-19 J. G. is supported by the PFR6 SARS-CoV-2 & COVID-19 grant.

References

[1] Sartori-Rupp A, Nat Commun. 2019;10: 342
[2] Witwinowski J, et al. Nat Microbiol. 2022;7: 411
[3] Sartori A, et al. J Struct Biol. 2007; 160: 135. doi: 10.1016/j.jsb.2007.07.011.
[4] Lepper S, et al. J Microsc. 2010 238: 21. doi: 10.1111/j.1365-2818.2009.03327.x.
[5] Xue L, et al. Nature 2022; 610: 205. doi: 10.1038/s41586-022-05255-2.
[6] Zimmermann L, et al. Curr Opin Virol. 2023; 61: 101338. doi: 10.1016/j.coviro.2023.101338.

Keywords: Cryo- Electron Tomography, cryo-Correlative Light and Electron Tomography, pathogens, host-pathogen interactions

LESSONS LEARNED FROM MOVING BETWEEN AN ACADEMIC JOB TO INDUSTRY AND BACK

Matthijn Vos (France)[1]

1 – NanoImaging core facility, Institut Pasteur

Abstract

Moving between academics and industry is often seen as unusual. The move from academics to industry is often seen as being motivated by salary, but possible. However, moving from industry to academics is poorly understood. Industry has a reputation of being only driven by sales and return on investment, while academics are sometimes viewed by the general audiences as wasteful if no direct application can be provide. Nevertheless, it is the combination between industry and academics that is often the most powerful route to innovation. Basic understanding of physical, chemical and biological processes is essential in providing solutions to our daily problems and the scientific validation and feasibility of the proposed ideas. Moving from the scientific drawing table to the productization and mass adoption of innovative ideas does require the full commitment of the industrial sector. Funding of scientific projects directly by the industry is, however, often seen as non-academic since the published data should be unbiased. In addition there is a notion that industry will not develop new improved products by themselves without the pressure of competition. Understanding both the academic and industrial way of working, one can eliminate many misconceptions present on both sides about the other side and work more effectively towards innovative new products. In this lecture, I'll present how to best engage each side and more successfully promote new ideas both in front of industry as well as in academics.

THE NEW (UA)GE - ALTERNATIVES TO THE USE OF URANYL ACETATE IN ELECTRON MICROSCOPY

Beatriz Tomaz (Portugal)[1]; Sofia Pachecho (Portugal)[2]; Ana Laura Sousa (Portugal)[1]; Erin Tranfield (Portugal)[1]

1 - Instituto Gulbenkian de Ciência; 2 - Instituto de Investigação e Inovação em Saúde

Abstract

Uranyl Acetate is one of the most frequently used reagents in Electron Microscopy. Known for its versatility, the applications range from staining of thin sections in plastic-embedded samples, to high-contrast negative staining (1). Its salts combine with the phosphate groups in nucleic acids and the phosphate and carboxyl groups on the cell surface – providing electron density to the sample and contrasting the various cellular elements (2, 3).

Despite most radioactive nuclides being depleted from uranyl salts used in Electron Microscopy, the chemical is still classified as radioactive. It is highly toxic, and subsequently needs a lot of precautions surrounding its use (2). Therefore the purchase of the reagent is limited and subject to tedious bureaucratic processes, followed by a notorious difficulty for the storage and disposal (1). The establishment of a non-hazardous alternative in the community, would decrease the health and environmental issues for those who work with Uranyl Acetate, but also for the surrounding environment.

With this purpose in mind, three non-toxic reagents (UAR-EMS, UA-Zero and Neodymium) were tested alongside Uranyl Acetate, to evaluate their performance in Negative Staining Conventional Processing and Post-Staining. UAR and UA-Zero were selected because of their availability on the market and the reported good results (1, 4). Neodymium was selected after excellent reports in the community of its suitability to replace Uranyl Acetate (5). For the Negative Staining tests, we selected *E. coli*, *Lactobacillus spp.,* HIV-VLP ad exossomes samples, while for the Conventional Processing and Post-Staining the tests used 793T cell pellets.

After the image collection in the Tecnai G2 Spirit BioTWIN Transmission Electron Microscope, using the Olympus-SIS Veleta CCD Camera, an evaluation key was created and distributed amongst various blind observers in and out of the field of Electron Microscopy. The mean of each score attributed was calculated for each reagent and condition tested; statistical analysis was then performed.

Preliminary results point to UAR-EMS being a strong contender, followed by Neodymium and with UA-Zero having the weakest performance. The current hypothesis points to the lack of a “one size fits all” answer - with different reagents performing better depending on the sample and protocol. Our best option may be to ration the remaining Uranyl Acetate for very specialized protocols.

Acknowledgments

I would like to extend my gratitude to Dr. Erin Tranfield and Technician Ana Laura Sousa, for entrusting me with this project but also for all the help and guidance they have provided. I'd also like to thank Technician Sofia Pacheco, for building the foundation for this project before me. Finally, we thank – AB Santos, Ana Pires, Dagmar Zeuschner, Ivo Telley, Joana Gomes Antunes, José Melero, Karina Mildner, Lilo Greune, Mariana Ferreira, Michael J. Hall, Pedro Faísca and Rob Mesman – for lending us their knowledge and time by evaluating the date we obtained.

References

1 - Nakakoshi M, Nishioka H, Katayama E. New versatile staining reagents for biological transmission electron microscopy that substitute for uranyl acetate. Journal of Electron Microscopy. 2011 Dec 1;60(6):401–7.

2 - Suvarna KS, Layton C, Bancroft JD. Theory and practice of histological techniques. 7. ed. Edinburgh: Elsevier Churchill Livingston; 2013. 637 p.

3 - Hayat MA. Principles and Techniques of Electron Microscopy. 3rd edition. Basingstoke: Palgrave Macmillan; 1989. 480 p.

4 - Pinto AL, Rai RK, Shoemark A, Hogg C, Burgoyne T. UA-Zero as a Uranyl Acetate Replacement When Diagnosing Primary Ciliary Dyskinesia by Transmission Electron Microscopy. Diagnostics. 2021; 11(6):1063. https://doi.org/10.3390/diagnostics11061063

5 - Kuipers J, Giepmans BNG. Neodymium as an alternative contrast for uranium in electron microscopy. Histochem Cell Biol. 2020 Apr;153(4):271-277. doi: 10.1007/s00418-020-01846-0. Epub 2020 Feb 1. Erratum in: Histochem Cell Biol. 2020 Dec;154(6):683.

Keywords: Uranyl Acetate, UAR-EMS, UA-Zero, Neodymium, Alternative, Electron Microscopy, Negative Staining, Conventional Processing, Post-Staining

MINERAL DEPOSITION IN TYPE I COLLAGEN MATERIALS OCCURS THROUGH SPHERULITIC-LIKE CRYSTAL GROWTH

Elena Macías-Sánchez (Spain)[1]; Nadezda V. Tarakina (Germany)[2]; Danail Ivanov (Germany)[3]; Stéphane Blouin (Austria)[4]; Andrea M. Berzlanovich (Austria)[5]; Peter Fratzl (Germany)[2]

1 - University of Granada; 2 - Max Planck institute of Colloids and Interfaces; 3 - Fritz Haber Institute of the Max Planck Society; 4 - Ludwig Boltzmann Institute of Osteology; 5 - Medical University of Vienna

Abstract

The formation of the hard tissues that provide support and mobility to our organism is achieved by the interaction of tiny inorganic crystals and an organic framework composed mainly of collagen. The mechanical properties of bone depend on the size, orientation and degree of crystallinity of the mineral phase. However, the mechanisms driving mineralization remain poorly understood, with competing hypotheses on the location and orientation of the nanocrystals in relation to collagen fibrils.

Combining a variety of sample preparation methods with three-dimensional electron tomography and high-resolution electron microscopy imaging and spectroscopy, we demonstrate that mineralization occurs through a spherulitic-like crystal growth process, in which the collagen matrix serves as an organic scaffold where the apatite crystals grow. First, aggregates of disordered crystals form in the interfibrillar spaces, which form the core of the spherulites. As the mineral expands and penetrates into the collagen fibrils, both the shape and the arrangement of the nanocrystallites are no longer arbitrary, but arrange in overlapping curved layers, apparently following the internal helical structure of the collagen fibril.

Each of these spherulites is formed by a tight structure of overlapping curved layers crowded with small crystallites. The spherulitic intergrowth of the collagen structure by the mineral creates an interlocking tessellated macrostructure that seems to be responsible of the extraordinary mechanical performance of bone.

Acknowledgments

EMS is supported by a Juan de la Cierva Incorporación fellowship (IJC2020-043639-I) funded by MCIN/AEI/10.13039/501100011033 and European Union NextGenerationEU/PRTR.

Authors gratefully acknowledge financial support from the Max Planck Society.

References

1. E. Macías-Sánchez,* N. V. Tarakina, D. Ivanov, S. Blouin, A. M. Berzlanovich, and P. Fratzl*. *Spherulitic Crystal Growth Drives Mineral Deposition Patterns in Collagen-Based Materials.* Advanced Functional Materials, 2022. **32**(31): p. 2200504.

2. Buss, D.J., N. Reznikov, and M.D. McKee, *Crossfibrillar mineral tessellation in normal and Hyp mouse bone as revealed by 3D FIB-SEM microscopy.* Journal of Structural Biology, 2020. **212**(2): p. 107603.

3. Shah, F.A., K. Ruscsák, and A. Palmquist, *Transformation of bone mineral morphology: From discrete marquise-shaped motifs to a continuous interwoven mesh.* Bone Reports, 2020. **13**: p. 100283.

Keywords: Bone mineralization, collagen, S/TEM, 3D tomography, spcectroscopy

INFLUENZA A VIRUS LIQUID CONDENSATES – AN ULTRASTRUCTURAL STUDY

Ana Laura Sousa (Portugal)[1]; Sílvia Vale-Costa (Portugal)[1]; Maria João Amorim (Portugal)[1,2]; Erin M Tranfield (Portugal)[1]

1 - Fundação Calouste Gulbenkian - Instituto Gulbenkian de Ciencia; 2 - Católica Biomedical Research Centre

Abstract

Influenza A virus (IAV) viral inclusions are viewed as critical hubs for concentrating and exchanging viral genome RNA segments in the cytosol and promoting viral genome assembly[1,2]. Genome assembly is challenging and involves the combination of eight distinct viral RNAs that must be packaged into a virion to form infectious particles. Identifying viral inclusions key-features may thus provide means to control their formation and halt viral production.

To our knowledge, the only host factor directly implicated in the biogenesis of IAV liquid inclusions is Rab11[3-6], the major regulator of the recycling compartment that sorts and transports cargo to the apical cell surface[1,7]. During infection, Rab11 recycling function is impaired[8,9] and Rab11 accumulates near specific Endoplasmic Reticulum (ER) subdomains – the ER exit sites (ERES)[10,11]. At these sites, viral inclusions develop as biomolecular condensates that enlarge as infection progresses, and display properties of liquids including the ability to dynamically exchange contents and swiftly adjust to physiological changes[10].

Ultrastructural analysis of sites positive for Rab11, using correlative light and electron microscopy (CLEM), revealed that liquid viral inclusions, despite lacking a delimiting membrane, harbor clusters of heterogeneous vesicles of double and single membrane inside. Using immunogold labeling, we assessed that single membranes are decorated with structures that correspond to the viral genome segments[8,10]. Another group observed similar vesicles, protruding from a dilated and tubulated ER[11]. In both reports, ultrastructural studies were performed using chemical fixation and plastic sectioning which can introduce artifacts and structural distortions.

To overcome methodological limitations, the 3D organisation of viral inclusions was resolved by using high-pressure freezing/freeze substitution and electron tomography. The study revealed numerous single membrane vesicles clustered around double membrane vesicles in the vicinity of the ER. Importantly, we detected ER invaginations, whorls and large vacuoles, which are characteristic ER-alterations induced early in autophagy.

We conclude that both ER alterations together with single and double vesicles are not chemical fixation induced artifacts and that further studies using cryo-electron microscopy should be pursued to reveal the ultrastructure of IAV viral inclusions and lead to a better understanding of IAV replication cycle.

Acknowledgments

This project is supported by the European Research Council (ERC) under the European Union's Horizon 2020 research and innovation program (No 101001521 - LOFlu), by Fundação para a Ciência e a Tecnologia (FCT, 2022.02716.PTDC_EXPL) and also by Fundação Calouste Gulbenkian-Instituto Gulbenkian de Ciência (FCG-IGC, Portugal). M.J.A. is an Auxiliary Professor at Universidade Católica Portuguesa. S.V.-C. is funded by a Junior Researcher working contract from FCT/FCG. A.L.S. is funded by FCG.

References

[1] Vale-Costa S, Amorim MJ. Viruses. 2016;8: 64
[2] Amorim MJ. Frontiers in Cell and Developmental Biology. 2019;6: 176
[3] Amorim MJ, et al. Journal of Virology. 2011. pp. 4143–4156. doi:10.1128/jvi.02606-10
[4] Bruce EA, Digard P, Stuart AD. J Virol. 2010;84: 5848–5859
[5] Eisfeld AJ, et al. Journal of Virology. 2011. pp. 6117–6126. doi:10.1128/jvi.00378-11
[6] Staller E, Barclay WS. Cold Spring Harb Perspect Med. 2020. doi:10.1101/cshperspect.a038307
[7] O'Sullivan MJ, Lindsay AJ. Int J Mol Sci. 2020;21: 6074
[8] Vale-Costa S, et al. J Cell Sci. 2016;129: 1697–1710
[9] Kawaguchi A, et al. PLoS Pathog. 2015;11: e1005284
[10] Alenquer M, et al. Nat Commun. 2019;10: 1629
[11] de Castro Martin IF, et al. Nat Commun. 2017;8: 1396

Keywords: Influenza A virus, Transmission Electron Microscopy, High-Pressure Freezing, Electron Tomography

XEDS-STEM SPECTROKINETIC ANALYSIS OF BEAM SENSITIVE OXIDE NANOSTRUCTURES

Miguel Lóez-Haro (Spain)[1]; Isabel Gómez-Recio (Spain)[2]; Huiyan Pan (Spain)[1]; Juan José Delgado (Spain)[1]; Xiaowei Chen (Spain)[1]; Miguel Ángel Cauqui (Spain)[1]; José Antonio Pérez-Omil (Spain)[1]; María Luisa Ruiz-González (Spain)[1]; Marina Parras (Spain)[2]; María Hernando (Spain)[2]; José M. González-Calbet (Spain)[2]; José Juan Calvino (Spain)[1]

1 - Departamento de Ciencia de los Materiales e Ingeniería Metalúrgica y Química Inorgánica. Facultad de Ciencias. Universidad de Cádiz; 2 - Departamento de Química Inorgánica. Facultad de Ciencias Químicas. Universidad Complutense de Madrid

Abstract

Understanding the structural and compositional features of the oxygen sublattice becomes crucial to rationalize the functional properties of oxide type materials. In this context, determining the oxygen composition al local level is the most fundamental piece of information. However, the precise and accurate quantification of oxygen content in a metallic or multi-metallic oxide by means of nanoanalytical techniques, particularly XEDS, is not, in general, a straightforward question, due to the occurrence of absorption effects. This absorption contribution leads to underestimations of the oxygen content.

Likewise, oxygen evolution from the samples induced by the interaction with the electron beam during the acquisition of the spectroscopic information may further complicate a precise quantitative oxygen analysis. This additional effect will be particularly significant for nanostructured oxides, due to the large value of their surface to volume ratio.

Taking advantage of the improved detection capabilities of recent SDD multidetector systems, like that offered by the ChemiSTEM equipment, we have developed a novel experimental methodology which allows to overcome these limitations. The approach combines time-resolved XEDS-STEM mapping with precise quantifications performed using a new implementation of the so-called z-factors method (1). The former provides a series of spectra as a function of irradiation time. The latter allows to deconvolve the influence of absorption effects in the quantification of the oxygen content in each of the spectra in the time series. From this analysis, the evolution of oxygen content can be monitored as a function of electron dose and, consequently, traced-back to zero-dose conditions, Figure 1(d). In other words, using this method it is possible to obtain the O/M ratio in the pristine, undamaged, material.

The methodology has been applied to determine the exact oxygen content of individual nanorods of a potassium-manganese oxide with hollandite type structure, Figure 1(a-c). A very good agreement has been observed with compositional results determined at macroscopic level using Neutron Diffraction and Temperature Programmed Reduction experiments (2), which fully validates the proposed approach.

Moreover, the results observed during the interaction of these oxides with the electron beam have demonstrated as key to propose a compositional path for the reduction of K-Mn hollandites under hydrogen at increasing temperatures (2).

Acknowledgments

This work has received support from Projects: PID2020-113006-RB-I00 funded by MCIN/AEI/ 10.13039/501100011033, PID2019-110018GA-I00, PID2020-113753RB-I00 and PID2020- 113809RB-C33. This work has also been co-financed by the Department of Economy, Knowledge, Business and University of the Regional Government of Andalusia, Project references: FEDER-UCA18-107139 and PY18-2727. STEM experiments were recorded at the DME-UCA Node of the Spanish Singular Infrastructure for Electron Microscopy of Materials (ICTS ELECMI). HRTEM images were obtained at the CNME node of ELECMI. The authors acknowledge funding from the European Union's Horizon 2020 research and innovation program under Grant 823717−ESTEEM3.

References

(1) Watanabe, M.; Williams, D. B., The quantitative analysis of thin specimens: a review of progress from the Cliff-Lorimer to the new zeta-factor methods. *J. Microsc.J. Microsc.* **2006,** *221*, 89-109.
(2) Miguel López-Haro, Isabel Gómez-Recio, Huiyan Pan, Juan J. Delgado, Xiaowei Chen, Miguel A. Cauqui, José A. Pérez-Omil, María L. Ruiz-González, María Hernando, Marina Parras, José M. González-Calbet, José J. Calvino. *Quantitative, spectro-kinetic, analysis of oxygen in electron-beam sensitive, multi-metallic, oxide nanostructures. Microscopy and Microanalysis,* 2023, early view, https://doi.org/10.1093/micmic/ozad037

Keywords: Time-resolved XEDS spectroscopy, oxygen quantification, zeta-factors method, Electron Tomography, beam sensitive materials, hollandites

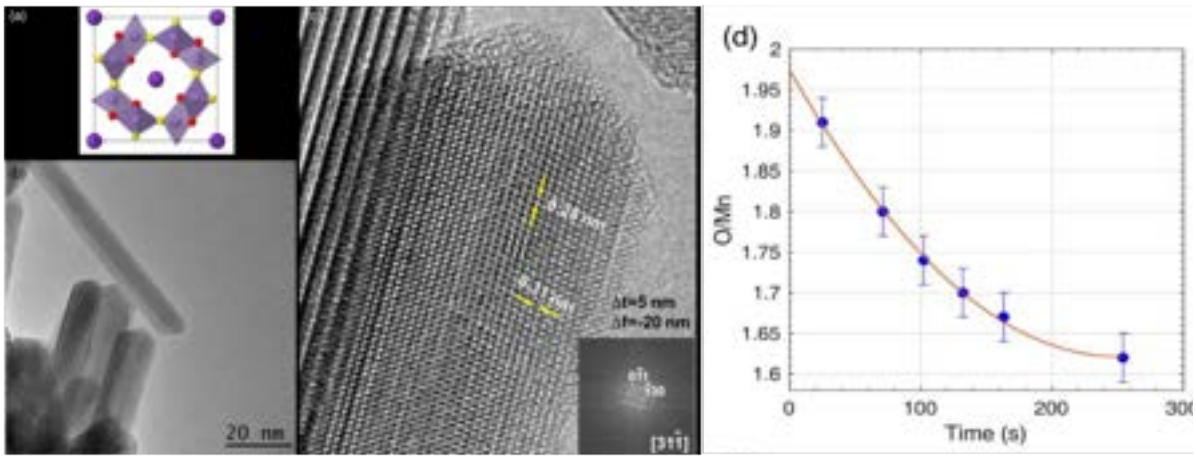

USE OF AUTOFLUORESCENCE AS A COMPLEMENTARY METHOD TO ASSESS DIFFERENCES IN ANATOMY AND STRUCTURAL DISTRIBUTION UNDERLYING EVOLUTIVE VARIATION IN COMMON BEAN SEED DISPERSALANATOMY

Ana M. Santos (Spain)[1]; Ana M. González (Spain)[2]; Juan De Dios Alché (Spain)[3]; Marta Santalla (Spain)[2]

1 - Centro de Instrumentación Científica, University of Granada; 2 - Grupo de Genética del Desarrollo de Plantas, Misión Biológica de Galicia—Consejo Superior de Investigaciones Científicas (MBG-CSIC); 3 - Estación Experimental del Zaidín, CSIC and

Abstract

Common bean is frequently used as a model plant for legume studies, however scarce information concerning the morphology of its pods and the relation of this morphology to the loss of seed dispersal and/or the pod string is available, in spite that they are key agronomic traits for legume domestication. Weakening of the dorsal and ventral dehiscence zones and the tensions of the pod walls are key features of pod tissues through dehiscence. Such tensions are attributed to the differential mechanical properties of lignified and non-lignified tissues and changes in turgor associated with fruit maturation. In the present report, we have studied the histological characteristics of the dehiscence zone of the ventral and dorsal sutures of the pod in two contrasting genotypes for the dehiscence and string, and we have compared different histochemical methods with autofluorescence. The secondary cell wall modifications of the ventral suture of the pod were clearly different between the PHA1037 genotype (dehiscence-susceptible and stringy) and the PHA0595 one (dehiscence-resistant and stringless). Thus, the susceptible genotype had cells of bundle caps arranged in a more easily breakable bowtie knot shape. The resistant genotype had a larger vascular bundle area and larger fibre cap cells (FCCs), and due to their thickness, the external valve margin cells were significantly stronger than those from PHA1037. These findings suggest that the FCC area, and the cell arrangement in the bundle cap, might be partial structures involved in the pod dehiscence of the common bean. When autofluorescence visualization methods were used, the dehiscent phenotype was quickly identified by the pattern at the ventral suture, allowing a better understanding of cell wall tissue modifications that took place along the bean's evolution, which had an impact on crop improvement. We propose the use of this simple autofluorescence detection protocol as a reliable method to identify secondary cell wall organization and its relationship to the dehiscence and string in the common bean [1].

Acknowledgments

We gratefully acknowledge the support and facilities of the Misión Biológica de Galicia (Consejo Superior de Investigaciones Científicas), the Microscopy Facilities of Centro de Instrumentación Científica (University of Granada), and the Estación Experimental del Zaidín-CSIC.

References

[1] Santos, A.M.; González, A.M.; De Dios Alche, J.; Santalla, M. Microscopical Analysis of Autofluorescence as a Complementary and Useful Method to Assess Differences in Anatomy and Structural Distribution Underlying Evolutive Variation in Loss of Seed Dispersal in Common Bean. Plants 2023, 12, 2212. https://10.3390/plants12112212

Keywords: Anatomy, autofluorescence, cell wall, legume, microscopy, Phaseolus vulgaris, pod

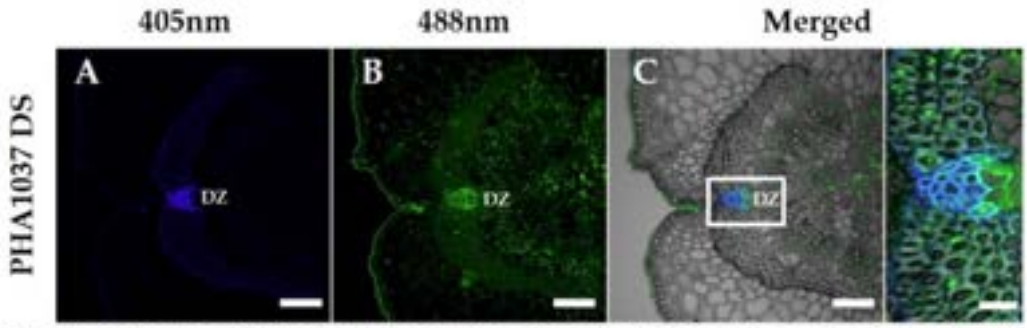

Transverse sections of dorsal sutures in the dehiscent and stringy genotype PHA1037 at 45 days after anthesis (DAA). Excitation at 405 nm with emissions in the range of 400–475 nm (blue, first column), and excitation at 488 nm with emissions in the range of 500–545 nm (green, second column). Images for each channel are maximal projections of five confocal optical sections. The merging of both fluorescent channels is shown in the third and fourth columns, where the bright field was used for anatomical reference. The fourth column shows an optical magnification of the central region of the sutures (white squares in the third column). Ventral suture: VS, dorsal suture: DS, dehiscence zone: DZ. Scale bars, 100 µm in panoramic views and 30 µm in the magnified regions.

MICROSCOPY VISUALIZATION OF SUPEROXIDE GENERATION BY RBOH IN THE REPRODUCTIVE ORGANS OF OLIVE (OLEA EUROPAEA L.)

Antonio J. Castro (Spain)[1]; María José Jiménez-Quesada (Spain)[1]; Elena Lima-Cabello (Spain)[1]; Juan De Dios Alché (Spain)[1]

1 – Plant Reproductive Biology and Advanced Imaging Laboratory (BReMAP), Estación Experimental del Zaidín (CSIC), Granada 18008

Abstract

Reactive Oxygen Species (ROS) are compounds derived from oxygen with important implications in biological processes in plants, some of them related to reproduction [1]. Among ROS, superoxide is the primary oxidant, since an array of other ROS are eventually derived from this anion [2]. Therefore, the analysis of the molecular systems able to generate this molecule and the cellular compartmentalization of these events is of paramount importance. In this work, we have used the fluorochrome $DCFH_2$-DA and the chromogenic substrate NBT in association with DPI (diphenyleneiodonium chloride, a specific inhibitor of Rboh enzymes generating superoxide in plants) to identify cell localization of DPI-dependent superoxide accumulation in olive reproductive tissues by using stereomicroscopy, confocal microscopy and transmission electron microscopy [3]. The incubation of the samples with $DCFH_2$-DA revealed a specific accumulation of ROS in the stigma surface. Two peaks of DPI-dependent superoxide accumulation were detected, a first one at developmental stage 2 (white bud), and a second peak, similar in intensity to the first, at stage 4 (dehiscent anther). On the other hand, such superoxide accumulation only appeared to be significant at the time of dehiscence in the developing anthers (stage 4). A similar organ location pattern was found for the superoxide anion by NBT reduction. The decrease of the signal after the addition of DPI suggests that the generation of superoxide is largely due to Rboh or other flavin oxidase activity. At the subcellular level, accumulation of $O_2^{\cdot-}$ was found in the plasma membrane of mature pollen and pollen tubes, as well as in the rough endoplasmic reticulum and mitochondria. In this case, the origin of this superoxide anion might be diverse and not only attributable to Rboh activity.

Acknowledgments

This research was funded by projects BFU-2016-77243-P, PID2020-113324GB-100 from MICINN/AEI, and grants P18-RT-1577 and PYC20-RE-009-CSIC-EEZ from Junta de Andalucía, all of them co-funded by ERDF program of the EU.

References

[1] Jiménez-Quesada MJ, Traverso JA, Alché JD (2016). NADPH oxidase dependent superoxide production in plant reproductive tissues. Front. Plant Sci. 7: 00359.

[2] Sharma P, Jha AB, Dubey RS, Pessarakli M (2012). Reactive oxygen species, oxidative damage, and anti-oxidative defense mechanism in plants under stressful conditions. J. Bot. 2012: 217037.

[3] Jiménez-Quesada MJ, Castro AJ, Lima-Cabello E, Alché JD (2022). Cell localization of DPI-dependent production of superoxide in reproductive tissues of the olive tree (*Olea europaea* L.). Oxygen 2: 79-90.

Keywords: Rboh, Superoxide anion, TEM, CLSM, Olive tree

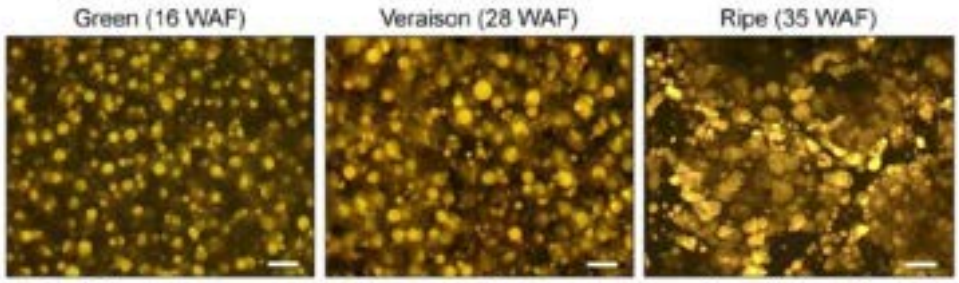

Figure 1. Lipid droplet accumulation dynamics during olive (cv. Picual) fruit development and ripening. From left to right, fluorescence microscopy photomicrographs of olive mesocarp 1 mm-width sections showing Nile red-stained LD (yellowish fluorescence) at three developmental stages: green (16 WAF, weeks after flowering), turning (28 WAF) and maturity (35 WAF). Bars, 50 µm.

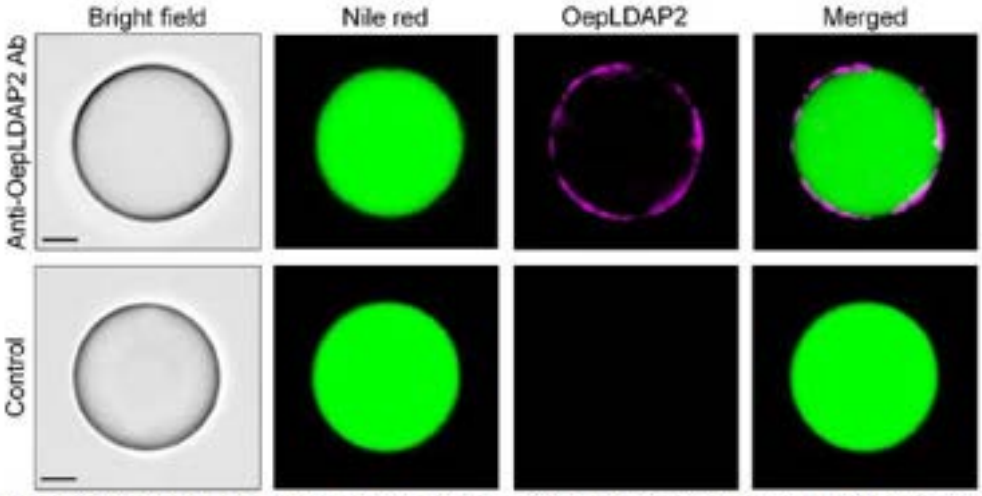

Figure 2. Confocal microscopy immunolocalization of OepLDAP2 protein on LD isolated from olive (cv. Picual) mesocarp cells. Upper panel, the OepLDAP2 protein (pink fluorescence) appears coating the surface of a Nile red-stained LD that is filled of neutral lipids (green fluorescence). Lower panel, negative control by omitting the anti-OepLDAP2 Ab. Bars, 10 µm.

LOCALIZATION OF 2S SEED STORAGE PROTEINS (SSPS) IN SEEDS OF OLIVE AND NUTS OF AGRICULTURAL/ALIMENTARY INTEREST.

Mohammed M'rani-Alaoui (Morocco)[1]; Antonio Jesús Castro (Spain)[2]; Elena Lima-Cabello (Spain)[2]; Adoración Zafra (Spain)[2]; Juan De Dios Alché (Spain)[2]

1 - Département de Biologie, Faculté des Sciences, Université Abdelmalek Essaâdi, Tétouan;
2 - Estación Experimental del Zaidín. CSIC

Abstract

The olive tree is an important economic crop in the Mediterranean area. Olive oil is usually obtained by using the whole fruit (olive) as the primary raw material. However, the olive seed is becoming a source of a differential oil and a unique flour, with increasing uses and applications in cosmetics, nutrition and health. Other seeds of alimentary interest include almond, walnut, cashew, pistachio, hazelnuts, chestnuts and others.

Accumulation of different types of SSPs (seed storage proteins) including 11S -“legumins”- and 7S -"conglutin-like”- proteins in the olive seed tissues has been reported before.

In the present work, detailed subcellular localization of 2S -“globulin-like proteins”- in the endosperm and embryo of a wide panel of nuts (and in the olive seed as a comparison) is described. For this purpose, samples of mature olive seeds of the Picual cultivar, and a wide panel of commercial crude nuts were processed for both LM/TEM immunolocalization of 7S proteins. Samples were fixed in a mix of paraformaldehyde/glutaraldehyde, and embedded in Unicryl resin (BBinternational) at low temperature. Immunolocalication of 2S proteins was performed either on thin sections (1µm) or ultrathin sections (70 nm) obtained using a Reichert-Jung ultramicrotome and picked up using glass slides or 200 mesh nickel grids coated with formvar, respectively. The sections were then sequentially treated with a blocking solution (5% (w/v) bovine serum albumin, 0.1% (v/v) Tween 20 in phosphate-buffered saline), a diluted (1:100) solution of an anti-2S antiserum (custom made antibody) in blocking solution, a 1:1000 solution of the secondary antibody (goat anti-rabbit IgG:Alexa 480 or :30 nm gold, respectively), and finally observed in a Nikon Ti-U inverted fluorescence microscope, or contrasted using a 5% (w/v) uranyl acetate alternative solution (Ted Pella INC. CA) and observed in a JEM-1011 (JEOL) transmission electron microscope, respectively. Negative control sections were treated as above but using preimmune serum instead of the anti-2S antiserum. Morphometric measurements were performed using the UTHSCSA ImageTool (version 3.00 for Windows) software.

Acknowledgments

This research was funded by projects PID2020-113324GB-100 and TED2021-130015B-C22 from MICIU/AGE, together with projects P18-RT-1577 and PYC2O REOO9CSIC. EEZ from Junta de Andalucía, all of them cofinanced by the FEDER program of the European Union.

Keywords: 2S, Cotyledon, Endosperm, Globulin, Histology, Immunolocalization, Olive, Oil bodies, Protein bodies, Seed Storage Proteins

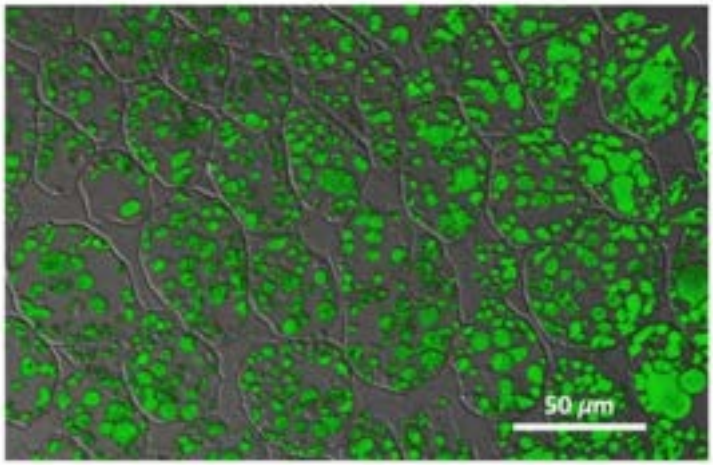

Transverse sections of pistachio seed endosperm showing immunolocalization of 2S ("globulin-like") seed storage proteins (green fluorescence), merged with transmitted light (differential interferential contrast). 2S proteins appear discretely located in protein bodies thoroughly present in the endosperm cells.

CELLULAR LOCALIZATION OF CARBONYLATED PROTEINS IN OLIVE (OLEA EUROPAEA L.) POLLEN BY FLUORESCENCE MICROSCOPY.

Salvador Priego (Spain)[1]; Elena Lima-Cabello (Spain)[1]; Antonio Jesús Castro (Spain)[1]; Juan De Dios Alché (Spain)[1]

1 – Estación Experimental del Zaidín. CSIC

Abstract

Understanding the mechanisms that govern pollen biology and plant reproduction is crucial to ensure optimal crop yield. Carbonylation (the addition of reactive carbonyl groups to biomolecules) is a post-translational modification that is essential for regulating gene expression and protein activity under normal conditions. Oxidative reactions induced by reactive oxygen species increase the level of carbonylation and produce irreversible cell damage. Carbonylated proteins and lipids have been extensively studied and associated with the onset or the progression of oxidative stress-related disorders. Nevertheless, their spatial distribution in either cells and tissues have been less investigated. In the present work, we have germinated olive (*Olea europaea* L.) pollen either under normal and enhanced oxidative stress conditions (with the addition of paraquat at several concentrations at the culture medium) and detected the location of carbonylated proteins using fluorescence microscopy. For this purpose, carbonyl compounds were derivatized with DNPH (2,4-Dinitrophenylhydrazine) and later treated sequentially with an anti-DNP antibody and an Alexa Fluor®488-conjugated secondary antibody. Samples were observed in a Nikon Ti-U inverted fluorescence microscope using a 488-diode source for excitation. Our results show that germinating pollen grains harbor basal levels of fluorescence (associated to carbonylation), which do not affect pollen viability. On the other hand, carbonylated species tend to accumulate in the cytoplasm of those pollen grains under oxidative stress, also leading to decreased viability. More detailed experiments are needed to understand what proteins are preciselycarbonylated and how that alters their function.

Acknowledgments

This research was funded by projects PID2020-113324GB-100 and TED2021-130015B-C22 from MICIU/AGE, all of them cofinanced by the FEDER program of the European Union. Salvador Priego was granted with a PhD fellowship from Junta de Andalucía (Spain).

Keywords: Carbonylation, olive, pollen, fluorescence

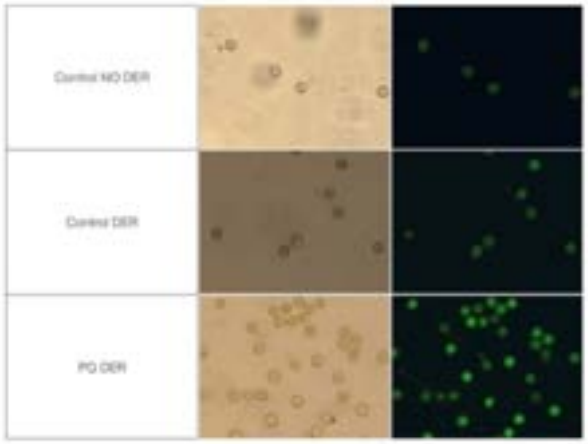

Detection of carbonylated proteins in pollen grains of olive (*Olea europaea* L.) cultured *in vitro*. Upper row: non-derivatized samples (negative control). Middle row: derivatized samples (positive control). Lower row: derivatized samples with enhanced production of ROS along in vitro culture (paraquat treatment). Note differential intensity of fluorescence in the pollen grains (higher intensity in the paraquat-treated samples compared to the remaining samples) whereas control samples show a basal fluorescence only.

INSIGHT INTO CHANGES IN EXTENSIN LOCALIZATION EVOKED BY GLOMUS SP. AND BACILLUS SP. IN DROUGHT-CULTIVATED POTATO

Agata Kućko (Poland)[1]; Juan De Dios Alché (Spain)[2]; Maciej Walczak (Poland)[3]; Jacek Karwaszewski (Poland)[4]; Kalisa Bogati (Poland)[3]; Małgorzata Kapusta (Poland)[5]; Emilia Wilmowicz (Poland)[4]

1 - Department of Plant Physiology, Institute of Biology, Warsaw University of Life Sciences-SGGW, Warsaw University of Life Sciences, Warsaw; 2 - Estación Experimental del Zaidín. CSIC; 3 - Chair of Environmental Microbiology and Biotechnology, Faculty of Biological and Veterinary Sciences, Nicolaus Copernicus University; 4 - Chair of Plant Physiology and Biotechnology, Faculty of Biological and Veterinary Sciences, Nicolaus Copernicus University; 5 - Laboratory of Electron Microscopy, Faculty of Biology, University of Gdańsk, 80-308 Gdańsk

Abstract

Drought affects the productivity of many crops, including potatoes (*Solanum tuberosum* L.). Tuber yield is associated with processes taking place in photosynthetically active tissues. Better tolerance to stress is guaranteed by the stability and proper architecture of plant cell wall. Additionally, plant strategy to cope with unfavorable conditions is related to the increasing strength and extensibility of cell wall. Extensins (EXTs) are a family of hydroxyproline-rich glycoproteins involved in the processes related to the improvement of the mechanical properties of cell wall. They are also responsible for the remodeling of its structure ensuring the extension of cells. There are studies supporting that EXTs increase tolerance to various stresses through anchoring polysaccharides. What is more, enriched in arabinose EXTs counteract dehydration under drought [1].

Nowadays, microorganisms producing beneficial compounds are used to help plants to increased tolerance against abiotic stress. One of them is bacteria - *Bacillus* or fungi, e.g. *Glomus* [2]. Presented study aimed to explore the differences in localization of EXTs in leaves of potatoes subjected to drought and the action of these microorganisms. Furthermore, we used specific monoclonal antibodies: JIM11 and JIM20 (Figure 1) recognized different EXTs epitopes: IgG2c and IgM, respectively [3].

Our research demonstrated that drought differentially regulates these epitopes' distribution. The stress caused the accumulation of EXTs recognized by JIM11 but negatively influenced EXTs detected by JIM20, which can be used as a great indicator of cell wall modification under drought. In turn, EXTs localization patterns in stressed plants that were pre-inoculated with *Glomus* sp. or *Bacillus* sp. support that both microorganisms modulate drought tolerance in potatoes.

We believe that our research contributes to a better understanding of drought responses and give hope for the improvement of crops yielding by plant-microbes interaction.

Acknowledgments

This research was partially funded by projects PID2020-113324GB-100 and TED2021-130015B-C22 from MICIU/AGE, both cofinanced by the FEDER program of the European Union.

References

[1] R Castilleux, B Plancot, M Ropitaux, A Carreras, J Leprince, I Boulogne, M-L Follet-Gueye, ZA Popper, A Driouich, M Vicré, J. Exp. Bot. **69** (2018) p. 4235-4247.

[2] E Wilmowicz, A Kućko, K Bogati, M Wolska, M Świdziński, A Burkowska-But, M Walczak, Front. Plant Sci. **13**(2022) 958004.

[1] R Castilleux, B Plancot, M Vicré, E Nguema-Ona, A Driouich, Ann. Bot. **127** (2021) p. 709-713.

Keywords: cell wall, crop, drought, extensins, JIM11 Ab, JIM20 Ab, potato

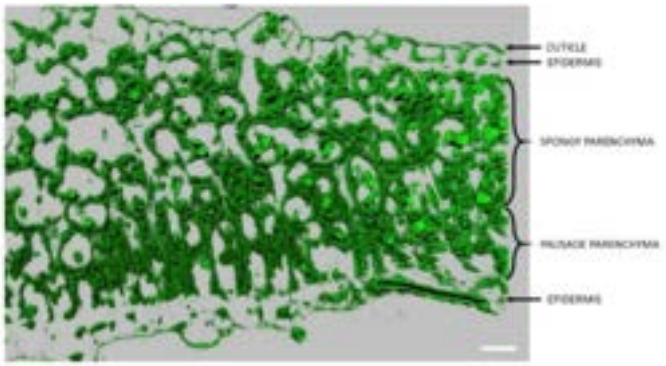

Figure 1. Representative image of immunodetection of extensin recognized by JIM11 antibody in the leaves of potato. Green labeling corresponds to the presence of extensin. Bar – 20 µm.

LIQUID PHASE ELECTRON CRYSTALLOGRAPHY ON LYSOZYME PROTEIN CRYSTALS AT ROOM TEMPERATURE

Sergi Plana-Ruiz (Spain)[1]; Alejandro Gómez-Pérez (Belgium)[2]; Monika Spano (France)[3]; Daniel L. Foley (United States of America)[4]; Joaquim Portillo-Serra (Spain)[2]; Edgar Rauch (France)[5]; Evangelos Grivas (Belgium)[2]; Partha Pratim Das (Belgium)[2]; Mitra L. Taheri (United States of America)[4]; Wai Li Ling (France)[3]; Stavros Nicolopoulos (Belgium)[2]

1 - Servei de Recursos Científics i Tècnics, Universitat Rovira i Virgili; 2 - NanoMegas SRPL; 3 - Université Grenoble Alpes, CEA, CNRS, IBS; 4 - Department of Materials Science and Engineering, Johns Hopkins University; 5 - SIMAP, Grenoble INP, Université Grenoble Alpes, CNRS,

Abstract

The characterization of proteins and their structural conformation is crucial for the understanding of the different mechanisms that organisms use to keep life going. In addition to X-ray crystallography and nuclear magnetic resonance, cryogenic transmission electron microscopy (cryo-EM) has been extensively and successfully applied and nowadays it has been established as an essential tool in the field of structural biology. However, the use of vitrified samples preserved at liquid nitrogen temperature limits the real-time observation of dynamics, and also raises the question if crystalline samples would have the same crystal structure as in their natural environment. This work tries to overcome this limitation by demonstrating how protein crystals can be encapsulated in their mother liquor for electron diffraction (ED) experiments in a transmission electron microscope (TEM) using a standard sample holder at room temperature.

Liquid samples are frequently isolated from the vacuum of the TEM by means of sophisticated liquid cells in the form of microfluidic chips fitted in specially designed holders[1]. They are highly versatile as they can give insights to inorganic[2] as well as biological specimens[3], yet their image resolution is ultimately limited by the scattering along the combined thickness of the liquid, sample, and the viewing windows. In this context, the use of graphene membranes to seal liquid pockets is preferred, the so-called graphene liquid cells (GLCs), as they are atomically thin but flexible and robust enough to keep the liquid encapsulated[4]. Here, we demonstrate how ED patterns of lysozyme crystals can be obtained up to 3 Å resolution using one-layer or three-layer graphene sheets supported by lacey C on Cu grids, as well as ultrathin continuous C films (3-4 nm in thickness) supported on Cu grids. The use of a very low-dose acquisition strategy and a hybrid-pixel direct electron detector is shown to be key to ensure the collection of statistically significant ED data prior to the crystallinity loss due to the electron beam illumination. The obtained ED patterns were indexed using a template-matching algorithm to prove that they belonged to the expected lysozyme crystal structure. The presented methodology provides a new way to explore crystallization dynamics in protein crystals and hydrated nanocrystals and serve to pave the way for liquid phase electron crystallography.

References

(1) Ring, E. A.; de Jonge, N. Microfluidic System for Transmission Electron Microscopy. *Microsc Microanal* **2010**, *16* (5), 622–629. https://doi.org/10.1017/S1431927610093669.

(2) Li, C.; Tho, C. C.; Galaktionova, D.; Chen, X.; Král, P.; Mirsaidov, U. Dynamics of Amphiphilic Block Copolymers in an Aqueous Solution: Direct Imaging of Micelle Formation and Nanoparticle Encapsulation. *Nanoscale* **2019**, *11* (5), 2299–2305. https://doi.org/10.1039/C8NR08922A.

(3) Peckys, D. B.; Macías-Sánchez, E.; de Jonge, N. Liquid Phase Electron Microscopy of Biological Specimens. *MRS Bulletin* **2020**, *45* (9), 754–760. https://doi.org/10.1557/mrs.2020.225.

(4) Cho, H.; Jones, M. R.; Nguyen, S. C.; Hauwiller, M. R.; Zettl, A.; Alivisatos, A. P. The Use of Graphene and Its Derivatives for Liquid-Phase Transmission Electron Microscopy of Radiation-Sensitive Specimens. *Nano Lett.* **2017**, *17* (1), 414–420. https://doi.org/10.1021/acs.nanolett.6b04383.

Keywords: Liquid Phase Electron Microscopy, Graphene Liquid Cells, Protein Electron Crystallography, Lysozyme

ZEISS VOLUTOME: VOLUME DATA ACQUISITION THROUGH AUTOMATED SECTIONING AND IMAGING

Abel Sainz, PhD,

Electron and X-ray Microscopy Specialist, Carl Zeiss

Abstract

New technologies and methods for 3D ultraresolution electron microscopy using SEM and focused ion beam SEM (FIB-SEM) have been emerging over the last two decades. ZEISS has been working together with scientists in neuroscience/connectomics, cancer research, developmental biology, plant biology, and other fields toward the shared goal of developing solutions for high-volume 3D electron microscopy (vEM). Also, many researchers are also showing success correlating data collected from light and/or X-ray microscopy.

The new ZEISS Volutome, an in-chamber ultramicrotome for ZEISS field emission scanning electron microscopes (FE-SEM) designed to image the ultrastructure of biological, resin-embedded samples in 3D over a large area, is presented. By activating the ZEISS patented Focal Charge Compensation (Focal CC), even the most charge-prone samples can be investigated without degrading image quality. Focal CC neutralizes charges directly at the block face with no compromise in signal-to-noise ratio or resolution.

ZEISS Volutome comes with ZEISS Volume BSD, the optimized detector for serial block-face imaging of resin-embedded biological samples. A new diode design and new electronics make this a highly sensitive detector specifically enhanced for the imaging with low acceleration voltages and fast scanning speeds.

ZEISS software combines the individual Volutome hardware components to make the serial blockface workflow smooth and easy-to-use. The cutting operation as well as the imaging process are controlled by ZEISS ZEN core. Once the data is collected and the pre-calculation is applied for stitching and z-stack alignment, the results can be visualized and processed with ZEISS arivis Pro.

LIPID DROPLET DYNAMICS AND LIPID DROPLET-ASSOCIATED PROTEIN (LDAP) SUBCELLULAR LOCALIZATION IN THE OLIVE (OLEA EUROPAEA L.) FRUIT DURING DEVELOPMENT AND RIPENING

Antonio J. Castro (Spain)[1]; José Manuel Martínez-Rivas (Spain)[2]; Juan De Dios Alché (Spain)[1]

1 - Plant Reproductive Biology and Advanced Imaging Laboratory (BReMAP), Estación Experimental del Zaidín (CSIC), Granada 18008; 2 - Department of Biochemistry and Molecular Biology of Plant Products, Instituto de la Grasa (CSIC), Seville 41013

Abstract

The olive tree (*Olea europaea* L.) has been cultivated for centuries for both oil and fruit production. Storage lipidsaccumulate in specialized cytoplasmic organelles called lipid droplets (LD) in the mesocarp cells of oleaginous fruits [1]. Understanding the biogenesis and function of olive LD and their associated proteins is essential to engineering this storage organelle in order to improve both oil production and quality. In this work, we investigated the accumulation dynamics of LD in the olive (cv. Picual) mesocarp cells during the development and maturation process by combining specific staining methods with fluorescence microscopy, as well as transmission electron microscopy (TEM). Young fruits at the “green” stage (16 WAF, weeks after flowering) contains numerous small LD scattered in the cytoplasm of mesocarp cells. As the fruit ripens, they become in close contact and fuse together, resulting in a few larger LD at the “turning” stage (28 WAF). Finally, at maturity (35 WAF), each mesocarp cell contains a single large LD that occupies almost the entire cell volume. We also observed an increasing gradient in the stored oil from the outer to the inner mesocarp layers, suggesting that oil accumulates from the inside during fruit ripening. At ultrastructural level, LD are bounded by a thin electron-dense coating that likely corresponds to the phospholipid monolayer that encircles the TAG matrix of LD. This coating is missing in zones where LD coalesce and appears discontinuous at the end of the maturation period.On the other hand, Lipid Droplet-Associated Proteins (LDAPs) have been described as the major LD proteins of oleaginous fruits like avocado [2]. Here, we studied the subcellular location of the most abundant lipid droplet-associated protein of the olive mesocarp, called OepLDAP2 (unpublished transcriptomic data). For this purpose, we isolated LD from olive (cv. Picual) mesocarp cells and carried out immunolocalization experiments by confocal microscopy using a specific anti-OepLDAP2 antibody. Our results showed that the OepLDAP2 protein is located on the surface of LD, as it was expected. Transmission electron microscopy experiments confirmed that this protein is specifically associated with cytosolic lipid droplets. Thus, no gold labeling was observed in the cell wall, extracellular junctions, the nucleus, the cytoplasm and other cell organelles like mitochondria and plastoglobuli-containing plastids.

Acknowledgments

This research was funded by projects AGL2017-84298-P and AGL2017-87871-R from MINECO/AEI, PID2020-113324GB-100 and TED2021-130015B-C22 from MICINN/AEI, and P18-RT-1577 from Junta de Andalucía, all of them co-funded by the ERDF program of the EU.

References

[1] AHC Huang (2018). Plant lipid droplets and their associated proteins: potential for rapid advances. Plant Physiol. 176: 1894-1918.

[2] PJ Horn, CN James, SK Gidda, A Kilaru, JM Dyer, RT Mullen, JB Ohlrogge, KD Chapman (2013). Identification of a new class of lipid droplet-associated proteins in plants. Plant Physiol. 162: 1926-1936.

Keywords: LDAP, Lipid droplet, Mesocarp, Olive tree

IT IS NOT EASY BEING GREEN: THE TECHNICAL PATH FOR THE ULTRASTRUCTURAL STUDY OF THE LOCOMOTORY APPARATUS OF THE MOSS PHYSCOMITRIUM PATENS

Ana Laura Sousa (Portugal)[1]; Sónia Gomes Pereira (Portugal)[1,3]; Alexander. J. Holmes (Portugal)[1,2]; Martin Schorb (Germany)[4]; Jörg D. Becker (Portugal)[5]; Mónica Bettencourt-Dias (Portugal)[1]; Erin M Tranfield (Portugal)[1]

1 - Instituto Gulbenkian de Ciência; 2 - Currently at: University of Cambridge, UK.; 3 - Currently at: University of Geneva, Switzerland; 4 - European Molecular Biology Laboratory; 5 - Instituto de Tecnologia Química e Biológica António Xavier, Universidade Nova de Lisboa

Abstract

Electron microscopy (EM) as a whole technique enables the ultrastructural studies of many samples from individual cells to full organisms. For the visualization of a single image under the electron beam, extensive time investment is made in technical preparation and several EM techniques often need to be applied until an image or model can be presented. The path is not always easy, and optimizations are commonly needed to avoid unintentional artifacts that can impact the final ultrastructural observation. This problem is even more pronounced when it comes to processing plant samples, such as the moss *Physcomitrium patens*, where there is a need to consider the existence of the cell wall, that provides rigidity and strength to cells, but also functions as a barrier for the chemicals needed to observe the ultrastructure using room temperature EM.

In this study, the challenge presented to our facility was the characterization of the locomotory apparatus of the moss *P.patens*, namely the de novo centriole assembly that is involved in the motility of the sperm cells during spermatogenesis. These sperm cells develop inside an antheridium located at the tip of the gametophore, a complex structure that contains leaves, rhizoids and both sexual organs (the antheridia and the archegonia). We addressed this question by combining the observations from Chemical Fixation, High-Pressure Freezing–Freeze Substitution, Correlative Light-Electron Microscopy (CLEM) and Electron Tomography.

Each of the different EM techniques helped to address different parts of the biological question. Chemical Fixation allowed to carefully identify the main stages of development and to do the initial ultrastructural characterization. High-Pressure Freezing – Freeze Substitution was used to confirm that the identified structures were not artifacts induced by chemical fixation and allowed a more accurate and detailed ultrastructural characterization of each structure. Electron Tomography gave three-dimensional models of the structures. CLEM helped to elucidate the protein composition of the sperm cells' locomotory apparatus and associate the light microscopy results with the structures observed by electron microscopy.

Overall, this work shows how complex the technical path in an EM study of a larger specimen can be and how crucial it is to keep optimizing and developing EM techniques that supports the answering of biological questions even when using bigger and more intricate specimens.

Keywords: Locomotory Apparatus, Physcomitrium patens, Chemical Fixation, High-Pressure Freezing–Freeze Substitution, Correlative Light-Electron Microscopy, Electron Tomography

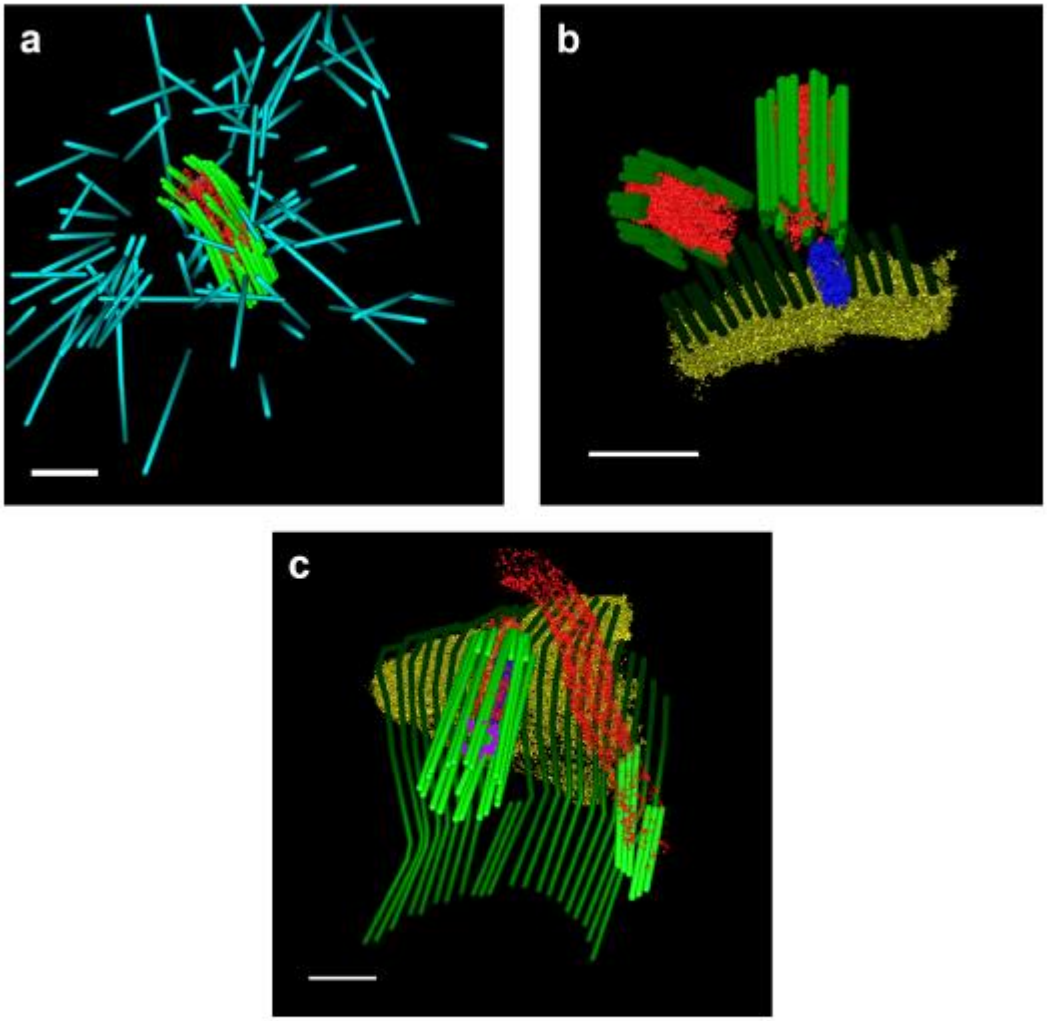

Figure 1: 3D models of different stages in centriole assembly and maturation in *Physcomitrium patens*. **a)** Bicentriole stage; **b)** Sister centrioles associated with the multilayered structure (MLS); **c)** Asymmetrical sister centrioles docked to the cell membrane, serving as basal bodies for ciliogenesis. Cyan – astral microtubules; Light green – centriolar microtubules; Red – Centriolar cartwheel; Dark green – microtubular spline of the MLS; Yellow – lamellar strip of the MLS; Magenta – ciliary transition zone. Scale-bars = 200nm. Adapted from: The 3D architecture and molecular foundations of de novo centriole assembly via bicentrioles (2021).

REAL-TIME DYNAMICS OF INFLUENZA A VIRUS TRANSCRIPTION: INSIGHTS FROM HIGH-SPEED ATOMIC FORCE MICROSCOPY

Rebeca Bocanegra (Spain)[2]; Shingo Fukuda (Japan)[3]; Diego Carlero (Spain)[1]; Borja Ibarra (Spain)[2]; Jaime Martín-Benito (Spain)[1]

1 – National Centre for Biotechnology; 2 - IMDEA Nanociencia Institute; 3 - WPI Nano Life Science Institute

Abstract

The Influenza A virus genome is composed of eight different single-stranded viral RNA (vRNA) segments assembled into viral ribonucleoprotein complexes (vRNP) in which the RNA polymerase (RNApol) binds to the 5' and 3' ends of the vRNA, while nucleoproteins (NPs) bind the remaining vRNA. The vRNP represents the minimal transcriptional machinery of influenza viruses, although its mechanism is not fully understood. Recent studies have proposed the so-called Processive Helical Track model (1), which suggests that vRNP undergoes conformational changes that allow RNApol to progressively access the entire template vRNA for copying, without disassembling the overall vRNP structure. This mechanism involves significant local restructuring of the vRNP, but the highly dynamic interactions between its components allow it to regain its initial structure after each transcription cycle, enabling it to perform several consecutive rounds of transcription. Monitoring these conformational changes is crucial for a better understanding of the mechanistic processes that take place during vRNA synthesis. Here, we aimed to address this challenge by following with High-Speed Atomic Force Microscopy (HS-AFM) the conformational dynamics of individual mini-recombinant vRNP (rRNP) (2) (3) during transcription. Our results support the Processive Helical Track model, showing reversible conformational changes in the rRNP and events of multiple consecutive rounds of such changes. In addition, we provide the first estimations of the average transcription rates of the RNApol within the rRNP complex and its modulation by NTP analogs that affect the structure of the nascent RNA.

References

[1] Coloma, R. et al. Nat Microbiol 5, 727–734 (2020).
[2] Coloma, R. et al. PLoS Pathog. 2009 Jun;5(6):e1000491
[3] Ortega J. J Virol. 2000 Jan;74(1):156-63

Keywords: transcription, influenza, virus, High Speed AFM

EXAMINING FLAGELLAR AND CELLULAR DIVISION DIVERSITY IN PROTISTS TO UNCOVER THE BASAL BODY (BB) CYTOSKELETON EVOLUTION

Luca Cirino (Italy)[1]; Mónica Bettencourt-Dias (Portugal)[1]

1 – Instituto Gulbenkian de Ciência

Abstract

The emergence of a microtubule-based cytoskeleton marked a turning point in eukaryotic evolutionary history, redefining fundamental cellular functions like motility, sensing, morphology, and division. Despite the cytoskeletal system's crucial importance, very little is known regarding its ancestral configuration, how the extant diversity originated, and what drivers shaped it. Basal Bodies (BBs), fundamental microtubule organizing centers providing the foundation of microtubular cytoskeletons and defining their spatial arrangement, may serve a critical role in answering these pending questions. The purpose of this work is to reconstruct the evolutionary history of the cytoskeletal system by determining BB morphological variations within eukaryotic lineages of particular interest. By serial sectioning transmission electron microscopy (TEM) and electron tomography, we will reconstruct 3D structures of BBs and associated cytoskeletal components from a wide array of phylogenetically diverse protists. As several targeted species exhibit multiple life stages, the same approach will also be applied to collect structural data regarding BBs structural changes throughout the diverse ontogenetic shifts. Altogether, these approaches will provide new insight into the evolution of a fundamental cellular component and potentially reveal fundamental forces guiding cellular evolution.

Keywords: Evolution, Basal Bodies, Microtubule Organizing Center, TEM, Tomography

ACCELERATING CRYO-TEM SAMPLE PREPARATION

Martin Suchánek

1 – Tescan Area Sales Manager

Abstract

Cryo-electron tomography (cryo-ET) has revolutionized structural biology by enabling the observation and characterization of biological samples at a molecular level in their near-native state. This technique provides an unprecedented level of structural detail, but it necessitates thin specimens (typically below 200nm) for effective electron beam penetration. Presently, the prevailing method for achieving such thinning involves Focused Ion Beam (FIB) milling. FIB instruments utilizing Gallium ion sources are widely employed, offering exceptional resolution and precise milling. However, the meticulousness of sample preparation becomes time-consuming, creating a bottleneck that restricts overall lab throughput.

Recently, there has been a surge of interest in adopting FIBs based on plasma ion sources to expedite cryo transmission electron microscopy (TEM) lamella preparation. Commonly employed ion sources include Xenon, Oxygen, and/or Argon. Among these options, Xenon stands out as the most suitable choice due to its highly focused beam profile, which facilitates precise lamella shaping and accelerates the milling rate.

In the lecture, we will delve into the practical advantages of optimized workflows, specifically focusing on on-grid lamella, waffle, and lift-out techniques, aimed at enhancing the speed and throughput of cryo-TEM lamella preparation. Furthermore, we will explore the TESCAN AMBER X cryo-plasma FIB-SEM as a robust and versatile workstation that serves as an indispensable tool for routine cryo-TEM sample preparation. This instrument not only excels in its primary function but also offers a remarkable range of additional capabilities, making it a comprehensive solution for various research needs.

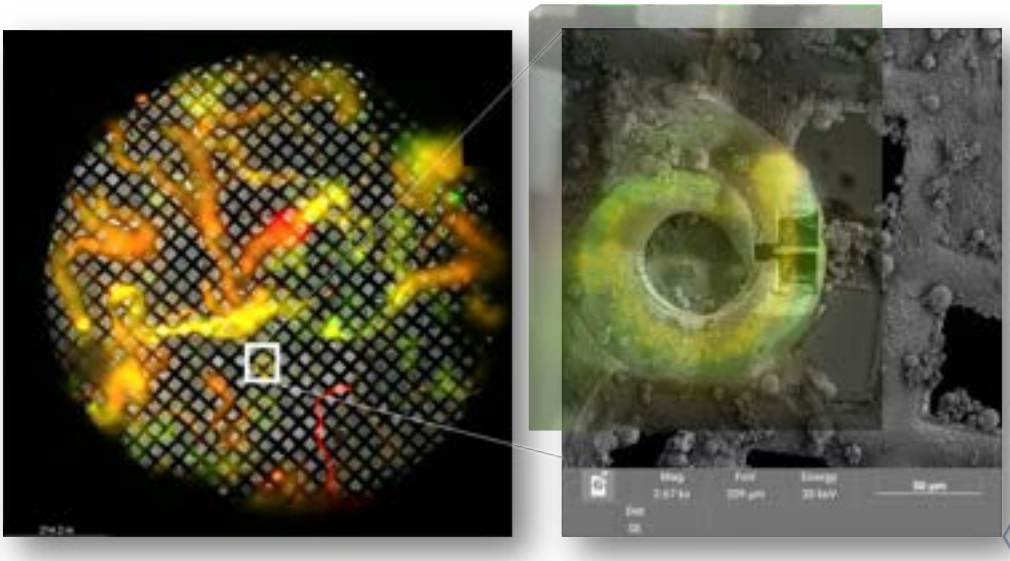

DECIPHERING A POTENTIAL TOXIC SYNERGY BETWEEN PERSISTENT ORGANIC POLLUTANTS

Ljiljana Puskar (Germany)[1]; Luisa Jordao (Portugal)[2]

1 – Helmholtz-Zentrum Berlin für Materialien und Energie GmbH, Infrared Beamline IRIS; 2 - Instituto Nacional de Saúde Dr Ricardo Jorge

Abstract

Plastic, massively used in everyday life, inevitably accumulates in the environment, becoming a persistent pollutant due to its reduced and/ or extremely slow recyclability[1]. Plastic particles in the micro and nano range, known as micro (MP) and nanoplastics (NP), respectively represent a huge ecotoxicological challenge. Due to their high surface areas, they might ad/absorb other persistent pollutants with similar chemical properties, such as polycyclic aromatic hydrocarbons (PAHs), with unpredictable effects on persistence and distribution in the environment[2]. MPs/NPs, with or without pollutants ad/absorbed, could enter the trophic chain at the level of invertebrates, inflicting toxicological effects through all levels of the ecosystem[3].

Polystyrene MPs and PAHs previously found in water samples (e.g. fluoranthene, phenanthrene)[4] and known to be adsorbed by MPs (Pyrene, benzo(a) pyrene)[5] will be used in the study. PAH's mixtures will be used to mimic environmental samples and single compounds will be used in order to understand the individual contribution of each compound for the observed toxic effect. This experimental approach will also allow to evaluate a potential synergy between compounds with effect on toxicity. Since PAHs and MPs have similar chemical properties, they are known to adsorb to each other. We will use PAHs adsorbed to MPs to test higher concentrations of PAHs (not soluble in aqueous solutions such as cell culture medium) and to document the intracellular distribution of adsorbed versus free PAHs. Concerning MPs only one material will be used at this stage. Polystyrene was selected because it is commercially available in spheres suitable for internalization by HepG2 cells and was previously isolated from environmental samples [4]. This study could contribute to identify differences in toxicity and contribute to the elucidation of the underlying toxicity mechanisms using molecular biology protocols, light/electron microscopy and FTIR micro/spectrometry.

Acknowledgments

Infrared spectroscopy measurements were carried out at the IRISbeamline at the BESSY II electron storage ring operated by the Helmholtz- Zentrum Berlin für Materialien und Energie (Proposals No 231-11744-ST/2022).

References

1. Kumar,P; Lee, J; Brown, RJC, Kim, K. Micro- and nano-plastic pollution : Behavior, microbial ecology and remediation technologies. *J. Clean. Prod.*, 2020,125240. doi.org/10.1016/j.jclepro.2020.125240

2. Camacho, M; Herrera, A; Gómez, M; Acosta-Dacal, A; Martínez, I; Henríquez-Hernández, LA; Luzardo, OP. Organic pollutants in marine plastic debris from Canary Islands beaches. Sci Total Environ. 2019 ,662:22-31. doi: 10.1016/j.scitotenv.2018.12.422.

3. Luo, H; Liu, C; He, D; Sun, J; Li, J; Pan, X. Effects of aging on environmental behavior of plastic additives: Migration, leaching, and ecotoxicity. *Sci Total Environ.* 2022, 849:157951. doi:10.1016/j.scitotenv.2022.157951.

4. Raposo, A; Mansilha, C; Veber, A; Melo, A; Rodrigues, J; Matias, R; Rebelo, H; Grossinho, J; Cano, M; Almeida, C; Nogueira, I; Puskar, L; Schade, U; Jordao, L. Occurrence of polycyclic aromatic hydrocarbons, microplastics and biofilms in Alqueva surface water at touristic spots.***Sci Total Environ.*** 2022, 13:157983. doi: 10.1016/j.scitotenv.2022.157983.

5. José, S & Jordao, L, Exploring the interaction between microplastics, polycyclic aromatic hydrocarbons and biofilms in freshwater. *Polycycl. Aromat. Compd.* 2020,1–12. doi.org/10.1080/10406638.2020.1830809.

Keywords: Polycyclic aromatic hydrocarbons (PAHS), Microplastics, Freshwater, Microscopy

Key benefits:

- ✓ **Perform large area – up to 1mm – high throughput FIB milling** using the high beam currents of the Plasma FIB
- ✓ **Prepare microsamples without risk of Ga implantation** thanks to the inert Xe ions
- ✓ **Investigate the widest range of materials using the ultra-high resolution imaging and nanoanalysis** capabilities of our BrightBeam™ field-free UHR-SEM column
- ✓ **Accelerate your 2D and 3D multi-modal characterization workflows** using our unique analytical geometry setup and smart beam spot optimization routines
- ✓ **Navigate to regions of interest quickly and safely** by utilizing extended field of view in the live SEM image together with our unique 3D chamber model for collision protection
- ✓ **Streamline work for everyone in the multi-user lab** thanks to our easy-to-use, modular Essence™ software

TESCAN

TESCAN AMBER X

A unique combination of Plasma FIB and field-free UHR SEM for the widest range of multiscale materials characterization applications

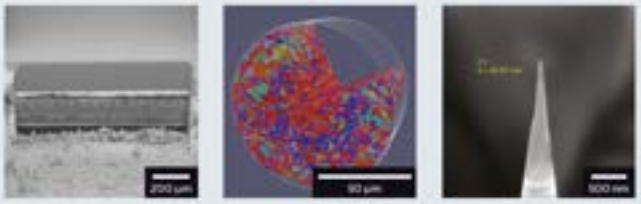

- 1 mm cross-section through a Li-ion battery electrode
- Large-volume 3D EBSD analysis
- Ga-free APT sample preparation

For more information

CONTACT US

Dias de Sousa

INSTRUMENTAÇÃO ANALÍTICA E CIENTÍFICA, S.A.

NenoVision

Next level of imaging

LiteScope

AFM-in-SEM for In-Situ Correlative Microscopy

We merge the forces of AFM and SEM

Key technology benefits

1. **Complex and correlative sample analysis**

Unique CPEM technology enables **simultaneous acquisition of AFM and SEM channels** and their seamless **correlation into 3D** images.

2. **In-situ sample characterization**

In-situ conditions inside the SEM ensure sample analysis at the **same time**, in the **same place** and under the **same conditions**.

3. **Precise localization of the region of interest**

Extremely precise and time-saving approach **uses SEM to navigate the AFM tip** to the region of interest, enabling its fast & easy localization.

For more information

CONTACT US

Dias de Sousa

INSTRUMENTAÇÃO ANALÍTICA E CIENTÍFICA, S.A.

MATERIAL SCIENCES

FAST 4D STEM WITH ARINA HYBRID-PIXEL DETECTOR

Daniel Stroppa (Switzerland)[1]; Matthias Meffert (Switzerland)[1]; Christoph Hoermann (Switzerland)[1]; Pietro Zambon (Switzerland)[1]; Luca Piazza (Switzerland)[1]

1 – DECTRIS

Abstract

Electron detection technology has been evolving over the last few years and improving TEM characterization in both Materials Sciences and Life Sciences, particularly when beam-sensitive samples are involved [1]. The hybrid-pixel detector (HPD) concept [2] has the distinctive advantage of a flexible design with respect to the sensor material and electronics, allowing the direct electron detection and counting optimization for a range of TEM experimental parameters (such as electron energy) and different applications.

Building on its HPD technology for X-ray detectors, DECTRIS fine-tuned its design to enable the precise detection of electrons. Its most recent development is an application-specific integrated circuit (ASIC) designed to allow read-out rates above 100 kHz and to perform electron counting up to 10 pA beam current per detector pixel with zero read-out noise [3].

ARINA detector combines this newly-designed ASIC with a flexible choice of sensor materials, an easy-to-use application programming interface (API), and a detector retraction mechanism, making it fit to most TEMs with electron energies from 30 to 300 keV and 4D STEM experiments requirements. Initial tests show that ARINA is suitable for flexible virtual STEM imaging with dwell time below 10 µs, allowing for flexible differential phase contrast (DPC) and ptychography with atomic resolution, and electron diffraction experiments with high dynamic range for crystal phase/orientation mapping.

Acknowledgments

We thank Mingjian Wu, Erdmann Spiecker, Phillip Pelz, and Benjamin Apeleo Zubiri at the Friedrich-Alexander-Universität in Erlangen, for the application tests concept, execution, and data analysis. We thank Anton Gladyshev and Christoph Koch at Humboldt University of Berlin and Colin Ophus at Lawrence Berkeley National Laboratory for their support on data analysis.

References

[1] A. R. Faruqi et al., Nucl. Inst. Meth. Phys. Res. A **878** 180-190 (2018)
[2] M. Bochenek et al. IEEE Trans Nucl Sci **65** (6), 1285-1291 (2018).
[3] P Zambon et al., Nucl. Inst. Meth. Phys. Res. A **1048** (2023).
[4] C. Ophus et al., Microsc. Microanal. 28, 390-403 (2022).

Keywords: TEM, 4D STEM, DPC, ptychography, orientation mapping

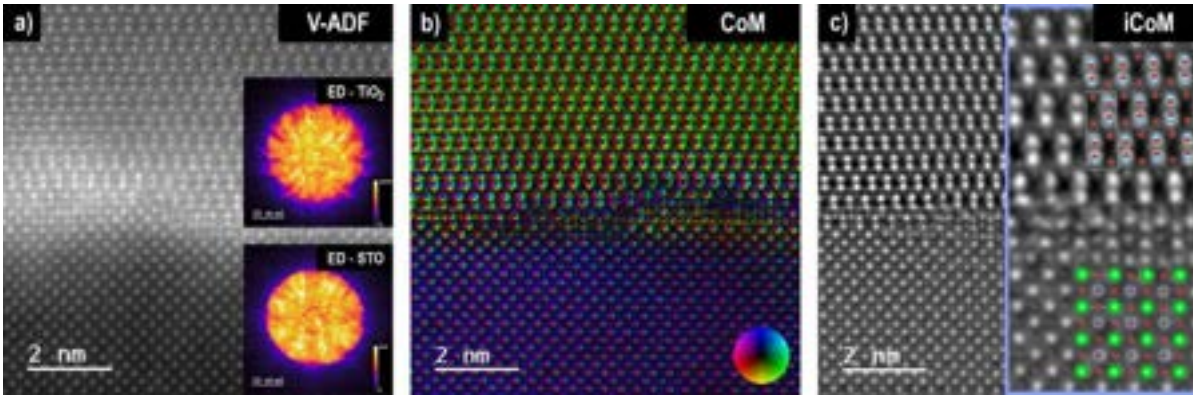
a)
V-ADF
ED - TiO_2
ED - STO
2 nm
b)
CoM
2 nm
c)
iCoM
2 nm

HOW TO OPTIMIZE TEM LAMELLA PREPARATION USING BROAD ION MILLING SYSTEM

Daniel Monville (France)[1]

1 – AMETEK SAS – GATAN – EDAX

Abstract

Broad ion milling system is a well-known and established technique for preparing TEM Lamella. Over the last decade, FIB (Focus Ion Beam) technique became a first-choice technique due to its capacity of precise area selection. However, this technique is costly (price and time) and generate artifacts, which are more and more visible thanks to the significant improvements of TEM performances and analysis, so that the preparation could be the limit. We will cover the different factors influencing ion milling and how we can combine both of these techniques (Broad and focus beam) to save time and money and get better lamellas free from artifacts.

TEM ANALYSIS OF ALTERNATIVE RU-W BARRIER LAYERS FOR CU METALLIZATION

Bruno M.C. Oliveira[1], R.F. Santos[1], P.J. Ferreira[2,3,4] , M F Vieira[1]

1 – INEGI, Dept. of Metallurgical and Materials Engineering, University of Porto, Portugal; 2 - Materials Science and Engineering Program, University of Texas at Austin, Austin, USA [3] International Iberian Nanotechnology Laboratory, Braga, Portugal; 3 - Instituto Superior Técnico, Lisboa, Portugal.

Abstract

Continuous development of modern circuitry entails state of the art studies of the physical properties of the structures used, seeing as the industry is currently in the nanometric range for its smallest components. One type of structure being pushed to the limits of the materials used is the barrier layers, which are responsible for inhibiting atomic diffusion from the interconnect layers to the neighboring layers. As miniaturization progresses, however, the electrical performance of the materials used until this moment has peaked, and as such there is a push to find materials compatible with modern requirements. Ru-W has been studied as a potential replacement for the commonly used TaN layers, as it provides good electrical resistivity coupled with a processing range compatible with heat treatment.

This work seeks to analyze the microstructural effect of a vacuum annealing treatment on the atomic mobility of 40 nm Cu layers deposited over 20 nm Ru-W barrier layers, by resorting to TEM microscopy of FIB prepared lamellae.

CHARACTERIZATION OF A HIGH-CR WHITE CAST IRON WITH TIC AND WC-MMCS SURFACE REINFORCEMENTS

A.B. Moreira[1,2], L.M.M. Ribeiro[1,2], M.F. Vieira[1,2]

1 – Department of Metallurgical and Materials Engineering, University of Porto, Porto, Portugal; 2 - INEGI - Institute of Science and Innovation in Mechanical and Industrial Engineering, Porto, Portugal.

Abstract

Ferrous alloys locally reinforced by carbide particles are promising materials for wear resistance applications. The local reinforcement provides high wear resistance, while the bulk cast iron offers high strength and toughness. For this reason, this grade of material is of increasing importance in the oil, gas and mining industries. Considerable attention has been directed towards techniques in which the reinforcing phase is formed during casting or previously manufactured by ex-situ methods and incorporated into the molten metal [1-3].

To produce the reinforced specimens, mixtures of Ti, Al and graphite powders were produced for the TiC system, and WC and Fe powders for the WC system. The powders were mixed and homogenised in a shaker mixer for 7 hours, and the binder was added afterwards. The mixtures were cold pressed in a metallic mould with a pressure of 70 MPa. The placement of the compacts in the mould cavity and the high-Cr white cast iron pouring were the final steps. The mechanical response of reinforced zones and the base metal was evaluated by microabrasion and hardness tests. To understand the effect of localized reinforcement on material performance, the microstructure of the composites and bonding interfaces was characterised using XRD, SEM/EDS, EBSD and TEM techniques.

Regarding the TiC system, the microstructural characterisation shows a non-uniform distribution of TiC particles in the reinforced matrix. The average hardness of the metal matrix composite is 797 HV 30, corresponding to a 34% increase compared to the hardness of the base metal. Concerning the WC system, a homogeneous and random distribution of the WC particles in the reinforced matrix was observed. The average hardness of the composite is 721 HV 30, a 47% increase in hardness compared to the base metal.

The microstructural characterisation and mechanical properties results allow us to state that this fabrication technique shows great potential for industrial application.

References

[1] Moreira, A. B., Ribeiro, L. M., & Vieira, M. F. (2021). Production of TiC-MMCs Reinforcements in Cast Ferrous Alloys Using In Situ Methods. *Materials*, *14*(17), 5072.

[2] Olejnik, E., Sobczak, J. J., Szala, M., Kurtyka, P., Tokarski, T., & Janas, A. (2022). Dry sliding, slurry abrasion and cavitation erosion of composite layers reinforced by TiC fabricated in situ in cast steel and gray cast iron. *Journal of Materials Processing Technology*, *308*, 117688.

IN SITU OBSERVATIONS REVEAL THE FIVE-FOLD TWIN-INVOLVED GROWTH OF GOLD NANORODS BY PARTICLE ATTACHMENT

Leonard Francis (Portugal)[1]

1 – International Iberian Nanotechnology Laboratory

Abstract

Crystallization plays a critical role in determining crystal size, purity and morphology. Therefore, uncovering the growth dynamics of nanoparticles (NPs) atomically is important for the controllable fabrication of nanocrystals with desired geometry and properties (1-7). Herein, we conducted in situ atomic-scale observations on the growth of Au nanorods (NRs) by particle attachment within an aberration-corrected transmission electron microscope (AC-TEM). The results show that the attachment of spherical colloidal Au NPs with a size of about 10 nm involves the formation and growth of neck-like (NL) structures, followed by five-fold twin intermediate states and total atomic rearrangement. The statistical analyses show that the length and diameter of Au NRs can be well regulated by the number of tip-to-tip Au NPs and the size of colloidal Au NPs, respectively. The results highlight five-fold twin-involved particle attachment in spherical Au NPs with a size of 3–14 nm, and provide insights into the fabrication of Au NRs using irradiation chemistry (8,9).

References

[1] Francis Leonard Deepak et al. Cryst. Growth, 2016, 16, 7256.
[2] Francis Leonard Deepak et al. ACS Nano 2017, 11, 5590.
[3] Francis Leonard Deepak et al. Adv. Sci., 2018, 1700992; DOI:10.1002/advs.201700992.
[4] Francis Leonard Deepak et al. Nanoscale Horiz, 2019, 4, 1302.
[5] Francis Leonard Deepak et al. J. Phys. Chem. Lett., 2018, 9, 961.
[6] Francis Leonard Deepak et al. Chem Comm, 2020, 56, 4765.
[7] Francis Leonard Deepak et al. Adv. Sci., 2019, 6, 1802131.
[8] Francis Leonard Deepak et al. Chem. Rev., 2022, 122, 16911.
[9] Francis Leonard Deepak et al. Nanomaterials 2023, 13, 796.

Keywords: in situ observation, Au nanorod, particle attachment, transmission electron microscopy, crystal growth

CUTTING EDGE SOLUTIONS FOR TIME RESOLVED IN-SITU MICROSCOPY

G. Brunetti (France)[1]

1 - JEOL (EUROPE) SAS – Espace Claude Monet – 78290 Croissy-sur-Seine (France)

Abstract

Since 1949, JEOL's legacy has been one of the most remarkable innovations in the development of instruments used to advance scientific research and technology. JEOL has 70 years of expertise in the field of electron.

This presentation will be focused on the cutting edge development based on ultrafast shutter and laser injection inside the TEM column. Recently JEOL acquire IDES company and start developing technologies for transmission electron microscopes. IDES is a leader and pioneer in the field of Ultrafast and Dynamic TEM, specializing in pulsed lasers and high-speed electrostatic beam blanking and deflection technologies. these products add time resolution to the TEM's exceptional spatial resolution enabling new applications and the exploration of the dynamics of specimens across a range of very fast time scales. Here is a non exhaustive list of the innovation we will present: EDM Basic (Electrostatic Dose Modulator) / Programmable STEM with EDM Synchrony / Luminary Micro Compact Specimen Photoexcitation System.

Keywords: time resolved microscopy; STEM detectors; in-situ; dose modulation; laser

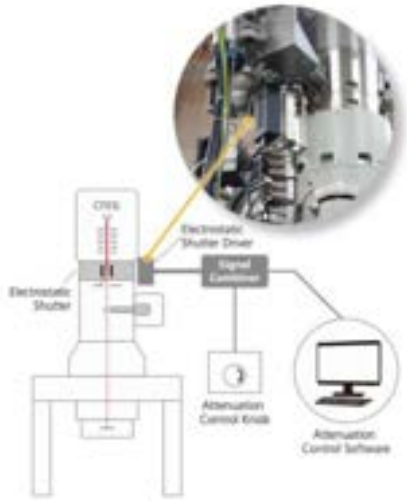

Figure 1. EDM: Electron Dose Modulator.

Figure 2. Luminary Micro: Compact Specimen Photoexcitation System

ADVANCES IN THE INVESTIGATION OF THE STRENGTHENING MECHANISM IN THE METAL MATRIX NANOCOMPOSITES

Sónia Simões[1,2]

1 - Faculty of Engineering of the University of Porto, R. Dr. Roberto Frias, 4200-465 Porto, Portugal
2 - INEGI/LAETA - Institute of Science and Innovation in Mechanical and Industrial Engineering, R. Dr. Roberto Frias, 4200-465 Porto, Portugal

Abstract

The development of metal matrix nanocomposites (MMNCs) has been a focus of attention by the scientific community in recent years. The most promising reinforcements are the carbon-based nanomaterials, since they have significantly improved properties, exceeding those of composites containing micro-scale reinforcements [1]. Nevertheless, the full potential of this type of reinforcement is compromised due to the need for knowledge about the effects of its introduction in the metal matrices. The improvement in the mechanical properties of the MMNCs results from several contributions of strengthening mechanisms, which can occur simultaneously and are difficult to identify separately [2-4]. A microstructural characterization at different scales is essential to identify the strengthening mechanisms.

In this context, this investigation aims to show the recent advances in the investigation of the strengthening mechanisms in the metal matrix nanocomposites. Aluminum powders and multi-walled carbon nanotubes (MWCNTs) were dispersed and mixed in one step by ultrasonication in isopropanol for 15 min. The mixtures were then uniaxially pressed with 300 MPa and pressureless sintered at 640 ºC for 90 min in a vertical furnace under a vacuum of 10^{-2} Pa. Microstructural characterization of the samples was performed by scanning and transmission electron microscopy (SEM and TEM) and electron backscatter diffraction (EBSD).

The reinforcement effect occurs due to several strengthening mechanisms that act simultaneously. For the Al-CNT nanocomposites produced by ultrasonication as a dispersion/mixture technique, the observed improvement in the mechanical properties of nanocomposites can be attributed to the load transfer from the matrix to the CNTs. The strain hardening and the second-phase hardening can also strengthen the nanocomposites.

References

[1] Kainer, K., Metal Matrix Composites: Custom-Made Materials for Automotive and Aerospace Engineering, Wiley-VCH Verlag GmbH & Co, 2006.
[2] Chen, B., Li, S., Imai, H., Jia, L., Umeda, J., Takahashi, M. and Kondoh, K., Load transfer strengthening in carbon nanotubes reinforced metal matrix composites via in-situ tensile tests. Composites Science and Technology, 2015, 113: p. 1-8.
[3] Choi, H.J., Shin, J.H. and Bae, D.H., Grain size effect on the strengthening behavior of aluminum-based composites containing multi-walled carbon nanotubes. Composites Science and Technology, 2011, 71(15): p. 1699-1705.
[4] Mokadad, F., Chen, D.L., Liu, Z.Y., Xiao, B.L., Ni, D.R. and Ma, Z.Y., Deformation and strengthening mechanisms of carbon nanotube reinforced aluminium composites. Carbon, 2016, 104: p. 64-77.

SPECTRA 300 (S)TEM: A NEW TOOL FOR MATERIALS SCIENCE RESEARCH AT JEMCA IN ALBA SYNCHROTRON

Bernat Mundet (Spain)[1]; Jordi Arbiol (Spain)[1]; Belén Ballesteros (Spain)[1]

1 - Institut Català de Nanociència i Nanotecnologia (ICN2)

Abstract

The integration of electron microscopes with synchrotrons has been a growing field of research and development in the recent years. The combination of these two powerful techniques has been pursued by scientists and engineers to enhance the capabilities and expand the applications of both instruments. The integration of these techniques facilitates breakthroughs in various scientific fields, including materials science, nanotechnology, biology, and energy research. With these ideas in mind, several institutions (ICN2, ICMAB, CSIC, UAB, IBMB, CRG, IRB and ALBA) have collaborated together in order to create the Joint Electron Microscopy Center at ALBA (JEMCA), in the ALBA synchrotron, which is one of the funding members of e-DREAM.1 Up to now, two high-end transmission electron microscopes have been already installed - a Thermofisher Glacios cryo-TEM and a Thermofisher Spectra 60-300kV -, together with a focus ion beam Thermofisher Helios 5UX, while a third (S)TEM (devoted to in-situ experiments) will also be installed in the following years. Besides the researchers belonging to those institutions, external users will also have the opportunity to access this equipment through competitive open calls that will be periodically announced in the ALBA website.

The installed Spectra 300 is equipped with a double aberration corrector, a thermally-assisted field emission gun (X-FEG) with monochromator, a pixelated EMPAD detector, a 16-segment panther detector for differential phase contrast acquisitions, a highsensitivity, windowless Super-X EDX detector system and a Continuum K3 Gatan Energy Filter with a CMOS and a retractable K3 direct-detection electron camera. This instrument is very versatile as it can be operated at 4 different high-tensions (60kV, 80kV, 200kV and 300kV), providing ultimate spatial and energy resolution: below 25meV (at 60kV) and 50pm (at 300kV). In this contribution, I will present the JEMCA infrastructure, I will describe the experimental possibilities offered by this new tool, showing some preliminary results obtained during the commissioning period, and also I will show how external users can apply to exploit it for their own research.

Acknowledgments

We acknowledge funding from Generalitat de Catalunya 2021SGR00457.We also acknowledge the Advanced Materials programme supported by MCIN with funding from European Union NextGenerationEU (PRTR-C17.I1) and Generalitat de Catalunya. This research is part of the CSIC program for the Spanish Recovery, Transformation and Resilience Plan funded by the Recovery and Resilience Facility of the European Union, established by the Regulation (EU) 2020/2094 and “ERDF A way of making Europe”, by the “European Union”. ICN2 is supported by the Severo Ochoa program from Spanish MCIN / AEI (Grant No.: CEX2021-001214-S) and is funded by the CERCA Programme / Generalitat de Catalunya. We acknowledge support from CSIC Interdisciplinary Thematic Platform (PTI+) on Quantum Technologies (PTI-QTEP+). We acknowledge support from EU HORIZON INFRA TECH 2022 project IMPRESS (Ref.: 101094299) and the Horizon Europe call HORIZON-INFRA-2021-SERV-01 project ReMade@ARI under grant agreement number 101058414.

References

R. Ciancio, et al., e-DREAM: the European Distributed Research Infrastructure for Advanced Electron *Microscopy. Microscopy and Microanalysis*, 28, 2900 (2022)

Keywords: STEM, Aberration-corrected, Infraestructure, advanced characterization, EDX, EELS

PHASE AND COMPOSITION MAPPING OF GENERATION 3B HIGH-ENERGY-DENSITY LINIXCOYMNZO2 BATTERY CATHODES WITH TRANSMISSION ELECTRON MICROSCOPY

C. F. Almeida Alves (Portugal)[1]; R. Ferreira (Portugal)[1]; S. Calderon V. (United States of America)[2]; A. Manthiram (United States of America)[3]; P. J. Ferreira (Portugal)[1,3,4]

1 - International Iberian Nanotechnology Laboratory; 2 - Department of Materials Science and Engineering, Carnegie Mellon University; 3 - Materials Science and Engineering Program, University of Texas at Austin; 4 - Mechanical Engineering Department and IDMEC, Instituto Superior Técnico, University of Lisbon.

Abstract

LiNixCoyMnzO2 (NCM), one of the most common cathode battery materials, exhibits a specific capacity and operating voltage comparable to LiCoO2, while being less toxic, thus representing the new generation of Li-ion batteries (LIBs). It is reported that NCM is composed of a mixture of LiMO2/ Li2MnO3 layers (where M=Ni, Co or Mn). LiMO2 is associated with a trigonal (R3m) phase whereas Li2MnO3 is associated with a monoclinic (C2/m) phase being responsible for storing and providing Li+ during Li-extraction of LiMO2. Nevertheless, these layered materials exhibit a large degree of cation disorder, and hence, Ni exchanges with Li in the Li2MnO3 layer, which disrupts the Li+ pathways and creates a continuous MO2 layer, lowering the Li mobility, deteriorating the cycling performance. So far, all these phenomena were studied in single-crystalline particles. However, at the industrial scale, this process results in porous micrometer polycrystalline particles, where the primary micron size particles possess a very complex microstructure, in particular an agglomeration of many nano sized particles, porosity, as well as chemical and phase heterogeneity.

In this regard, this work aims to fundamentally understand the changes in chemical distribution as a function of Ni content in polycrystalline NCM cathode materials. In particular, the chemical composition and structure of porous micrometer polycrystalline particles with Ni compositions ranging from 0.70 up to 0.90 wt. % were investigated using FIB-SEM, aberration-corrected STEM, EDS mapping, and precession electron diffraction. Slice-and-view SEM/FIB analysis revealed a geode-like morphology, independently of the composition. Yet, as the Ni content increases, the particle porosity decreases. STEM-EDS revealed variations in chemical composition across a single particle, in particular Ni content. Despite precession electron diffraction results suggesting the presence of only one crystal structure, atomic-resolution STEM images revealed that variations in the composition may be related to variations in orientation within a single crystalline grain

Keywords: Li-ion batteries; Slice and View FIB tomography; STEM-EDS; Precession electron diffraction

ON THE ACCURACY OF ATOMIC-RESOLUTION DPC-STEM MEASUREMENTS

Rafael V. Ferreira (Portugal)[5,6]; Sebastian V. Calderon (United States of America)[1]; Ricardo M. Ribeiro (Portugal)[2]; Deji Akinwande (United States of America)[3,4]; Paulo J. Ferreira (Portugal)[4,5,6]

1 - Department of Materials Science and Engineering, Carnegie Mellon University; 2 - Department and Centre of Physics, University of Minho; 3 - Microelectronics Research Center, Department of Electrical and Computer Engineering, The University of Texas at Austin; 4 - Materials Science and Engineering Program, The University of Texas at Austin; 5 - International Iberian Nanotechnology Laboratory; 6 - IDMEC, Instituto Superior Técnico.

Abstract

The study of prevalent defects and their impact on functional properties is a critical issue for the successful implementation of 2D materials in next-generation devices. However, the direct quantitative characterization of a specific defect is a challenging task, requiring atomic-resolution measurements that are sensitive to the electronic structure of the material. The use of differential phase contrast (DPC) in scanning transmission electron microscopy (STEM) is particularly promising for this purpose, leveraging the natural coupling between the electron probe and the atomic-scale electric fields within a sample, which leads to a redistribution of intensity at the diffraction plane. For thin specimens, the centre of mass (CoM) of the diffraction disc is then directly related to the phase gradient, allowing for the mapping of electrostatic forces between atoms of the material structure, a capability which has already been demonstrated in the study of several 2D materials [1–4].

CoM measurements can be performed with pixelated detectors, capable of recording the entire diffraction disc, or with segmented annular detectors that integrate the intensity of the disk over independent quadrants. Pixelated detectors offer the greatest accuracy, but the faster processing times associated with segmented detectors allow for the generation of DPC-STEM images in real time, making it easier to identify interesting features and to correct aberrations. These benefits, along with the fact that segmented detectors are still the most accessible option, make it worthwhile to explore methodologies to manage their reduced accuracy. For this reason, it is essential to understand the precise effect of instrumental parameters on segmented-detector DPC-STEM, such that their influence may be accounted for when analysing the results.

In this work, the influence of key instrumental parameters – probe convergence angle, defocus and detector orientation – on atomicresolution segmented-detector DPC-STEM measurements is evaluated through extensive image simulations of MoS2 and some of its defects. The qualitative effects on electrostatic field and potential maps are identified, along with the quantified impact on the accuracy of the measurements. Finally, conclusions applicable to the observation of 2D materials in general are drawn from this simulation-based study. The gathered observations are then employed in the analysis of experimental images from similar materials and defects.

Acknowledgments

Rafael V. Ferreira acknowledges funding from the Portuguese Science and Technology Foundation (FCT) through the Ph.D. studentship SFRH/BD/149390/2019

References

[1] Ishikawa, R., et al, Nat. Commun. 9 (2018), p. 3878.

[2] Müller-Caspary, K., et al, Phys. Rev. B 98 (2018), p. 121408.
[3] Fang, S., et al, Nat. Commun. 10 (2019), p. 1127.
[4] Calderon V., S., et al, Nano Letters 21(24) (2021), p.10157.

Keywords: Differential Phase Contrast, 2D materials, Multislice simulations

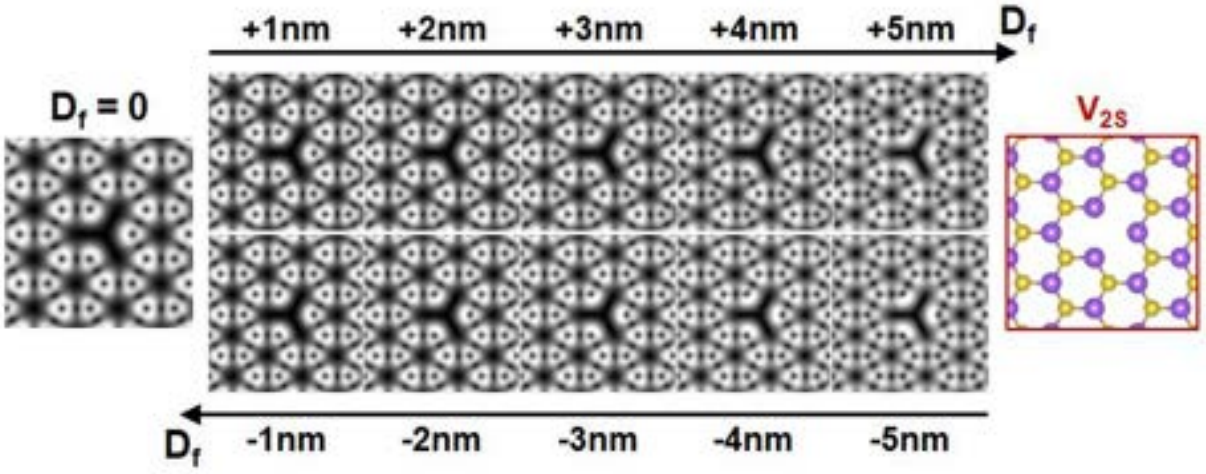

LITESCOPE: IN-SITU SAMPLE PREPARATION AND CORRELATIVE ANALYSIS BY AFM IN SEM.

Radek Dao

Application Specialist at NenoVision s.r.o.

Correlative microscopy has become an essential tool helping us understand the complexity of the sample properties. Not only does combining different imaging systems provide deeper understanding of the material, but it can also allow elegant solutions to problems with sample preparation and experimental workflow. Two such devices are especially well-suited for integration within each other: the Atomic Force Microscope (AFM) and Scanning Electron Microscope (SEM). The range of information these instruments can provide is almost mutually exclusive, with AFM being capable of imaging the 3D topography, electrical, magnetic, or mechanical properties of the sample, and SEM providing lightning-fast imaging for navigation, chemical analysis by Energy Dissipative Spectroscopy (EDS), and surface modification by Focused Ion Beam (FIB) or Gas Injection Systems (GIS).

Many applications require obtaining information which cannot be provided by one of these instruments alone. Such is the case with mapping of conductivity on the surface of battery components. The cross-sections of cathode/anode tapes, traditionally analyzed in SEM, must not be exposed to air and humidity to prevent degradation of the surface. This further complicates transfer to AFM, which is often not a vacuum system by nature.

Using the LiteScope AFM installed in a dual-beam SEM with GIS, we show a workflow which allows preparation of a fresh cross-section on demand anywhere on the sample. The surface is subsequently analyzed by Conductive AFM.

To demonstrate the use of LiteScope in other areas of material analysis, additional selection of use-cases, such as Magnetic Force imaging on a TEM lamella, will be shown.

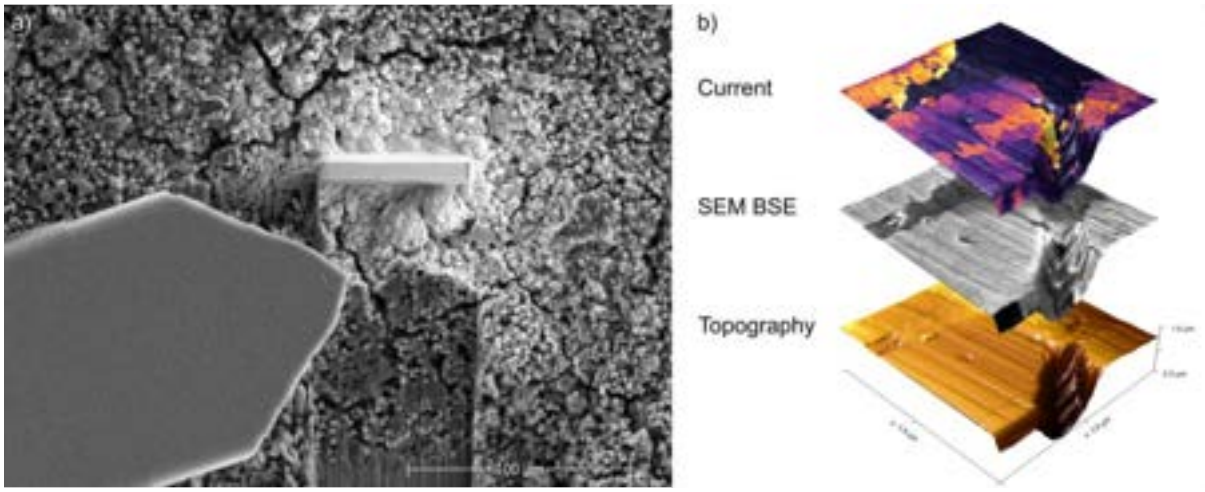

Figure 1 a) SEM overview of the AFM probe near the prepared surface, where the correlated C-AFM/SEM imaging was performed, b) resulting 3D maps of conductivity and BSE contrast

072

IDPC STEM IMAGING OF B IN DEFECTIVE MOALB THIN FILMS

Rajib Sahu (Germany)[1,2], Dimitri Bogdanovski[2], Christian Liebscher[2], Jan-Ole Achenbach[2], Jochen M. Schneider[1,2], Christina Scheu[1,3]

1 - Max-Planck-Institut für Eisenforschung and RWTH Aachen University; 2 - Materials Chemistry, RWTH Aachen University, Kopernikusstr. 10, 52074 Aachen; 3 - Materials Analytics, RWTH Aachen University, Kopernikusstr.

Abstract

Light elements play a significant role in designing advanced functional materials. Direct imaging of light atoms and their defect states by advanced scanning transmission electron microscopy (STEM) is still challenging due to local tilt and sample thickness. Here, we demonstrate that integrated differential phase contrast (iDPC) STEM imaging allows determination of the precise positions of B atoms, enabling detection of B defects in MoAlB MAB phase thin films. The iDPC results are compared with annular bright field (ABF) and annular dark field (ADF) STEM imaging as well as with results from density functional theory (DFT) calculations. The measurement was performed on a probe-corrected ThermoFisher Titan Themis at an accelerating voltage of 300 kV. TEM cross-sectional and plan view samples were prepared and thinned down below 20 nm by conventional mechanical polishing and Ar ion milling in a Gatan PIPS. MoAlB, a ceramic nanolaminate, shows promising potential for various applications such as protective coatings, oxidationresistant materials, conductors, battery electrodes etc. MoAlB also works as the precursor to synthesize the two-dimensional (2D) MBene MoB, which is used in sustainable energy research.

The MoAlB thin film was deposited by direct current magnetron sputtering at 700 °C. The shortest in-plane B-B distances of 82 pm and 168 pm were observed along the [001] and [100] zone axes (ZA). A statistical mean average measurement considering at least twenty bond lengths was performed and values of 89±8 pm and 185±3 pm were obtained along those directions. The experimental projected B-B bond distance (along [001]) is compared to DFT results, which yield a value of 93 pm for the corresponding bond. Hence, the experimental and calculated values agree well with a deviation of approx. 4%. Further, optimized DFT models are considered as input for STEM image simulations using the abTEM code for the interpretation of the experimental iDPC image contrast. A similar agreement between the experimental and simulated data is also seen along the direction of the [100] ZA. Additionally, missing B atomic columns are identified in the MoAlB phase due to sub-stochiometric composition. Due to prolonged electron beam irradiation, the number of missing B atomic columns increases with time. It is observed that more B vacancies lead to the growth of a 3D amorphous defect in the film. The existence of these missing B atomic columns can be rationalized due to the very small energetic barrier towards defect formation in the MoAlB MAB phase as calculated by DFT in literature. Our analyses validate that the formation of B defects is energetically feasible compared to the removal

of Al and Mo atomic columns in MoAlB. This can be identified as a significant issue in the synthesis of 2D MoB MBene derivatives from its parental MoAlB MAB phase. Also, the iDPC STEM imaging method is used to analyze accurate positions of B in the compositional defect phase Mo3Al2B4 coexisting inside the MoAlB matrix. Overall, our study compares various STEM imaging methods to characterize B atom positions and distances and utilize the advantages of iDPC imaging over the ABF and ADF techniques by removing overlapping contrast of Mo and B accurately in STEM micrographs

Keywords: Light element, iDPC STEM, defects, DFT, image simulation

UNSUPERVISED CLUSTERING FOR LOW-LOSS EELS: A NOVEL COMBINATION OF MACHINE LEARNING STRATEGIES FOR SURFACE PLASMON DETECTION

Vanessa Costa Lesdesma (Spain)[1]; Daniel Del Pozo Bueno (Spain)[1]; Catalina Coll (Spain)[5]; Josep Nogues (Spain)[2,5]; Borja Sepúlveda (Spain)[4]; Laura Bocher (France)[3]; Mathieu Kociak (France)[3]; Javier Blanco-Portals (Spain)[1]; Sonia Estradé (Spain)[1]; Francesca Peiró (Spain)[1,2]

1 - LENS - MIND, Department of Electronics and Biomedical Engineering and Institute of Nanoscience and Nanotechnology (IN2UB), University of Barcelona (UB); 2 - Catalan Institution for Research and Advanced studies, ICREA Academia, Barcelona; 3 - Laboratoire de Physique des Solides (LSP), Microscopie électronique STEM, Orsay; 4 - Instituto de Microelectrónica de Barcelona (IMB-CNM, CSIC)Campus UAB, Bellaterra, 08193 Barcelona; 5 - Catalan Institute of Nanoscience and Nanotechnology (ICN2)CSIC and BISTCampus UAB, Bellaterra.

Abstract

A plasmon is quasiparticle that quantizes the free-electron density oscillations in a metal, analogous to a phonon that quantizes the atomic vibrations in a crystalline material [1]. Surface Plasmon Polariton (SPP) is a phenomenon that arises from the interaction between incident electromagnetic radiation and the collective oscillation of electrons confined in the interface of a metal and a dielectric material. Morever, Localised Surface Plasmon Resonance (LSPR) is a non-propagating electron-density wave that is confined at the surface of a metallic nanoparticle, which geometry and surrounding medium determines the family of solutions to the Maxwell equations [2–4]. LSPRs have gained significant attention in the photonics and electronics communities due to their ability to concentrate electromagnetic radiation into sub-wavelength volumes; and due to their tunability, which is geometrydependent due to its resonance. This unique property opens a wide range of applications across various fields of applied research such as nanophotonics, robotics, environmental studies, energy, biology, and medicine [5–9].

Electron Energy Loss Spectroscopy (EELS) within a Scanning Transmission Electron Microscope (STEM) has revealed remarkable capabilities in the analysis of Surface Plasmons (SPs) at nanometric scale, offering the ability to achieve sub-angstrom spatial resolution and excite the complete range of Localized Surface Plasmon Resonance (LSPR) modes supported by metallic nanostructures. By employing EELS, the plasmonic properties can be correlated with geometric or structural characteristics, enabling a more comprehensive understanding of the plasmonic response. Therefore, it is as an ideal technique for studying SPs [10].

Clustering techniques correspond to a branch of unsupervised machine learning strategies where algorithms are given the task of independently identifying patterns, structures, or relationships within the data.

In this study, based on the analysis of Au/Si Nanowires samples, we demonstrate that clustering techniques can be used for detecting LSPRs in EELS data by reducing the dimensionality of the data. This allows for the identification of distinct spectra in a large EELS dataset, without the need for prior knowledge or labelling of the data [11].

Acknowledgments

This work has been supported by the Spanish Project PDC2021-121366-I00, financed by MCIN/AEI/ 10.13039/501100011033 and by the European Union NextGenerationEU/PRTR. The authors acknowledge the financial aid of the MICIIN under the project PID2019- 106165GB-C21, and of the Generalitat de Catalunya under project 2021SGR00242. The authors also acknowledge the support received from the ELECMI - ICTS Electron Microscopy for Materials Science and from ESTEEM3 program.

References

[1] Maier S A and Atwater H A 2005 Plasmonics: Localization and guiding of electromagnetic energy in metal/dielectric structures
Journal of Applied Physics 98(1)
[2] Ammari H, Ruiz M, Yu S and Zhang H 2016 Mathematical analysis of plasmonic resonances for nanoparticles: the full maxwellequations Journal of Differential Equations 261(6):3615-3669
[3] Mayer K M and Hafner J H 2011 Localized Surface Plasmon Resonance Sensors Chemical Reviews 111(6):3828-3857
[4] Yu H, Peng Y, Yang Y and Li Z Y 2019 Plasmon-enhanced light–matter interactions and applications npj Computational Materials 5(45)
[5] Pujol-Vila F, Güell-Grau P, Nogués J, Alvarez M and Sep úlveda B 2023 Soft optomechanical systems for sensing, modulation, and actuation Advanced Functional Materials 33 (14):2213109
[6] Paulillo B, Jr Bareza N and Pruneri V 2021 Controlling mid-infrared plasmons in graphene nanostructures through post-fabrication chemical doping J. Phys. Photonics 3:034001
[7] Ye T, Peng Y, Yuan M, Cao H, Yu J, Li Y and Xu F 1997 A “turn-on” fluorometric assay for kanamycin detection by using silver nanoclusters and surface plasmon enhanced energy transfer Microchim Acta 186:40 [8] Mamer S B, Page P, Murphy M, Wang J, Gallerne P, Ansari A and Imoukhuede P I 2019 The convergence of cell-cased surface plasmon resonance and biomaterials: the future of quantifying bio-molecular interactions—a review Annals of Biomedical Engineering 17:761
[9] Huang X, Jain P K, El-Sayed I H and El-Sayed M A 2007 Gold nanoparticles: interesting optical properties and recent applications in cancer diagnostics and therapy Nanomedicine 2(5):681-693
[10] Wu Y, Li G and Camden J P 2018 Probing nanoparticle plasmons with Electron energy loss spectroscopy Chemical Reviews 118(6):2994-3031
[11] Ryu J, Kim H, Kim R M, Kim S, Jo J, Lee S, Nam K T, Joo Y C, Yi G C, Lee J and Kim M 2021 Dimensionality reduction andunsupervised clustering for EELS-SI Ultramicroscopy 231:113314

Keywords: Surface Plasmon, machine learning, clustering, EELS

ADAPTABLE TRANSMISSION ELECTRON MICROSCOPY CHARACTERIZATION OF FUNCTIONAL CARBON-BASED AND HYBRID IRON-CARBON NANOMATERIALS

José M. Vila Fungueiriño (Spain)[1]; Carlos Herreros-Lucas (Spain)[1]; Lucía Vizcaíno-Anaya (Spain)[1]; María Del Carmen Giménez-López (Spain)[1]

1 - Center for Research in Biological Chemistry and Molecular Materials (CiQUS), University of Santiago de Compostela, Galicia

Abstract

Tunable carbon-based nanomaterials with an easy design of their size, morphology, surface, and other chemical features such as defects and oxidation state are a smart way to expand the properties of carbon at the nanoscale.[1] However, the properties of carbon nanostructures are strongly determined by the fabrication process, limiting their application to a single purpose, and preventing their functional and reliable use. For this reason, it is crucial to develop a methodology that, starting from a feasible carbon source, can obtain high quality products that can be employed in multiple functions. Here, we present the electron microscopy characterization of the production of homogeneous graphite nanoplatelets (GNP) that can be used either in energy storage or in chemical sensing by exploiting the interiors of hollow carbon nanofibers (CNF) using dry ball-milling.[2]

In addition, the confinement of metallic nanoparticles (MNP) within carbon nanostructures represents a sophisticated approach that serves a dual purpose. Firstly, it ensures the protection and stability of the MNP within the carbon nanostructure framework. Secondly, it safeguards the surrounding environment from potential toxicity caused by the MNP, particularly in biological conditions. In this work, we discuss the use of TEM in combination with advanced physical techniques to refine the conditions to protect iron nanoparticles within graphitic carbon layers by a thermal treatment of the NPs.[3] Acknowledgments This work has received financial support from the Ministry of Science of Spain (RYC-2016-20258, RTI2018-101097-A-I00, EIN2019- 103246, PID2021-127341OB-I00, TED2021-131451BC21 and PDC2022-133925-I00 for M.d.C.G.-L., IJC2020-044369-I for J.M.V.-F. and Ministry of Universities of Spain (FPU20/01072) for L.V.-A.), the European Research Council (ERC) [Starting Grant (NANOCOMP679124) and ZABCAT (966743) for M.d.C.G.-L.], the Xunta de Galicia (Centro singular de investigación de Galicia accreditation 2019−2022, ED431G 2019/03), and the European Union (European Regional Development Fund ERDF).

References

[1] Jin, X., Gu, T. H., Kwon, N. H., & Hwang, S. J. (2021). "Synergetic advantages of atomically coupled 2D inorganic and graphene nanosheets as versatile building blocks for diverse functional nanohybrids." Advanced Materials 33.47 (2021): 2005922.
[2] Herreros-Lucas, Carlos, Vila-Fungueiriño, José M., and María del Carmen Giménez-López. "Electrochemically Versatile Graphite Nanoplatelets Prepared by a Straightforward, Highly Efficient, and Scalable Route." ACS Applied Materials & Interfaces 15.17 (2023):21375-21383.

[3] Vizcaíno-Anaya, L., Herreros-Lucas, C., Vila-Fungueiriño, J. M., and del Carmen Giménez-López, M. (2022). "Magnetic Hyperthermia Enhancement in Iron-based Materials Driven by Carbon Support Interactions." Chemistry–A European Journal 28.67 (2022): e202201861

Keywords: Carbon nanofibers, graphite nanoplatelets, carbon supports, hybrid materials, confined nanoparticles

TRANSMISSION AND AUGER ELECTRON MICROSCOPY OF SPIN-VALVE NANOSTRUCTURES

Martynas Skapas (Lithuania)[1]; Nerija Žurauskienė (Lithuania)[1]; Voitech Stankevič (Lithuania)[1]; Vilius Vertelis (Lithuania)[1]

1 - Center for Physical Sciences and Technology

Abstract

The detection of magnetic fields with increased spatial resolution to micro-nanoscales is very important for magnetometry [1]. It is of great interest to have low-dimension sensors with increased sensitivity and extended capabilities. The discovery of magnetoresistive (MR) effects (AMR, TMR, GMR and CMR) in magnetic structures encouraged fundamental research leading to a number of laboratory-scale and commercially available devices [2]. Moreover, nowadays, the magnetosensorics becomes very important for wearable electronics and soft robotics. Each application has its specific requirements for sensitivity, temperature and magnetic field ranges of operation, accuracy, sensor's positioning, etc. Therefore, the choice of material with specific properties and design of sensing element becomes very important.

High-resolution transmission electron microscopy (HRTEM) study on layered Heusler alloy Co2MnSi structures is presented in this work. These films were grown by using magnetron sputtering, serves as a main active element of magnetoresistive sensor with tunable sensitivity. Series of samples, including dependence on layers' thicknesses (5 - 200 nm) and annealing temperature (400-650 oC) were analysed. Such novel hybrid sensor would provide possibilities to decrease its dimensions for measuring magnetic fields in small volumes, especially for measurement of field direction in respect to reference plane, when in conventional methods three sensors are used. Other complex structures, including LSMO based sensors, were also analysed.

Auger electron microscopy provides medium resolution (up to 10nm) elemental analysis, together with depth profiling capabilities. As requiring no sample preparation, this method is advantageous for initial analysis and TEM sample selection.

These structural peculiarities, unresolvable by other techniques, affect magnetic properties, such as magnetoresistance anisotropy and sensor sensitivity, so in-depth structural analysis is crucial in sensor development and could be used for the development of magnetic field sensors with predetermined parameters for operation at low or high temperatures.

Acknowledgments

This project has received funding from the Research Council of Lithuania (LMTLT), agreement No. S-PD-22-6

Keywords: Heusller alloy, STEM, Auger microscopy

TECHNOLOGY PLATFORM FOR IN-SITU/OPERANDO TEM CHIPS FABRICATION

Jose Rodrigues (Portugal)[1]; Paulo Ferreira (Portugal)[1]; Carlos Calaza (Portugal)[1]

1 – International Iberian Nanotechnology Laboratory

Abstract

Advances in transmission electron microscopy (TEM) providing sub-Angstrom resolution along with fast and sensitive electron detection have recently enabled direct in-situ observation of dynamic phenomena at the atomic scale. Furthermore, the use of specialized specimen holders has played a crucial role in the experiments, allowing precise control of the stimulus being applied to the samples along with overall system stability, which is critical to ensure the atomic-scale resolution. For this reason, the use of MEMS-based TEM sample holders has become the preferred route for in-situ TEM applications, enabling high precision in parameter measurement for more reproducible data.

Current challenges for in-situ TEM specimen holders include the operation of an appropriate reaction environment allowing both the penetration of the electron beam and the reconstruction of the work conditions within a limited space while minimizing the possible systematic artifacts induced by the electron beam. The fabrication of thin and robust cell windows is crucial to hold real experimental environments and, in addition, decreasing window thickness or gap between windows enhances the imaging resolution. Consequently, MEMS microfabrication technologies become crucial to realize such membranes as well as many other functional elements that may be required on a chip holder or a closed gas/liquid cell. Custom chips for heating, mechanical deformation, polarization, solid-gas, and solid-liquid reactions have already been demonstrated, allowing researchers to measure mechanical properties, electromechanical properties, cyclic voltammetry/discharge profile properties, current-voltage curve (I-V), gas partial pressure, and so on using application-specific designs.

The scope of this work is to develop the basic set of microfabrication process steps required to produce MEMS chips with robust SiNx membranes, to be later used for the accomplishment of more complex microfabricated platforms specifically designed for a broad range of in-situ TEM applications. The primary role of the technology platform developed at the INL MNF facility will be to support the users of INL in-situ specimen holders providing custom chips to meet the unique needs of each experiment or process. INL MNF capabilities allow us to take the design of a device completely from concept to completion.

Acknowledgments

International Iberian Nanotechnology Laboratory and Universidade de Vigo.

References

Zhang, X.; Zhou, Y.; Chen, Y.; Li, M.; Yu, H.; Li, X. Advanced In Situ TEM Microchip with Excellent Temperature Uniformity and High Spatial Resolution. Sensors 2023, 23, 4470. https://doi.org/10.3390/s23094470

Keywords: Transmission Electron Microscopy, In-situ, fabrication, MEMS

STRUCTURAL CHARACTERIZATION OF TOPOLOGICAL POLAR TEXTURES IN TWISTED FREESTANDING OXIDE LAYERS

Gabriel Sanchez Santolino (Spain)[1]; Victor Rouco (Spain)[1]; Sergio Puebla (Spain)[2]; Hugo Aramberri (Spain)[3]; Victor Zamora (Spain)[1]; Fabian Cuellar (Spain)[1]; Carmen Munuera (Spain)[2]; Federico Monpean (Spain)[2]; Mar García-Hernandez (Spain)[2]; Andrés Castellanos-Gómez (Spain)[2]; Jorge Íñiguez (Spain)[3]; Carlos Leon (Spain)[1]; Jacobo Santamaria (Spain)[1]

1 – GFMC. Dept. Fisica de Materiales. Facultad de Fisica. Universidad Complutense; 2 - Instituto de Ciencia de Materiales de Madrid ICMM-CSIC 28049 Cantoblanco; 3 - Materials Research and Technology Department, Luxembourg Institute of Science and Technology (LIST), Avenue des Hauts-Fourneaux 5, L-4362 Esch/Alzette, Luxembourg.

Abstract

Several studies on ferroelectric oxide materials have recently shown how complex polar topologies can be stabilized by imposing electrical and mechanical boundary conditions [1, 2]. These findings open the possibility of creating new states of matter, such as polar skyrmions, with potential applications for the development of high-density memory devices. In this work we study the formation of ferroelectric topological textures in twisted freestanding ferroelectric perovskite bilayers. Epitaxially grown ferroelectric layers are isolated from the substrate by selective etching and adhered to a polymer film, which can then be transferred deterministically. This approach allows us to produce complex mechanical boundary conditions by stacking oxide layers with controllable twisting angles. To study these systems, we have used aberration-corrected scanning transmission electron microscopy in combination with density-functional theory calculations. We have performed real-space measurements of the local polar displacements in atomic resolution images and relate them to the complex strain fields originating in the twisted ferroelectric bilayers [3]. This approach presents an interesting perspective for creating polar topologies using the unique modulations that are possible in Moiré bilayers.

References

[1] Yadav, A. K. et al. Observation of polar vortices in oxide superlattices, Nature, 2016, 530, 198–201.
[2] Rusu, D. et al. Ferroelectric incommensurate spin crystals, Nature, 2022, 602, 240–244.
[3] G. Sánchez-Santolino et al., A 2D ferroelectric vortex lattice in twisted BaTiO3 freestanding layers, arXiv:2301.04438

Keywords: complex oxides, ferroelectrics, scanning transmission electron microscopy

NANOMETER MAPPING OF STRAIN-INDUCED BAND STRUCTURE VARIATIONS IN SEMICONDUCTOR DEVICES

Marc Botifoll (Spain)[1]; Sara Martí-Sánchez (Spain)[1]; Quentin Ramasse (United Kingdom)[2]; F. Javier García De Abajoc (Spain)[3,5]; Ernesto Joselevich (Israel)[4]; Jordi Arbiol (Spain)[1,5]

1 - ICN2, CSIC and BIST; 2 - SuperSTEM Laboratory, STFC Daresbury Campus; 3 - . ICFO, BIST; 4 - Department of Molecular Chemistry and Materials Science, Weizmann Institute of Science; 5 - ICREA

Abstract

Germanium and silicon-based devices for quantum computing are experiencing a huge rise in popularity over the last few years. They have proven to be magnificent candidates for efficient qubit generation, and are flexible enough to hold different quantum computing paradigms. Based on the morphology and dimensionality of the devices they may act as either spin qubits or (topological) superconducting qubits. For this purpose, heterostructures contacting combinations of pure Ge, pure Si, and alloyed SiGe with varying Si/Ge ratios are successful candidates towards the obtention of qubits [1].

Interestingly, the low effective mass and the electrically tuneable g factors that are key for the qubit performance closely correlate with the strained interface that rules the energy splitting. This constitutes an interesting materials science problem that is worth tackling at the high spatial resolutions the transmission electron microscope can offer, in search of local effects. Therefore, in the present contribution we present a new methodology that can sub-nanometrically map the band structure of semiconductor devices.

The proposed new methodology is based on the correlation of high-resolution low-loss electron energy loss spectroscopy (EELS) and strain mapping to link the accumulations of strain with bandgap shifts [2]. Importantly, we ensure the obtained results are physically meaningful by removing and cleaning the parasitic signals that can arise when studying the low-loss spectral regime (i.e., Cherenkov radiation). The original methodology was developed and applied to an optoelectronic device based on a planar ZnSe/ZnTe core-shell heterojunction, although preliminary results will be shown on quantum devices, more specifically Ge/SiGe quantum wells for holding spin qubits and Ge/Si nanowires aiming towards topological quantum computing.

References

[1] Jirovec, D. et al. *Nature Materials*, (2021) doi.org/10.1038/s41563-021-01022-2
[2] Martí-sánchez, S. et al, Nat. Commun. 13, 4089 (2022).

Keywords: EELS, bandgap, strain, methodology

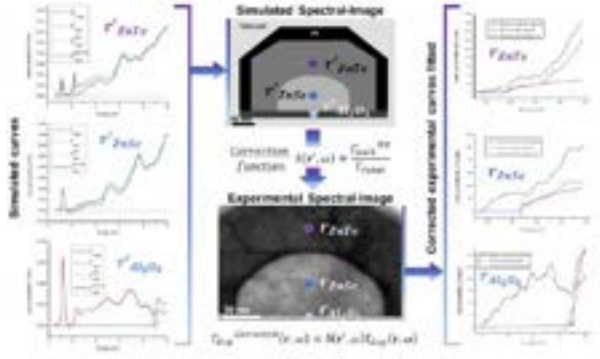

Figure 1: Scheme of the methodology for low-loss EELS cleaning and bandgap mapping

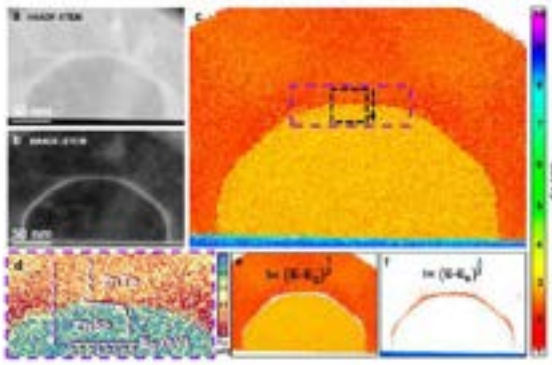

Figure 2: Bandgap maps obtained from applying the proposed methodology to a ZnSe/ZnTe core-shell nanowire

MEASUREMENT OF LOCAL DIELECTRIC FUNCTION OF HFO2 THIN LAYER WITH DIFFERENT CRYSTALLOGRAPHIC PHASES FROM EELS ANALYSIS

Beatriz Vargas (Spain)[1]; Déspina Nasiou (Germany)[2]; Leopoldo Molina-Luna (Germany)[2]; Catalina Coll (Spain)[3]; Daniel Del Pozo Bueno (Spain)[1]; Pranjal Nandi (Spain)[1]; Sonia Estradé (Spain)[1]; Lluis Yedra (Spain)[1]; Lambert Alff (Germany)[4]; Niko Kaiser (Germany)[4]; Lluis López-Conesa (Spain)[1]; Francesca Peiró (Spain)[1,5]

1 - LENS, Department of Electronics and Biomedical Engineering and Institute of Nanoscience and Nanotechnology, University of Barcelona, Barcelona, Spain.; 2 - Department of Materials and Earth Sciences, Advanced Electron Microscopy, Technical University of Darmstadt, Darmstadt, Germany.; 3 - Catalan Institute of Nanoscience and Nanotechnology (ICN2), CSIC and BIST, Campus UAB, Bellaterra, Spain.; 4 - Department of Materials Science, Advanced Thin Film Technology, Technical University of Darmstadt, Darmstadt, Germany.; 5 - Catalan Institution for Research and Advanced studies, ICREA Academia, Barcelona, Spain.

Abstract

Hafnium oxide (HfO_2) is a material with a high dielectric response, making it widely used in the fabrication of advanced semiconductor devices. The dielectric function is an important parameter in the study of its optical and electronic properties [1]. At the nanoscale, the dielectric response of HfO_2 can differ from its behavior in bulk, due to a variety of factors such as defects and surface effects [2].

In this study, we compare the dielectric function and energy loss function of HfO_2 thin layers, with hexagonal and rhombohedral phases. Thin films of 20 nm HfO_{2-x} were grown on a TiN substrate, and each one was extracted from a vacuum atmosphere to an air atmosphere where an oxygen-rich nanolayer was formed at the top of the HfO_{2-x} layer. After this, each sample was deposited in a vacuum atmosphere to sputter a Pt bottom electrode by using molecular beam epitaxy (MBE), obtaining two multilayer devices as shown in Fig. 1. Electron transparent cross-sectional TEM lamellas were fabricated using a JEOL 4600F Focused Ion Beam (FIB), and EELS data were acquired in a JEOL-ARM200F at 200 kV.

The dielectric function and electron energy loss function of HfO_2 have been studied using electron energy loss spectroscopy (EELS) by Kramers-Kronig (KK) analysis, using the algorithm reported by Eljarrat [3]. The effects of crystalline structure on the optical properties of HfO_2 have been observed through the analysis of the dielectric function (see Fig. 2). Additionally, for each sample, the procedure was applied to several regions of the HfO_2 layer with the same size and dimensions, sweeping the area of measurement from one interface to the other, in order to observe how the oxygen variation affects the optical response. KK calculations revealed a shift to higher energies of the ELF, and consequently on the dielectric response of the HfO_2 layer with a hexagonal phase near the oxygen-rich nanolayer. Further, Density Functional Theory (DFT) calculations have been carried out to co-relate with the experimental findings.

Acknowledgments

The authors would like to acknowledge funding from MICIIN under project reference No. PID2019-106165GB-C21, the support received from the ELECMI-ICTS Electron Microscopy for Materials Science and funding from Gencat under project reference No. 2021SGR00242.

References

E. I. Suvorova, O. V. Uvarov, N. A. Arkharova, A. D. Ibrayeva, V. A. Skuratov, and P. A. Buffat. Structure evolution, bandgap, and dielectric function in La-doped hafnium oxide thin layer subjected to swift Xe ion irradiation. *J Appl Phys*, vol. 128, no. 16, Oct. 2020, doi: 10.1063/5.0025536.

J. Park and M. Yang, 'Determination of complex dielectric functions at HfO2/Si interface by using STEM-VEELS', *Micron*, vol. 40, no. 3, pp. 365–369, Apr. 2009, doi: 10.1016/J.MICRON.2008.10.006.

A. Eljarrat and C. T. Koch. Design and application of a relativistic Kramers–Kronig analysis algorithm. *Ultramicroscopy*, vol. 206, Nov. 2019, doi: 10.1016/j.ultramic.2019.112825.

Keywords: Kramers-Kronig, EELS, HfO2

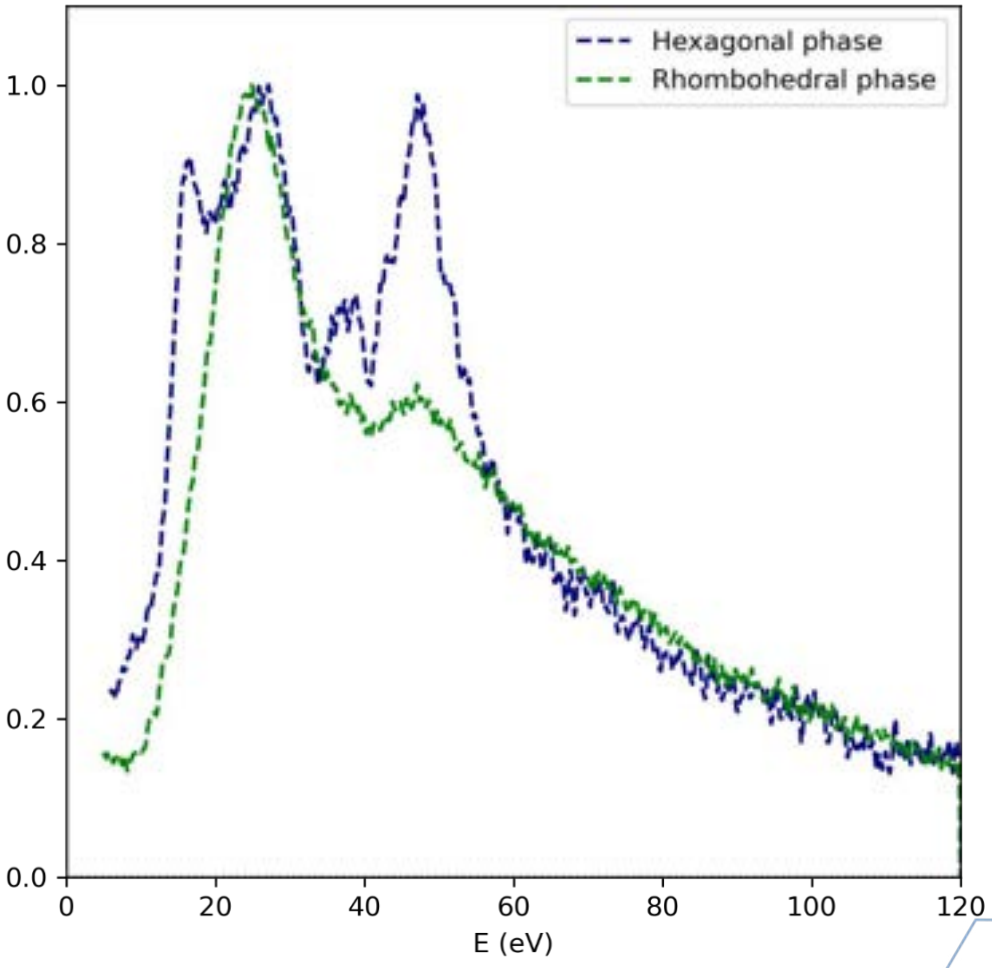

NEW TOOLS FOR ELECTRON MICROSCOPY OF AIR-SENSITIVE AND ELECTRON BEAM-SENSITIVE MATERIALS

Alpesh Khushalchand Shukla[1]

1 – ZoNexus LLC

Abstract

In recent years, there has been increased interest in characterizing air-sensitive materials such as lithium metal, which is a promising material for development of all-solid-state batteries. ZoNexus has developed several tools that aid in sample preparation as well as electron microscopy of such air-sensitive materials. In this presentation, I will discuss several such products, namely: 1) a high-throughput air-free transfer TEM holder that allows transfer of up to three samples from an inert gas glove box to the TEM, 2) a double-tilt, biasing air-free transfer holder for in situ cycling studies of batteries and 3) an air-free transfer module for scanning electron/focused ion beam microscopes. Recent development of cryo-biasing and cryo-transfer holders will also be presented. Finally, an example showing sample preparation for a Li-S micro-battery in focused ion beam microscope and operando studies showing cycling of the battery in the transmission electron microscope will be discussed.

Keywords: air-free transfer, batteries, cryo-electron microscopy, air-sensitive materials, in situ TEM holders.

UNVEILING VACANCIES AND ANISOTROPIC DEFECTS IN LA1-XSRXMNO3 (LSMO) THROUGH STEM AND IDPC SIMULATION IMAGING.

Pranjal Nandi (Spain)[1]; Juri Barthel (Germany)[2]; Miguel López-Haro (Spain)[3]; José J. Calvino (Spain)[3]; Francesco Chiabrera (Spain)[4]; Federico Baiutti (Spain)[4]; Albert Tarancón (Spain)[4,5]; Francesca Peiró (Spain)[6,7]; Lluís Yedra (Spain)[6]; Sònia Estradé (Spain)[6]

1 - Laboratory of Electron Nanoscopies (LENS), Micro Nanotechnology and Nanoscopies for electrophotonic Devices (MIND), Department of Electronics and Biomedical Engineering and Institute of Nanoscience and Nanotechnology (IN2UB), University of Barcelona; 2 - Ernst Ruska-Centre (ER-C 2), Forschungszentrum Jülich GmbH; 3 - Universidad de Cádiz; 4 - Institut de Recerca en Energia de Catalunya; 5 - Catalan Institution for Research and Advanced Studies; 6 - Laboratory of Electron Nanoscopies (LENS), Micro-Nanotechnology and Nanoscopies for electrophotonic Devices (MIND), Department of Electronics and Biomedical Engineering and Institute of Nanoscience and Nanotechnology (IN2UB), University of Barcelona; 7 - ICREA Academia, Passeig Lluís Companys 23, Barcelona 08010

Abstract

$La_{1-x}Sr_xMnO_3$ (LSMO) has been widely considered as a promising candidate in fields of mixed ionic−electronic conductors and solid oxide fuel cells. A great amount of effort has been focused on its oxygen mass transport properties[1]. Faster diffusion through dislocations has been generally attributed to higher vacancy concentration or to a higher mobility of oxygen vacancies[2]. It has been reported that oxygen vacancies and antisite defects in LSMO can strongly affect its electronic and magnetic properties [3,4]. We therefore propose a novel method to detect vacancies and antisite defects from scanning transmission electron microscopy (STEM) images by image simulation and analysis software. LSMO thin films with antisite defects of variable Mn/(La+Sr) ratio were grown by combinatorial pulsed laser deposition on $SrTiO_3$ and the control of stoichiometry was achieved by using an alternate deposition of Mn-deficient LSM and Mn_3O_4 followed by an in-situ annealing in oxygen[5]. The samples were observed in a FEI Titan^3 Themis 60-300 Transmission Electron Microscope operated at 200 KV equipped with segmented STEM detectors.

In this study, we simulated STEM images of LSMO with variable oxygen vacancies from four segmented detectors[6]. The images obtained were then processed to generate integrated differential phase contrast (iDPC) images. Comparing the theoretical iDPC with the experimental images, we could correlate the reduced intensities on O columns with the presence of oxygen vacancies as shown in Fig 1. Further, we introduced antisite defects and simulated the corresponding STEM and iDPC images. The comparison of integrated intensities along the atomic column between different positions in the perovskite and the simulated controlled composition images provide a method to estimate antisite defects supplementary to elemental mapping. Our approach contributes to illustrate the relevance of simulations for analysing STEM images.

Acknowledgments

We acknowledge the funds received from AGAUR FI grants (2021 FI_B 00157) and the support received from the ELECMI - ICTS Electron Microscopy for Materials Science. L.Y. acknowledges support from the MINECO (Spain) through the IJC2018-037698-I grant. The authors would also like to acknowledge the financial support from the Spanish project PID2019-106165GB-C21, and the Catalan project 2021SGR00242.

References

1. Saranya, A. M. *et al.* Unveiling the Outstanding Oxygen Mass Transport Properties of Mn-Rich Perovskites in Grain Boundary-Dominated La0.8Sr0.2(Mn1- xCox)0.85O3±δ Nanostructures. *Chemistry of Materials* **30**, 5621–5629 (2018).
2. Navickas, E. *et al.* Dislocations Accelerate Oxygen Ion Diffusion in La0.8Sr0.2MnO3 Epitaxial Thin Films. *ACS Nano* **11**, 11475–11487 (2017).
3. Kumari, S. *et al.* Effects of Oxygen Modification on the Structural and Magnetic Properties of Highly Epitaxial La0.7Sr0.3MnO3 (LSMO) thin films. *Sci Rep* **10**, (2020).
4. Gu, M. *et al.* Antisite defects in La0.7Sr0.3MnO3 and La0.7Sr0.3FeO3. *Appl Phys Lett* **102**, (2013).
5. Chiabrera, F. M. *et al.* The impact of Mn nonstoichiometry on the oxygen mass transport properties of La0.8Sr0.2Mn y O3±δ thin films. *JPhys Energy* **4**, (2022).
6. Barthel, J. Dr. Probe: A software for high-resolution STEM image simulation. *Ultramicroscopy* **193**, 1–11 (2018).

Keywords: vacancy, defect, anisotropy, simulation, STEM, iDPC

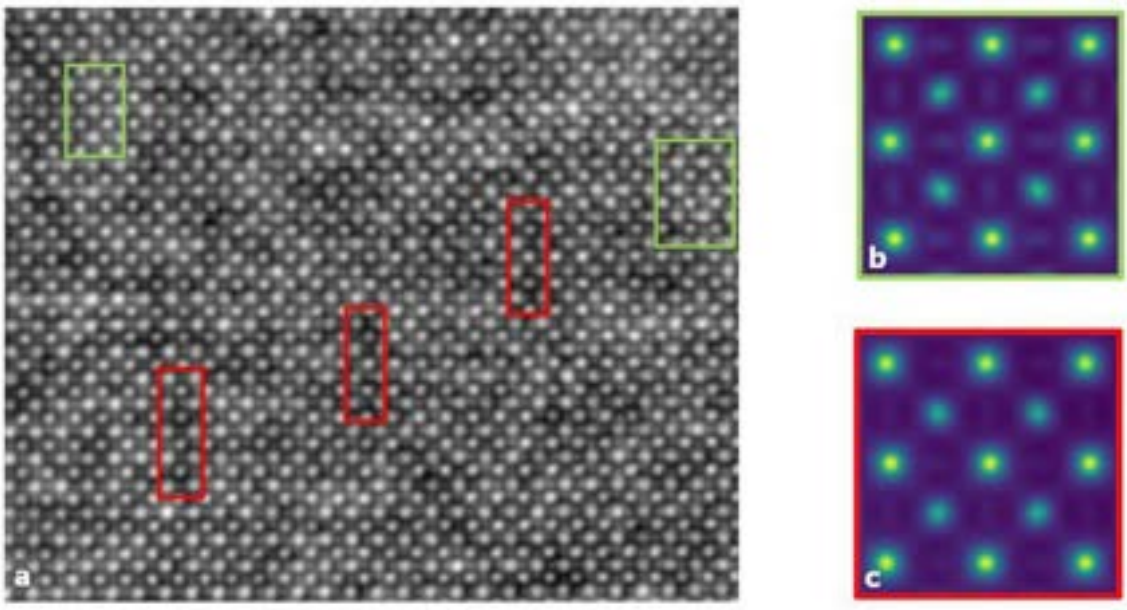

Fig 1. LSMO (a) Experimental iDPC image where regions with oxygen vacancies (in red) and without (in green) are highlighted. (b) Simulated iDPC image with no vacancies. (c) Simulated iDPC image with vacancies.

RADIATION TOLERANT PIXEL DESIGN FOR SEM IMAGING BETWEEN 500 EV TO 30 KEV

Juan Antonio Leñero Bardallo (Spain)[2]; Lionel Cervera Gontard (Spain)[3]; Jorge Johanny Sáenz Noval (Spain)[1]

1 - Universidad de Cádiz; 2 - Institute of Microelectronics of Seville (IMSE-CNM) CSIC-Universidad de Sevilla; 3 - Department of Physics of Condensed Matter and IMEYMAT, University of Cádiz

Abstract

State-of-the art image sensors for 4D STEM are based on radiation hard, or *radhard*, monolithic active pixel sensors (MAPS) fabricated with conventional CMOS integrated circuits hardened with hybrid structures [1]. Such detectors would be of interest also for measuring diffraction patterns in the largely unexplored field of low-voltage 4D STEM-in-SEM at energies between 500 eV and 30 keV [2]. Nevertheless, *radhard* MAPS are efficient only at well-defined primary electron energies, and they are not very sensitive to low-energy electrons, thus, hindering their general application in SEM [3].

Here we describe a new type of pixel that is at the same time, *radhard*, sensitive to electrons in a wide range of energies and with high dynamic range. Therefore, it can be used as the sensing unit of a MAPS for SEM. Figure 1(a) and 1(b) show the building blocks and pixel placement in the stacked layers of the CMOS process, respectively. A charge sensitive amplifier connected to the metallic electrode of a capacitor converts the electron signal from the beam into a voltage, which is then compared with two thresholds (V_H and V_L) to determine whether there is a positive or negative change in charge. A conductive layer of some micrometers (for example, of platinum or tungsten) is grown on top of the CMOS top metal. This conductive layer serves two purposes: (i) it gathers free electric charge, and (ii) it acts as a barrier against unintentional charges from entering the oxides, which reduces the risk of radiation damage. Figure 2(a) shows an SEM image of the integrated circuit, bonding wires and ceramic package fabricated with an UMC CMOS@180nm process. Figure 2(b) shows a photograph of one single pixel. Preliminary pixel measurements demonstrate sensitivity to electrons with electron energies within the SEM range, high radiation tolerance (tested up to 30keV@100 nA), and a high dynamic range of 110 dB.

Acknowledgments

The authors want to acknowledge funding from MCIU/AEI/ERDF-EU through projects PGC2018-101538-A-I00. Financial support from the program Plan Propio-UCA Ref 18INPPPR05 and from the grant Proyectos de I+D+i DE entidades públicas – Convocatoria 2020 P20_01206 (VERSO) are also acknowledged.

References

[1] W. Snoeys, “CMOS monolithic active pixel sensors for high energy physics,” *Nucl. Instruments Methods Phys. Res. Sect. A Accel. Spectrometers, Detect. Assoc. Equip.*, vol. 765, no. 2014, pp. 167–171, 2014, doi: 10.1016/j.nima.2014.07.017.

[2] B. W. Caplins, J. D. Holm, R. M. White, and R. R. Keller, "Orientation mapping of graphene using 4D STEM-in-SEM," *Ultramicroscopy*, vol. 219, no. May, p. 113137, 2020, doi: 10.1016/j.ultramic.2020.113137.
[3] L. C. Gontard, J. A. Leñero-Bardallo, F. M. Varela-Feria, and R. Carmona-Galán, "Vertically stacked CMOS-compatible photodiodes for scanning electron microscopy," *Proc. - IEEE Int. Symp. Circuits Syst.*, vol. 2020-Octob, no. c, pp. 4–8, 2020, doi: 10.1109/iscas45731.2020.9181208.

Keywords: MAPS, Radhard, SEM, 4D STEM-in-SEM

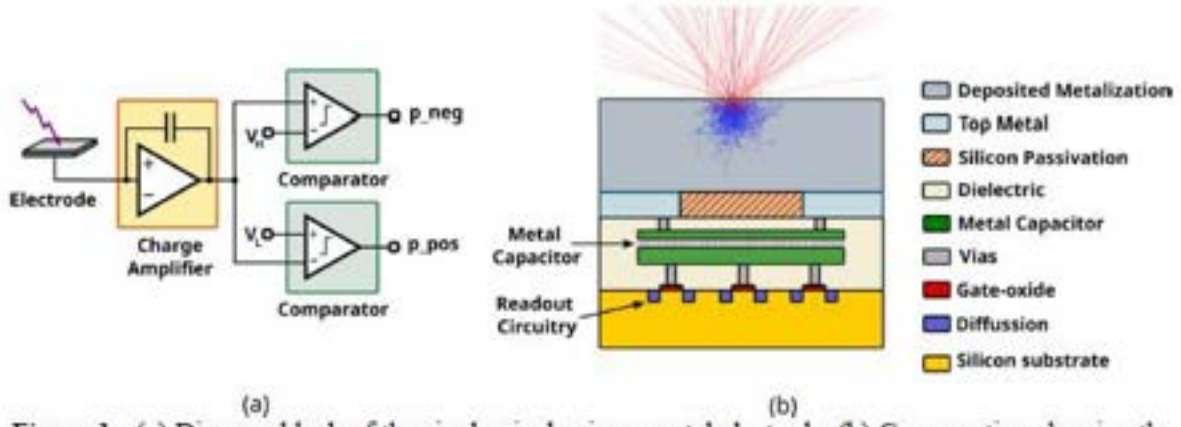

Figure 1. (a) Diagram block of the single pixel using a metal electrode. (b) Cross section showing the physical arrangement and connections of the pixel. Detector capacitance was made using metal capacitors available in CMOS process.

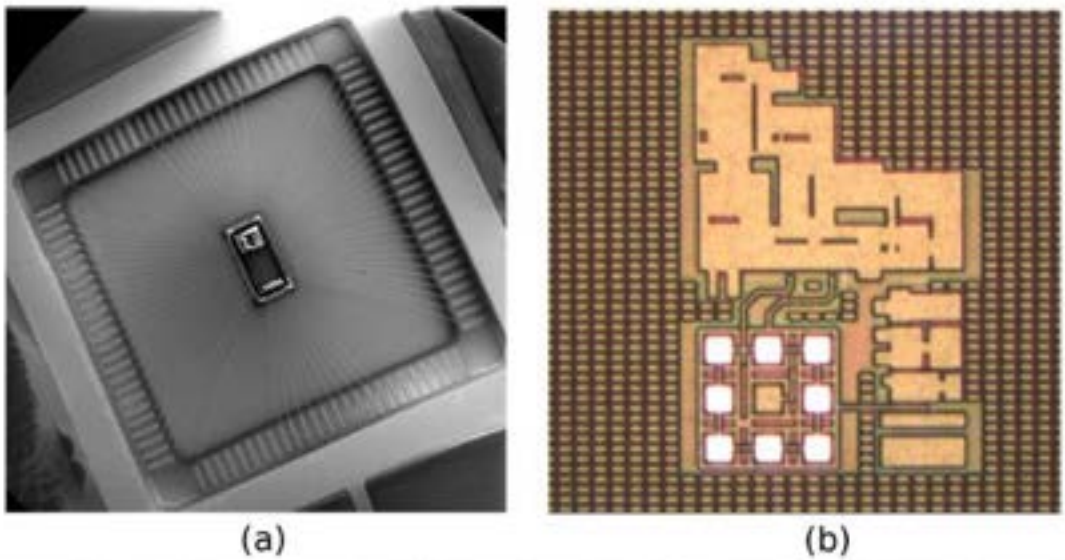

Figure 2. (a) SEM image of the CMOS integrated circuit detailing bonding metal connections and die. (b) Light microscope photograph of single pixel detailed the metal electrodes and circuitry.

UNDERSTANDING THE MECHANISMS OF FLASH SINTERING OF SEMICONDUCTOR OXIDE MATERIALS BY ADVANCED ELECTRON MICROSCOPY

Fátima Zorro (Portugal)[1,2]; Camila Ribeiro (Portugal)[3]; Ana Senos (Portugal)[3]; Paula M. Vilarinho (Portugal)[3]; Paulo Ferreira (Portugal)[1,2,4]

1 - Instituto Superior Técnico; 2 - International Iberian Nanotechnology Laboratory; 3 - Department of Materials and Ceramic Engineering, CICECO – Aveiro Institute of Materials; 4 - Materials Science and Engineering Program, University of Texas at Austin

Abstract

With the rising demand for energy-efficient technologies, it has become crucial to develop cost-effective processes for producing materials. Flash sintering (FS) offers a promising alternative to conventional sintering methods, as it significantly reduces processing times from hours to seconds and operating temperatures by several hundreds of degrees. While the recent literature reports successful room temperature FS for materials such as ZnO and YSZ, the relationship between the micro/nanoscale properties and the underlying physical mechanism(s) during FS is not yet fully understood. Furthermore, there is a lack of research regarding these mechanisms in semiconductor oxides [1], [2]. This is significant since this category of materials exhibits various attractive properties, such as superconductivity, ferroelectricity, and dielectric behavior, making them applicable in a wide range of industries [3].

In this study, the objective is to understand the room temperature flash-sintering process of $La_{0.75}Sr_{0.25}CrO_3$ at the nano/atomic scale. This material has applications in the catalytic and energy-related fields. Specifically, the investigation is focused on the development of a novel method for the preparation of lamellas from porous and brittle materials and its transfer to MEMS chips for in-situ experiments. To observe the changes in the nano/atomic structure of electron transparent samples, an electric field will be applied in-situ in the TEM to simulate the flash sintering process at room temperature (Figure 1). This allows the observation in real-time of the physical mechanism(s) occurring in the selected material. Additionally, to access the possibility of the Joule heating mechanism the study is focused on the grain boundaries through its characterization using aberration-corrected TEM/STEM and DSTEM to identify the presence of amorphous phases resulting from local melting.

Acknowledgments

Fátima Zorro acknowledges the financial support of FCT – Portugal, through the studentship 2021.05950.BD of the 2021 Call for Ph.D. Studentships. This work was supported by FCT, through IDMEC, under LAETA, project UIDB/50022/2020.

References

[1] N. Yan *et al.*, “Ethanol-Induced Flash Sintering of ZnO Ceramics at Room Temperature,” *Materials (Basel)*, vol. 15, no. 3, pp. 1–9, 2022.

[2] Y. Zhu *et al.*, “Gas-discharge induced flash sintering of YSZ ceramics at room temperature,” *J. Adv. Ceram.*, vol. 11, no. 4, pp. 603–614, 2022.

[3] R. Catlow and A. Walsh, “Semiconducting oxides,” *J. Phys. Condens. Matter*, vol. 23, no. 33, pp. 2010–2011, 2011.

Keywords: Flash Sintering, Semiconductor Oxide Materials, TEM, in-situ TEM

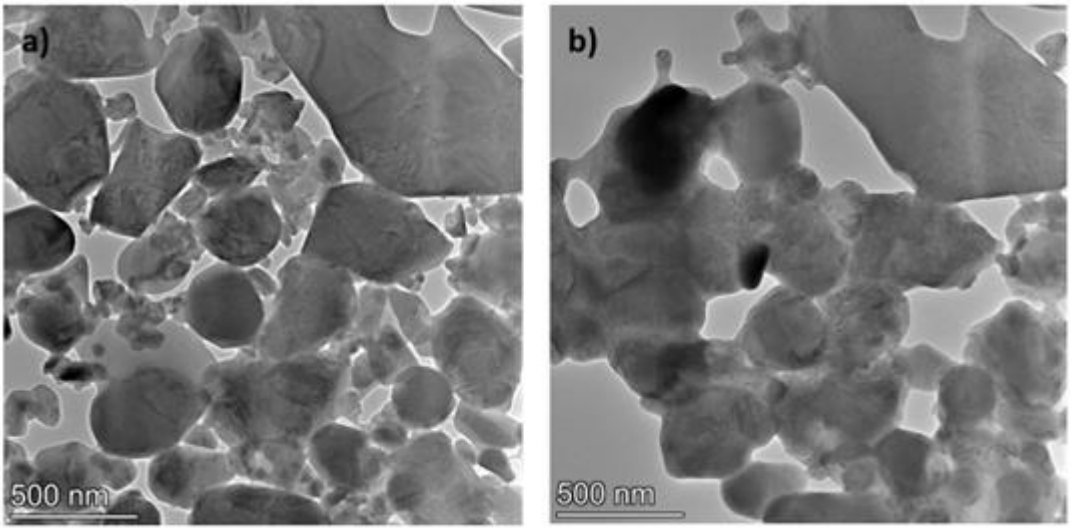

ON THE ACCURACY OF ATOMIC-RESOLUTION DPC-STEM MEASUREMENTS

Rafael V. Ferreira (Portugal)[5,6]; Sebastian V. Calderon (United States of America)[1]; Ricardo M. Ribeiro (Portugal)[2]; Deji Akinwande (United States of America)[3,4]; Paulo J. Ferreira (Portugal)[4,5,6]

1 - Department of Materials Science and Engineering, Carnegie Mellon University; 2 - Department and Centre of Physics, University of Minho; 3 - Microelectronics Research Center, Department of Electrical and Computer Engineering, The University of Texas at Austin; 4 - Materials Science and Engineering Program, The University of Texas at Austin; 5 - INL – International Iberian Nanotechnology Laboratory; 6 - IDMEC, Instituto Superior Técnico

Abstract

The study of prevalent defects and their impact on functional properties is a critical issue for the successful implementation of 2D materials in next-generation devices. However, the direct quantitative characterization of a specific defect is a challenging task, requiring atomic-resolution measurements that are sensitive to the electronic structure of the material. The use of differential phase contrast (DPC) in scanning transmission electron microscopy (STEM) is particularly promising for this purpose, leveraging the natural coupling between the electron probe and the atomic-scale electric fields within a sample, which leads to a redistribution of intensity at the diffraction plane. For thin specimens, the centre of mass (CoM) of the diffraction disc is then directly related to the phase gradient, allowing for the mapping of electrostatic forces between atoms of the material structure, a capability which has already been demonstrated in the study of several 2D materials [1–4].

CoM measurements can be performed with pixelated detectors, capable of recording the entire diffraction disc, or with segmented annular detectors that integrate the intensity of the disk over independent quadrants. Pixelated detectors offer the greatest accuracy, but the faster processing times associated with segmented detectors allow for the generation of DPC-STEM images in real time, making it easier to identify interesting features and to correct aberrations. These benefits, along with the fact that segmented detectors are still the most accessible option, make it worthwhile to explore methodologies to manage their reduced accuracy. For this reason, it is essential to understand the precise effect of instrumental parameters on segmented-detector DPC-STEM, such that their influence may be accounted for when analysing the results.

In this work, the influence of key instrumental parameters – probe convergence angle, defocus and detector orientation – on atomic-resolution segmented-detector DPC-STEM measurements is evaluated through extensive image simulations of MoS_2 and some of its defects. The qualitative effects on electrostatic field and potential maps are identified, along with the quantified impact on the accuracy of the measurements. Finally, conclusions applicable to the observation of 2D materials in general are drawn from this simulation-based study. The gathered observations are then employed in the analysis of experimental images from similar materials and defects.

Acknowledgments

Rafael V. Ferreira acknowledges funding from the Portuguese Science and Technology Foundation (FCT) through the Ph.D. studentship SFRH/BD/149390/2019.

References

[1] Ishikawa, R., et al, Nat. Commun. 9 (2018), p. 3878.
[2] Müller-Caspary, K., et al, Phys. Rev. B 98 (2018), p. 121408.
[3] Fang, S., et al, Nat. Commun. 10 (2019), p. 1127.
[4] Calderon V., S., et al, Nano Letters 21(24) (2021), p.10157.

Keywords: Differential Phase Contrast, 2D materials, Multislice simulations

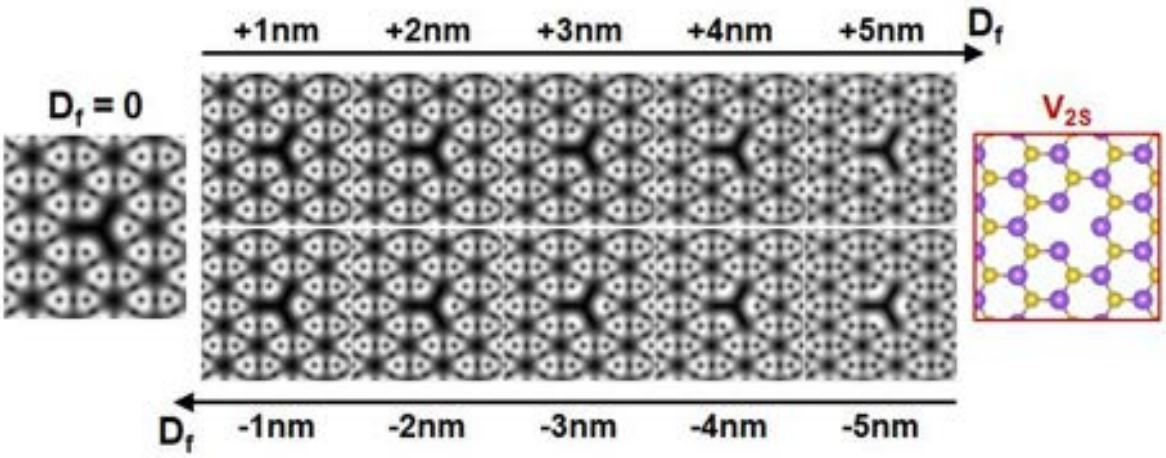

TRACKING ATMOSPHERE-DEPENDENT PHASE TRANSFORMATIONS: EXPLORING THE CAPABILITIES OF GAS-CELL IN SITU ELECTRON MICROSCOPY

Ramón Manzorro (Spain)[1]; Carmen Mora (Spain)[1]; Lidia E. Chinchilla (Spain)[1]; Miguel López-Haro (Spain)[1]; José A. Pérez-Omil (Spain)[1]; José J. Calvino (Spain)[1]; Ana B. Hungría (Spain)[1]

1 - Universidad de Cádiz, Departamento de Ciencia de los Materiales e Ingeniería Metalúrgica y Química Inorgánica

Abstract

Environmental catalysis has always been a topic that has received significant attention, although given the current energy crisis seeking for renewable, green energy sources is now of primary interest. O_2 and/or H_2 are usually involved, either as reactants or as products, and accordingly redox reactions play a key role in the understanding of the reaction pathway and its mechanism, which is intimately linked to the catalyst performance. Therefore, an in-depth study of these systems opens up the opportunity to improve the catalytic activity and selectivity. However, catalysts are dynamic entities prone to suffer structural and chemical transformations [1], which lay out of the scope of conventional electron microscopy, which provides information about a ground state before the reaction and post-mortem state after the reaction. In this context, gas-cell *in situ* electron microscopy has recently arisen as a crucial tool to directly visualize at the nano and even atomic-scale the phenomena taking place during catalytic reactions.

To gain a valuable insight about the behavior of reducible materials under reaction conditions, we have characterized CuO and CeO_2 samples, which are typically employed in catalytic formulations for redox reactions, in reducing and oxidizing atmospheres by means of *in situ* electron microscopy. To do so, a DENS Solutions Climate holder in a double-corrected FEI Titan Cubed at 200 kV has been employed. The phase transformations related to temperature and gas flow in electron-transfer reactions entail chemical changes, like a shift in the valence state, and structural changes triggering a modification in the crystal lattice. In spite of intrinsic limitations of the system itself, e. g. membrane thickness, this gas-dependent evolution has been determined using electron diffraction, electron energy loss spectroscopy and imaging techniques, when possible.

Finally, it has been lately reported that besides chemical environment and temperature, total pressure inside the reactor may also change drastically the outcome of the catalytic reaction [2], meaning that boundary conditions are of major importance in the final results. To evaluate phenomena potentially related to heat and mass transport, we have compared our *in situ* findings related to the behavior of reducible oxides with macroscopic ex situ measurements carried out in a conventional reactor.

Acknowledgments

The authors gratefully acknowledge funding from Junta de Andalucía, 18INPA2003, and Plan Propio from UCA (20 VI.IN.0605).

References

[1] J. L. Vincent et al. Nature Communications, 2021. 12, 5789.

[2] A. Beck et al. Nature Catalysis, 2021. 4, 488.

Keywords: In situ TEM, Nanoparticles

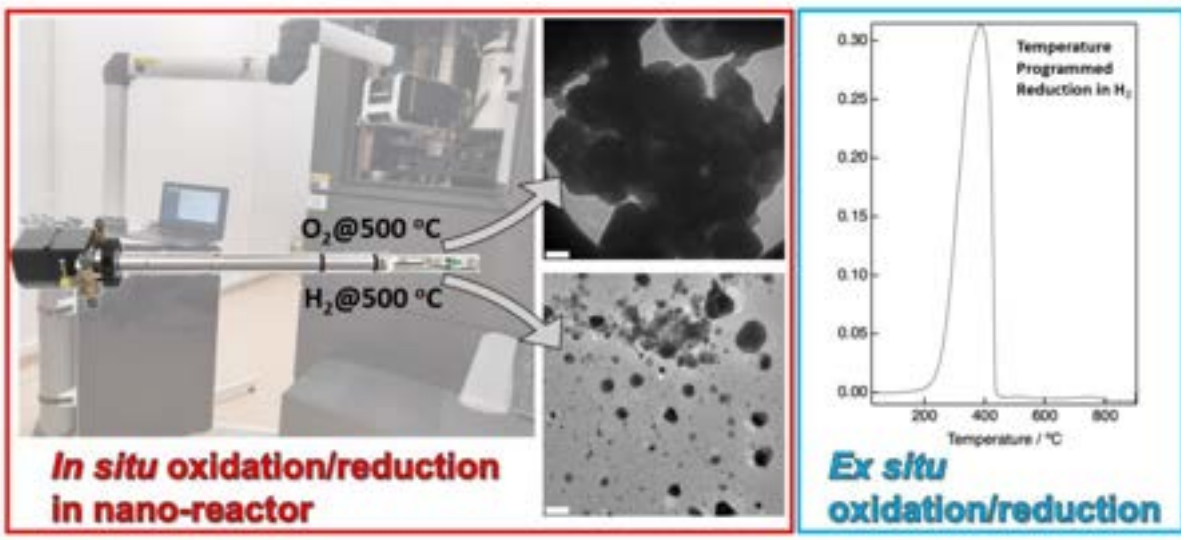

COMBINING TEM IN-SITU AND MONOCHROMATED EELS EXPERIMENTS WITH ELECTROCHEMICAL AND PHOTOELECTROCHEMICAL CHARACTERIZATIONS OF AU@MOS2 NANOPARTICLES TO UNRAVEL THEIR PHYSICAL AND CHEMICAL PROPERTIES TOWARDS HYDROGEN EVOLUTION REACTION

Juan José Quintana González (Spain)[1]; Antonio Jesus Medina Olivera (Spain)[1,2]; Ramón Manzorro Ureba (Spain)[1,2]; Cédric Pardanaud (France)[3]; Ana Belén Hungría (Spain)[1,2]; Laura Cubillana Aguilera (Spain)[2,4]; José María Palacios Santander (Spain)[2,4]; Juan Carlos Hernández Garrido (Spain)[1,2]; Luc Lajaunie (Spain)[1,2]

1 - Department of Materials Science, Metallurgical Engineering and Inorganic Chemistry. Faculty of Sciences. University of Cadiz. Campus Universitario de Puerto Real. 11510 Puerto Real, Spain.; 2 - University Institute of Research on Electron Microscopy and Materials (IMEYMAT), Faculty of Sciences. Campus Universitario de Puerto Real. University of Cadiz, 11510 Puerto Real, Spain; 3 - Aix-Marseille Université, CNRS, PIIM UMR 7345, F-13397, Marseille, France; 4 - Department of Analytical Chemistry, Faculty of Sciences. University of Cadiz. Campus Universitario de Puerto Real, 11510 Puerto Real, Spain

Abstract

One of the biggest challenges facing the development and profitability of new ways to obtain H_2 by water splitting method is to find new materials for Hydrogen Evolution Reaction (HER) electrocatalysis that are not based on Pt, with the aim to obtain electrodes which are both performant and sustainable [1]. The synthesis of MoS_2-based materials is one of the most promising strategies. In particular MoS_2-Au hybrid systems have shown high HER activity, and the plasmonic properties of gold makes it an interesting proposal in photoelectrocatalysis. [2-4].

In this work, we report the synthesis and complete physical and chemical characterization of Au@MoS_2 core-shell nanostructures that have been submitted to a thermal reduction in hydrogen to increase the activity of these particles via a precise control of the number of shell layers and associated defects. The samples have been characterized in a double-corrected FEI Titan Cubed, by means of HR-(S)TEM and STEM-EDS techniques. These analyses have confirmed the formation of core-shell nanostructures with a mean diameter of 9.8 ± 4.2 nm for the pristine sample. Moreover, the study of the reduced samples establishes an inverse relationship between the treatment temperature and the number of shell layers. In order to further confirm this trend determined in conventional TEM studies, gas-cell in-situ TEM experiment (Climate Holder, DENS Solutions) has been performed to track the evolution of these structures while increasing the temperature under H_2 atmosphere, which supports the ex-situ studies. In addition, Raman and XPS spectroscopies were performed too, revealing the presence of chemical inhomogeneities and highlighting the presence of defects.

To rule out the influence of these structural modifications in the electrochemical HER behaviour under acidic conditions, electrochemical properties of the Au@MoS_2 hybrids samples were also measured. HER experiments were performed in a standard three-electrodes cell with H_2SO_4 0.5 M as electrolyte. Au@MoS2 nanostructures have exhibited better activity compared to the MoS_2 bulk sample, and additionally, the H_2-reduced Au@MoS_2 sample even better, showing the best HER activity. Finally, it has been demonstrated as well that when the sample is irradiated with different led lamps (different wavenumber), the plasmonic response of these nanostructures increases their activity respect to the dark conditions.

Acknowledgments

The authors acknowledge the use of (S)TEM instrumentation provided by the National Facility ELECMI ICTS ("División de Microscopia Electrónica", Universidad de Cádiz, DMEUCA). This research was funded by the European Union's Horizon 2020 research and innovation program (grant agreement 823717–ESTEEM3), the Spanish Ministerio de Economía y Competitividad (PID2019-107578GA-I00), the Ministerio de Ciencia e Innovación MCIN/AEI/10.13039/501100011033, and the European Union "NextGenerationEU"/PRTR (RYC2021-033764-I, CPP2021-008986).

References

[1] Q. Ding, B. Song, et al. Chem. 2016, 1(5), 699-726.
[2] G. Zhang, H. Liu, et al. Energy Environ. Sci. 2019, 128, 274-297.
[3] R. Bar-Ziv, P. Ranjan, et al. ACS Appl. Energy Mater. 2019, 2(8), 6043-6050. [5] L. Li, Z. Qin, et al. ACS Nano. 2019, 13(6), 6824–6834.
[4] L. Li, Z. Qin, et al. ACS Nano. 2019, 13(6), 6824–6834.

Keywords: Plasmonic Materials, in-situ gas cell, H2 Production, HER Reaction, 2D Materials

RATIONALIZING THE ROLE OF METAL-SUPPORT INTERFACE STRUCTURE ON THE CATALYTIC PERFORMANCE OF PD/CEO2 NANOCATALYSTS IN CO OXIDATION: CONTRIBUTION OF QUANTITATIVE 3D ELECTRON TOMOGRAPHY

José Marqueses (Spain)[2]; Justyna Grzonka (Spain)[2]; Antonio Jesús Jiménez-Benítez (Spain)[2]; Lionel C. Gontard (Spain)[1]; Ana Belén Hungría (Spain)[2]; José Juan Calvino (Spain)[2]; Miguel López-Haro (Spain)[2]

1 - Departamento de Física de la Materia Condensada. Facultad de Ciencias. Universidad de Cádiz; 2 - Departamento de Ciencia de los Materiales e Ingeniería Metalúrgica y Química Inorgánica. Facultad de Ciencias. Universidad de Cádiz

Abstract

The role of the interface structure between metal nanoparticles and oxide substrates is a hot topic in Heterogeneous Catalysis. To this end, the catalytic performance of materials in which the metal particles are distributed over the surface of substrates with different morphologies is investigated. Routinely, in these studies, the crystallography of metal-oxide contacts is determined from 2D High Resolution (HRTEM or HRSTEM) images. Nevertheless, this is an incorrect approach, since 2D images cannot reveal the actual distribution of the metal particles onto the surface of the support; for this, 3D information is required. Strictly speaking, the combination of HR images with Electron Tomography (ET) experiments is necessary to face this question on reliable basis.

HAADF-STEM ET has proven quite useful to reveal the spatial distribution of metal nanoparticles onto the surface of a variety of supports, including even some which incorporate heavy (high Z) elements, as it is the case of 4f element oxides (1). Among these, CeO_2 is the most studied in relation with the role of interface structure.

ET studies of nanoparticles supported on CeO_2 is quite challenging (2), due to the limitations imposed by the contrast mechanisms of HAADF images. In fact, ET becomes particularly complex when the metal nanoparticles are made of elements lighter than Ce (Z=58), like Pd (Z=46). Thus, in Pd/CeO_2 nanocatalyst, ET studies based on conventional procedures totally fail to detect the light metal nanoparticles and to reveal the details of their distribution onto the CeO_2 crystallites, Figure 1(a).

In this contribution we will report how by using an approach which combines advanced Compressed-Sensing based reconstruction algorithms with the use of different types of Deep Learning Neural Networks, it is not only possible to precisely detect even subnanometer-sized Pd nanoparticles, but also to determine, in full quantitative terms, their morphology, distribution over the CeO_2 crystallites and some growth parameters related to the strength of metal-support interaction, Figure 1(b). The information obtained after the analysis of different catalysts allows also to conclude about the influence of crystallographic planes exposed at the surface of ceria on the intrinsic catalytic performance of the metal atoms.

The developed DL-CS methodology can be fruitfully applied to a wide range of other nanomaterials mixing a light (low Z) component with a second, heavier one.

Acknowledgments

This work has received support from Projects: PID2020-113006-RB-I00, PID2019-110018GA-I00, funded by MCIN/AEI/10.13039/501100011033. This work has also been co-financed by the 2014–2020 ERDF Operational Program, the Department of Economy, Knowledge, Business and University of the Regional Government of Andalusia, Project references: FEDER-UCA18-107139 and by MCIU/AEI/ERDF-EU through project PGC2018-101538-A-I00. STEM ET experiments were recorded at the DME-UCA Node of the Spanish Singular Infrastructure for Electron Microscopy of Materials (ICTS ELECMI).

References

(1) W. Jiang, W. Ji, C.-Tong Au, *ChemCatChem*, 2018, 10, 2125 – 2163

(2) J.C. González, J.C. Hernández, M. López-Haro et al., *Angew. Chem. Int. Ed*. 2009, 48 (29), 5313-5315

Keywords: Electron Tomography, Compressed Sensing, Deep Learning, Neural Networks, Nanocatalysts

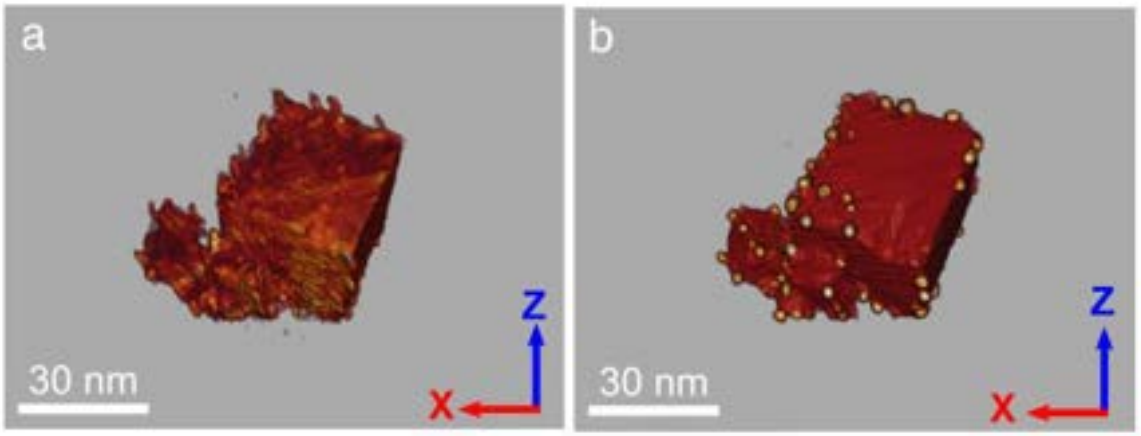

DEGRADATION MECHANISM OF ACRYLIC RESIN BASED MATERIALS UNDER STEM CONDITIONS

Luisa Valencia (Spain)[1]; Alberto Sanz De Leon (Spain)[1]; Miriam Herrera (Spain)[1]; Sergio Molina (Spain)[1]; María De La Mata (Spain)[1]

1 - Universidad de Cádiz

Abstract

Polymers offer a rich playground for the development of novel lightweight materials with appealing processing capabilities for 3D printing technologies, whose smart engineering strongly benefits from (S)TEM analyses. Within this context, acrylic resins are versatile candidates widely employed themselves or combined within other phase leading to composites. Regrettably, the possible electron beam damage during (S)TEM measurements hinders the analysis of polymer based materials and composites, comprising the attainable resolution and accurateness of the measurements, due to the interplay of several factors, including the quality of the specimen, electrostatic charging effects, radiolysis and knock-on phenomena.

We have analyzed the induced electron beam damage during STEM-EELS analyses performed on acrylic-based materials[1,2]. We have monitored the spectral changes with the accumulated electron dose by means of dual-EELS time series acquisition in order to address compositional changes and structural variations of the acrylic resin until breakage. The acrylic resin losses mass as function of the accumulated electron dose by the sequential effect of radiolysis followed by knock-on damage[3]. Moreover, the addressed core-loss changes with increasing electron doses indicates differentiated losing rates for carbon and oxygen, along with an increasing π character of the C (see Figure 1), suggesting likely decomposition pathways involving the removal of CO and CO_2 from acyl and carboxylic radicals. The results also allow estimating the critical electron doses for the different phenomena driving the material degradation, ensuring safe experimental conditions for the successful STEM characterization of acrylic-based materials

Acknowledgments

This work has been co-financed by the 2014-2020 ERDF Operational Programme and by the Department of Economy, Knowledge, Business and University of the Regional Government of Andalucía (Ref: FEDER-UCA18-106586). Co-funding from UE and Junta de Andalucía (research group INNANOMAT, ref. TEP946) are also acknowledged. TEM/STEM measurements were carried out at the DME-SC-ICyT-ELECMI-UCA.

References

[1] L. M. Valencia, M. Herrera, M. de la Mata, A. S. de León, F. J. Delgado, S. I. Molina. *Synthesis of Silver Nanocomposites for Stereolithography: In Situ Formation of Nanoparticles*. Polymers **14**, 1168 (2022).
[2] L. M. Valencia, M. Herrera, M. de la Mata, J. Hernández-Saz, I. Romero-Ocaña, F. J. Delgado, J. Benito, S. I. Molina. *Stereolithography of Semiconductor Silver and Acrylic-Based Nanocomposites*. Polymers **14**, 5238 (2022).

[3] L. M. Valencia, M. de la Mata, M. Herrera, F.J. Delgado, J. Hernández-Saz, S. I. Molina. *Induced damage during STEM-EELS analyses on acrylic-based materials for Stereolithography*. Polymer Degradation and Stability **203**, 110044 (2022).

Keywords: STEM-EELS, degradation mechanisms, acrylic resin, accumulated electron dose, radiolysis, knock-on damage

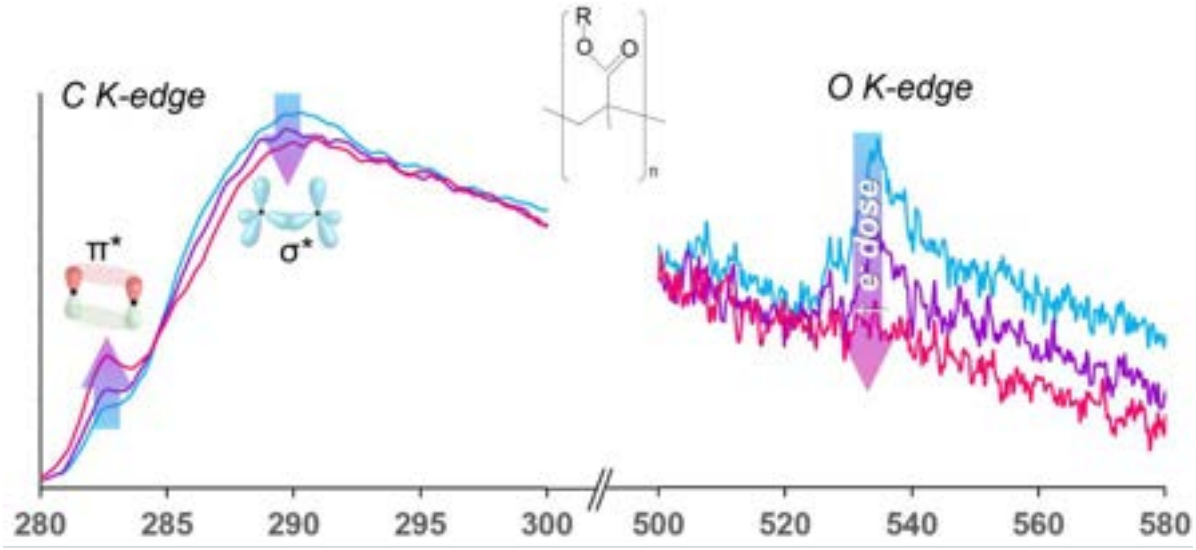

Figure 1. EELS C and O K-edges from the acrylic resin for different accumulated electron doses (arrows point towards increasing electron doses), evidencing the spectral evolution due to the electron irradiation[3].

PLASMONIC, PHOTOCATALYTIC AND HYDROGEN EVOLUTION REACTION PERFORMANCES OF (TBA)2AG2[MO8O26] NANOWIRES AND A NEW AG@(TBA)2AG2[MO8O26] NANOSTRUCTURE

Luc Lajaunie (Spain)[1]; Juan José Quintana Gonzalez (Spain)[1]; José Manuel Montes Monroy (Spain)[1]; Juan Carlos Hernandez Garrido (Spain)[1]; José Antonio Pérez Omil (Spain)[1]; Rémi Dessapt (France)[2]

1 - Department of Materials Science, Metallurgical Engineering and Inorganic Chemistry. Faculty of Sciences. University of Cadiz; 2 - Nantes Université, CNRS, Institut des Matériaux de Nantes Jean Rouxel

Abstract

Plasmonic hybrid nanostructures assembling nanoparticles (NPs) of noble metal and metal-oxide nanowires (NWs) are interesting since they combine the localized surface plasmon resonance (LSPR) of metals with the specific photochemical properties of oxides [1-2]. In this work, we report the synthesis, plasmonic and catalytic properties of hybrid organic-inorganic $(TBA)_2Ag_2[Mo_8O_{26}]$ (TBAAgMo) NWs (TBA = tetrabutylammonium), and of a new plasmonic nanostructure. Upon UV irradiation, the NWs form an unprecedented plasmonic $Ag@(TBA)_2Ag_2[Mo_8O_{26}]$ nanostructure. The physical and chemical properties of the NWs were investigated in details before and after UV irradiation. In particular, the structure and local chemistry of the NWs were investigated by aberration-corrected transmission electron microscopy as well as Raman and XPS spectroscopies. In addition, monochromated EELS measurements were performed to determine the plasmonic properties of the nanostructure at the nanoscale. Photocatalytic measurements were performed through the oxidation of methylene blue (MB) under simulated sunlight. Hydrogen evolution reaction (HER) measurements were carried out in a standard three-electrode cell in 0.5 M H_2SO_4.

Figure 1a show the SEM micrograph of the TBAAgMo NWs which have aa length of several microns. After UV irradiation, NPS can be observed by TEM at the surface of the NWs (Figure 1b). The NPs have a size of several hundreds of nm and the EDS analyses show that the NPs correspond to areas rich in Ag. In addition, the HRTEM micrographs highlight the high crystalline quality of the Ag NPs with a crystallographic structure corresponding to metallic Ag. All these results show that UV irradiation induced the formation of Ag^0 NPs. In addition, the presence of strong localized surface plasmon resonance excitations can be observed at the surface of the Ag NPs (Fig. 1c). Several resonance modes are highlighted including one located between 2.3 and 3.7 eV in the energy range expected for Ag LSPR. In addition, in both dark and under light-irradiation, a strong adsorption of MB can be highlighted at the surface of the NWs. The complete degradation of MB is then observed after ~ 30 min. The TBAAgMo NWs present better photocatalytic properties than TiO_2 P25 reference sample. The reduction of Ag also induces a decrease of both the overpotential and Tafel slope making theses samples interesting candidates for photoelectrochemical HER. All these results will be presented in details.

Acknowledgments

This research was funded by the Andalusian regional government (FEDER-UCA18-107490), the European Union's Horizon 2020 research and innovation program (grant agreement 823717–ESTEEM3), the Spanish Ministerio de Economía y Competitividad (PID2019-107578GA-I00), the Ministerio de Ciencia e Innovación MCIN/AEI/10.13039/501100011033, and the European Union "NextGenerationEU"/PRTR (RYC2021-033764-I, CPP2021-008986). The authors acknowledge the use of (S)TEM instrumentation provided by the National Facility ELECMI ICTS ("División de Microscopía Electrónica", Universidad de Cadiz, DME-UCA).

References

[1] Hakouk et al. "Plasmonic properties of an $Ag@Ag_2Mo_2O_7$ hybrid nanostructure easily designed by solid-state photodeposition from very thin $Ag_2Mo_2O_7$ nanowires." J. Mater. Chem. C . 6.41 (2018): 11086-11095.

[2] Hakouk et al. "Novel soft-chemistry route of $Ag_2Mo_3O_{10}{\cdot}2H_2O$ nanowires and in situ photogeneration of a $Ag@Ag_2Mo_3O_{10}{\cdot}\ 2H_2O$ plasmonic heterostructure." Inorg. Chem. 52.11 (2013): 6440-6449.

Keywords: EELS, Plasmonic, Photocatalysis, Electrocatalysis

Figure 1: a) SEM Image of the $(TBA)_2Ag_2[Mo_8O_{26}]$ nanowires, b) Superposition of TEM micrograph and EDS elemental maps. The red circle highlights the area used to acquire the EELS data c) Dark field (DF) image (DF) and EELS plasmonic maps acquired in the energy range 2.3-3.7 eV.

THE USE OF FIB AS A NEW TECHNIQUE FOR CHARACTERIZING SURFACE DEFECTS IN STAINLESS STEELS

Andrés Ruiz Flores (Spain)[1]; Andrés Nuñez Galingo (Spain)[1]; Irene Collado García (Spain)[2]; Ana Vargas Velasco (Spain)[3]; Juan Francisco Almagro Bello (Spain)[3]

1 - Laboratory & Research section, Technical Department, Acerinox Europa S.A.U; 2 - LABCYP, Materials Sciences and Inorganic Chemistry Department, University of Cadiz (Spain).; 3 - Laboratory & Research section, Technical Department, Acerinox Europa S.A.U.

Abstract

Over the last 20 years, Focused Ion Beam (FIB) has become one of the dominant techniques for 3D characterization of the materials [1,2]. New advances in the knowledge of stainless steel could not be conceived without the rise of this technique [3]. FIB offers a large number of advantages over traditional characterization methods [4]: it is extremely selective and allows to be sure that the most superficial layers of the sample are being observed [5].

In this study, FIB technique was used to achieve a better understanding of some surface defects related to stainless steels. In this case, a “sliver” or internal oxidation defect [6] and oxide scale were characterised by FIB-SEM.

References

[1] V. Le, M. Milani, F. Tatti, 2010 *Focused ion beam (FIB)/ scanning electron microscopy (SEM) in tissue structural research*, Protoplasma. 246 41–48.

[2] L. Gu, N. Wang, X. Tang, H.G. Changela, 2010 *FIB-SEM Techniques for the Advanced Characterization of Earth and Planetary Materials*, Wiley.

[3] J. Perret, E. Boehm-courjault, M. Cantoni, S. Mischler, A. Beaudouin, W. Chitty, J. Vernot, 2010 *EBSD , SEM and FIB characterisation of subsurface deformation during tribocorrosion of stainless steel in sulphuric acid*, Wear. 269 383–393.

[4] L.A. Giannuzzi, B.W. Kempshall, S.M. Schwarz, J.K. Lomness, B.I. Prenitzer, F.A. Stevie, 2005 *in: Introduction to Focused Ion Beams* Chapter 10. FIB lift-out specimen preparation techniques.

[5] D. Drobne, M. Milani, V. Leser, 2007 *Surface Damage Induced by FIB Milling and Imaging of Biological Samples is Controllable*, Microsc. Res. Tech. 70.

[6] G. Wenfang, 2012 *Formation and Prevention of Sliver Defects on the Surface of Cold-rolled Strip*, Adv. Mater. Res. 402 221–226.

[7] I.A. Carlos. C.S. Caruso 1997 *Electrodeposition of iron fragile layer on nickel substrate with emphasis on iron powder production*, Journal of Power Sources. 73 199-203

Keywords: Stainless Steel, Focused Ion Beam, Surface Characterization, Oxide Layer, Surface Defects

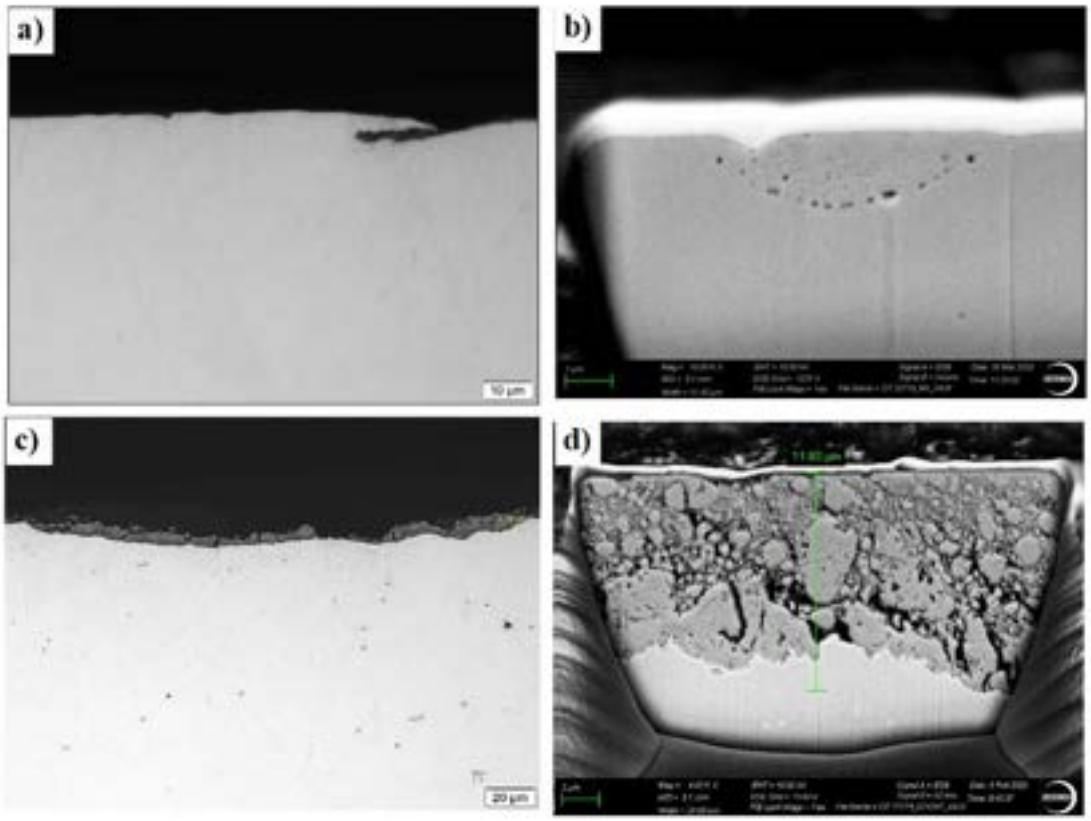

Fig. 1 a) and b) shows a comparison between traditional polishing methods and a cross section on austenitic stainless steel EN 1.4301, respectively. No inclusions nor internal oxidation was observed through traditional cross-sections, Fig. 1 a). On the other hand, Fig. 1 b) shows that the internal oxidation can be observed using FIB. Normally, when the sliver defect is formed in the subsurface region of the steel, it is likely to be removed by traditional polishing. Therefore, the characterization of this defect it is not possible to be carried out without the FIB technique.

Fig. 1 c) and d) shows the results of the cross section characterization of an oxide scale formed on a stainless steel EN 1.4509 during hot rolling process. Considering that this oxide scale is very fragile, the use of specific conventional methods for its maintenance is not adequate [7], therefore, its characterization can only be carried out by FIB. Fig. 1 c) provides a cross section of the oxide scale obtained by traditional polishing methods, whereas Fig. 1 d) shows a cross section achieved by FIB-SEM. According to the optical image of Fig. 2 (a), using traditional polishing methods, the observed thickness of the oxide scale is around 8.68 µm. On the other hand, FIB polishing method allowed to estimate that the thickness of the oxide scale is about 11.92 µm. Moreover, a high-quality cross section is reached by FIB-SEM, where the fragility of the oxide scale could be confirmed and EDS analysis was developed. This analysis allowed to obtain elemental concentration profiles of the oxide scale, where the strata distribution of the different species was studied as well as the oxidation kinetic of stainless steels EN 1.4509 during the hot rolling process.

TRANSMISSION ELECTRON MICROSCOPY AND RELATED TECHNIQUES APPLIED TO INDUSTRIAL FERRITIC STAINLESS STEEL: UNDERSTANDING THE ORIGIN OF THE GOLD DUST DEFECT

Andrés Ruiz Flores (Spain)[1]; José Juan Calvino Gámez (Spain)[2]; Andrés Núñez Galindo (Spain)[1]; Juan Francisco Almagro Bello (Spain)[1]; Luc Lajaunie (Spain)[2]; Beatriz Amaya Dolores (Spain)[1]

1 - Acerinox Europa S.A.U. Avenue ACERINOX EUROPA, s/n 11379, Los Barrios (Cádiz), Spain.; 2 - Department of Materials Science and Metallurgical Engineering and Inorganic Chemistry. University of Cádiz, Avenue República Árabe Saharaui, 11519, Puerto Real (Cádiz), Spain.

Abstract

Introduction. Some difficulties remain in the production process of the AISI 430 ferritic stainless steels (FSS) which need to be overcome. In particular, a surface defect called the gold dust defect (GDD) can be observed sometimes at the end of the production process, which is not completely controlled. [1–4]. It was shown that the GDD is correlated to an inadequate recrystallization of the ferritic grains resulting in a particular top-layer structure with smaller grains than those in the FSS matrix [1,2].

Experimental. In this work, we have studied the morphology, the chemical composition and the recrystallization of the microstructure of a FSS affected by the GDD flake. To this end, we combined several techniques such as optical microscopy, a FIB microscopy, EBSD, TEM as well as electron spectroscopies including monochromated EELS and EDS. In particular, monochromated EELS was analysed by using K-means clustering algorithms in order to shed a new light on the local chemistry of the FSS affected by the GDD. Finally, to study the relationship between the GDD and the recrystallization of the grains as well as to determine the origin of the GDD, the same AISI 430 FSS sample was studied in different stages of the production line.

Results and conclusions. The lamella made on a GDD flake (Figure 1a) shows that it is composed by a top-layer which is usually separated from the FSS matrix by cracks (Figure 1b). The cracks are usually oxidised and rich mostly in O, Cr and Mn where Cr and Mn are distributed heterogeneously. The results of the Cr-L_3,L_2 ratio map (Figure 1c) coincides with the K-means clustering results (Figure 1d). Specifically, the ratios 1.3 ± 0.1 and 1.7 ± 0.1 correspond according to the literature to Cr^0 and Cr_2O_3. Another ratio of 2.4 ± 0.2 was found which coincides with areas where the Mn content is higher (highlighted as “2” in Figure 1) and might be ascribed to the spinel $MnCr_2O_4$, which has already been identified in this FSS [5,6]. In addition, EBSD results (Figure 1e) show that the flake usually presents a random crystalline orientation compared to the rest of the grains which have recrystallized properly after the final annealing. The studies have shown that hot-rolling is a decisive step in the production process. All these results will be described in detailed in order to highlight the origin of the GDD in FSS and to demonstrate the contribution of electron microscopy to extract a maximum of information from the defect.

Acknowledgments

The authors acknowledge the use of (S)TEM instrumentation provided by the National Facility ELECMI ICTS ("División de Microscopía Electrónica", Universidad de Cadiz, DME-UCA) and the use of the Microscope for EBSD analysis provided by ACERINOX EUROPA S.A.U. The authors also acknowledge Dr. Lidia Esther Chinchilla who carried out the monochromated EELS measurements.

References

[1] B. Amaya, A. Ruiz, A. Núñez, J. Calvino, J. Almagro and L. Lajaunie., "Textural, Microstructural and Chemical Characterization of Ferritic Stainless Steel Affected by the Gold Dust Defect"., Materials. 16 (2023) 1825. https://doi.org/10.3390/ma16051825.

[2] Beatriz Amaya Dolores, Ilse Letofsky-Papst, Manuel Domínguez, Andrés Núñez Galindo, José Juan Calvino Gámez, Juan Francisco Almagro Bello and Luc Lajaunie., "Multiscale Analysis of the Gold Dust Defect in AISI 430 Industrial Stainless Steels: Influence of the Aluminum Content". Vol, 2-3, 2022., Materials. 74 (2022) 4059–4068.

[3] S. Mithra, P. G. Venkatakrishnan, D. Noorullah and V. Karthik., "Sensitization of Gold Dust in 430 Grade Stainless Steel"., Int. J. Adv. Eng. Manag. Sci. (2017) 4–110.

[4] S. Mithra, P. G. Venkatakrishnan, D. Noorullah, V. Karthik., (2018). "Failure Analysis of Gold Dust defect in 430 grade Stainless Steel"., Materials and Manufacturing. (2018) 1–2. https://doi.org/10.1088/1757-899X/314/1/012003.

[5] P. Navarro, A. Núñez, J. Almagro and J. Odriozola., "Analysis of oxide scales on oxidised EN 1.4509 ferritic stainless steel catalyst support by scanning electron microscopy"., Mater. Sci. Eng. (2020) 891. https://doi.org/10.1088/1757-899X/891/1/012017.

[6] I. Collado, A. Núñez, J. Almagro, J. González and J. Botana., "Characterisation of High Temperature Oxidation Phenomena during AISI 430 Stainless Steel Manufacturing under a Controlled H2 Atmosphere for Bright Annealing"., Metals. 11 (2021) 191. https://doi.org/10.3390/met11020191.

Keywords: Ferritic Stainless Steels, Surface Defect, Gold Dust Defect, FIB, EELS, Kmeans-Clustering

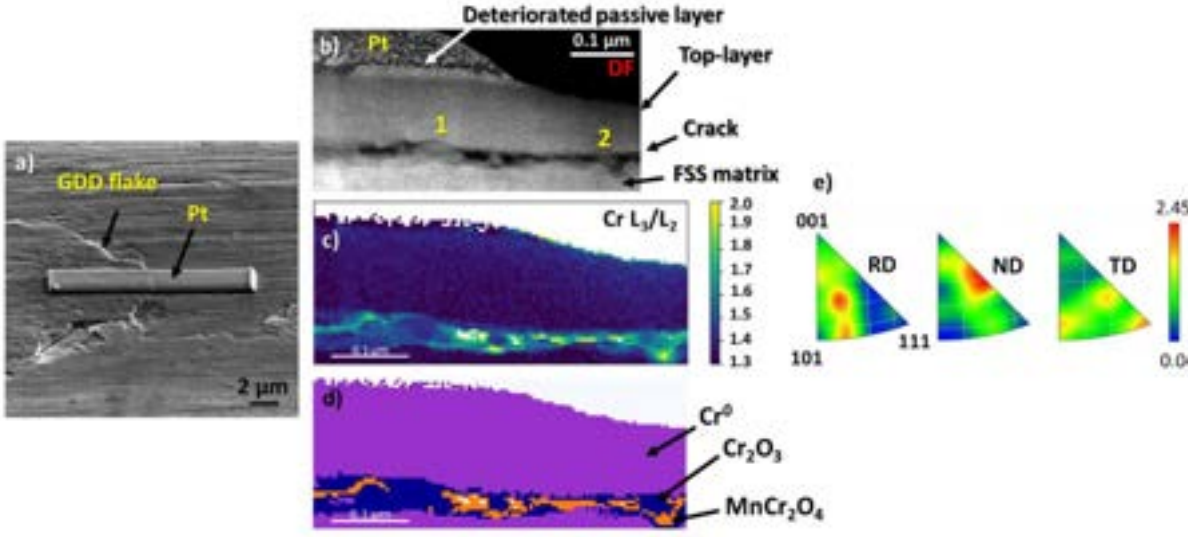

A NOVEL APPROACH USING GENERATIVE ADVERSARIAL NETWORKS FOR DATA AUGMENTATION IN ELECTRON ENERGY LOSS SPECTROSCOPY SUPERVISED CLASSIFICATION

Daniel Del Pozo Bueno (Spain)[1,2]; Francesca Peiró (Spain)[1,2]; Sònia Estradé (Spain)[1,2]

1 - LENS-MIND, Departament d'Enginyeria Electrònica i Biomèdica, Universitat de Barcelona; 2 - Institute of Nanoscience and Nanotechnology (IN2UB)

Abstract

In recent years, Transmission Electron Microscopy (TEM), and more specifically, Scanning Transmission Electron Microscopy (STEM), has experienced considerable advancements in its technical capabilities. These improvements stem not only from technological enhancements of the equipment, such as aberration correctors and direct electron detectors, but also from increases in computer processing power. As a result, the acquisition of large amounts of data has become usually, leading to a need within the STEM community for innovative tools to manage and analyze this wealth of data efficiently and accurately. In particular, the Electron Energy Loss Spectroscopy (EELS) community has reported numerous studies wherein Machine Learning (ML) strategies have successfully been employed for spectral analysis.

In this study, we focus on EELS technique and ML algorithms, which can broadly be categorized into two main branches: supervised and unsupervised learning. Supervised algorithms necessitate prior data, i.e., labels, of the attributes we aim to examine to train the models. In contrast, unsupervised algorithms do not require prior data for data analysis. Both types have been applied to EELS spectra; supervised learning as a classifier[1,2], and unsupervised learning for tasks such as classifying different regions in spectrum images based on their composition or for denoising tasks[3–5]. However, it's crucial to apply unsupervised methods with caution, as their interpretations can be significantly more complex, as they do not necessarily identify the properties in which we are interested.

Concerning supervised algorithms, they necessitate a substantial amount of labeled data to generate generalizable and reliable models. This requirement presents a challenge in the context of EELS, as samples are often susceptible to damage under the electron beam. To address this issue, we introduce a novel data augmentation method for EEL spectra, leveraging Generative Adversarial Networks (GANs)[6]. Utilizing GANs, we only require a small quantity of training spectra to produce generators capable of creating synthetic spectra that are suitable for training supervised classification models. Consequently, this approach enables us to establish EELS classifiers using a significantly reduced number of spectra while simultaneously maintaining a substantial training data set for the classifier.

Acknowledgments

This work has been supported by the Spanish Project PDC2021-121366-I00 financed by MCIN/AEI/10.13039/501100011033 and by the European Union NextGenerationEU/PRTR. The authors also acknowledge funding from MICIIN under the project PID2019-106165GB-C21, the support received from the ELECMI - ICTS Electron Microscopy for Materials Science and the funding from Gencat under project 2021SGR00242 and the 2020 FI-SDUR grant from the AGAUR agency of the Generalitat de Catalunya.

References

(1) del-Pozo-Bueno; Peiró; Estradé. *Ultramicroscopy* 2021, *221*, 113190.

(2) Chatzidakis; Botton. *Sci Rep* 2019, *9* (1), 2126.

(3) Torruella; Estrader; López-Ortega; Baró; Varela; Peiró; Estradé. *Ultramicroscopy* 2018, *185*, 42–48.

(4) Blanco-Portals; Peiró; Estradé. *Microscopy and Microanalysis* 2022, *28* (1), 109–122.

(5) Pate; Hart; Taheri. *Sci Rep* 2021, *11* (1), 19515.

(6) Goodfellow; Pouget-Abadie; Mirza; Xu; Warde-Farley; Ozair; Courville; Bengio. *Generative Adversarial Nets*; 2014.

Keywords: Machine Learning, STEM, EELS, Generative Adversarial Networks, Data Augmentation

CORE@SHELL TERNARY NANOSTRUCTURES: AU@MO(W)S2 FOR THE HYDROGEN EVOLUTION REACTION

Antonio Jesús Medina Olivera (Spain)[1]; Juan Jose Quintana González (Spain)[1]; Juan Carlos Hernández Garrido (Spain)[1]; Luc Cyrille Jacques Lajaunie (Spain)[1]; Rong Sun (Spain)[1]

1 - Universidad de Cádiz (UCA)

Abstract

One of the most interesting ways to produce clean energy and, therefore, to help mitigate climate change, is by obtaining hydrogen from the process called water splitting. To achieve this, it is essential to go beyond Pt-baed electrode and to search for new catalysts which present both good catalytic activity and sustainability. Layered transition metal dichalcogenides (TMDs), such as MoS_2, have attracted interest from various chemical and catalytic processes, including the hydrogen evolution reaction (HER). Furthermore, core@shell nanostructures in which a metallic core is encapsulated by a TMD layer, such as Au@MoS_2, have been shown to enhance HER performance[1]. In this work, we investigate the influence of W-based heteroatoms on the HER performance of Au@MoS_2 nanostructures.

The samples were obtained by borohydride reduction method from an Au precursor, followed by mixing the MoS_2 and WS_2 precursors in different molar ratios. This process was finalized by a thermal treatment. The structural and compositional analysis of the samples was carried out using XPS spectroscopies and TEM microscopy. In order to study the relationship between the structure and catalytic activity, measurements of the HER were carried out in a standard three-electrode cell in a 0.5 M H_2SO_4 solution. The electrodes were fully characterized by combining linear scanning voltammetry (LSV), cyclic voltammetry (CV) and impedance spectroscopy (EIS).

The formation of the core@shell nanostructures is clearly highlighted in the STEM images. Fig. 1a in particular, the presence of a single layer around the metallic core is observed. It should be noted that the presence of W inside the layer was confirmed by the EELS analyses, in good agreement with the XPS results. The STEM image presented belongs to the Au@Mo(W)S_2-3 sample in which there is a 3% mole of the tungsten precursor (within the total moles of the dichalcogenide precursors). Fig. 1b shows the results of electrochemical activity. It was observed that ternary samples with lower proportions of WS_2 presented HER performances, translated into a drop in overpotential and Tafel slope. The worst performances being obtained for samples with only one type dichalcogenide shell such as Au@MoS_2 Au@WS_2. These results show that the HER performances of core-shell nanostructures based on Au core can be further improved thanks to a simple easy synthetic design that allows the introduction of a low number of W-based defects.

Acknowledgments

This research has been funded by the Junta de Andalucía (FEDER-UCA18-107490), the European Union's Horizon 2020 research and innovation program (grant agreement 823717-ESTEEM3), the Spanish Ministry of Economy and Competitiveness (PID2019- 107578GA-I00), the Ministry of Science and Innovation MCIN/AEI/10. 13039/501100011033, and the European Union "NextGenerationEU"/PRTR (RYC2021-033764-I, CPP2021-008986). The authors appreciate the use of

the (S)TEM instrumentation provided by the National Installation ELECMI ICTS ("Division of Electron Microscopy", University of Cádiz, DME-UCA).

References

[1] Bar-Ziv, R., Ranjan, P., Lavie, A., (...), Lajaunie, L., Bar-Sadan, M. (2019). Au-MoS2 Hybrids as Hydrogen Evolution Electrocatalysts. ACS Applied Energy Materials 2(8), pp. 6043-6050

Keywords: HER, Au@MoS2, dichalcogenides

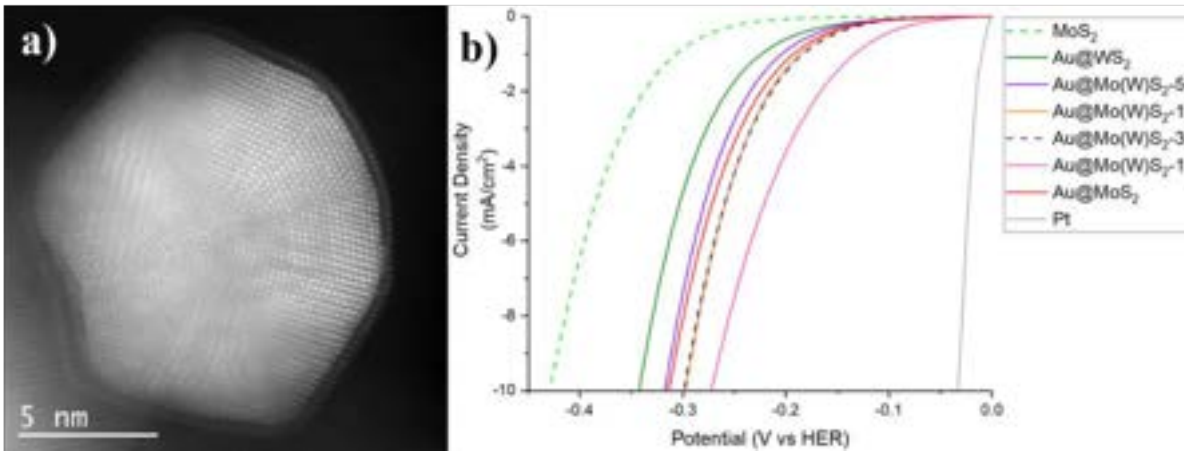

Fig 1a. HAADF-STEM images of the Au@Mo(W)S2-3 sample

Fig 1b. Polarization curve of the samples with different proportions of dichalcogenides (core-shell), together with the Pt reference.

1D NANOSTRUCTURES WITH LAYERED COBALT DIOXIDE SYNTHESIZED BY CRYSTAL CONVERSION PROCESS

Simon Hettler (Spain)[1,2]; Kankona Singha Roy (Spain)[3]; Raul Arenal (Spain)[1,2,4]; Leela Panchakarla (Spain)[3]

1 - Laboratorio de Microscopias Avanzadas (LMA), Universidad de Zaragoza, Mariano Esquillor Gomez, Zaragoza, 50018, Spain; 2 - Instituto de Nanociencia y Materiales de Aragon (INMA), CSIC-Universidad de Zaragoza, Mariano Esquillor Gomez, Zaragoza, 50018, Spain; 3 - Department of Chemistry, Indian Institute of Technology Bombay, Mumbai, 400076, Powat, India; 4 - Araid Foundation, Zaragoza, 50018, Spain

Abstract

Layered cobalt dioxide in bulk form is only meta-stable and its synthesis is mostly obtained from de-intercalation of Li_xCoO_2 and similar structures [1] or by intercalation in the form of misfit-layered compounds (MLCs) [2]. Crystal structures, which are unstable in bulk form, may have a stable form if its size is reduced to the nano-regime. For such nanomaterial synthesis routes, the starting material is either a mixture of the individual elements or the corresponding bulk structure. Recently, we introduced a novel synthesis method based on a crystal conversion process, which parts from a bulk structure with a different crystal structure [3]. Here, we will present the in-depth electron microscopy analysis of nanotubes and scrolls based on layered CoO_2 that have been obtained using this method with two different starting compounds [3,4].

The process starts from bulk material with a quasi 1D crystal structure, e.g. $Sr_6Co_5O_{15}$ [3] or $Ca_3Co_2O_6$ [4], which is treated in a hydrothermal process in basic environment. This environment renders the structure unstable and dissolves the Sr or Ca ions leaving cobalt oxide chains behind. These chains then bind to nanotubular or scrolled forms.

The resulting products are studied by electron microscopy and spectroscopy and related techniques. The electronic properties of the nanotubes are analyzed in detail on the individual nanotube level. In case of Sr-based bulk precursor, nanotubes of a misfit-layered compound $Sr_xCoO_2 – CoO_2$ are observed, which is Sr-deficient compared to the nanotubes obtained by a classical synthesis route [2], see Figure 1a. In the case of Ca, nanoscrolls made of pure layered CoO_2 are obtained. The scrolls all possess a similar size and wall width suggesting that the CoO_2 stabilization occurs under specific circumstances. Electron energy-loss spectroscopy of the nanostructures are consistent with a high valence state of up to Co^{4+}, see Figure 1b.

The $Sr_xCoO_2 – CoO_2$ nanotubes possess an extremely high ampacity (10^9 A cm^{-2}) and an extraordinary breakdown power per channel length (P/L 38 W cm^{-1}) [3]. The results on structure and properties show that the crystal conversion route is promising to synthesize structures unstable in its bulk counterpart.

Acknowledgments

This work was supported by the Spanish MICINN (project grant PID2019-104739GB-100/AEI/10.13039/501100011033), and European Union H2020 programs Marie Skłodowska-Curie-IF “PROMISES” (889546), Graphene Flagship CORE3 (881603) and “ESTEEM3” (823717).

References

[1] Mizushima, K. et al. *Materials Research Bulletin* **15**, 783–789 (1980).

[2] L. Panchakarla et al, *Chem. Mater.* **28**, 9150–9157 (2016).

[3] K. Singha Roy, S. Hettler, R. Arenal, L. Panchakarla, *Materials Horizons* **9**, 2115-2127 (2022).

[4] S. Hettler, K. Singha Roy, R. Arenal, L. Panchakarla, submitted.

[5] Takada, K. et al. *Nature* **422**, 53–55 (2003).

Keywords: layered cobalt dioxide, 1D nanostructures, transmission electron microscopy, electron energy-loss spectroscopy, crystal conversion

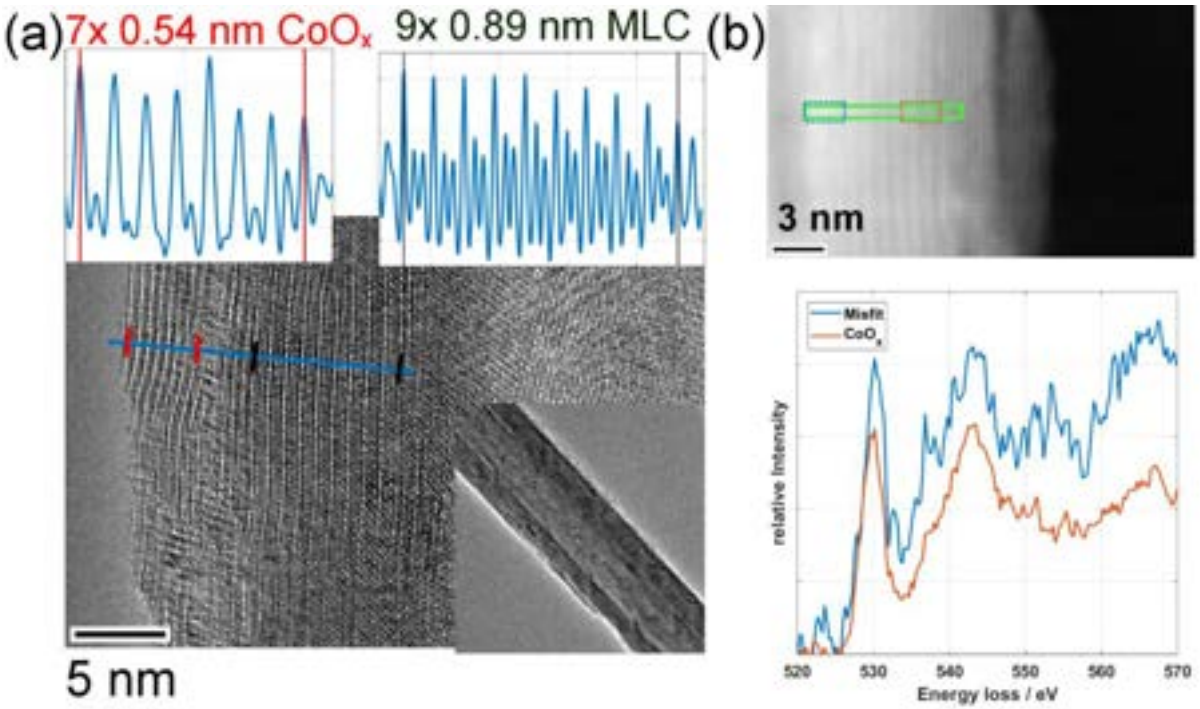

Figure 1: (a) TEM images of Sr_xCoO_2 – CoO_2 nanotube with line profile of different wall areas revealing two different lattice spacings. (b) STEM image showing outer wall of nanotube. EEL spectra of O-K edge obtained from marked areas show dominant pre-peak indicating a high Co valence state.

GATHERING INFORMATION ON THE HYDROSCOPIC BEHAVIOUR OF AEROSOLS IN AN ENVIRONMENTAL TEM USING A NOVEL MICRO-PELTIER-BASED COOLING SAMPLE-HOLDER TO CONTROL THE CONDENSATION/EVAPORATION OF WATER

Francisco J. Cadete Santos Aires (France)[1]; Eric Ehret (France)[1]; Joseph V. Vas (Singapore)[2]; Mimoun Aouine (France)[1]; Laurence Massin (France)[1]; Martial Duchamp (Singapore)[2]; Thierry Epicier (France)[1]

1 - IRCELYON (UMR5256 CNRS/UCBL); 2 - Majulab/Lision (UMI 3654 CNRS/NTU-Singapore)

Abstract

Micro and nanoscale in situ studies of dynamics of water condensation/evaporation requiring water vapour-liquid equilibrium conditions are of paramount importance in many domains such as textile wettability, virus/bacteria spreading, reduction of chemical impact in agriculture, atmospheric chemistry, etc. Notwithstanding their unmatched adequacy for a wide range of in situ/operando studies of nanomaterials in liquids or liquids themselves within a TEM, water vapour-liquid equilibrium is extremely difficult to achieve (if not beyond the reach) within closed liquid cells. Conversely, in a dedicated environmental TEM, where sealing membranes are not required, conditions necessary to work around the dewpoint of water are attainable within the available pressure range (≤ 20 mbar) when the sample is cooled down to a few degrees Celsius (~ 0 to 18°C).

Our main interest relates to atmospheric chemistry and in particular the hygroscopic behaviour of aerosols [1] and their role in the formation of water droplets ultimately leading to the formation of clouds. We have thus studied the deliquescence and efflorescence of NaCl model aerosols (typical of a marine environment) within the Ly-EtTEM (TFS Titan ETEM G2 60-300 kV) using, in a first step, a classic LN_2 cryo-holder ELSA (Gatan/Ametek). More recently, we have initiated a new approach in developing a cooling holder based on a micro-Peltier element mounted on the tip a commercial MEMS-based heating holder (DENSsolutions) taking advantage of the electric contacts available to power the micro-Peltier element (Figure 1A) [2]. This system is far more adequate to work within the required range of temperatures (~ 0 to 18°C) than a LN_2 cryo-holder: it is easier to operate, the required temperature is attained much faster and there is a fine control of the relative humidity (RH) through the micro-Peltier input power; it also provides more stability of the operating conditions over time despite a still improvable thermal dissipation of the Peltier element. These advantages are illustrated in Figure 1B.

Acknowledgments

The authors acknowledge the French National Research Agency (ANR) for financial support through the WATEM project (n°ANR-20-CE42-0008) and the Consortium Lyon – St-Etienne de Microscopie (CLYM, www.clym.fr) for access to the Lyon Environmental and tomographic TEM (Ly-EtTEM).

References

[1] C. Chatre *et al.*, Langmuir **39** (2023) 2957.

[2] J.V. Vas *et al.*, Microscopy and Microanalysis **28 (Suppl. 1)** (2022) 818.

condensation/evaporation, Deliquescence/Efflorescence, NaCl aerosols, , Peltier-based sample-holder

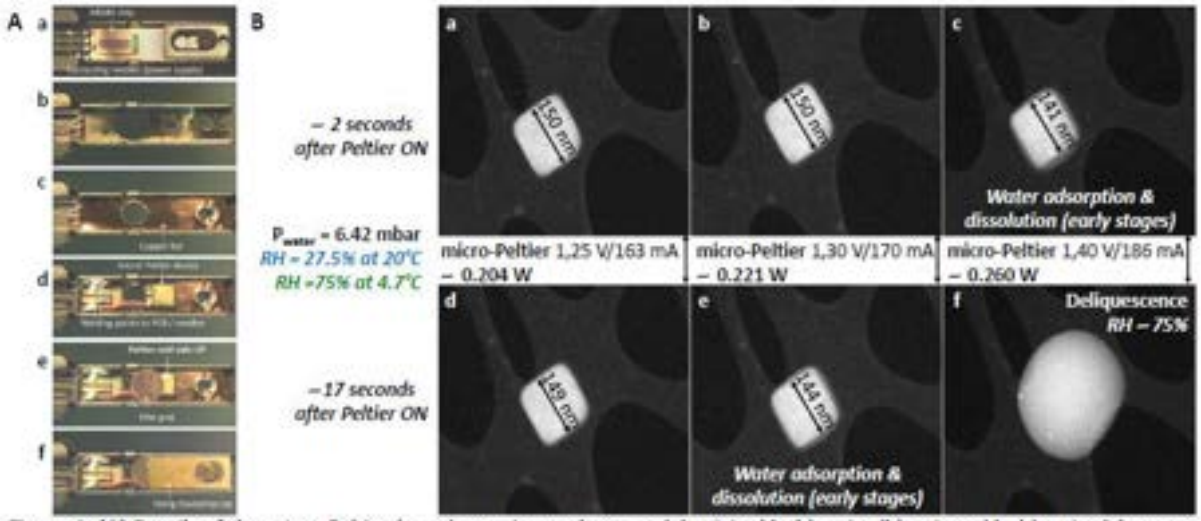

Figure 1: (A) Details of the micro-Peltier-based experimental set-up: (a) original holder-tip; (b) stripped holder-tip; (c) copper foil for thermal conduction; (d) positioning and contact welding of the micro-Peltier device (cold face upwards); (e) positioning of the TEM grid; (f) insulating piece for assuring a firm contact of the TEM-grid on the Peltier cold surface.

(B) Deliquescence of a NaCl nanocube. Frames taken from dynamic sequences 2 seconds (a-c) and 17 seconds (d-f) after turning the Peltier power ON under 6.42 mbar of H_2O vapour showing the prompt achievement of the working conditions and the fine control over the applied power (0.204W: a,d; 0.221W: b,e; 0.260W: c,f) thus of the attained temperature and the relative humidity (RH).

IN-SITU ATOMIC RESOLUTION STUDIES OF BI-DOPED CU NANOWIRES FOR SPINTRONIC APPLICATIONS

Alejandra Guedeja-Marron (Spain)[1,4]; Matilde Saura-Muzquiz (Spain)[1]; Sandra Ruiz-Gomez (Spain)[2]; Claudia Fernandez-Gonzalez (Spain)[2]; Ines Garcia-Manuz (Spain)[3]; Henrik L. Andersen (Spain)[1]; Paolo Perna (Spain)[3]; Lucas Perez (Spain)[1,3]; Maria Varela (Spain)[1,4]

1 - Universidad Complutense de Madrid; 2 - Max Planck Institute for Chemical Physics of Solids, Dresden, Germany; 3 - Instituto Madrileño de Estudios Avanzados – IMDEA Nanociencia, Madrid, Spain; 4 - Instituto Pluridisciplinar, Universidad Complutense de Madrid, Spain

Abstract

The spin Hall effect (SHE) is a spin-charge conversion phenomenon that plays a key role in spintronics, [1] so the search for materials that exhibit giant SHE has grown significantly within the last decades. [2, 3] Recently, SHE in $Cu_{95}Bi_5$ films has been directly detected by X-ray spectroscopy, [4] confirming this material as a good candidate for integration in spintronic devices. Achieving CuBi structures with tunable composition and structure [5] can provide an ideal model-system for exploring and optimizing the extrinsic SHE.

Here, we present a detailed structural characterization of Bi-doped Cu nanowires (NWs) with different Bi doping levels and degrees of crystallinity, grown by template-assisted electrochemical deposition. *In-situ* heating experiments combining atomic resolution scanning transmission electron microscopy (STEM), electron energy-loss spectroscopy (EELS) and high-resolution synchrotron powder X-ray diffraction (PXRD), allow studying in detail the atomic structure of the NWs along with evolution with temperature, aimed at controlling Joule heating effects in future devices. These results pave the way towards the realization of spin-dependent transport measurements complemented with *in-situ* polarization in CuBi NWs.

Acknowledgments

Electron microscopy observations were carried out at the Centro Nacional de Microscopía Electrónica at Universidad Complutense de Madrid. PXRD experiments were performed at the MSPD beamline, ALBA, Spain, and ID22 beamline, ESRF, France.

References

[1] J. Sinova et al., *Rev. Mod. Phys*. **87** (2015) 1213.
[2] T. Jungwirth et al., *Nature*. **11** (2012) 5.
[3] Y. Niimi et al., *Phys. Rev. Lett*. **109** (2012) 15.
[4] S. Ruiz-Gomez et al., *Phys. Rev. X.* **12** (2022) 3.
[5] S. Ruiz-Gomez et al., *J. Magn. Magn. Mater*. **545** (2022) 168645.

Keywords: spintronics, alloys, HR-STEM, EELS

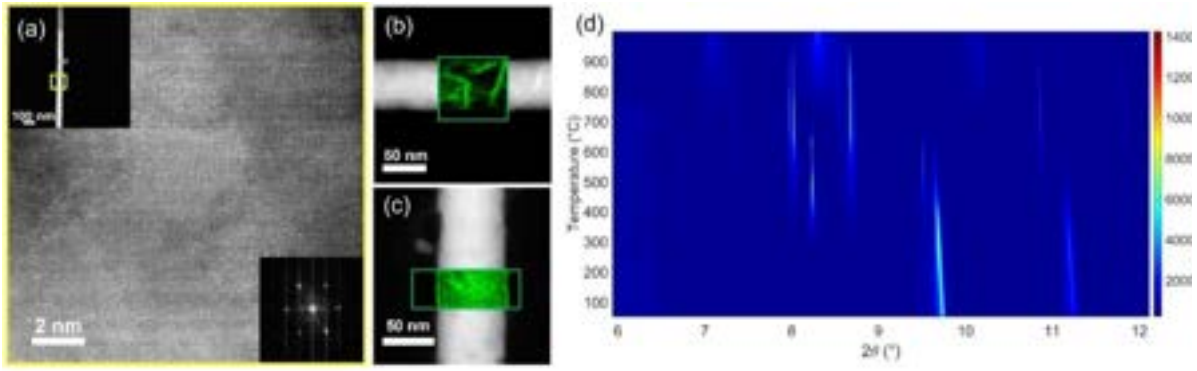

Figure 1: (a) High-angle annular dark field STEM atomic resolution images corresponding to a single-crystal CuBi nanowire. Bottom right (a) image displaying the fast Fourier transform [111] zone axis. EELS maps depicting the Bi $M_{4,5}$ edge integrated signal in a (b) polycrystal and (c) single-crystal NW. (d) PXRD heating 2D map showing the material decomposition at around 300ºC.

RECENT WORKS ON TMDS NANOMATERIALS: STUDIES OF THEIR STRUCTURAL AND OPTOELECTRONIC PROPERTIES

Raul Arenal (Spain)[1]; Mario Pelaez-Fernandez (Spain)[1]; Simon Hettler (Spain)[1]

1 - Laboratorio de Microscopias Avanzadas, Universidad de Zaragoza

Abstract

Atomically thin low-dimensional nanomaterials based on transition metal dichalcogenides (TMDs; e.g.: molybdenum/tungsten disulfide (Mo/WS_2)…) offer very interesting applications in a large variety of fields of nanoscience and nanotechnology due to their attractive mechanical, electronic, optical and thermal properties [1-6].

In this presentation, we will present several works, where high-resolution scanning transmission electron microscopy (HRSTEM) studies and local electron energy-loss spectroscopy (EELS) analyses have developed on different of these materials. These works will concern the investigation of these systems in pristine and functionalized forms, with particular interest in elucidating their crystal phase, their chemistry, their growth mechanism, as well as their optoelectronic properties [2-7]. Thus, these studies deal with crucial questions concerning the structure, the local composition (atomic configuration) of these nanomaterials. This detailed knowledge is essential for better understanding their outstanding properties.

Acknowledgments

Funding from the following institutions & programs is acknowledged: Spanish MICN (PID2019-104739GB-100/AEI/10.13039/501100011033), Government of Aragon (project DGA E13-20R) and EU-H2020 “Graphene Flagship” (881603), “ESTEEM3” (823717), MSCA-Promises (823717) and Margarita Salas (MICINN).

References

[1] R. Tenne et al., Nature 360, 444-446 (1992).
[2] R. Canton-Vitoria, et al. Angewandte Chemie International 59, 3976-3981 (2019).
[3] A. Kagkoura, R., N. Tagmatarchis, Adv. Funct. Mat. 31, 2105287 (2021).
[4] M. Pelaez-Fernandez et al. Nanomaterials 11, 3218 (2021).
[5] M.B. Sreedhara et al. J. Amer. Chem. Soc. 144, 10530–10542 (2022).
[6] A. Cohen, et al., ACS Nano 17, 5399–5411 (2023).

Keywords: 2D Materials, Transition Metal Dichalcogenides, HRSTEM, EELS

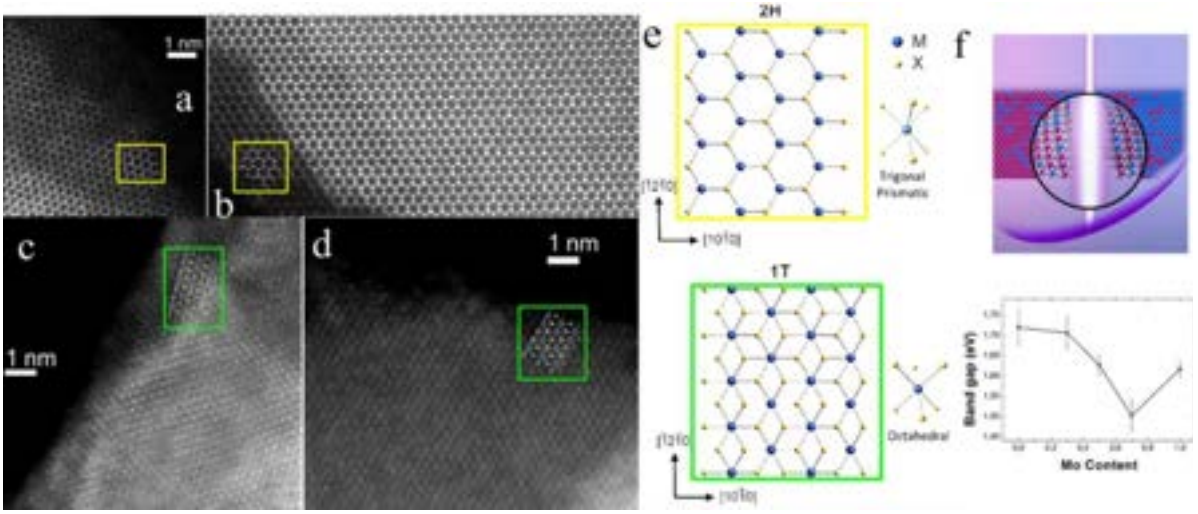
1 nm
a
b
c
d
1 nm
1 nm
e
2H
M
X
Trigonal Prismatic
[12$\bar{1}$0]
[10$\bar{1}$0]
1T
Octahedral
[12$\bar{1}$0]
[10$\bar{1}$0]
f
Band gap (eV)
Mo Content

Cellular ultrastructure in 3D context

Posters - MATERIAL SCIENCES

MORPHOLOGY INFLUENCE ON THE LUMINESCENCE OF ZN2GEO4 NANOPHOSPHORS

Miguel Tinoco (Spain)[1]; Javier García-Fernández (Spain)[1]; José Miguel Lendínez (Spain)[1]; Bianchi Méndez (Spain)[1]; Pedro Hidalgo (Spain)[1]; Julio Ramírez-Castellanos (Spain)[1]; José María González-Calbet (Spain)[1]

1 - Universidad Complutense de Madrid

Abstract

Novel semiconductor technology is devoted to the production of non-toxic and critical material-free phosphors due to the last recommendations from the EU and US Government.

Among these, several ternary oxides have emerged as possible alternatives to current luminescent semiconductors. In particular, Zn2GeO4 nanoparticles have shown outstanding luminescent properties. Varying nanoparticle size and morphology has been suggested to alter the emitted signal in Zn2GeO4. This opens a new promising scientific avenue to prepare toxic- free nanophosphors with tunable optoelectronic properties.

In this work, Zn2GeO4 nanoparticles have been synthesized by coprecipitation (CP-Zn2GeO4 sample) and a hydrothermal method (HT-Zn2GeO4 sample).

The willemite-like structure of both Zn2GeO4 samples was verified by X-ray diffraction. Although no impurities are distinguished in HT-Zn2GeO4 sample, additional maxima attributed to ZnO are visible in the CP-Zn2GeO4 diffractogram.

TEM images evidence that nanocrystallites in CP-Zn2GeO4 sample possess a nanorod morphology with relatively pointed ends, apart from the presence of other particles without a defined shape. X-EDS results suggest that nanorods possess a cationic ratio corresponding to the composition of Zn2GeO4 , whereas ill-defined nanoparticles are much richer in Zn, which may imply that these crystallites correspond to the ZnO impurities previously observed in XRD. On the contrary, HT-Zn2GeO4 sample consists of smaller short nanorods, with either straight or rounded basal planes. This sample is remarkably homogeneous, with no apparent impurities, and no appreciable variations in morphology among nanoparticles. HRTEM images confirm the willemite-like Zn2GeO4 structure of the nanorods present on both samples, with its characteristic tunnels clearly distinguishable along the [111] zone axis. No obvious variations were detected in the crystal structure of both nanophosphors.

Photoluminescence is rather similar between both samples, and notoriously analogous to Zn2GeO4 microrods and nanowires. However, it is noticeably different than Zn2GeO4 in bulk form, or Zn2GeO4 thin layers. These results may confirm that emission is tightly related to particle morphology. Therefore, the improvement of the luminescence response of this material may depend on the optimization of the synthesis of homogeneous controlled morphology Zn2GeO4 nanoparticles.

Acknowledgments

The authors acknowledge the National Centre for Electron Microscopy (ELECMI National Singular Scientific Facility) for the access to corrected microscopy facilities. Authors acknowledge financial support to Spanish Ministry of Science and Innovation through Research Project PID 2020-113753RB-100.

References

[1] Yan C., Singh N. & Lee P. S. Wide-bandgap Zn2GeO4 nanowire networks as efficient ultraviolet photodetectors with fast response and recovery time. Applied Physics Letters (2010), 96, 053108.

[2] Luo S. et al. Ultrawide bandgap willemite-type Zn2GeO4 epitaxial thin films. Appled Physics Letters (2023), 122, 031601.

[3] Dolado J. et al. Intense cold-white emission due to native defects in Zn2GeO4 nanocrystals. Journal of Alloys and Compounds. (2022), 898, 162993.

[4] Hidalgo P., López. A., Méndez B. & Piqueras J. Synthesis and optical properties of Zn2GeO4 microrods. Acta Materalia. (2016), 104, 84-90.

Keywords: Luminescence, Controlled morphology, Hydrothermal synthesis

ENHANCING ACTIVITY AND STABILITY OF THE OXYGEN ELECTRODE SURFACE IN REVERSIBLE PROTONIC CERAMIC ELECTROCHEMICAL CELLS

Shunrui Luo (Spain)[1]; Kai Pei (China)[2]; Yu Chen (China)[2]; Jordi Arbiol (Spain)[1]

1 - Catalan Institute of Nanoscience and Nanotechnology (ICN2); 2 - South China University of Technology

Abstract

Reversible protonic ceramic electrochemical cells (R-PCECs) offer promising opportunities for energy conversion and storage at low-intermediate temperatures (400-700°C), enabling efficient electrolysis of H2O to H2 in electrolysis mode and the production of electricity in fuel cell mode. However, the sluggish kinetics of oxygen reduction/evolution reaction (ORR/OER) at reduced temperatures and in humid environments, along with undesired surface segregation and structural degradation, have presented challenges in developing R-PCEC devices.[1] For instance, PrBaCo2O5+δ (PBC), a double perovskite material renowned for its high ORR and OER activities, has attracted significant interest. However, the presence of barium in the interstitial positions within the PBC lattice often leads to segregation at the electrode interface, resulting in performance and structural degradation. [2]

In this presentation, we focus on the development of a stable surface for the oxygen electrode in PBC double perovskite to enhance its activity and durability.[3] Our approach involves the implementation of an efficient fluorite catalyst coating on the oxygen electrode, which has been further modified with an active and robust shell of Pr0.1Ce0.9O2+δ (PCO). Through this modification, PCO-PBC composite exhibits an elevated concentration of oxygen vacancies, facilitating enhanced surface exchange processes, ion diffusion, and providing multiple active reaction sites. Importantly, this surface modification also prevents the segregation of barium under operation conditions. As a result, the PCO-PBC oxygen electrode shows good performances on a fuel-electrode supported single cell at 650 oC, which displays a typical peak power density of 1.21 Wcm-2 (FC mode) and a typical current density of 2.69 Acm-2 at 1.3 V (EL mode), which also demonstrates exceptional performance and minimal degradation in both electrolysis and fuel cell modes over 25 cycles and 100 hours at 650°C with 3 vol.% H2O.

Acknowledgments

ICN2 acknowledges funding from Generalitat de Catalunya 2021SGR00457. This study was supported by MCIN with funding from European Union NextGenerationEU (PRTR-C17. I1) and Generalitat de Catalunya. This research is part of the CSIC program for the Spanish Recovery, Transformation, and Resilience Plan funded by the Recovery and Resilience Facility of the European Union, established by the Regulation (EU) 2020/2094. The authors thank the support from the project NANOGEN (PID2020-116093RB-C43), funded by MCIN/ AEI/10.13039/501100011033/ and by “ERDF A way of making Europe”, by the “European Union”. ICN2 is supported by the Severo Ochoa program from Spanish MCIN/AEI (Grant No.: CEX2021-001214-S) and is funded by the CERCA Programme / Generalitat de Catalunya. This study is financially supported by the Natural Science Foundation of Guangdong Province (2021A1515010395), the National Natural Science Foundation of China (22179039 and

22005105), the Fundamental Research Funds for the Central Universities (2022ZYGXZR002), the Pearl River Talent Recruitment Program (2019QN01C693), and the Introduced Innovative R&D Team of Guangdong (2021ZT09L392). K.P. appreciates the support of the China Postdoctoral Science Foundation Project (2020M682700). S.L. appreciates the support of the Science and Technology Innovation Program of Hunan Province (2021RC2007).

References

[1] S. Kim, D.W. Joh, D.-Y. Lee, J. Lee, H.S. Kim, M.Z. Khan, J.E. Hong, S.-B. Lee, S.J. Park, R.-H. Song, M.T. Mehran, C.K. Rhee, T.-H. Lim, Microstructure tailoring of solid oxide electrolysis cell air electrode to boost performance and long-term durability, Chemical Engineering Journal, 410 (2021) 128318.
[2] E. Marelli, J. Gazquez, E. Poghosyan, E. Müller, D.J. Gawryluk, E. Pomjakushina, D. Sheptyakov, C. Piamonteze, D. Aegerter, T.J. Schmidt, M. Medarde, E. Fabbri, Correlation between Oxygen Vacancies and Oxygen Evolution Reaction Activity for a Model Electrode: PrBaCo2O5+δ, Angewandte Chemie International Edition, 60 (2021) 14609-14619.
[3] K. Pei, S. Luo, F. He, J. Arbiol, Y. Xu, F. Zhu, Y. Wang, and Y. Chen, Constructing an Active and Stable Oxygen Electrode Surface for Reversible Protonic Ceramic Electrochemical Cells. Applied catalysis. B, Environmental, 330 (2023) 122601.

Keywords: Reversible protonic ceramic electrochemical cells, Water electrolysis, Durability, Oxygen reduction reaction, Oxygen evolution reaction

LEVERAGING ON ZINC PHOSPHIDE FOR NEXT GENERATION PHOTOVOLTAICS

Francesco Salutari (Spain)[5]; Maria Chiara Spadaro (Italy)[1]; Helena Freitas Rabelo (Spain)[5]; Simon Escobar Steinvall (Sweden)[2]; Sebastian Lehmann (Sweden)[3]; Kimberly A. Dick (Sweden)[2]; Jordi Arbiol (Spain)[4,5]

1 - Department SIMAU, Marche Polytechnic University, Ancona, Italy; 2 - Center for Analysis and Synthesis and NanoLund, Lund University, Box 124, 221 00 Lund, Sweden; 3 - Division of Solid State Physics and NanoLund, Lund University, Box 124, 221 00 Lund, Sweden; 4 - ICREA, Pg Lluis Companys 23, 08010 Barcelona, Catalonia, Spain.; 5 - Catalan Institute of Nanoscience and Nanotechnology (ICN2), CSIC and BIST, Campus UAB, Bellaterra, 08193 Barcelona, Catalonia, Spain.

Abstract

The ever-growing need for clean energy has boosted the research on innovative solar energy technologies that can enter the photovoltaics (PV) market and compete with the leading silicon-based technology. Reaching high power conversion efficiencies (PCE) is only a side of the desired requirements for these novel technologies: sustainability, environmental and human health impact reduction, and end-of-life recyclability are challenges that cannot be overlooked anymore. In this scenario, zinc phosphide (Zn3P2) has been proposed as an alternative semiconductor for the realization of thin and flexible solar cells. Thanks to its favourable optoelectronic characteristics and direct bandgap, theoretical studies and simulations have shown the potentialities of Zn3P2 in terms of PCE [1]. Moreover, its earth-abundance can support the development of a sustainable technology and ultimately reduce the impact on global warming [2]. However, many limitations still need to be overcome, from the growth of a high-quality crystalline layer, through the stacking of the latter with suitable materials to achieve the final device architecture, to finally the scaled-up production and field installation of the PV panels.

At this stage of the research, it becomes essential to comprehensively investigate the crystalline quality and elemental homogeneity of the produced material. Different fabrication processes are being tested in order to fulfil these requirements and, above all, selective area epitaxy (SAE) has shown promising results [3]. Here, we report our recent findings onto the study of high-quality Zn3P2 nanowires via high resolution transmission electron microscopy (HRTEM) and high angle annular dark field scanning transmission electron microscopy (HAADF-STEM). The deep atomic-level investigation will be key in order to unveil the growth mechanism behind the adopted approaches, like the aforementioned SAE, and highlight the peculiar features that strongly impact the electronic properties of the final device.

Acknowledgments

This study was supported by HORIZON EIC PATHFINDER OPEN 2021 project SOLARUP (Ref.: 101046297).

References

1. Elias Z. Stutz et al., Mater. Adv., 2022,3, 1295-1303; 2. S. Escobar Steinvall et al. Nanoscale Adv., 2021, 3(2), 326–332 ; 3. M. C. Spadaro et al. Nanoscale 2021, 13, 18441-18450

Keywords: Zinc Phosphide, Solar Energy, Electron Microscopy

IN-DEPTH ELECTRON NANOSCOPY INVESTIGATIONS OF (NANO)MATERIALS FOR GREEN ENERGY APPLICATIONS

Helena Rabelo Freitas (Spain)[1]; Thomas Hagger (Switzerland)[2]; Raphaël Lemerle (Switzerland)[2]; Didem Dede (Switzerland)[2]; Anna Fontcuberta I Morral (Switzerland)[2]; Maria Chiara Spadaro (Italy)[3]; Jordi Arbiol (Spain)[4]

1 - Catalan Institute of Nanoscience and Nanotechnology; 2 - École Polytechnique Fédérale de Lausanne; 3 - Marche Polytechnic University; 4 - ICREA

Abstract

There has been an ever-growing demand for the development of novel and sustainable energy conversion devices that act as alternatives to the conventional and often, non-renewable, or intermittent sources of energy. The crucial drive for the development of a new generation of sophisticated devices has been motivating the effort for discovering innovative nanostructured materials that play a key role in enhancing performance and protecting the environment. It is known that the understanding of a material's compositional and structural characteristics at the nano and atomic level, as the configuration of the active atoms, crystalline phase, and defects, is unprecedent to determining the structure-performance relationship that guides the designing new materials and improving existing ones. Transmission electron microscopy (TEM) is among the techniques employed in the characterization of functional nanomaterials, as it provides opportunities for the investigation of crystal structure at a particularly local scale. When complemented by techniques such as Electron Energy Loss Spectroscopy (EELS), it offers a clear and complete map of elemental information and atomic arrangements, which can be useful for giving insights on the most various promising applications. In this scope, this work presents an overview of the advantages of implementing the previously mentioned investigation tools on the mapping of layer growth, thickness, and morphology of nanostructured Zinc Phosphide (Zn3P2) thin films grown by Molecular Beam Epitaxy (MBE) on graphene and designed for solar energy applications.

Acknowledgments

This project has received funding from the European Innovation Council and SMEs Executive Agency (EISMEA) under grant agreement No 101046297 funded by the European Union. Views and opinions expressed are however those of the author(s) only and do not necessarily reflect those of the European Union or European Innovation Council and SMEs Executive Agency (EISMEA). Neither the European Union nor the granting authority can be held responsible for them.
This work was supported by the Swiss State Secretariat for Education, Research and Innovation (SERI) under contract number 22.00018.

References

1. Elias Zsolt Stutz, Santhanu Panikar Ramanandan, Mischa Flór, Rajrupa Paul, Mahdi Zamani, Simon Escobar Steinvall, Diego Armando Sandoval Salaiza, Claudia Xifra, Maria Chiara Spadaro, Jean-Baptiste Leran, Alexander P. Litvinchuk, Jordi Arbiol, Anna Fontcuberta i Morral, Mirjana Dimitrievska. Faraday Discussions, 239, 202-218 (2022).
2. Spadaro, M. C., Steinvall, S. E., Dzade, N. Y., Martí-Sánchez, S., Torres-Vila, P., Stutz, E. Z., ... & Arbiol, J. (2021). Rotated domains in selective area epitaxy grown Zn3P2: formation mechanism and functionality. Nanoscale, 13(44), 18441-18450.

Keywords: Photovoltaics, Zinc Phosphide, Graphene, Solar energy

METAL ORGANIC FRAMEWORK DERIVED TRANSITION METAL-BASED COMPOUNDS TO BOOST HIGH-PERFORMANCE METAL-SULFUR BATTERIES

Chen Huang (Spain)1; Andreu Cabot (Spain)1; Jordi Arbiol (Spain)2; Jing Yu: (Spain)3

1 - IREC; 2 - ICN2& ICREA; 3 - ICN2 & IREC

Abstract

Lithium-sulfur batteries (LSBs) hold practical potential as next-generation energy storage devices due to their high energy density and potential for low cost [1] . However, the shuttle effect of lithium polysulfides (LiPSs) and the poor electrical conductivity of sulfur and lithium sulfides limit their practical application [2]. In this work, a sulfur host material based on nitrogen-doped carbon coated with small amounts of transition metal tellurides is developed. Firstly, introducing the concept of metal-organic frameworks to restrict polysulfides of shuttle effect. Secondly, based on the electronic control strategy to improve the catalytic performance of the host material, specifically, the adsorption capacity of polysulfides were promoted by designing heterostructure is conducive to Li + diffusion and fast electron transport of catalyst.

In the present work, we have used electron energy loss spectroscopy (EELS) elemental composition maps obtained together with HAADF STEM micrographs to reveal that the spherical nanoparticles show a homogeneous distribution of N in the whole structure, while Co, Te and Zn are concentrated in different regions, with Co-Te and Zn-Te rich areas. HRTEM images and the corresponding power spectra obtained revealed that the obtained nanostructure has a crystal phase that can be assigned to the cubic ZnTe (space group = F-43m) with a=b=c=6.106(1)Å. From the crystalline domains observed when visualizing the ZnTe lattice fringe distances, we could measure distances and angles corresponding to 0.202 nm, 0.270 nm and 0.201 nm, at 69.02º and 137.4º, which could be interpreted as the cubic ZnTe phase, visualized along its [1-22] zone axis.2 (space group = Pnn2) with a=5.3294(6)Å, b= 6.3223(8)Å, c= 3.9080(6)Å. The above results prove that ZnTe and CoTe 2 nanostructures coexist in v-ZnTe/CoTe 2 @NC.

Benefiting from designed heterostructure, sulfur cathodes containing the composite additive, ZnTe/CoTe 2 @NC/S, showed excellent initial capacities up to 1608 mAh g –1 at 0.1 C and stable cycling with an average capacity decay rate of only 0.022% per cycle at 1 C for 500 cycles. Even at a high load of 5.4 mg cm –2, a high capacity of 1273 mA hg –1 at 0.1 C is retained.

Acknowledgments

ICN2 acknowledges funding from Generalitat de Catalunya 2021SGR00457. This study is part of the Advanced Materials program and was supported by MCIN with funding from European Union NextGenerationEU (PRTR-C17.I1) and by Generalitat de Catalunya. The authors thank support from the NANOGEN project (PID2020-116093RB-C43), funded by MCIN/ AEI/10.13039/501100011033/ and by “ERDF A way of making Europe”, by the “European Union”. ICN2 is supported by the Severo Ochoa program from Spanish MCIN / AEI (Grant No.: CEX2021-001214-S) and is funded by the CERCA Program

/ Generalitat de Catalunya. Jing Yu and Chen Huang are grateful for financial support from the Chinese Scholarship Council (CSC).

References

[1]C. Zhang, B. Fei, D. Yang, H. Zhan, J. Wang, J. Diao, J. Li, G. Henkelman, D. Cai, JJ Biendicho, JR Morante, A. Cabot, Advanced Functional Materials 2022 , 32, 2201322.

[2] R. Xiao, D. Luo, J. Wang, H. Lu, H. Ma, EM Akinoglu, M. Jin, X. Wang, Y. Zhang, Z. Chen, Advanced Science 2022 , 9, 2202352

Keywords: Energy material, HRTEM, nanomaterials

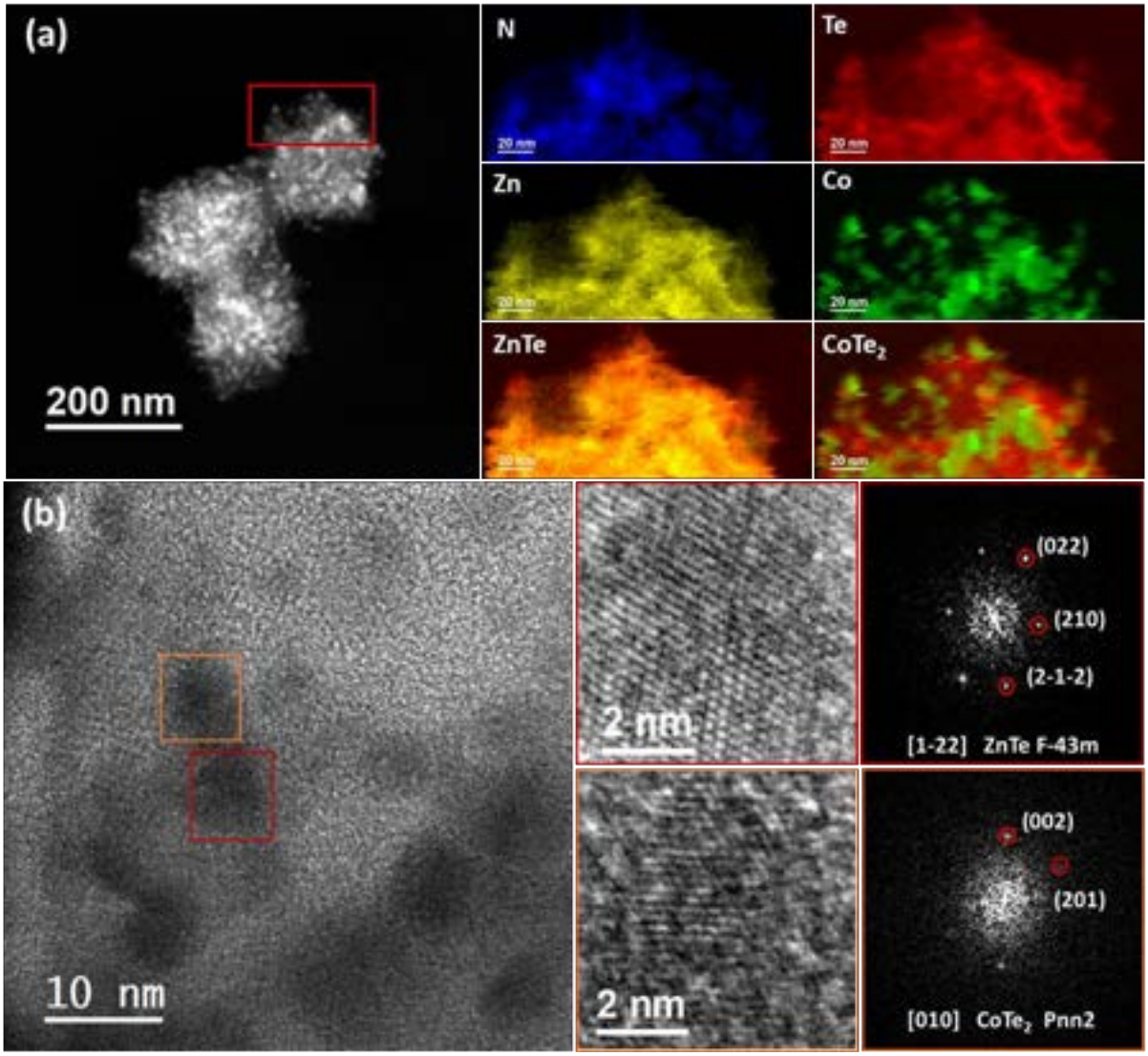

NOISE REDUCTION IN FFTS THROUGH MACHINE LEARNING ALGORITHMS FOR THE STUDY OF GE-BASED QUANTUM COMPUTING DEVICES

Ivan Pinto (Spain)[1]; Marc Botifoll (Spain)[1]; Jordi Arbiol (Spain)[1,2]

1 - ICN2; 2 - ICREA

Abstract

Ge quantum devices have become increasingly relevant and widely studied in recent years due to their applications in quantum computation. One of the most effective techniques for characterizing these materials and studying their physical properties is High Angle Annular Dark Field imaging in a Scanning Transmission Electron Microscope (HAADF-STEM). This technique allows researchers to study the crystallography of the material and determine its composition and the presence of defects.

A commonly used methodology for studying these materials involves calculating the Fast Fourier Transform (FFT) spectrum from various regions of interest in the device. These spectra provide information about the crystal phase and orientation of the region. By applying a mask to different frequencies, researchers can visualize the different crystallographic planes and possible defects in the material. However, FFT spectra often have noise that can impede the study of these materials.

To address this issue, in this work, we used a Convolutional Neural Network (CNN) to denoise FFT spectra. The CNN was trained on over 5000 simulated spectra from various materials, typically used in quantum devices, and in different orientations. Denoising the FFTs facilitated a more thorough study of these spectra, allowing us to conduct a comprehensive study of these Ge devices. Furthermore, this CNN model may become a key and common step in the analytical workflow towards cleaner microscopy data analysing quantum devices and beyond.

Acknowledgments

ICN2 acknowledges funding from Generalitat de Catalunya 2021SGR00457. This study is part of the Advanced Materials programme and was supported by MCIN with funding from European Union NextGenerationEU (PRTR-C17.I1) and by Generalitat de Catalunya. The authors thank support from the project NANOGEN (PID2020-116093RB-C43), funded by MCIN/ AEI/10.13039/501100011033/ and by “ERDF A way of making Europe”, by the “European Union”. ICN2 is supported by the Severo Ochoa program from Spanish MCIN / AEI (Grant No.: CEX2021-001214-S) and is funded by the CERCA Programme / Generalitat de Catalunya. Ivan Pinto and Marc Botifoll are greatful for financial support from FI Agaur Scolarship.

References

[1] S. Roddaro et al., “Spin states of holes in Ge/Si Nanowire quantum dots,” Phys. Rev. Lett., vol. 101, no. 18, 2008.
[2] O. Ronneberger, P. Fischer, and T. Brox, “U-Net: Convolutional Networks for Biomedical Image Segmentation,” in Lecture Notes in Computer Science, Cham: Springer International Publishing, 2015, pp. 234–241.

Keywords: ML, AI, FFT, denoising

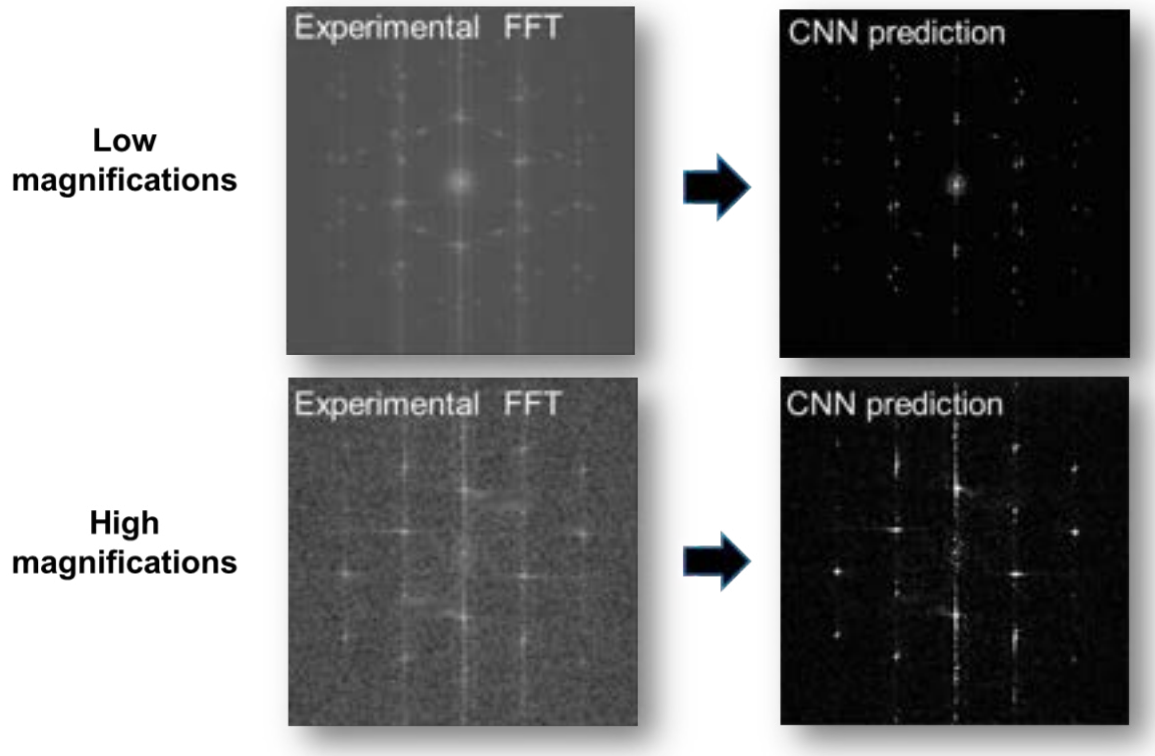

IN-SITU LIQUID (SCANNING) TRANSMISSION ELECTRON MICROSCOPY STUDIES OF COBALT OXIDE CATALYST FOR THE OXYGEN EVOLUTION REACTION

David Llorens Rauret (Spain)[1]; Ranit Ram (Spain)[3]; Fengli Yang (Germany)[4,5]; Alba Garzón Manjón (Spain)[1]; Francisco Pelayo García De Arquer (Spain)[3]; See Wee Chee (Germany)[4,5]; Jordi Arbiol (Spain)[1,2]

1 - ICN2; 2 - ICREA; 3 - ICFO; 4 - FHI; 5 - MPG

Abstract

In the context of the global energy crisis and of the advancements in clean energy technologies, the oxygen evolution reaction (OER) has emerged as a key process in some of the most important systems for sustainable energy conversion and storage. However, the 4-electron transfer mechanism of the reaction arises as a challenge for its large-scale implementation.1 Cobalt oxides are promising, cost-effective, noble metal-free catalyst for OER owing to its outstanding physicochemical properties.2 Specifically, they exhibit low overpotentials and high stability in acid mediums, which result in a viable high-performance catalyst. Nonetheless, long exposures to the harsh conditions of electrocatalytic OER can cause changes in nanoparticles' size, composition, and morphology.3

In recent years, in-situ (scanning) transmission electron microscopy ((S)TEM) has emerged as a powerful tool for studying the structure-property relationship of catalytic materials. The high spatial resolution, integrated chemical analysis spectroscopy techniques, and the ability to apply external stimuli, such as electrochemical potential bias, make in-situ (S)TEM a valuable technique for investigating dynamical effects in catalytic systems within their natural or operational environment.4 In addition to microscopy, spectroscopy, or diffraction data from conventional TEM experiments, in-situ studies can also offer insights into catalyst activity, selectivity, and stability.

By exploring the behaviour of the cobalt oxides under an applied bias voltage, e.g., during a cyclovoltammetry, using an in-situ liquid cell, the stability of the material can be studied. The degradation mechanisms responsible for the catalyst structural transformations can be revealed, and ways to extend their life cycle can be implemented. The study of nanostructured cobalt oxide catalyst under realistic working conditions using in-situ (S)TEM represents a ground-breaking approach in catalysis research. The real-time correlation between structure (TEM images) and activity (electrochemical data) can benefit the development of a highly efficient and stable catalyst.

Acknowledgments

ICN2 acknowledges funding from Generalitat de Catalunya 2021SGR00457. This study is part of the Advanced Materials programme and was supported by MCIN with funding from European Union NextGenerationEU (PRTR-C17.I1) and by Generalitat de Catalunya. The authors thank support from the project NANOGEN (PID2020-116093RB-C43), funded by MCIN/ AEI/10.13039/501100011033/ and by "ERDF A way of making Europe", by the "European Union". ICN2 is supported by the Severo Ochoa program from Spanish MCIN / AEI (Grant No.: CEX2021-001214-S) and is funded by the CERCA Programme / Generalitat de Catalunya.

References

1. Wen, Y. et al. Introducing Brønsted acid sites to accelerate the bridging-oxygen-assisted deprotonation in acidic water oxidation. Nature Communications 2022 13:1 13, 1–11 (2022).
2. Bagwade, P. P. et al. Nanocrystalline cobalt tungstate thin films prepared by SILAR method for electrocatalytic oxygen evolution reaction. Int J Hydrogen Energy 48, 8465–8477 (2023).
3. Liu, L. & Corma, A. Structural transformations of solid electrocatalysts and photocatalysts. Nature Reviews Chemistry 2021 5:4 5, 256–276 (2021).
4. Wu, Z.-P., Zhang, H., Chen, C., Li, G. & Han, Y. Applications of in situ electron microscopy in oxygen electrocatalysis. Microstructures 2, 2022002 (2022).
5. He, B., Zhang, Y., Liu, X. & Chen, L. In-situ Transmission Electron Microscope Techniques for Heterogeneous Catalysis. ChemCatChem 12, 1853–1872 (2020).

Keywords: in-situ, Cobalt oxide, oxygen evolution reaction, energy materials

PD-RICH PDAU NETWORKS OF NANOPARTICLES: EVOLUTION UNDER O2 AND CO2 WITHIN AN ENVIRONMENTAL TEM

Francisco J. Cadete Santos Aires (France)[1]; Eric Ehret (France)[1]; Bruno Domenichini (France)[2]; Laurence Burel (France)[1]

1 - IRCELYON (UMR5256 CNRS/UCBL); 2 - ICB (UMR6303 CNRS/UTMB/UB)

Abstract

The di-block copolymer approach is well suited to obtain well controlled (size, composition, ordered arrays) supported NPs which can be used as supported metallic catalysts on both flat (model catalysts) and powder (realistic catalysts) supports [1]. In this approach, an amphiphilic di-block copolymer dissolved in toluene yields a system of inverse micelles. We can then metallize the cores of these micelles by introducing metal salts. Such systems can then be deposited on flat surfaces by dip or spin coating for instance. We have already extended this method to the synthesis of bimetallic model catalysts [2] and have previously showed, using an Environmental TEM (Ly-EtTEM), that, for the Au-rich PdAu system under O2 pressure, the individual NPs formed between 350°C and 500°C and the network is stable up to 900°C and is only disrupted when the individual NPs begin to decompose above 1000°C [3]. Here we present a complementary study on a Pd-rich PdAu system and its behaviour under oxidizing (O2) and reducing (CO2) conditions within the Ly-EtTEM (TFS Titan ETEM G2 60-300kV, operated at 300kV under gas pressures up to 20 mbar and variable temperature). To perform the experiments, an Pd-rich AuPd core-metallized PS-b-P2VP micellar solution was deposited by spin-coating on dedicated heating microchips, positioned on a WildFire support holder with (DENSsolutions), capable of reaching temperatures up to 1300°C. Special care was taken to minimize/prevent any influence of the electron beam on the observed events. For this Pd-rich PdAu system (≈ 80% at. Pd), under O2, the bimetallic seeds begin to sinter around 300°C to form individual NPs and, at 450°C, demixing of the NPs leading to Janus NPs (Au-rich/PdO; Figure 1a) is observed (Figure 1d-e); the latter are readily reduced and bimetallic NPs reform upon CO exposure (Figure 1f-h). These results will be comparatively discussed with those obtained previously on the Au-rich PdAu system.

Acknowledgments

The authors acknowledge the French Microscopy and Atom probe network (METSA, www.metsa.fr) for supporting this work and the Consortium Lyon – St-Etienne de Microscopie (CLYM, www.clym.fr) for access to the Lyon Environmental and tomographic TEM (Ly-EtTEM).

References

[1] B. Roldan Cuenya, Accounts of Chemical Research 46 (2013) 1682.
[2] E. Ehret et al., Nanoscale 7 (2015) 13239.
[3] E. Ehret et al., Microscopy and Microanalysis 27 (Suppl. 2) (2021) 77.

Keywords: di-block copolymer inverse micelles, Pd-rich PdAu NP networks, Oxidation/Reduction, Environmental TEM

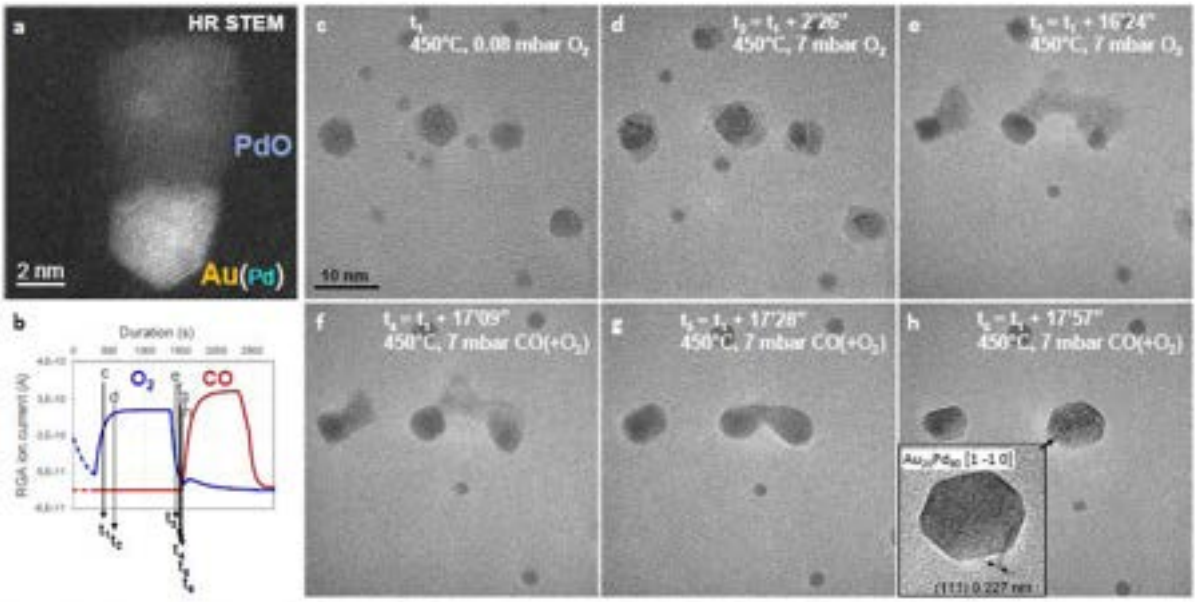

Figure 1: Detail of a Janus NP [PdO-Au(Pd)] formed during oxidation (7 mbar O_2) of a Pd-rich AuPd bimetallic NP at 450° (a) and sequence showing in situ ETEM oxidation of bimetallic Pd-rich AuPd NPs (c) under O_2 (d-e) followed by a prompt reduction under CO (f-h + HR image as insert in h) at 450°C and 7 mbar of gas according to the RGA profile shown in (b).

IMPROVING PHASE CONTRAST IN ABERRATION-CORRECTED TEM USING A THIN-FILM ZERNIKE PHASE PLATE

Simon Hettler (Spain)[1,2]; Raul Arenal (Spain)[1,2,3]

1 - Laboratorio de Microscopías Avanzadas (LMA), Universidad de Zaragoza, Spain; 2 - Instituto de Nanociencia y Materiales de Aragón (INMA), Universidad de Zaragoza, Spain; 3 - ARAID Foundation, Zaragoza, Spain

Abstract

The development of aberration correctors has pushed the limits of transmission electron microscopy (TEM). Although the resolution is strongly enhanced and in a range that allows resolving almost all crystal lattices, the contrast in acquired images is low. In fact, in a completely aberration-free microscope under focused conditions, phase-contrast transfer is zero. This low transfer leads to weak contrast of many nanomaterial and related thin material science specimens, which only weakly modify the phase of the transmitted electron wave. In biology and life science, physical phase plates (PPs), which allow enhancing phase contrast, have been applied in a large variety of forms [1].

In this work, we studied the application of a thin-film Zernike PP in aberration-corrected TEM to study nanomaterial samples [2]. The PP, consisting of a thin amorphous carbon film, was implemented in the plane of the objective aperture in an image-corrected Titan microscope and applied to a Fe3-δO4 nanoparticles sample [3]. In the comparison between two focused images acquired with (Figure 1a) and without the PP (Figure 1d), the strong enhancement in contrast is obvious. A small defocus difference induced by the PP presence might affect the lattice-fringe contrast at atomic resolution, but the main effect on contrast is clearly attributed to the action of the PP. The contrast enhancement is also visible as brighter contrast in the corresponding power spectra at intermediate spatial frequencies (Figure 1b and c).

A thorough study of the experimental PP performance accompanied with phase-contrast transfer function calculations shows that PPs are not only promising for life science applications but may increase contrast in material science analysis as well. Simulations also indicate that interpretability is increased when using PPs [4].

Acknowledgments

Funding from DFG (He 7675/1-1), the EU Horizon 2020 programme (MSC-IF: GA No. 889546, ESTEEM3: GA No. 823717) and Spanish MICN (PID2019-104739GB-100/AEI/10.13039/501100011033) is acknowledged.

References

[1] M Malac et al, Microscopy 70, 1, 75-115 (2020).
[2] S Hettler, R Arenal, Ultramicroscopy, 239, 113564 (2022).
[3] K. Sartori et al, ACS Appl. Mater. Interfaces 13, 14, 16784-16800 (2021).
[4] S Hettler, R Arenal, Ultramicroscopy 2a (1), 113319, (2021).

Keywords: transmission electron microscopy, phase plate, aberration correction

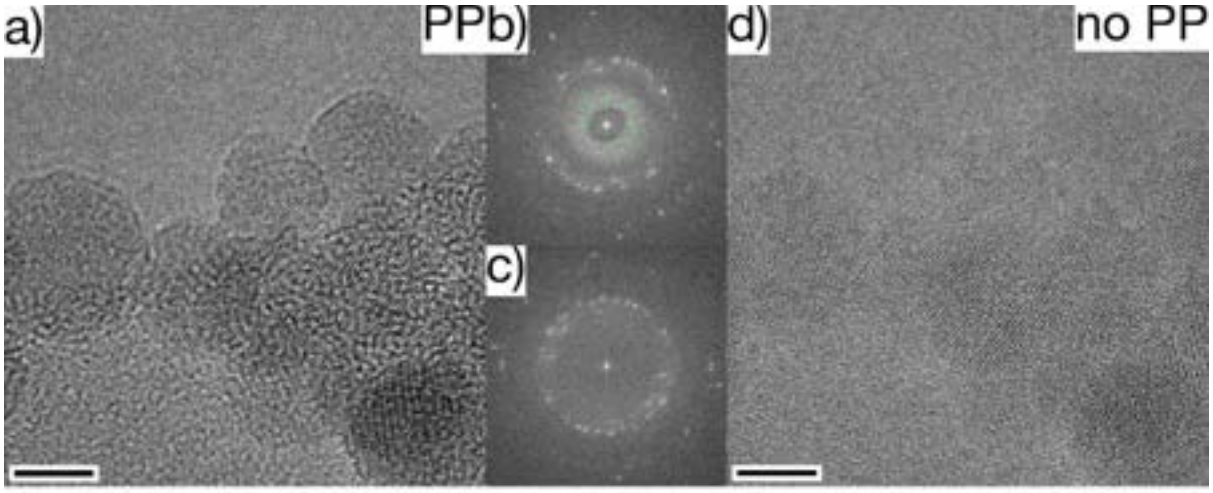

Fig. 1: (a,d) HRTEM images of Fe3-δO4 NPs with (b,c) corresponding FFTs (size of 14.3 nm-1 x 14.3 nm-1) acquired (a,b) with and (c,d) without Zernike PP (hole radius of 5 µm). Contrast settings for (a,d) are identical. Scale bars 5 nm.

INORGANIC NANOTUBES FROM MISFIT LAYERED COMPOUNDS (SMX,Y1-X)S-TAS2 – AN ELECTRON MICROSCOPE STUDY

Mohammad Furqan (Spain)[1]; Simon Hettler (Spain)[1]; Raul Arenal (Spain)[1]

1 - UNIVERSIDAD DE ZARAGOZA

Abstract

Misfit layered compounds (MLCs) have garnered considerable attention due to the fascinating chemistry and their properties [1]. MLCs are composed of two distinct layered chalcogenides that are stacked alternately along the 'c' direction. The MLC stack is composed of metal chalcogenide (MX) and a transition metal dichalcogenide (TX 2) structures [1,2]. The properties of MLCs can be tuned by the chemical and structural interplay between MX and TX 2. The nanotubes (NTs) from these MLCs offer potential applications in thermoelectrics due to the complementary properties of the two layered compounds [1]. Recently, a modified synthesis method of MLC-NT has permitted the introduction of additional elements to form a quaternary compound starting from LaS-TaS 2 [3,4]. Here, we present an electron microscopy analysis of the novel family of (Sm, Y)S-TaS 2 nanostructures. The partial exchange of Sm(S) by Y(S) provides a pathway for the fine control of the MLC structure and its properties.

Different transmission electron microscopy (TEM) techniques including (high-resolution (scanning)TEM (HR(S)TEM) imaging, electron diffraction and energy-dispersive x-ray spectroscopy (EDS)) have been employed to profoundly analyze these nanotubes. HRSTEM and STEM-EDS provide information about the NT's composition and atomic arrangement. Electron diffraction patterns allow to determine the crystal structure of NTs. In Fig. 1c and d, two STEM images are presented, illustrating the repetitive layers of (Sm, Y)S and TaS 2 . The results obtained from Electron Diffraction show that the substitution of Sm by Y is homogeneous and in-phase, with negligible effects on the material's lattice parameter. The study of the elemental composition of these NTs by EDS reveals the atomic weight percentage of the Sm and Y in each batch (Sm x ,Y 1-x)S-TaS 2 . Materials similar to NTs (Fig 1a) were observed in addition to NTs themselves (Fig 1b), but further examination revealed that these additional materials cannot be classified as NTs.

In summary, through comprehensive EM analysis, we have demonstrated the successful synthesis of an unexplored group of quaternary MLC-nanomaterials. These works provide interesting information about their structure and composition.

Acknowledgments

This work was supported by the Spanish MICN (project grant PID2019-104739GB-100/AEI/10.13039/501100011033), and European Union H2020 programsMarie Skłodowska-Curie-IF “PROMISES” (889546), Graphene Flagship CORE3 (881603) and “ESTEEM3” (823717).

References

1 - M. Serra, R. Arenal, R. Tenne, (2019). Nanoscale 11, 8073-8090.
2 – MB Sreedhara Chemistry of Materials 2022 34 (4), 1838-1853
3 - S. Hettler et al (2020), ACS Nano 14, 5, 5445–5458
4 - G. Radovsky et al. (2016). J Mater Chem C 4, 89–98.

Keywords: misfit-layered compounds, electron microscopy, ((S)TEM), nanotubes

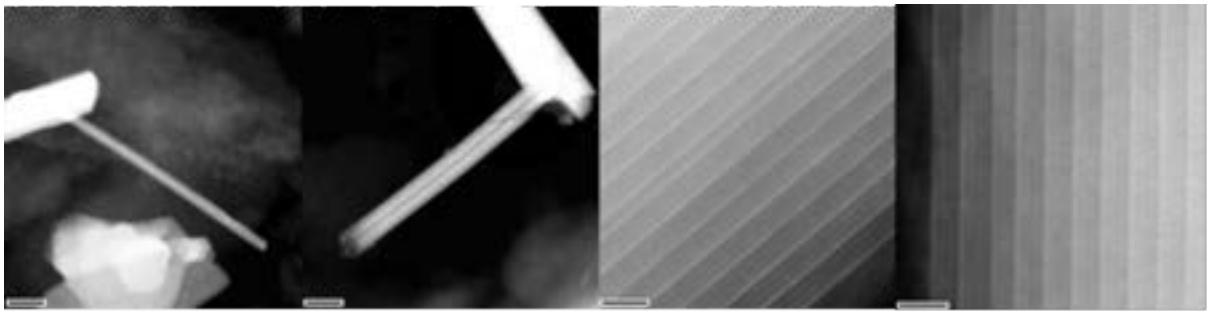

Figure 1: , (a) 200 nm and (b) 400 nm, STEM-HAADF images of (Sm,Y)S-TaS 2 NTs with 40% percent of Y. Scale bars are (c,d) 2 nm respectively

STUDY OF MICROSTRUCTURAL EVOLUTION OF HIGH CURRENT DENSITY YBCO SUPERCONDUCTING THIN FILMS AND COATED CONDUCTORS GROWN BY ULTRAFAST TRANSIENT LIQUID ASSISTED GROWTH (TLAG)

Kapil Gupta (Spain)[1,2]; Lavinia Saltarelli (Spain)[2]; Albert Queraltó (Spain)[2]; Roger Guzmán (Spain)[2]; Laia Soler (Spain)[2]; Júlia Jareño (Spain)[2]; Juri Banchewski (Spain)[2]; Silvia Rasi (Spain)[2]; Diana Garcia (Spain)[2]; Valentina Roxana Vlad (Spain)[2]; Aiswarya Kethamkuzhi (Spain)[2]; Joffre Gutierrez (Spain)[2]; Susagna Ricart (Spain)[2]; Cristian Mocuta (France)[3]; Belén Ballesteros (Spain)[1]; Xavier Obradors (Spain)[2]; Teresa Puig (Spain)[2]

1 - Institut Català de Nanociència i Nanotecnologia (ICN2); 2 - Institut de Ciència de Materials de Barcelona (ICMAB-CSIC); 3 - Synchrotron SOLEIL

Abstract

The outstanding ability of YBa2Cu3O7−x (YBCO) films to carry high currents at high magnetic fields offers an unprecedented opportunity to be used in large-scale superconducting power applications and high-field magnets. In an essential need of high-performance and low-cost manufacturing, chemical-solution deposition (CSD) has become a cost-effective and scalable methodology to grow epitaxial YBCO films [1]. However, their growth rates are rather small (0.5-1 nm/s). For this purpose, we have developed a novel growth approach, entitled, Transient Liquid Assisted Growth (TLAG) [2-4], by combining CSD methodologies with ultra-fast growth rates (100-1000 nm/s) using a non-equilibrium liquid-mediated approach. Critical current densities (Jc) up to 5MA/cm2 at 77K are already realized in TLAG-CSD thin films [2], but understanding of initial nano precursor phases and fine-tuning of growth parameters are essential to further improve the Jc in thicker films [4]. Therefore, the microstructure of multi-deposited nanocrystalline and grown YBCO films, investigated via HR-TEM, STEM, and EELS, will be presented. Moreover, a phenomenon of re-orientation of homogeneous-to-heterogeneous epitaxial growth of YBCO will also be discussed.

Furthermore, the control over the YBCO film microstructure is essential to enhance Jc, which can be achieved by well-controlled nano-defects embedded in the epitaxial superconducting-matrix acting as vortex-pinning-centers. We found that the microstructure of pristine YBCO could be tuned significantly via TLAG-CSD by optimizing different growth parameters. Besides, the addition of secondary phase, like nanoparticles nano inclusions can also increase flux-pinning at high fields by incorporating pre-formed nanoparticles to the metal-organic-inks [2]. Therefore, the detailed microstructure of pristine YBCO, YBCO nanocomposites, and coated-conductors with varying growth parameters on different substrates investigated via HR-TEM, atomic-resolution STEM, and EELS will also be discussed.

References

[1] J. Gutierrez, A. et al., Nat. Mat., 6, 367 (2007)
[2] L. Soler et al, Nat. Commun., 11, 344 (2020)
[3] S. Rasi et al, Adv Sci, 9, 2203834 (2022)
[4] L. Saltarelli, K.Gupta et al, ACS Appl. Mater. Interfaces 14 48582 (2022)

Keywords: YBCO, TLAG-CSD, TEM, Superconductivity

THE STRUCTURAL CHARACTERIZATION OF BI2TE3 ORDERED 3D NANO-NETWORKS BY MEANS OF ELECTRON TOMOGRAPHY AND PRECESSION-ASSISTED 4D-STEM

Sergi Plana-Ruiz (Spain)[1]; Javier Blanco-Portals (Spain)[2]; Sònia Estradé (Spain)[2]; Lluís López-Conesa (Spain)[2]; Beatriz Vargas-Carosi (Spain)[2]; Alejandra Ruiz-Clavijo (Spain)[3]; Olga Caballero-Calero (Spain)[3]; Miguel López-Haro (Spain)[4]; Marisol Martín-González (Spain)[3]; Francesca Peiró (Spain)[2]

1 - Servei de Recursos Científics i Tècnics, Universitat Rovira i Virgili; 2 - LENS-MIND, Departament d'Enginyeria Electrònica i Biomèdica, Universitat de Barcelona; 3 - Instituto de Micro y Nanotecnología (IMN-CNM), CSIC (CEI UAM+CSIC); 4 - Departamento de Ciencia de los Materiales e Ingeniería Metalúrgica y Química Inorgánica, Universidad de Cádiz

Abstract

Tetradymite chalcogenides such as Bi2Te3 are small band gap semiconductors that are strong 3D topological insulators with applications in Peltier cooling devices or thermoelectric power generators. Interestingly, while thin films and individual nanowires (NWs) have shown a reduced thermoelectric performance, the ordered 3D networks of these motifs have shown competitive properties for these applications1. In this context, we present here the structural characterization in a TEM of 3D networks of Bi2Te3 NWs fabricated via template-assisted electrochemical deposition2. The network consists in a highly ordered hexagonal array of free-standing NWs that are connected by nanochannels perpendicular to the length of the NWs at a periodic distance of 417 ± 10 nm. First, an image electron tomography was performed to determine the three-dimensional morphology of the NWs and their distribution in the network3. This allowed to measure the length and width of the NWs as well as their transversal connections in different positions and from different perspectives. The period of 417 nm between the connections was confirmed, the NWs diameter was determined to be 57 ± 5 nm, the distance between different NWs was averaged to be 67 ± 5 nm and the width of the nanochannels was taken at 28 ± 5 nm. Second, precession-assisted 4D-STEM maps were collected to assess the crystallinity of the NWs and their junctions. These diffraction maps consist of electron diffraction patterns collected in a defined area that allowed the generation of orientation maps by means of a template-matching algorithm based on simulated patterns4. The obtained orientation maps demonstrated that the NWs are not formed by a single-crystalline domain, but rather several grains between 200 and 500 nm in length, which are rotated with respect to each other around the [110] crystallographic direction. Furthermore, it was observed that the crystalline orientation of the transversal connections was the same as the grains from both connected NWs. In this way, the 3D networks of Bi2Te3 NWs could be fully structurally characterised at the nanoscale by methods employed in the real and diffraction space, respectively.

Acknowledgments

We acknowledge the support received from the ELECMI - ICTS Electron Microscopy for Materials Science. The authors would also like to acknowledge the financial support from the Spanish project PID2019-106165GB-C21, and from the Catalan Government through 2021SGR00242.

References

(1) Ruiz-Clavijo, A.; Caballero-Calero, O.; Manzano, C. V.; Maeder, X.; Beardo, A.; Cartoixà, X.; Álvarez, F. X.; Martín-González, M. 3D Bi2Te3 Interconnected Nanowire Networks to Increase Thermoelectric Efficiency. ACS Appl. Energy Mater. 2021, 4 (12), 13556–13566. https://doi.org/10.1021/acsaem.1c02129.

(2) Martín, J.; Martín-González, M.; Francisco Fernández, J.; Caballero-Calero, O. Ordered Three-Dimensional Interconnected Nanoarchitectures in Anodic Porous Alumina. Nat Commun 2014, 5 (1), 5130. https://doi.org/10.1038/ncomms6130.

(3) Goris, B.; Van den Broek, W.; Batenburg, K. J.; Heidari Mezerji, H.; Bals, S. Electron Tomography Based on a Total Variation Minimization Reconstruction Technique. Ultramicroscopy 2012, 113, 120–130. https://doi.org/10.1016/j.ultramic.2011.11.004.

(4) Viladot, D.; Véron, M.; Gemmi, M.; Peiró, F.; Portillo, J.; Estradé, S.; Mendoza, J.; Llorca-Isern, N.; Nicolopoulos, S. Orientation and Phase Mapping in the Transmission Electron Microscope Using Precession-Assisted Diffraction Spot Recognition: State-of-the-Art Results. Journal of Microscopy 2013, 252 (1), 23–34. https://doi.org/10.1111/jmi.12065.

Keywords: 3D nano-networks, Image Tomography, 4D-STEM, TEM

STRUCTURAL MODEL OF NEW PRECIPITATES OBSERVED IN NI-MN-GA-HF/ZR HIGH TEMPERATURE SHAPE MEMORY ALLOYS

Shoukai Xu (China)[2]; Jaume Pons (Spain)[1]; Ruben Santamarta (Spain)[1]

1 - Universitat de les Illes Balears; 2 - Xi'an Rare Metal Materials Institute Co., Ltd.

Abstract

Shape memory alloys (SMA), such as Ni-Ti, Cu-Zn-Al, Cu-Al-Ni, Au-Cd, Ni-Mn-Ga, … undergo a thermoelastic martensitic transformation, which is the basis of their functional properties, including the shape memory and superelasticity effects, and high damping capacity [1]. High Temperature Shape Memory Alloys (HTSMAs), working above 370 K, have been largely demanded in the last decade, particularly by aerospace, automotive and energy industries [2]. Among the different SMA families, Ni-rich Ni-Mn-Ga alloys have emerged as potential candidates for HTSMAs due to their excellent functional properties in single crystalline state and exceptional thermal stability for some specific compositions [3]. Nevertheless, the practical application of Ni-Mn-Ga polycrystals is hindered by their intrinsic brittleness and intergranular fracture. An effective approach to solve this problem is the formation of a ductile second phase along the grain boundaries. For Ni-Mn-Ga alloys, the precipitation of a ductile face-centered cubic (f.c.c.) phase, referred to as the γ phase, can be achieved by increasing the Ni content or by addition of quaternary elements, resulting in an enhancement of the ductility in many cases [4-6].

This study investigates the effect of low amounts of Hf or Zr addition on the functional properties and microstructure of a Ni-rich Ni-Mn-Ga HTSMA, not previously explored in the literature. The diffraction patterns obtained from second phase precipitates in these alloys exhibit an apparent f.c.c. structure similar to the γ phase (Fig. a), but with nearly twice the lattice parameter reported for the normal γ phase [7, 8]. Combining the information from SAEDPs in different zone axes with the composition obtained by EDX, the proposed structural model is built-up from an array of 8 (2x2x2) basic f.c.c. cells in which the Hf or Zr atoms occupy specific positions. As for the rest of elements, two possibilities are considered: i) disordered model with random positions of the Ni, Mn and Ga atoms (Fig. b); ii) ordered model for the Ni atoms, which occupy specific positions while the rest of lattice sites are randomly occupied by Mn and Ga (Fig. c). Both models give rise to simulated XRD and TEM diffraction patterns that match the experimental results. However, the structure is more accurately described in a different set of crystallographic axes (Fig. d), which results in an A6 face-centered tetragonal unit cell (space group I4/mmm, No. 139), as shown in Figs. e and f.

Acknowledgments

Drs. F. Hierro and J. Cifre from the Serveis Cientificotecnics-UIB are acknowledged for their assistance in the SEM-EDX and XRD experiments. This work has been supported by the Spanish "Ministerio de Ciencia e Innovación - Agencia Estatal de Investigación (MCIN-AEI)" and "Fondo Europeo de Desarrollo Regional (FEDER), EU" under the project RTI 2018-094683-B-C51.

References

[1] K Otsuka, CM Wayman, eds. “Shape memory materials” (Cambridge University Press) 1998.
[2] J. Ma, I. Karaman, R.D. Noebe, High temperature shape memory alloys, Int. Mater. Rev. 55 (2010) 257–315. https://doi.org/10.1179/095066010X12646898728363.
[3] R. Santamarta, E. Cesari, J. Muntasell, J. Font, J. Pons, P. Ochin, Thermal and microstructural evolution under ageing of several high-temperature Ni-Mn-Ga alloys, Intermetallics. 18 (2010) 977–983. https://doi.org/10.1016/j.intermet.2010.01.016.
[4] Y. Xin, Y. Li, Microstructure, mechanical and shape memory properties of polycrystalline Ni-Mn-Ga high temperature shape memory alloys, Mater. Sci. Eng. A. 649 (2016) 254–262. https://doi.org/10.1016/j.msea.2015.09.123.
[5] E. Villa, E. Villa, M. Melzi D’Eril, A. Nespoli, F. Passaretti, The role of γ-phase on the thermo-mechanical properties of NiMnGaFe alloys polycrystalline samples, J. Alloys Compd. 763 (2018) 883–890. https://doi.org/10.1016/j.jallcom.2018.06.028.
[6] J. Wang, H. Bai, C. Jiang, Y. Li, H. Xu, A highly plastic Ni50Mn25Cu18Ga7 high-temperature shape memory alloy, Mater. Sci. Eng. A. 527 (2010) 1975–1978. https://doi.org/10.1016/j.msea.2009.12.021.
[7] H.B. Xu, Y. Li, C.B. Jiang, Ni-Mn-Ga high-temperature shape memory alloys, Mater. Sci. Eng. A. 438 (2006) 1065–1070. https://doi.org/10.1016/j.msea.2006.02.187.
[8] S. Yang, Y. Ma, H. Jiang, X. Liu, Microstructure and shape-memory characteristics of Ni56Mn25−xCoxGa19 (x= 4, 8) high-temperature shape-memory alloys, Intermetallics. 19 (2011) 225–228. https://doi.org/10.1016/j.intermet.2010.08.009.

Keywords: Shape Memory Alloys, Precipitation, Structural model, Martensitic Transformation

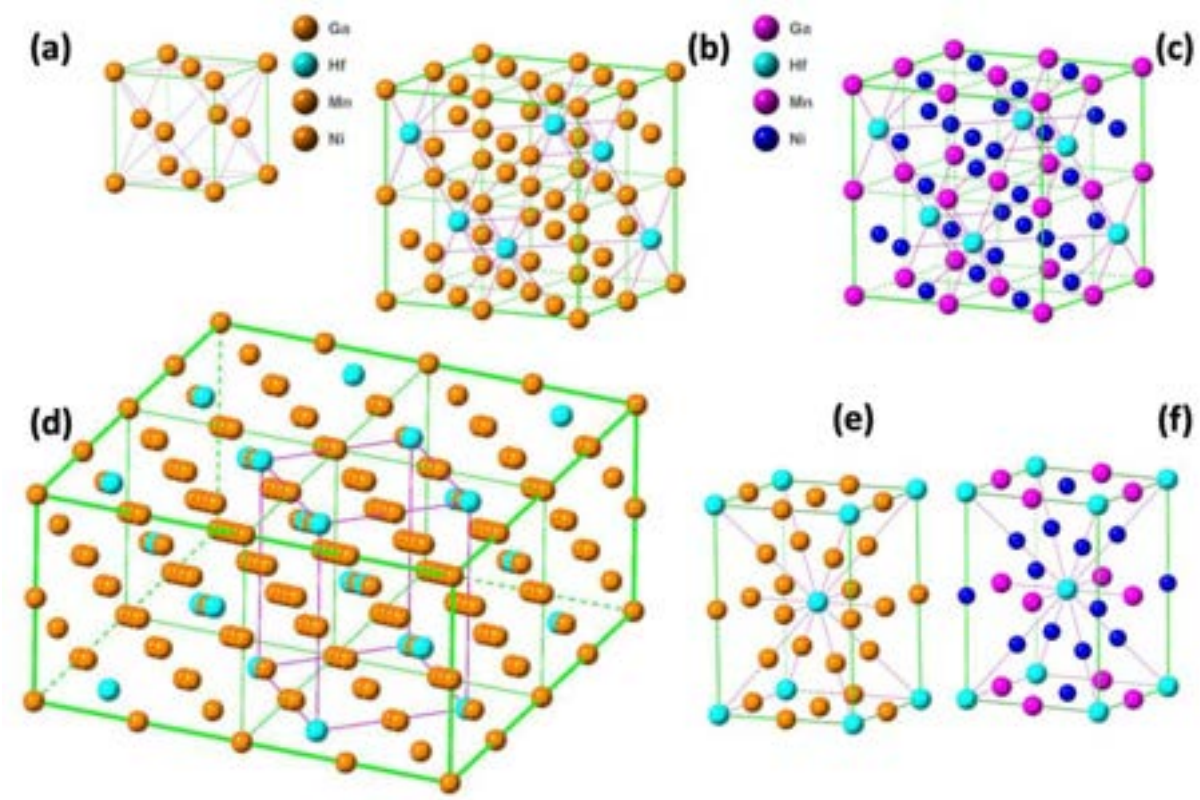

TEMPERATURE-DRIVEN STRUCTURAL AND COMPOSITIONAL EVOLUTION OF AUPD AND AURU BIMETALLIC CATALYSTS SUPPORTED ON CE-ZR MIXED OXIDE UNDER DIFFERENT ATMOSPHERES. NEW INSIGHTS FROM IDENTICAL LOCATION SCANNING TRANSMISSION ELECTRON MICROSCOPY STUDIES

Ramón Manzorro (Spain)[1]; Carol Olmos (Spain)[1]; Xiaowei Chen (Spain)[1]; José Calvino (Spain)1; Ana Hungría (Spain)[1]; Lidia Chinchilla (Spain)[1]

1 - Universidad de Cádiz

Abstract

Understanding the correlations between synthesis, structure and functionality in the field of catalysis is closely linked to the development of electron microscopy. In fact, the last decades have seen great developments in the field of in situ electron microscopy in order to obtain insights of transformation pathways that reflect intrinsic catalysts properties under very realistic reaction, which requires a specific infrastructure.[i] As an alternative to in-situ microscopy, Identical Location Transmission Electron Microscopy (ILTEM) [ii] analysis can be applied, which in a more simplistic way allows us to illustrate the interaction of the sample with the environment characteristic of the chemical process used in a macro-scale reactor.

Here, the evolution of the structure and composition of the system of particles in two Ce0.68Zr0.32O2 supported bimetallic catalysts based on Au and Ru (Fig.1) or Pd under high temperature conditions and different redox environments has been followed in STEM mode. In particular, the specific potential of a methodology based on characterizing, both in imaging (High Angle Annular Dark Field contrast) and nanoanalytical (X-Ray Energy Dispersive spectroscopy) modes, exactly the same areas before and after the thermochemical treatments is illustrated. It is proved that these so-called Identical Location STEM-HAADF-XEDS experiments, in which the spatial correlation between the investigated catalyst aggregates is retained, provide information which is unavoidably lost in conventional STEM studies.
From our observations on a sufficiently large number of metallic entities it has been possible to reveal the influence of particle size and nature of the redox environment on the temperature-driven mobilization of the different metals involved in these catalysts. Thus, oxidizing environments evidenced a much higher capacity to mobilize the three metals, preferentially Au. Moreover, prolonged exposure under an oxidising environment has been proved to induce significant modifications in these bimetallic system, even at room temperature. Irrespective of the type of redox environment, bimetallic systems showed better thermal resistance, which demonstrates a beneficial effect of the second metal. Finally, IL-STEM studies have shown how scaling from macroscopic to nanoscopic conditions involves intrinsic changes in heat and mass transfer phenomena, which must be taken into account in the comparative analysis of both type of experiments.

Acknowledgments

This work has been supported by the Junta de Andalucía project P20_00968 and by the Ministry of Science, Innovation and Universities of Spain projects PID2019-110018GA-I00 and PID2020-113006-RB-I00 funded by MCIN/AEI/ 10.13039/501100011033

References

[i] van der Wal, L. I.; Turner, S. J.; Zečević, J. Catal. Sci. Technol. 2021, 11, 363
[[ii]] K. J.J. Mayrhofer, S. J. Ashton, J.osef C. Meiera Gustav K.H. Wiberg, M. Hanzlik, M.Arenz, J. Power Sources 2008, 185, 734.

Keywords: ILSTEM, Bimetallic catalysts, nanostructural evolution, thermochemical treatments

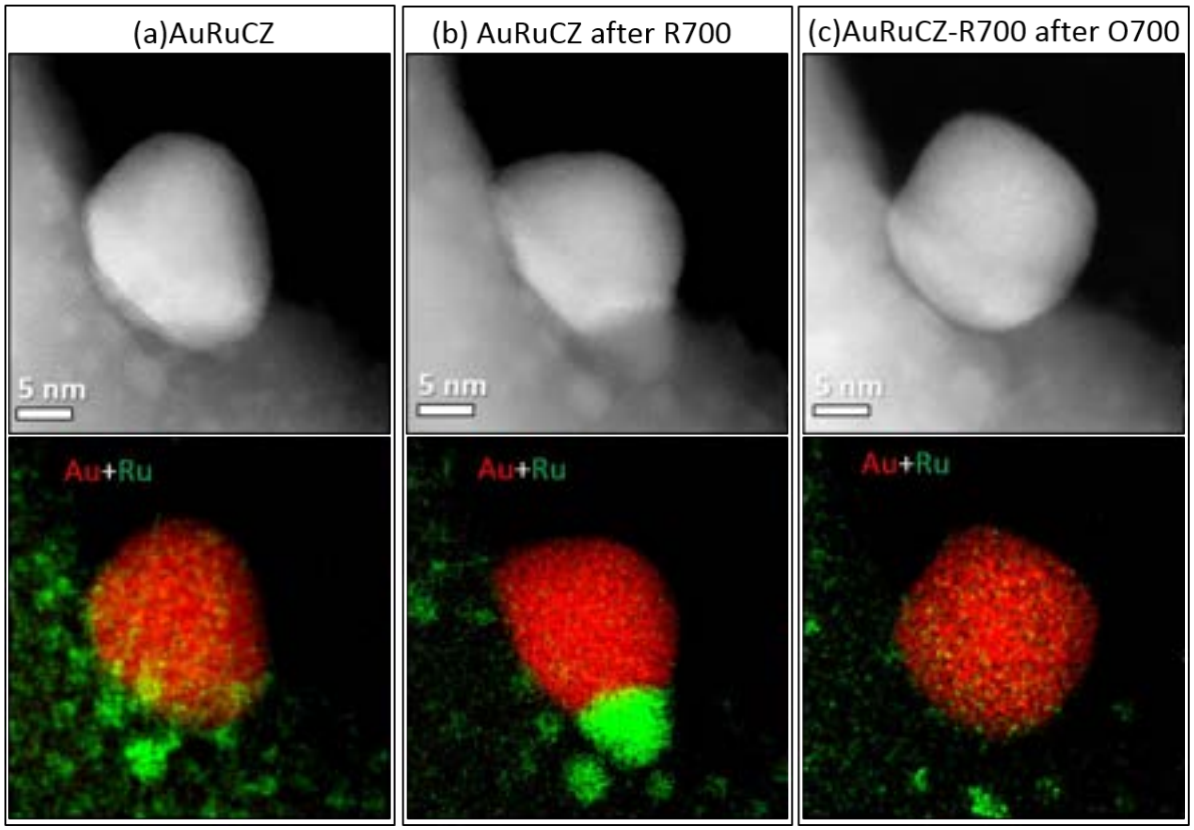

IN SITU HEATING ELECTRON MICROSCOPY OF A NICKEL THIN FILM ACROSS THE CURIE TEMPERATURE

Sergi Plana-Ruiz (Spain)[1]; Mariana Stefanova Trifonova (Spain)[1]; Eric Pedrol Ripoll (Spain)[1]
1 - Servei de Recursos Científics i Tècnics, Universitat Rovira i Virgili

Abstract
The use of a transmission electron microscope (TEM) for in situ experiments has been gaining attention during the last years due to the availability of more stable goniometric stages as well as specifically designed holders, which enable heating, biasing, liquid, and gas experiments at the nanoscale. Although this technology has shown very impressive results in materials science1–3, the preparation of thin-enough multilayer systems for in situ TEM measurements remain a challenge in most laboratories. That is because a lamella needs to be placed and thinned down in a MEMS chip without damaging the different electrodes in a focused ion beam. This work shows as a case study how this can be done for a 50-nm Nickel thin film placed on a heating MEMS chip. Nickel is a ferromagnetic material with plenty of applications, from batteries and fuel cells to special cements or guitar strings. Its Curie temperature is ~ 355 °C, thus it's a perfect candidate to observe in situ how the different crystalline grains behave when the material becomes paramagnetic above such temperature.

The Ni thin layer was deposited by means of a physical vapour deposition process in a magnetron sputtering system. A 10-nm thick titanium layer was previously deposited as adhesion promoter onto a silicon wafer substrate. A high-power delivery in DC was maintained for the Ar plasma to increase the sputtered grain size distribution hence promoting the creation of differentiated bulk domains within the deposited film. The subsequent lamella was prepared using a Thermo Fisher Scios 2 dual beam system. Before thinning and polishing, the extracted chunk was transferred to a DENSsolutions heating MEMS chip and attached to it by deposition of platinum paths. The lamella was thinned to a thickness less than 100 nm and then polished using very low ion beam voltage and current in order not to amorphize the layer. The resulting lamella-on-a-chip was placed on a DENSsolutions Lightning holder and inserted on a JEOL F200 Cold FEG operated at 200kV. Full characterization of the thin film was carried out by means of in situ high-resolution TEM and STEM imaging, EDS mapping and 4D-STEM below and above the Curie temperature.

References
(1) Tsoukalou, A.; Abdala, P. M.; Stoian, D.; Huang, X.; Willinger, M.-G.; Fedorov, A.; Müller, C. R. Structural Evolution and Dynamics of an In2O3 Catalyst for CO2 Hydrogenation to Methanol: An Operando XAS-XRD and In Situ TEM Study. J. Am. Chem. Soc. 2019, 141 (34), 13497–13505. https://doi.org/10.1021/jacs.9b04873.
(2) Ling, Y.; Sun, T.; Guo, L.; Si, X.; Jiang, Y.; Zhang, Q.; Chen, Z.; Terasaki, O.; Ma, Y. Atomic-Level Structural Responsiveness to Environmental Conditions from 3D Electron Diffraction. Nat Commun 2022, 13 (1), 6625. https://doi.org/10.1038/s41467-022-34237-1.
(3) Das, P. P.; Cookman, J.; Pérez, A. G.; Plana-Ruiz, S.; López-Haro, M.; Calvino, J. J.; Casablanca, J. G.; Grivas, E.; Antipas, G. S. E.; Ntallis, N. A.; Nicolopoulos, S. High Angle Liquid Cell TEM Tomography for In Situ Observation and 3D Reconstruction in Liquid. Microsc Microanal 2022, 28 (S1), 854–856. https://doi.org/10.1017/S1431927622003804.

Keywords: TEM, 4D-STEM, In situ heating microscopy

CRYO-EM

AUTOMATIC DETECTION OF ALIGNMENT ERRORS IN CRYO-ELECTRON TOMOGRAPHIC RECONSTRUCTIONSAUTOMATIC DETECTION OF ALIGNMENT ERRORS IN CRYO-ELECTRON TOMOGRAPHIC RECONSTRUCTIONS

Federico P. De Isidro-Gómez (Spain)[1]; Carlos O. S. Sorzano (Spain)[1]; Jose M. Carazo (Spain)[1]

1 - National Center for Biotechnology (CNB-CSIC)

Abstract

Cryogenic electron tomography is a widely used technique for the structural study of biological complexes. It allows the three-dimensional characterization in native state of a broad variety of samples, from cellular environments to purified complexes. The structural information is inferred from a set of images containing projective information in transmission. These images, called tilt series, are acquired by tilting the sample at different tilt angles. Unfortunately, the tilting process can introduce slight but significant displacements and rotations around the tilt axis. To properly combine the acquired images and obtain a 3D reconstruction of the sample, it is mandatory to correct these misalignments, this is the tilt series alignment process. If the alignment parameters are not properly estimated, the final reconstruction will present artifacts and its reliability is compromised. In this work, we present two different approaches to identify the existence of misalignment in the reconstructions without requiring the manual exploration of the data by the scientist. First, an algorithm for the detection of misalignment based on the trajectories described by markers (fiducials) through the tilt-series. And secondly, a deep neural approach for artifact detection over gold beads present in the tomographic reconstruction.

Acknowledgments The authors acknowledge the economical support from MICIN to the Instruct Image Processing Center (I2PC) as part of the Spanish participation in Instruct-ERIC, the European Strategic Infrastructure Project (ESFRI) in the area of Structural Biology, Grant PID2019-104757RB-I00 funded by MCIN/AEI/ 10.13039/501100011033/ and “ERDF A way of making Europe”, by the “European Union.

European Union (EU) and Horizon 2020 through grant: HighResCells (ERC - 2018 - SyG, Proposal: 810057)

References

Sorzano, C. O. S., de Isidro-Gómez, F., Fernández-Giménez, E., Herreros, D., Marco, S., Carazo, J. M., & Messaoudi, C. (2020). Improvements on marker-free images alignment for electron tomography. Journal of Structural Biology: X, 4, 100037.

de la Morena, J. J., Conesa, P., Fonseca, Y. C., de Isidro-Gómez, F. P., Herreros, D., Fernández-Giménez, E., ... & Carazo, J. M. (2022). ScipionTomo: Towards cryo-electron tomography software integration, reproducibility, and validation. Journal of structural biology, 214(3), 107872.

Turoňová, B., Marsalek, L., & Slusallek, P. (2016). On geometric artifacts in cryo electron tomography. Ultramicroscopy, 163, 48-61.

Mastronarde, D. N., & Held, S. R. (2017). Automated tilt series alignment and tomographic reconstruction in IMOD. Journal of structural biology, 197(2), 102-113.

Keywords: cryo-EM

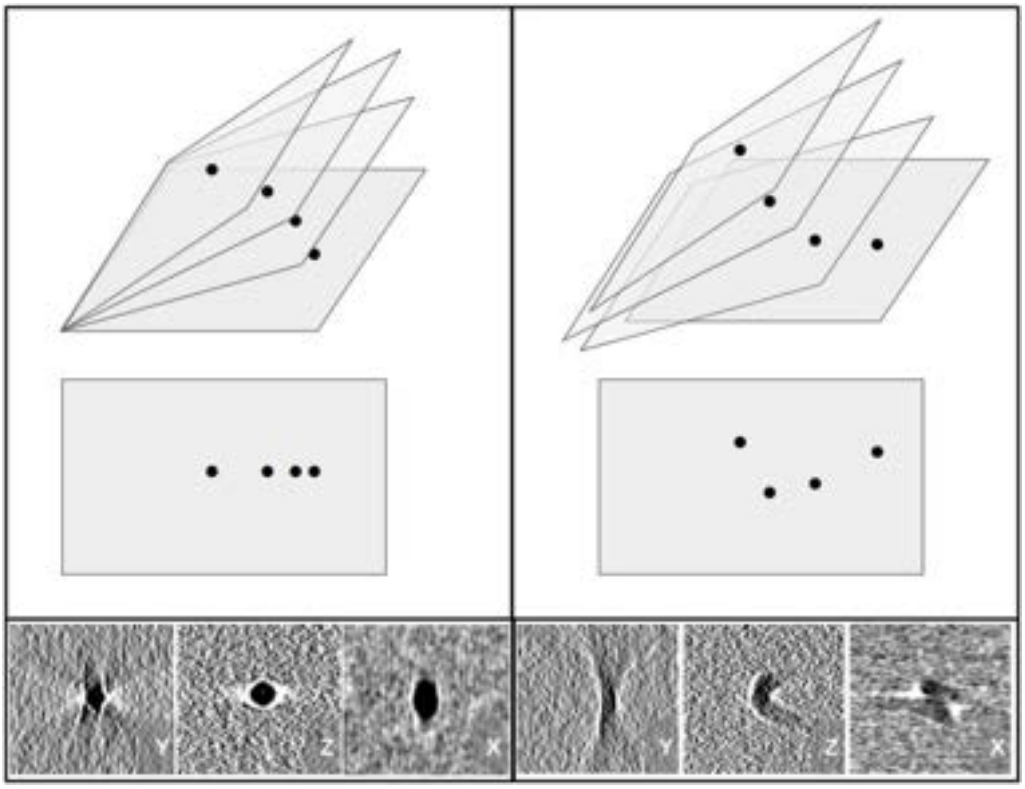

Top left: Schematic of an aligned tilt series in which it can be observed a single marker along the series (top) and its projection in the central plane (bottom). Top right: Same as topo left, but in this case the tilt-series presents some misalignment. It can be observed that the disposition of the protected markers does not present a straight line (as in the case of the aligned tilt-series). Bottom: views of 3-slides average of the same gold bead reconstruction at Y-plane (left), Z-plane (center), and X-plane (right). Bottom left gold bead present no misalignment and bottom right presents twisters (rotation of the tilt axis).

IMPACT AND EXAMPLES OF STRUCTURE-BASED DRUG DESIGN THROUGH CRYOEM AT MSD

Yacob Gomez Llorente (United States of America)[1]; Kaspar Hollenstein (United States of America)[1]; Giovanna Scapin (United States of America)[1,2]; Rachel Palte (United States of America)[1]

1 – MSD; 2 – Nanoimaging Services.

Abstract

Over the past decade, single particle cryo-electron microscopy (cryoEM) has transitioned from a niche technique to a powerful tool for structural biology. This is due, in part, to technological breakthroughs which have made it relatively routine to achieve near atomic resolutions for protein targets of pharmacological interest in complex with drug candidates. Industry has historically relied heavily on Xray crystallography to enable structure-based drug design (SBDD); however, we are seeing that cryoEM is playing an ever-increasing role in that process, especially for challenging samples like large multimeric complexes, proteins that are flexible, or proteins that are difficult to express or purify. In the last few years, cryoEM has allowed to expand dramatically the range of attractive targets that could be "structurally enabled", some of which have been long out of reach, like membrane proteins. Five years after its adoption at MSD, the number of projects and structures solved by cryoEM has increased steadily every year (with >150 structures solved and >30 projects enabled by 2022). Good examples that highlight the use of cryoEM at MSD are the Orexin 2 receptor (Hong, C. et al, 2021), insulin receptor (Scapin, G. et al, 2018), human arginase (Palte, R.L. et al, 2021) and the study of TGFβ antibody complexes (patent US WO 2020/076969, 2020). In those examples, cryoEM supported the design of new drugs by either defining drug-protein interactions, allowing the rational design of the molecules, or by improving the understanding of the mechanism of action of the different targets. For example, in the case of the Orexin 2 receptor, cryoEM structures were used to elucidate the mechanism of binding for an endogenous peptide and small molecule agonist which enabled SBDD of therapeutic agonists, while in the case of the human arginase, cryoEM structures allowed the understanding of the inhibitory mechanism of the antibodies. Though cryoEM is a powerful tool by industry production standards, it is still limited by the need for increased throughput and automation in most of the steps of the process, and the ability to routinely work with difficult cases. One such example are ligands that occupy transmembrane binding pockets that are otherwise occupied by lipids of unknown functional relevance, mimicking the overall lipid structure, or interacting with lipids on the exposed side of a shallow pocket.

At MSD, we use SBDD to steer the development and optimization of chemical matter, increasing our efficiency and ability to bring our products to the market. Building off the success that cryoEM has had on our pipeline over the past five years, MSD is investing in a brand new cryoEM facility with three state-of-the-art microscopes: a Titan Krios, Glacios, and Arctis. While we continue to rely heavily on single particle cryoEM in our pipeline, we are continually looking towards the future; including the ability to image macromolecular complexes in their native environment of the cell through cryo-electron tomography

Keywords: Drug discovery, Structure based drug design

CHARACTERIZATION OF A HIGH-CR WHITE CAST IRON WITH TIC AND WC-MMCS SURFACE REINFORCEMENTS

A.B. Moreira[1,2*], L.M.M. Ribeiro[1,2], M.F. Vieira[1,2]

1 – Department of Metallurgical and Materials Engineering, University of Porto, Porto, Portugal; 2 - INEGI - Institute of Science and Innovation in Mechanical and Industrial Engineering, Porto, Portugal.

Abstract

Ferrous alloys locally reinforced by carbide particles are promising materials for wear resistance applications. The local reinforcement provides high wear resistance, while the bulk cast iron offers high strength and toughness. For this reason, this grade of material is of increasing importance in the oil, gas and mining industries. Considerable attention has been directed towards techniques in which the reinforcing phase is formed during casting or previously manufactured by ex-situ methods and incorporated into the molten metal [1-3].

To produce the reinforced specimens, mixtures of Ti, Al and graphite powders were produced for the TiC system, and WC and Fe powders for the WC system. The powders were mixed and homogenised in a shaker mixer for 7 hours, and the binder was added afterwards. The mixtures were cold pressed in a metallic mould with a pressure of 70 MPa. The placement of the compacts in the mould cavity and the high-Cr white cast iron pouring were the final steps. The mechanical response of reinforced zones and the base metal was evaluated by microabrasion and hardness tests. To understand the effect of localized reinforcement on material performance, the microstructure of the composites and bonding interfaces was characterised using XRD, SEM/EDS, EBSD and TEM techniques.

Regarding the TiC system, the microstructural characterisation shows a non-uniform distribution of TiC particles in the reinforced matrix. The average hardness of the metal matrix composite is 797 HV 30, corresponding to a 34% increase compared to the hardness of the base metal. Concerning the WC system, a homogeneous and random distribution of the WC particles in the reinforced matrix was observed. The average hardness of the composite is 721 HV 30, a 47% increase in hardness compared to the base metal.

The microstructural characterisation and mechanical properties results allow us to state that this fabrication technique shows great potential for industrial application.

References

[1] Moreira, A. B., Ribeiro, L. M., & Vieira, M. F. (2021). Production of TiC-MMCs Reinforcements in Cast Ferrous Alloys Using In Situ Methods. Materials, 14(17), 5072.
[2] Olejnik, E., Sobczak, J. J., Szala, M., Kurtyka, P., Tokarski, T., & Janas, A. (2022). Dry sliding, slurry abrasion and cavitation erosion of composite layers reinforced by TiC fabricated in situ in cast steel and gray cast iron. Journal of Materials Processing Technology, 308, 117688.

STRUCTURAL RECOGNITION AND STABILIZATION OF TYROSINE HYDROXYLASE BY THE J-DOMAIN PROTEIN DNAJC12

José M. Valpuesta (Spain)[1]

1 - Centro Nacional de Biotecnología (CNB-CSIC)

Abstract

Pathogenic variants of the J-domain protein DNAJC12, a co-chaperone of Hsp70, cause parkinsonism, which seems associated with a defective interaction of DNAJC12 with tyrosine hydroxylase (TH), the rate limiting enzyme in dopamine synthesis. Here, we report the characterization of TH:DNAJC12 complex formation and show that DNAJC12 binding stabilizes TH and delays its time-dependent aggregation in an Hsp70-independent manner, while does not affect TH activity and regulatory inhibition by dopamine. Interestingly, although neither TH nor DNAJC12 alone significantly activate Hsc70, the complex stimulates its ATPase activity. Cryoelectron microscopy reveals two DNAJC12 monomers bound per TH tetramer, each embracing one of the two regulatory domain dimers, leaving all active sites available for substrate and dopamine interaction. Biochemical data confirm the key role of the DNAJC12 last eight residues in TH binding, explaining the molecular disease mechanism of C-terminal truncated DNAJC12 variants.

Acknowledgments

This research was supported by the grant PID2019-105872GB-I00/AEI/10.13039/ 501100011033 from the Spanish Ministry of Science and Innovation to J.M.V. and J.C. as well as FRIMEDBIO (261826) from the Research Council of Norway to A.M.; the Western Norway Regional Health Authorities (912246 to A.M. and 912264 to R.K.), the K.G. Jebsen Foundation (SKJ-MED-02) and Neuro-SysMed (to A.M.). The access to the Cryo-EM CNB-CSIC facility is acknowledged.

Keywords: Tyrosyne hydroxilase, molecular chaperones, Hsp40, DnaJC12

CRYOEM REVEALS A MECHANISM USED BY VACCINIA VIRUS TO INACTIVATE CYTOSOLIC DNA SENSING

Angel Rivera-Calzada (Spain)[1]; Raquel Arribas-Bosacoma (United Kingdom)[2]; Laurence H. Pearl (United Kingdom)[2]; Oscar Llorca (Spain)[1]

1 - Spanish National Cancer Research Centre (CNIO), Melchor Fernández Almagro 3, 28029 Madrid, Spain.; 2 - Genome Damage and Stability Centre, School of Life Sciences, University of Sussex, Falmer, Brighton BN1 9RQ, UK

Abstract

The Ku70-Ku80 heterodimer has a central role in the non-homologous end-joining (NHEJ) pathway of DNA repair. In the nucleus Ku70-Ku80 recognizes DNA ends generated after double strand breaks. However, in the cytosol, Ku70-Ku80 works as a sensor of dsDNA from viruses that replicate in the cytoplasm and activates an inflammatory response [1, 2]. Some viruses have found ways to counteract this defence mechanisms. Two proteins from Vaccinia virus, C4 and C16, are some of the best characterized examples of viral proteins that inactivate Ku70-Ku80 dependent DNA sensing and enhance virulence, but the structural basis for their inactivation mechanism have been poorly understood [3].

We have used cryo-Electron Microscopy (cryoEM) to determine the structure of Ku70-Ku80 bound to C16 [4]. Ku70-Ku80 consists on a preformed ring that it is used to bind and recognise dsDNA. C16 binds Ku70-Ku80 and sterically blocks this ring, thus preventing the binding to dsDNA and signalling into the downstream innate immunity system. C4 mimics these activities using a domain with 54% sequence identity to C16. Our results reveal how C4 and C16, two proteins with not fully redundant functions, evolved similar strategies to subvert the capacity of Ku70-Ku80 to recognize viral DNA. We also find that this mechanism is conserved in other poxvirus such as the causative agents of variola and monkeypox.

References

1. Hristova, D. B. *et al. J. Gen.Virol.*101, 1133–1144 (2020).
2. Chaplin, A. K. *et al. Mol. Cell* 81, 3400–3409 e3 (2021).
3. Scutts, S. R. *et al. Cell Rep.* 25, 1953–1965 e4 (2018).
4. Rivera-Calzada, A. *et al. Nat. Commun.* 13, 7062 (2022).

Keywords: NHEJ, Ku70-Ku80, Vaccinia virus, cytosolic DNA sensing

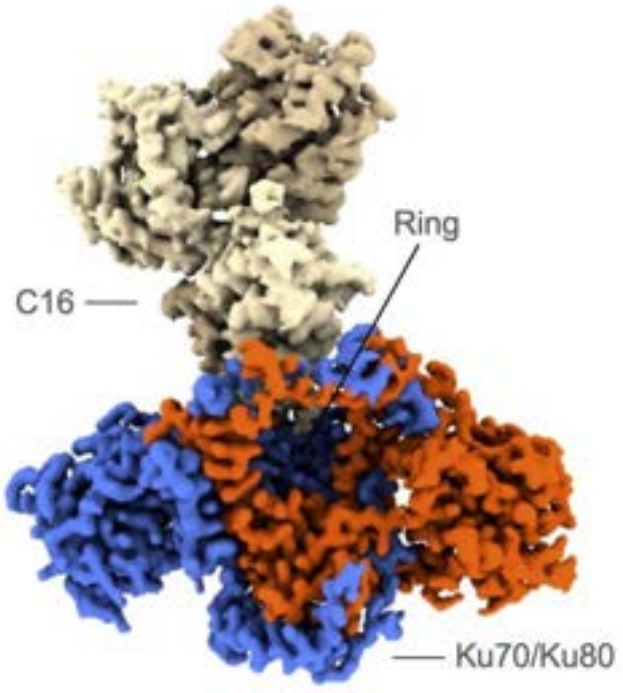

C16 – Ku (cryoEM map)

STRUCTURAL AND FUNCTIONAL CHARACTERIZATION OF SUBSTRATE SPECIFICITY IN THE HUMAN ASC1 AMINO ACID TRANSPORTER

Maria Martinez Molledo (Spain)[1]; Josep Rullo-Tubau (Spain)[2]; Manuel Palacin (Spain)[2]; Oscar Llorca (Spain)[1]

1 - Spanish National Cancer Research Center (CNIO); 2 - Institute for Research in Biomedicine (IRB Barcelona)

Abstract

Amino acid transport across biological membranes is essential to feed the cell with building blocks for protein synthesis, energy sources for growth, and metabolite and signaling molecule precursors. In humans, heteromeric amino acid transporters (HATs) are amino acid exchangers involved in the transport of amino acids in and out of the cell [1]. Furthermore, impaired amino acid transport is related to severe metabolic diseases, tumor growth or neurological disorders and therefore, HATs have great pharmacological interest [2].

Recent advances on cryo-electron microscopy (cryo-EM) have enabled the determination of the first human HAT structures, such as human LAT1 [3] and LAT2 (the latter also determined by the group of Oscar Llorca [4]). Despite having similar structural architecture, HATs present specific substrate preferences which define their physiological role [5]. As part of the HAT family, the Asc1 transporter is regarded as an important drug target as it is mostly expressed throughout the central nervous system both in astrocytes and neurons, participating in glutamatergic synapses [6]. Thus, Asc1 displays high affinity for small neutral amino acids (alanine, cysteine, glycine) and is unusually able to transport both serine stereoisomers, L- and D-serine.

We have recently determined a 4 Å resolution cryo-EM apo-structure of Asc1 inward-open partially occluded conformation. Using a multidisciplinary approach which combined cell-based transport assays, computational simulation and cryo-EM, we have now molecular insights to explain Asc1 substrate specificities. Moreover, the slightly different conformation to the already reported models completes our understanding on amino acid exchange and rises new hypothesis on undescribed alternative transport mechanisms for Asc1, so-called diffusion [7]. Ultimately, our experimental model paves the way on the design of Asc1-targeted drugs, helping to alleviate severe neurological disorders.

References

1. Kandasamy P, Gyimesi G, Kanai Y, Hediger MA (2018) “Amino acid transporters revisited: New views in health and disease”, Trends Biochem Sci, 43, 752-789.

2. Bröer S, Palacín M (2011) “The role of amino acid transporters in inherited and acquired diseases”, Biochem J, 436, 193-211.

3. Yan R, Zhao X, Lei J, ZHou Q (2019) “Structure of the human LAT1–4F2hc heteromeric amino acid transporter complex”, Nature, 568, 127-130.

4. Mikou A, Cabayé A, Goupil A, Bertrand H-O, Mothet J-P, Achner FC (2020) “Asc-1 transporter (SLC7A10): Homology models and molecular dynamics insights into the first steps of the transport mechanism” Sci Rep, 10: 3731.

5. Rullo-Tabau J, Bartoccioni P, Llorca O, Errasti-Murugarren E, Palacin (2022) “HATs meet structural biology”, Curr Opin Struct Biol, 74, 102389.

6. Rodriguez CF, Escudero-Bravo P, Diaz L, Bartoccioni P, Garcia-Martin C, Gilabert JG, Boskovic J, Guallar V, Errasti-Murugarren E, Llorca O, Palacin M (2021) “Structural basis for substrate specificity of heteromeric transporters of neutral amino acids” Proc Natl Acad Sci USA 118, e2113573118.

7. Sanson H, Billard JM, Smith GP, Safory H, Neame S, Kaplan E, Rosenberg D, Zubedat S, Foltyn VN, Christoffersen CT, Bundgaard C, Thomsen C, Avital A, Christensen KV, Wolosker H (2017) “Asc-1 transporterregulation of synaptic activity via the tonic reléase of d-serine in the forebrain”, Cerb Cortex, 27, 1573-1587.

Keywords: Heteromeric amino acid transporter, cryo-EM, Integral membrane proteins

THE SELF-ASSOCIATION OF HSP40 DNAJA2 INTO ORDERED OLIGOMERS REGULATES ITS INTERACTION WITH CLIENTS PROTEINS AND WITH HSC70

Jorge Cuéllar (Spain)[1]; Lorea Velasco-Carneros (Spain)[2]; Leire Dublang (Spain)[2]; César Santiago (Spain)[1]; Jaime Martín-Benito (Spain)[1]; Jean-Didier Maréchal (Spain)[3]; Moisés Maestro (Spain)[1]; José Ángel Fernández-Higuero (Spain)[2]; Natalia Orozco (Spain)[2]; Fernando Moro (Spain)[2]; José María Valpuesta (Spain)[1]; Arturo Muga (Spain)[2]

1 - National Centre for Biotechnology (CNB-CSIC); 2 - Biofisika Institute (CSIC-UPV/EHU); 3 - Insilichem, Department de Química (UAB)

Abstract

Members of the J-domain proteins family tune the specificity of Hsp70s, engaging them in precise functions. Despite their essential role, the structure and function of many J-domain proteins remain largely unknown, particularly those able to self-assemble into oligomers. We explored DnaJA2, a human class A J-domain protein, finding that it reversibly oligomerises into highly-ordered, tubular structures that interact with Hsc70, the constitutively expressed Hsp70 isoform. Cryoelectron microscopy and crosslinking mass spectrometry revealed that self-association occurs through multivalent interactions involving the J domain, a region of the C-terminal peptide-binding domain, the zinc finger and the C-terminal domains. The disordered C-terminal domain, comprising the last 52 residues, is essential for its holding activity and regulates the productive interaction with Hsc70. Although oligomers and dimers interact with unfolded clients preventing their aggregation, the holding activity of the dimer is higher. Oligomeric DnaJA2 could provide an array of closely spaced J domains that allows transfer of several Hsc70 molecules to the unfolded substrate, explaining the efficient recovery of DnaJA2-bound clients. The ATP-dependent conformational changes of Hsc70 induce oligomer dissociation. These *in vitro* findings suggest that the association equilibrium of DnaJA2 could regulate the interaction of the cochaperone with client proteins and with Hsc70.

Acknowledgments

This research was supported by grants PID2019-111068GB-I00 (AEI/FEDER, UE) to AM, PID2020-117752RB-I00 (AEI/FEDER, UE) to JMB, and PID2019-105872GB-I00 (AEI/FEDER, UE) to JMV, and by the Basque Government (grant IT1201-19 to FM).

Keywords: molecular chaperones, Hsp40, DnaJA2, Hsp70, oligomers, cryoEM

ENABLING REAL-TIME DATA OPTIMIZATION FOR CRYO-EM WITH SMART EPU

Singh, Dhirendra (The Netherlands)[1], Grollios, Fanis (The Netherlands)[1], Kohr, Holger (The Netherlands)[1]

1 - Thermo Fisher Scientific, Materials & Structural Analysis, Eindhoven

Abstract

Cryo-EM has revolutionized the field of structural biology due to its capabilities resolving the three-dimensional structure of proteins, protein complexes, and other biological macromolecules at high or even atomic resolutions. However, acquiring high-quality data for single particle analysis (SPA) still largely depends on the expertise of the microscope operator and their ability to judge the microscope output and optimize the acquisition process. The dependence on this empirical expertise emphasizes the need for more robust automation and real-time feedback throughout the data acquisition process. Here we will present the latest developments on the Thermo Scientific Smart EPU software that simplify and automate processing and data curation in addition to opening possibilities for AI automation of workflows. These developments free operators from tedious and repetitive tasks and makes Cryo-EM accessible to a wider audience.

Smart EPU with EPU Quality Monitor processes every acquired image in real-time and performs motion correction and CTF determination. Quality metrics are generated that allow curation of large single particle datasets and selective export of data for further processing. Results are presented for inspection in a web interface that is accessible from any modern internet-capable device.

The Smart EPU platform goes a step further to connect algorithms (“Smart Plugins”) to an ongoing acquisition and optimizes it in terms of efficiency and quality by monitoring image quality parameters and metadata. One example algorithm utilizes a neural network to automatically predict and discard inappropriate acquisition targets that would lead to inferior micrographs. This is complemented with another algorithm that works on real-time results of the processing routines, such as CTF fitting confidence, to recognize areas that still produce inferior micrographs and move the acquisition to other places on the grid or even switch grids. This dual check enables even entry level users to do efficient set-ups and reduces waste during acquisition.

Finally, we will also present Smart EPU Open API, an open application programming interface for Smart EPU Software. This API allows users with programming skills to develop their own User Plugins, so that they can influence an ongoing acquisition in certain critical steps according to their specific needs. The design of the API ensures that decisions made by algorithms don’t conflict between themselves or compromise the stability of the microscope This Open API enables the broader Cryo-EM community to develop its own routines and drive innovation.

SCIPION FLEXIBILITY HUB: A NEW FRAMEWORK TO SIMPLIFY THE DESIGN OF ADVANCED FLEXIBILITY WORKFLOWS

David Herreros (Spain)[1]; James Krieger (Spain)[1]; Yunior Fonseca (Spain)[1]; Pablo Conesa (Spain)[1]; Mohamad Harastani (France)[2]; Remi Vuillemot (France)[2]; Ilyes Hamitouche (France)[2]; Ricardo Serrano (Spain)[1]; Marcos Gragera (Spain)[1]; Roberto Melero (Spain)[1]; Slavica Jonic (France)[2]; José María Carazo (Spain)[1]; Carlos Óscar Sánchez (Spain)[1]

1 - National Centre for Biotechnology (CSIC); 2 - IMPMC-UMR 7590 CNRS, Sorbonne Universite, MNHN, Paris, France

Abstract

CryoEM ability to capture macromolecular heterogeneity is progressively shifting the field towards a new way of understanding how structure and function meet to drive biological processes. However, extracting flexibility information from CryoEM data is a challenging task, increasing the need for new and advanced methods specifically designed to address the heterogeneity problem through the approximation of conformational landscapes obtained from CryoEM data.

Therefore, many new algorithms designed to tackle the previous challenge have been recently introduced: Zernike3D [1], CryoDRGN [2], Gaussian Mixtures [3], 3D Flex [4]... Each algorithm approaches the problem from a different perspective, providing unique ways to analyze and understand conformational heterogeneity.

Nevertheless, integrating all the previous heterogeneity algorithms in a single flexibility workflow remains a difficult task. However, their combination would allow users to take advantage of their strengths to better explore and represent conformational landscapes, thus increasing the knowledge that could be extracted from a given study.

In this work, we introduce a novel framework called the Flexibility Hub, a new integration tool to define flexibility workflows inside Scipion [5]. The Flexibility Hub integrates advanced flexibility software (Zernike3D, CryoDRGN, ContinuousFlex [6]…) and handles their interaction, allowing to do combined flexibility analysis. In addition, it provides advanced tools to explore and annotate conformational landscapes, as well as a novel consensus method to merge different landscape estimations to posteriorly analyze the consistency of the estimated conformational states.

References

1. Herreros et al., Nat Comm., 2023
2. Zhong et al., Nat Methods, 2021
3. Chen et al., Nat Methods, 2021
4. Punjani et al., Biorxiv, 2021
5. de la Rosa Trevin et al., Struct. Biology, 2016
6. Harastani et al., Struct. Biology, 2022

Keywords: Molecular flexibility, Scipion

STRUCTURAL INSIGHTS OF THE POTENTIAL THERAPEUTIC MODULATORS OF THE EUKARYOTIC CHAPERONIN CCT

Sergio Pipaón (Spain)[1]; Svein I. Støve (Norway)[2]; Aurora Martínez (Norway)[2]; Jorge Cuéllar (Spain)[1]; José María Valpuesta (Spain)[1]

1 - National Center for Biotechnology (CNB-CSIC); 2 - University of Bergen

Abstract

Chaperonins, also known as Hsp60s, are a family of chaperones whose structure consists of two juxtaposed oligomeric rings with a cavity in their interior, where the folding process takes place (1). CCT (Chaperonin Containing TCP-1) is the most complex of all chaperonins, and it participates in the folding of over 10% of newly synthesized proteins (2). There are many evidences that prove that CCT has crucial roles in the development of different diseases. The first of these diseases is cancer, where CCT has shown to be upregulated, promoting tumor growth and mobility. Furthermore, CCT inhibition has been linked to tumor regression (3–5). On the other hand, CCT has been observed to be inhibited during neurodegenerative diseases such as Huntington disease, in accordance with the fact that CCT can inhibit the aggregation of polyQ proteins *in vitro* and *in vivo* (6,7). Although CCT has proven to play crucial roles in the development of many diseases, there has not been a relevant effort in the discovery of small molecules capable of modulating the activity of this proteins with a potential therapeutic effect; probably due to the structural complexity of the chaperonin. That is why in this work we screened the compounds included in the Prestwick chemical library using Differential Scanning Fluorimetry, from which three stabilizers and five destabilizers were identified. We then performed functional assays in order to characterize the effect that these small molecules have over CCT. ATPase and folding assays have allowed us to identify two molecules that inhibit both activities of CCT, and another molecule that enhances them. We are now optimizing the vitrification conditions for CCT in the presence of these three molecules. Although the presence of DMSO in the buffer with the samples -in which the small molecules are diluted- is hindering the proper distribution of the chaperonin in the cryo-electron microscopy grids, a preliminary 3D processing of CCT incubated with the inhibiting molecule Omeprazole has reached a ~4 Å resolution. Although the resolution could still be further improved, some densities can be attributed to the Omeprazole molecule, which seems to be binding to the ATP binding pocket of the CCT8 subunit. This structural information provides precise insight on the inhibiting mechanism of this small molecule, and supports its use as an inhibitor of the CCT chaperonin. These results can set the basis for the development of new drugs targeting CCT.

Acknowledgments

This research was supported by the grant PID2019-105872GB-I00/AEI/10.13039/ 501100011033 from the Spanish Ministry of Science and Innovation (JMV). The Centro Nacional de Biotecnología (CNB) is a Severo Ochoa Center of Excellence (MINECO award SEV 2017- 0712).

References

1. Bueno-Carrasco MT, Cuéllar J. Mechanism and Function of the Eukaryotic Chaperonin CCT. eLS. 2018;1–9.

2. Grantham J. The Molecular Chaperone CCT/TRiC: An Essential Component of Proteostasis and a Potential Modulator of Protein Aggregation. Front Genet. 2020;11(March):1–7.

3. Carr AC, Khaled AS, Bassiouni R, Flores O, Nierenberg D, Bhatti H, et al. Targeting chaperonin containing TCP1 (CCT) as a molecular therapeutic for small cell lung cancer. Oncotarget. 2017;8(66):110273–88.

4. Guest ST, Kratche ZR, Bollig-Fischer A, Haddad R, Ethier SP. Two members of the TRiC chaperonin complex, CCT2 and TCP1 are essential for survival of breast cancer cells and are linked to driving oncogenes. Exp Cell Res. 2015;332(2):223–35.

5. Showalter AE, Martini AC, Nierenberg D, Hosang K, Fahmi NA, Gopalan P, et al. Investigating Chaperonin-Containing TCP-1 subunit 2 as an essential component of the chaperonin complex for tumorigenesis. Sci Rep. 2020;10(1):1–14.

6. Shahmoradian SH, Galaz-Montoya JG, Schmid MF, Cong Y, Ma B, Spiess C, et al. TRiC's tricks inhibit huntingtin aggregation. Elife. 2013;2013(2):1–17.

7. Neef DW, Turski ML, Thiele DJ. Modulation of heat shock transcription factor 1 as a therapeutic target for small molecule intervention in neurodegenerative disease. PLoS Biol. 2010;8(1).

Keywords: Therapeutic target, Molecular chaperones, CCT, Small molecules, Omeprazole, Cryo-electron microscopy

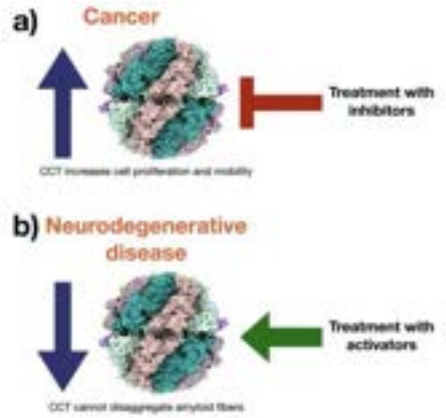

Figure 1. Depending on the different cell scenarios, CCT can be regulated in a variety of ways. **a)** During cancer, CCT is upregulated, promoting cell proliferation and mobility, which is why a treatment with inhibitors is desirable. **b)** During neurodegenerative diseases CCT is downregulated, so it cannot disaggregate amyloid fibers, which is why a treatment with activators is desirable.

BIOCHEMICAL AND STRUCTURAL CHARACTERIZATION OF A COMPLEX INVOLVED IN CHAPERONE-ASSISTED UPS DEGRADATION

Jimena Muntaner (Spain)[1]; Moisés Maestro-López (Spain)[1]; Margarita Menéndez (Spain)[3]; Tat Cheung Cheng (Germany)[2]; Eri Sakata (Germany)[2]; José María Valpuesta (Spain)[1]; Jorge Cuéllar (Spain)[1]

1 - Macromolecular Structures Department, National Center for Biotechnology. CNB-CSIC. Madrid, Spain; 2 - Institute for Auditory Neuroscience, University Medical Center Göttingen, 37077 Göttingen, Germany; 3 - Department of Biological Physical Chemistry, Institute of Physical Chemistry Rocasolano, CSIC. Madrid, Spain

Abstract

Protein homeostasis involves the balance between protein synthesis, folding, trafficking, and degradation essential for proper cellular function, where molecular chaperones operate as a regulatory network[1]. Their role is dictated by their interaction with different co-chaperones, which can either direct the Hsp70:substrate complex towards its folding or degradation through the ubiquitin-proteasome system (UPS) or the autophagy system[2]. One of these co-chaperones is Bag1 (Bcl-2-associated athanogene 1), a Nucleotide Exchange Factor of Hsp70 that contains a Ubiquitin like (UBL) domain shown to mediate the interaction with the proteasome[3].

In this work, we have addressed the proteasomal subunit involved in the interaction with Bag1 by cloning and purification of different proteasomal subunits, inferring a strong interaction with Rpn1. Binary (Rpn1:Bag1), ternary (Rpn1:Bag:Hsp70) and quaternary (Rpn1:Bag1:Hsp70:model substrate of Hsp70) complexes have been isolated and characterized using biochemical and biophysical techniques that will help to elucidate the substrate delivery mechanism that takes place between Hsp70 and the proteasome.

To further analize the interactions among these proteins, the purified complexes have been structurally characterized by cryo-EM. The Rpn1:Bag:Hsp70 3D reconstruction, complemented with cross-linking and mass spectrometry information, have allowed us to propose a model of the ternary complex. A high-resolution map of the complex between the 26S proteasome and Bag1 has been generated at an overall resolution of 3.21Å and a local resolution of the given interaction region between 3-5Å. This map shows the binding site of the UBL domain of Bag1 to the toroidal region of Rpn1 and a significant structural rearrangement within the 20S AAA-ATPase ring affecting the interface between the Rpt4 and Rpt5 subunits. This interaction and the subsequent conformational change would allow the positioning of Hsp70 in the vicinity of the proteasomal gate, thus favoring substrate transfer.

To gain further insight into the effects of the structural change affecting the 20S ATPases, we have performed degradation assays using Hsp70 substrates as α-synuclein. These results suggest that the interaction between Bag1 and the proteasome induces an open conformation, quite different from the known structures, that would facilitate the translocation of unfolded proteins inside the catalytic [illegible]cing degradation in an ATP-independent manner.

Acknowledgments

This research was supported by the grant PID2019-105872GB-I00/AEI/10.13039/ 501100011033 from the Spanish Ministry of Science and Innovation (JMV). The Centro Nacional de Biotecnología (CNB) is a Severo Ochoa Center of Excellence (MINECO award SEV 2017- 0712).

References

1. Hartl, F.U., Bracher, A., and Hayer-Hartl, M. (2011) Molecular chaperones in protein folding and proteostasis. Nature, 475, 324-332.

2. Shiber, A. And Ravid, T. (2014) Chaperoning Proteins for Destruction: Diverse Roles of Hsp70 Chaperones and their Co-Chaperones in Targeting Misfolded Proteins to the Proteasome. Biomolecules, 4, 704-724.

3. Lüders, J., Demand, J., & Höhfeld, J. (2000). The ubiquitin-related BAG-1 provides a link between the molecular chaperones Hsc70/Hsp70 and the proteasome. Journal of Biological Chemistry.

Keywords: Protein degradation, Proteasome, Molecular chaperones, Hsp70, Bag1, Cryo-EM

MODIFICATIONS IN THE INNER SURFACE OF THE SYNTHETIC POLY-CCT5 CHAPERONIN TO PROMOTE NANOPARTICLE ENCAPSULATION

Jorge Gutiérrez (Spain)[1]; Sergio Pipaón (Spain)[1]; Jesús G Ovejero (Spain)[2]; María Del Puerto Morales (Spain)[2]; Jorge Cuéllar (Spain)[1]; José M Valpuesta (Spain)[1]

1 - Department of Macromolecular Structures of the National Centre for Biotechnology (CNB-CSIC), Darwin 3, Campus of the Universidad Autónoma de Madrid, Cantoblanco, 28049 Madrid, Spain.; 2 - Department of Materials for Health of the Materials Science Institute of Madrid (ICMM), Sor Juana Inés de la Cruz 3, Campus of the Universidad Autónoma de Madrid, Cantoblanco, 28049 Madrid, Spain.

Abstract

To achieve their functional activities, cells possess a complex network of molecular chaperones, proteins that assist de novo protein folding and prevent protein aggregation (1). One of the most important chaperone families are the chaperonins (or Hsp60 chaperones), which are organized as two oligomeric back-two-back rings generating a cavity in each ring where the substrate will be placed for its folding (2). The most complex and important of all chaperonins is the eukaryotic CCT (Chaperonin Containing TCP-1) whose structure and the folding mechanism are key for nanotechnological applications (3,4).

The main aim of this project is to build a stable synthetic cylindrical CCT structure capable of encapsulating chemical reagents or small proteins. It has been shown that two of the eight human CCT subunits, CCT4 and most importantly CCT5, are able to self-oligomerize (5). When compared to the eukaryotic CCT (6), poly-CCT5 is easier to purify, can be genetically modified in all subunits at the same time and allows a more manageable image processing due to the asymmetric disposition of the different CCT subunits. These capabilities could enable poly-CCT5 to act as a nanocontainer delivering molecules to specific targets.

Negative staining EM was used to assess the encapsulation of various nanoparticles inside synthetic poly-CCT5. VENOFER, an iron-sucrose coating NP, produced the best results overall and was chosen for Cryoelectron microscopy (CryoEM) analysis. Data acquisition took place in a Talos Artica from the cryoEM facility at CNB-CSIC, and image processing reach a 3D reconstruction at 10 Å resolution of the NP-bound poly-CCT5, in which the NP is held by CCT5 apical domains. This preliminary 3D reconstruction was recently improved to 4.1 Å through a new image processing performed with data acquired at the Diamond Light Source (DLS) electron Bio-Imaging Centre (eBIC).

As part of this project, we are also designing and structurally characterizing two poly-CCT5 mutants, Cterm2 and Nterm1. The Cterm2 mutant involves substituting two negatively-charged residues with basic positively-charged ones to achieve attraction instead of repulsion. The Nterm1 mutant involves removing a third of the residues from the N-terminus to limit possible steric impediments. Both N- and C-termini have been identified within the CCT cavity around the equatorial domains and could be the reason (as steric hindrance) for the failure to achieve complete encapsulation of the NP.

Acknowledgments

Project of the Community of Madrid P2018/NMT-4389. “NANOBIOCARGO. Nanocontainers and nanovehicles directed to the transport and release of bioactive agents”.

References

(1) Kim YE, Hipp MS, Bracher A, Hayer-Hartl M, Ulrich Hartl F. Molecular Chaperone Functions in Protein Folding and Proteostasis. Annu Rev Biochem 2013 June 2,;82(1):323-355.

(2) Yébenes H, Mesa P, Muñoz IG, Montoya G, Valpuesta JM. Chaperonins: two rings for folding. Trends Biochem Sci 2011 -08;36(8):424-432.

(3) Bueno-Carrasco MT, Cuéllar J. Mechanism and Function of the Eukaryotic Chaperonin CCT. eLS: John Wiley & Sons, Ltd; 2018. p. 1-9.

(4) Skjærven L, Cuellar J, Martinez A, Valpuesta JM. Dynamics, flexibility, and allostery in molecular chaperonins. FEBS Letters 2015;589(19PartA):2522-2532.

(5) Sergeeva OA, Chen B, Haase-Pettingell C, Ludtke SJ, Chiu W, King JA. Human CCT4 and CCT5 Chaperonin Subunits Expressed in Escherichia coli Form Biologically Active Homo-oligomers. J Biol Chem 2013 -6-14;288(24):17734-17744.

(6) Grantham J. The Molecular Chaperone CCT/TRiC: An Essential Component of Proteostasis and a Potential Modulator of Protein Aggregation. Front Genet 2020;0.

Keywords: Poly-CCT5, Chaperonin, Nanocontainer, Nanoparticles, Cryo-EM, Image Processing, 3D Reconstruction

SUBVERSION OF RETROMER COMPLEX BY THE HUMAN PAPILLOMAVIRUS L2 CAPSID PROTEIN

Marta Pardo Piñón (Spain)[1]; María Lucas (Spain)[2]; Miguel Romano Moreno (Spain)[3]; Adriana Rojas (Spain)[1]; Aitor Hierro (Spain)[1]

1 - CIC bioGUNE; 2 - Instituto de Biomedicina y Biotecnología de Cantabria; 3 - Industrial Sector (LEV2050)

Abstract

The endosomal network is a major hub in protein trafficking. Proteins that enter in this pathway may be degraded in lysosomes or be recycled to continue developing their functions. Retromer is a highly conserved hetero-trimeric complex that mediates endosomal sorting of hundreds of integral membrane proteins, thus contributing to cellular proteostasis. Other accessory proteins such as members of the Sortin nexin (SNX) family work together with retromer recruiting it to the endosomal membrane to select cargo. Retromer machinery is also hijacked by several intracellular pathogens to facilitate host invasion, establish intracellular replicative niches and promote survival.

Human Papillomavirus (HPV) encodes L2, a minor capsid protein that interacts with the viral DNA and promotes its retrograde transport through the endomembrane system into the nucleus hijacking retromer complex. The C terminal region of the L2 protein contains a retromer binding motif followed by a membrane-destabilising sequence that functions as a cell-penetrating peptide. In this study we have used an integrative approach based on X-ray crystallography and cryo-electron microscopy combined with biochemical and functional assays to establish the mechanism by which the L2 protein subverts retromer function during HPV infection.

Keywords: Retromer, L2, Endosomal network, SNX

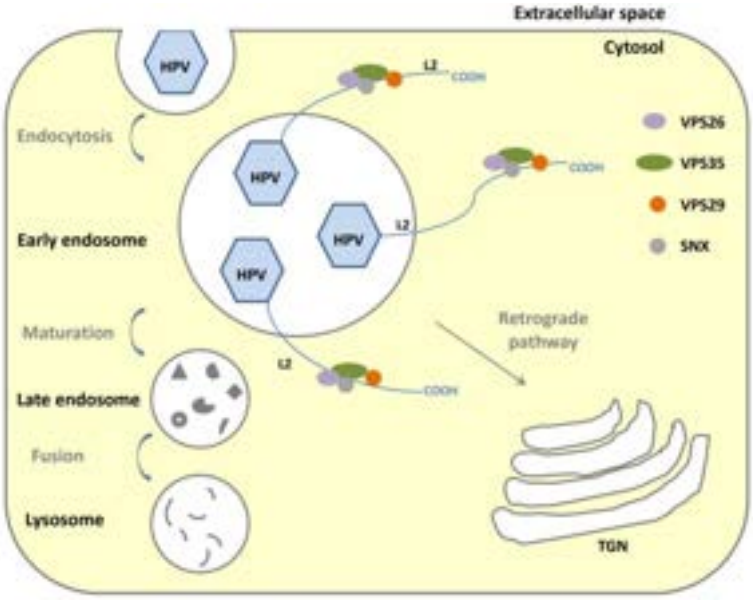

LOOKING FOR NON-ICOSAHEDRAL ELEMENTS IN THE ADENOVIRUS CAPSID: THE CASE OF PROTEIN VI

Marta Martinez (Spain)[1]; Mercedes Hernando-Perez (Spain)[2]; Jose Gallardo (Spain)[1]; Patrick Hearing (United States of America)[3]; Jose Maria Carazo (Spain)[1]; Roberto Marabini (Spain)[4]; Carmen San Martín (Spain)[1]

1 - Department of Macromolecular Structures, Centro Nacional de Biotecnología (CNB-CSIC). Madrid (Spain); 2 - Faculty of Sciences, Autonomous University of Madrid (Spain); 3 - Department of Microbiology & Immunology, Stony Brook University, New York (USA); 4 - Escuela Politécnica Superior, Autonomous University of Madrid (Spain)

Abstract

Adenoviruses are non-enveloped icosahedral viruses studied by their role as pathogens infecting vertebrates and by their utility as therapeutic vectors and models for virus assembly. Minor coat protein VI contains a membrane-disrupting peptide essential to ensure endosome escape in the early stages of the infection. In absence of the major core protein VII, the lytic peptide remains trapped in the hexon cavity[1], similarly as in maturation deficient TS1 virions[2]. Protein VII is thus required for protein VI maturation and viral infection[1]. Moreover, since N-terminal peptides of proteins VI (pVI_N) and VII ($pVII_{N2}$) bind alike residues in the hexon cavity[3], a model has been proposed in which both proteins compete for the same binding pockets in all hexon monomers during assembly[1]. Protein VI is problematic due to its uncertain stoichiometry and incomplete icosahedral order. To better characterize the arrangement of protein VI in the capsid, we built a high-resolution map of a particle lacking protein VII (HAdV-C5-VII$^-$) by single particle averaging cryo-electron microscopy. We processed 74,000 viral particles applying icosahedral symmetry, CTF per particle refinement and Ewald sphere correction to yield the best resolution map obtained so far for any Adenovirus (2.8 Å). Despite this resolution, the lower density of protein VI compared to the rest of the capsid and its lack of continuity according to DeepEMhancer[4] postprocessing suggested that protein VI folding could escape to icosahedral symmetry. We thus addressed the localized reconstruction of the four hexons in the asymmetric unit using LocalRec[5] without imposing symmetry. Hexon 2 yielded the best outcome due to protein VI density enrichment, resulting in a map continuous enough to fit a model, though we were unable to unequivocally assign protein VI residues. Nevertheless, we identified in hexon 2, as well as in hexons 1 and 4, connections between pVI_N and the core outer layer. Comparisons of maps from virions HAdV-C5-VII$^-$, TS1 (full[3] and lacking genome) and the delayed packaging mutant FC31_L3[6] (lacking genome) showed that connections do only occur after proteolytic maturation and are formed by capsid elements. We hypothesize that these connections may arise from interactions between protein VI, the core and other internal minor coat proteins. This would suggest that protein VI has a role in directing the assembly of hexons during adenovirus morphogenesis.

Acknowledgments

* Grant PID2019-104098GB-I00/AEI/10.13039/501100011033, cofunded by the Spanish State Research Agency and the European Regional Development Fund to C.S.M.

* Cryo-EM CNB-CSIC facility access via the CRIOMECORR project (ESFRI-2019-01-CSIC-16).

* Electron Bio-Imaging Centre (eBIC), Diamond Light Source, Oxfordshire, UK (BAG proposal BI22006)

* Ayudas a Proyectos de I+D para Jóvenes Doctores de la Universidad Autónoma de Madrid 2021, SI3/PJI/2021-00216 supported by the Community of Madrid and the University Autónoma de Madrid to M. H.P.

* TED2021-129937B-I00 from Spanish Ministry of Science and Innovation to M. H.P.

References

1. Hernando-Pérez M. *et al.* Dynamic competition for hexon binding between core protein VII and lytic protein VI promotes adenovirus maturation and entry. *Proc Natl Acad Sci U S A.* 2020, 117:13699-13707.

2. Yu X. *et al*. Structure of a Cell Entry Defective Human Adenovirus Provides Insights into Precursor Proteins and Capsid Maturation. *J Mol Biol.* 2022, 434:167350.

3. Dai X. *et al*. Atomic Structures of Minor Proteins VI and VII in Human Adenovirus. *J Virol.* 2017, 91:e00850-17.

4. Sanchez-Garcia R. *et al.* DeepEMhancer: a deep learning solution for cryo-EM volume post-processing. *Commun Biol.* 2021, 4:874.

5. Abrishami V. *et al.* Localized reconstruction in Scipion expedites the analysis of symmetry mismatches in cryo-EM data. *Prog Biophys Mol Biol.* 2021,160:43-52.

6. Condezo GN. e*t al.*. Structures of Adenovirus Incomplete Particles Clarify Capsid Architecture and Show Maturation Changes of Packaging Protein L1 52/55k. *J Virol.* 2015, 89:9653-64.

Keywords: Adenovirus, SPA, Protein VI

STRUCTURAL CHARACTERIZATION OF DICTYOSTELIUM DISCOIDEUM VAULTS

María González Álamos (Spain)[1]; Nuria Verdaguer Massana (Spain)[1]; Pablo Guerra Lahoz (Spain)[2]

1 - Instituto de Biología Molecular de Barcelona (IBMB-CSIC); 2 - Cryo-Electron Microscopy Platform - IBMB CSIC, Joint Electron Microscopy Center at ALBA (JEMCA)

Abstract

The vault particle, with a mass of 10 MDa and dimensions of 70 nm x 40 nm x 40 nm, is the largest ribonucleoprotein described in the eukaryotic kingdom. The vault shell is organized in two identical moieties, each consisting of 39 copies of the major vault protein (MVP, 100 kDa), which assemble to form a barrel-like cage with an enormous interior volume. The telomerase associated protein 1 (TEP1, 290 kDa), the vault poly (ADP)-ribose polymerase (vPARP, 193 kDa), as well as several short untranslated RNAs (vRNA) are localized in the interior volume of the vault, as minor components. Vaults are present and widely conserved in most eukaryotes, suggesting an essential biological role, which, however, remains poorly understood (Berger et al., 2009; Frascotti et al., 2021).

In a previous work, using a combination of vault recombinant reconstitution, biophysics and cryo-electron microscopy (cryo-EM) techniques, we characterized the structural dynamics of rat vaults, suggesting a mechanistic model for the vault opening-closing cycle with functional implications for cargo encapsulation, transport, and delivery (Guerra et al., 2022).

Dictyostelium discoideum is the only organism described so far possessing two different, although highly homologous isoforms of MVP (MVPα and MVPβ), and previous findings in our lab demonstrated that both monomers are essential for vault assembly. Solving the structure of these singular particle would allow us to decipher the evolutionary relationships linking vaults from an ancient microorganism to higher eukaryotes. Here we present the cryo-EM structures of recombinant *D. discoideum* vaults, unbound (3.8 Å resolution) and bound (3.7 Å resolution) to a nanobody recognizing a myc-tag, artificially inserted in an exposed loop of the R6 repeat in MVPβ, to differentiate the two isoforms.

Cryo-EM data were obtained at the ESRF cryo-EM facility, in a 300-kV Titan Krios, equipped with a Gatan K3 direct electron detection camera at ×81,000. The pixel size was measured to 1.06 Å on the specimen scale. RELION 4.0 was used to process the data. The 2D classification showed noticeable extra density, attributable to the presence of the nanobody in the vault-nanobody complex. High performance image computing is in process to figure out the distribution of the MVP isoforms forming the vault shell.

Berger, W., Steiner, E., Grusch, M., Elbling, L., & Micksche, M. (2009). Vaults and the major vault protein: Novel roles in signal pathway regulation and immunity. In *Cellular and Molecular Life Sciences* (Vol. 66, Issue 1, pp. 43–61). https://doi.org/10.1007/s00018-008-8364-z

Frascotti, G., Galbiati, E., Mazzucchelli, M., Pozzi, M., Salvioni, L., Vertemara, J., & Tortora, P. (2021). The Vault Nanoparticle: A Gigantic Ribonucleoprotein Assembly Involved in Diverse Physiological and Pathological Phenomena and an Ideal Nanovector for Drug Delivery and Therapy. *Cancers*, *13*, 707. https://doi.org/10.3390/cancers

Guerra, P., González-Alamos, M., Llauró, A., Casañas, A., Querol-Audí, J., de Pablo, P. J., & Verdaguer, N. (2022). Symmetry disruption commits vault particles to disassembly. *Science Advances*, *8*(6). https://doi.org/10.1126/sciadv.abj7795

Keywords: vault protein, cryo-EM structures

CRYO-CORRELATIVE LIGHT AND ELECTRON MICROSCOPY AT CNB CSIC

Jose Javier Conesa Muñoz (Spain)[1]; David Delgado-Gestoso (Spain)[1]; Jonathan Gabriel Piccirillo (Spain)[1]; Noelia Zamarreño (Spain)[1]; Francisco Javier Chichón (Spain)[1]; M. Teresa Bueno-Carrasco (Spain)[1]; Javier Collado-Ávila (Spain)[1]; Blanca Soler (Spain)[1]; Mario Mellado (Spain)[1]; José M. Valpuesta (Spain)[1]; Rocío Arranz (Spain)[1]

1 - CNB-CSIC

Abstract

Correlative light and electron microscopy (CLEM) is a structural biology methodology that allows to relate different microscopy techniques. This methodology, applied in cryogenic conditions, allows the extraction of high resolution structural 3D information in the native cellular context avoiding artefacts related to chemical fixation and dehydration. CLEM allows the study of cellular samples by means of cryo-fluorescence microscopy to locate interesting cellular events while cryo-focus ion beam-scanning electron microscopy (cryo-FIB-SEM) serial sectioning is used to analyse the cellular ultrastructure at the level of cellular organelles or, alternatively, cryo-electron tomography is used to analyse the 3D structure of protein complexes and their distribution at molecular resolution (Figure 1). At CNB-CSIC we are implementing a cryo-correlative platform aiming to provide users with dedicated tools to perform CLEM in cryogenic conditions in a variety of workflows, including the usage of cryo-epifluorescence, cryo-confocal fluorescence, cryo-FIB-SEM and cryo-ET, to investigate and answer questions to biological events occurring in the cell.

Keywords: Cryo-focus-ion-beam scanning electron microscopy, cryo-correlative light-electron microscopy, tomography

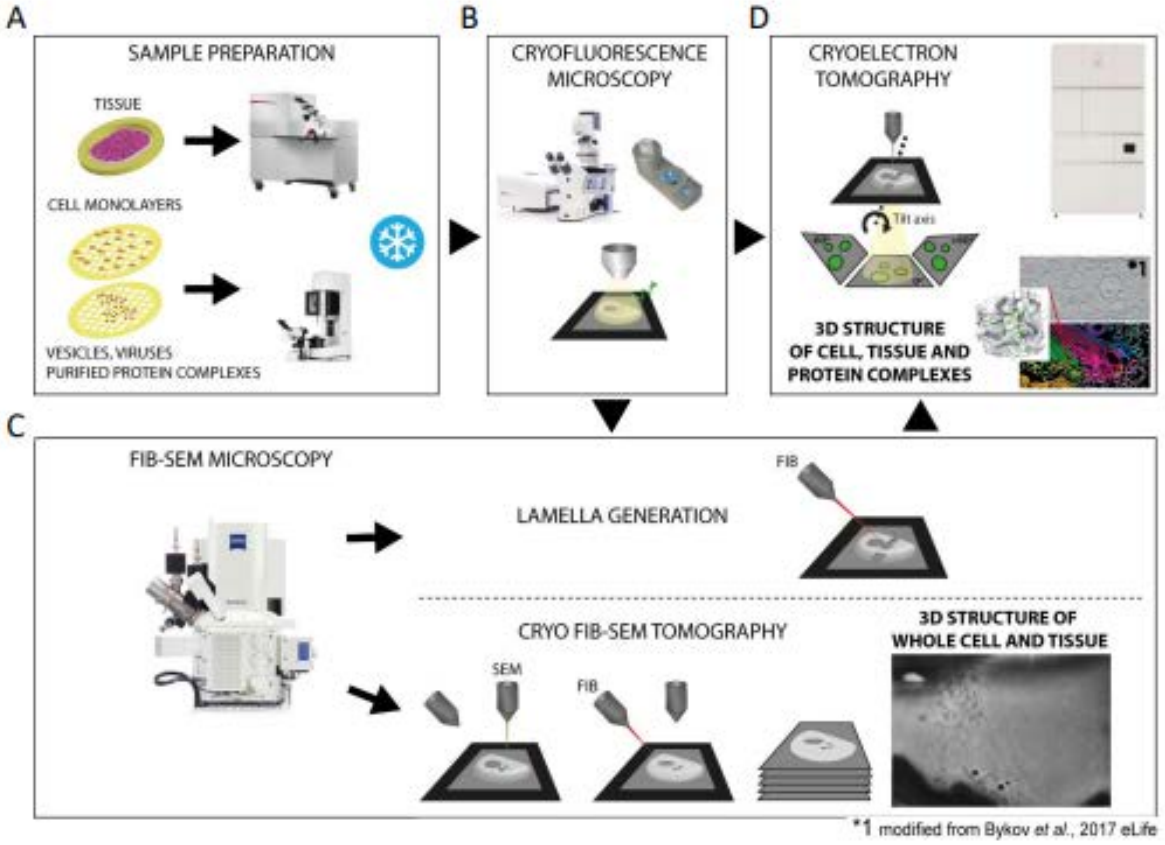

Figure 1. Correlative light and electron microscopy workflow being implemented at CNB-CSIC. **A**, Cryogenic preservation of cellular and tissue samples by plunge freezing and high pressure freezing. **B**, vitrified samples are transferred to a cryogenic sample carrier to be analysed by epi-fluorescence or confocal microscopy in order to determine sample quality and the location of events of interest. **C**, samples imaged by fluorescence are loaded in the cryo-focus ion beam-scanning electron microscope (cryo-FIB-SEM) to study the whole cellular structure at the level of organelle (cryo FIB-SEM tomography) or further processed (lamella generation) to make them compatible with cryo-electron tomography (cryo-ET). **D**, the lamellae prepared by cryo-FIB-SEM are loaded into a high voltage cryo-electron transmission microscope to be analysed by cryo-ET. The generated tomograms can be further processed *in silico* by subtomogram averaging approaches to obtain the 3D structure of macromolecular complexes at near atom resolution and their distribution in the whole cell context and in close to native conditions.

IMPLEMENTATION DATA PROCESSING PIPELINE FOR CRYO FIBSEM VOLUME IMAGING

Jonathan Gabriel Piccirillo (Spain)[1]; José Javier Conesa (Spain)[1]; Ana Cayuela (Spain)[1]; David Delgado-Gestoso (Spain)[1]; Rocío Arranz (Spain)[1]; Francisco Javier Chichón (Spain)[1]; Javier Collado-Avila (Spain)[1]; Noelia Zamarreño (Spain)[1]; María Teresa Bueno-Carrasco (Spain)[1]; Carlos Óscar Sánchez Sorzano (Spain)[1]; Noa Beatriz Martín Cófreces (Spain)[2]; Francisco Javier Sánchez Madrid (Spain)[2,3]; José María Valpuesta (Spain)[1]

1 - CNB-CSIC; 2 - Insituto de Investigación Sanitaria del Hospital de La Princesa; 3 - Universidad Autónoma de Madrid

Abstract

There is a growing interest in structural techniques that take advantage of the vitrification of water in biological samples in order to preserve their native conditions. Most of these techniques involve high-resolution methods that aim to solve the structure of purified biological complexes. Nevertheless, these approaches are hindered because the structure is analysed without its cellular context. For this reason, it is essential to integrate light microscopy techniques in the workflow of the cryotechniques to localize protein complexes and solve its structure in their native environment. The Valpuesta group and the cryo-electron microscopy platform at CNB-CSIC are implementing a new facility for cryocorrelative techniques that exploit the advantages of visible light and electron microscopy (cryo-CLEM). In this platform two cryo-CLEM approaches are available. First, the tomographic approach by lamellae preparation allows having a near-atomic resolution by the study of less than 300 nm thin windows opened into the cell (lamella FIB milling). Second, serial sectioning allows to obtain a whole cell volume at a resolution of 10 nm. This technique is based on the use of a iterative process of imaging with the SEM and surface milling with the FIB to obtain a stack of images containing the volume of the cell (cryo FIBSEM tomogram).

Serial sectioning imaging has technique-related artifacts that are unavoidable and hinder the images obtained. To overcome this issue, we are focusing on developing an open-source and user-friendly software package for the processing of cryo FIBSEM volumes to obtain more accurate insights. The first operation our package executes is the stripes elimination to get rid of the lines created by the so-called curtain artifact produced by the shielding of the downstream material by a harder one upstream. The second operation is the elimination of the charging artifact generated by the accumulation of electrons in the sample that result in darker and lighter areas in the image. The third part is the stack alignment. Since electrons are accumulated not homogenously in the sample, this also means that these areas deflect differently the electrons creating local deformations in the image, thus making the alignment a non-trivial problem. Last, deep learning segmentation is performed using Cellpose software. This pipeline will reduce significantly the image artifacts within cryo FIB-SEM data allowing the extraction of more reliable information.

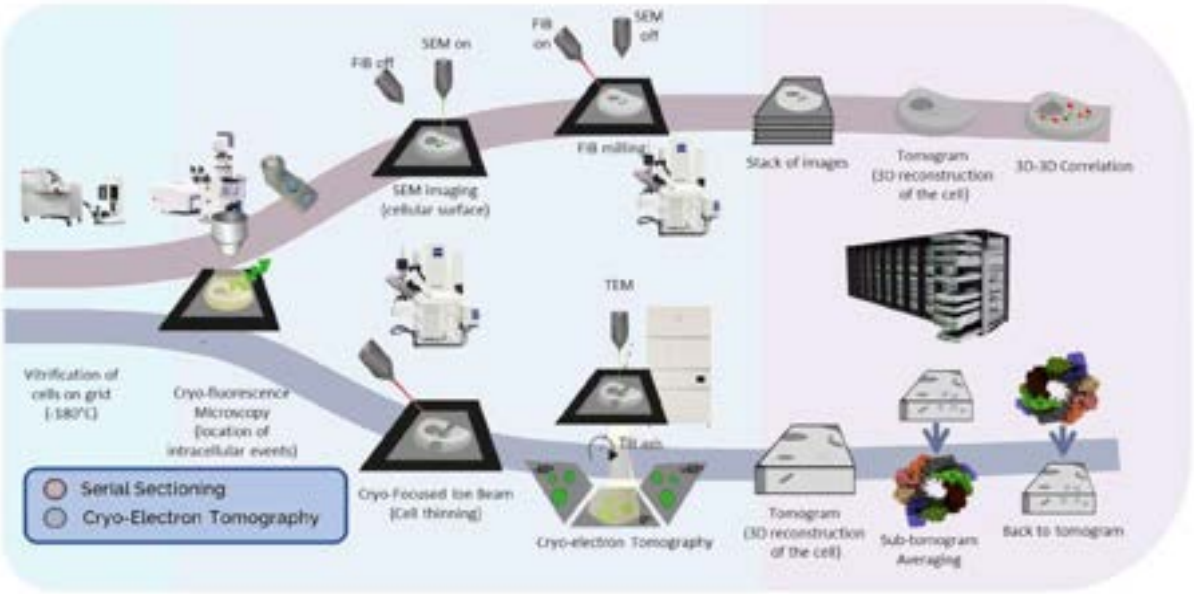
FIB on
SEM off
FIB off
SEM on
FIB milling
SEM Imaging
(cellular surface)
Stack of images
Tomogram
(3D reconstruction
of the cell)
3D-3D Correlation
TEM
Vitrification of
cells on grid
(-180°C)
Cryo-fluorescence
Microscopy
(location of
intracellular events)
Serial Sectioning
Cryo-Electron Tomography
Cryo-Focused Ion Beam
(Cell thinning)
Cryo-electron Tomography
Tomogram
(3D reconstruction
of the cell)
Sub-tomogram
Averaging
Back to tomogram

CRYOEM OF THE Γ-TUBULIN RING COMPLEX

Marina Serna (Spain)[1]

1 - Spanish National Cancer Research Center (CNIO)

Abstract

Microtubules are highly dynamic αβ-tubulin polymers whose continuous assembly and disassembly cycles serve to important cellular roles such as cell division, cell motility and intracellular transport.

While microtubules are spontaneously disassembled in the so-called catastrophe events, microtubule assembly occurs both spontaneously when αβ-tubulin dimers exceed a minimum critical concentration, and orchestrated by the γ-tubulin ring complex (γTuRC) in the so-called nucleation events. The γTuRC is a multi-subunit complex embedded into the pericentriolar material that nucleates and caps the minus end of the microtubules, allowing their assembly in a more spatio-temporal regulated manner. This tight control of the microtubules end up being critical for the formation and proper orientation of the mitotic spindle during cell division.

The most widely agreed hypothesis for the γTuRC-driven microtubule nucleation control considers that this complex serves as a template for the αβ-tubulin heterodimers to oligomerize. However, cryo-EM structures of both native and recombinant γTuRC complexes evidenced an asymmetric ring-like structure that does not match the microtubule geometry[1,2,3,4]. Accordingly, both the recombinant and native γTuRC complexes displayed a poor *in vitro* microtubule nucleation activity compared to cells. Thus, identification of the γTuRC activation factors as well as understanding the complex conformational transition remain elusive.

Our work focused on the study of the actors and conformational changes required for the γTuRC complex to become active using cryo-EM structures.

Acknowledgments

We acknowledge our collaborators Jens Luders (IRB, Barcelona, Spain), Fabian Zimmermann (MPI-Dortmund, Germany), and Thomas Surrey and Claudia Brito (CRG, Barcelona, Spain). We thank David Gil (BREM cryo-EM facility), C. Savva and C. Lacey (University of Leicester, UK) and eBIC (Oxford, UK) for data collection. We are grateful to J. Boskovic and J. Le Coq for support at CNIO Electron Microscopy Facilities (CNIO, Madrid, Spain), and R. F. Leiro (CNIO, Madrid, Spain) for image processing support and discussions.

References

1. T. Consolati, J. Locke, J. Roostalu et al., Developmental Cell 53 (2020), p. 603-617
2. P. Liu, E. Zupa, A. Neunet et al., Nature 578 (2020), p. 467-471.
3. M. Wieczorek, L. Urnavicius, S.C. Ti et al., Cell 180 (2020), p. 165-175.
4. F. Zimmermann, M. Serna, A. Ezquerra et al., Sci. Adv. 6 (2020), p. eabe0894.

Keywords: Cryo-EM, Microtubules, Tubulin, Nucleation

CHARACTERIZATION OF ACTIN STRUCTURES IN FISSION YEAST USING CRYO-CORRELATIVE ELECTRON TOMOGRAPHY

Olivia Muriel (Spain)[1]; Sophie Martin (Switzerland)[2]

1 - Department of Macromolecular Structures. National Center of Biotechnology. CSIC. C/Darwin nº3, 28049, Madrid.; 2 - Departament of Molecular and Cellular Biology, University of Geneva. 30, quai Ernest-Ansermet CH-1211, Geneva 4, Switzerland.

Abstract

The actin cytoskeleton in Schizosaccharomyces pombe functions in three distinct structures throughout the mitotic cell cycle: actin patches for endocytosis, actin cables for polarized delivery of cargoes and the contractile ring for cell division[1]. An additional structure, the actin fusion focus (AFF), functions during sexual reproduction to promote gamete fusion[2].

Although these structures have been characterized by fluorescence microscopy (FM)[1], only a few studies using electron microscopy (EM) have been performed[3-5], therefore a precise description of actin organization is lacking. This is due in part to the difficulty to visualize actin with resin embedding protocols, where actin structures and their amount appear significantly altered[5-7]. Furthermore, although live F-actin probes transiently label other cellular locations, these have not been confirmed as site of F-actin assembly due to the poor preservation of conventional EM.

Making use of recent developments in cellular cryo-electron tomography (cryo-ET), which provide unprecedented sample preservation and resolution[8], we have resolved the actin structures in a near-native state. For that we vitrified Schizosaccharomyces pombe cells, which were subsequently thinned by cryo-focused ion beam milling to obtain cryo-lamellae that are subjected to cryo-ET.

Moreover, after implementation of cryo-correlative light and electron microscopy (cryo-CLEM), by imaging cryo-lamellae by cryo-FM we have identified unequivocally not only the three main actin structures in vegetative cells, but also actin structures in new locations not yet described.

Finally, we have set up the cryo-CLEM pipeline during sexual reproduction. Using this approach, we can describe the organization of actin filaments in the AFF and laying the foundations for structural studies using subtomogram averaging.

Acknowledgments

I acknowledge Professor Sophie Martin (University of Geneva) for her scientific support, and the Electron Microscopy Facility (Univeristy of Lausanne) and the Dubochet Center for Imaging (Lausanne) for their technical support.

References

1. Kovar DR, Sirotkin V and Lord M. Three's company: The fission yeast actin cytoskeleton. Trends Cell Biol. 2011 March 21(3): 177–187.

2. Dudin O, Bendezú FO, Groux R, Laroche T, Seitz A, Martin SG. A formin-nucleated actin aster concentrates cell wall hydrolases for cell fusion in fission yeast. J Cell Biol. 2015 Mar 30;208(7):897-911.

3. Swulius MT, Nguyen LT, Ladinsky MS, Ortega DR, Aich S, Mishra M and Jensen GJ. Structure of the fission yeast actomyosin ring during constriction. Proc Natl Acad Sci U S A 2018 Feb 13;115(7):E1455-E1464.

4. Serwas D, Akamatsu M, Moayed A, Vegesna K, Vasan R, Hill JM, Schöneberg, Davies KM, Rangamani P and Drubin DG. Mechanistic insights into actin force generation during vesicle formation from cryo-electron tomography. Developmental Cell. 2022. Volume 57, Issue 9, 9 May 2022, Pages 1132-1145.e5

5. Muriel O, Minchon L, Kukulski W and Martin SG. Ultrastructural plasma membrane asymmetries in tension and curvature promote yeast cell fusion. J Cell Biol. 2021 Oct 4;220(10):e202103142.

6. Kamasaki T, Arai R, Osumi M and Mabuchi I. Directionality of F-actin cables changes during the fission yeast cell cycle. Nature Cell Biology. 2005. 7, 916-917.

7. Kamasaki T, Osumi M and Mabuchi I. Three-dimensional arrangement of F-actin in the contractile ring of fission yeast. J Cell Biol. 2007. 178 (5): 765–771.

8. Mahamid J, Pfeffer S, Schaffer M, Villa E, Danev R, Cuellar LK, Forster F, Hyman AA, Plitzko JM and Baumeister W. Visualizing the molecular sociology at the HeLa cell nuclear periphery. Science. 2016 351, 969-972.

Keywords: actin, cryo-FIBSEM, cryo-ET, cryo-CLEM

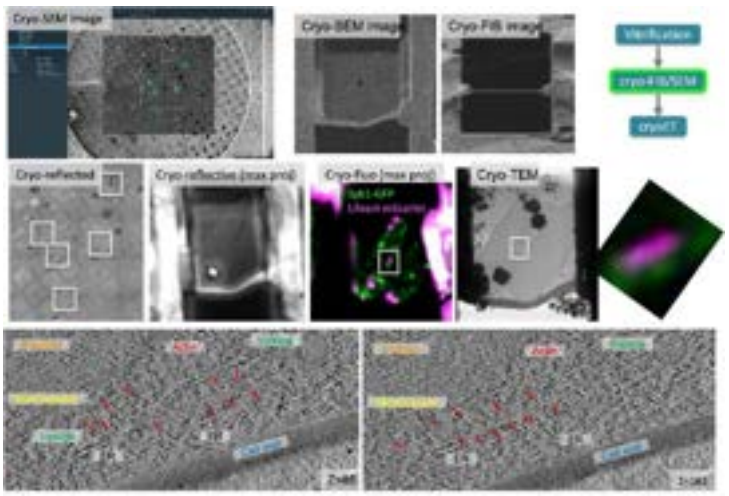

ORGANISATION OF THE ORTHOBUNYAVIRUS TRIPODAL SPIKE AND THE STRUCTURAL CHANGES INDUCED BY LOW PH AND K+ DURING ENTRY

Samantha Hover (United Kingdom)[1]; Frank W Charlton (United Kingdom)[1]; Jan Hellert (United Kingdom)[2]; Jessica J Swanson (United Kingdom)[1]; Jamel Mankouri (United Kingdom)[1]; John N Barr (United Kingdom)[1]; Juan Fontana (United Kingdom)[1]

1 - University of Leeds; 2 - Centre for Structural Systems Biology

Abstract

Following endocytosis, enveloped viruses employ the changing environment of maturing endosomes as cues to promote endosomal escape, a process often mediated by viral glycoproteins. We previously showed that both high [K^+] and low pH promote entry of Bunyamwera virus (BUNV), the prototypical bunyavirus. Here, we used sub-tomogram averaging and AlphaFold, to generate a pseudo-atomic model of the whole BUNV glycoprotein envelope. We unambiguously located the Gc fusion domain and its chaperone Gn within the floor domain of the spike. Furthermore, viral incubation at low pH and high [K^+], reminiscent of endocytic conditions, resulted in a dramatic rearrangement of the BUNV envelope. Further structural and biochemical assays indicated that pH 6.3/K^+ in the absence of a target membrane elicits a fusion-capable 'triggered' intermediate state of BUNV GPs; but the same conditions induce fusion when target membranes are present. Taken together, we reveal new mechanistic understanding of the requirements for bunyavirus entry.

Figure legend: a, Isosurface rendering of the BUNV GP trimer, identifying the three regions; head (light blue), stalk (light green) and floor (gold; where Gn also resides) on top of the viral membrane (grey). **b**, Alphafold model fitted into our subtomogram average in C3 symmetry (Gn-Gc ectodomains are shown; Gn is pink and Gc is blue). **c**, Subtomogram averaging of glycoproteins from the surface of pH 6.3/K^+ virions, showing how pH 6.3/K^+ disrupts the BUNV GP spike arrangements on the virion surface**. d & e**, Purified BUNV virions were mixed with liposomes for 2 hrs at 37 ˚C at pH 6.3/K^+, and then samples were vitrified on cryo-EM grids. Cryo-ET tilt series were collected and 3D tomographic reconstructions calculated. In **e** white arrowheads indicate vRNPs, and black arrowheads viral GPs attached to liposomes. Scale bars: a-c, 2 nm; d, 100 nm.

References

1. Organisation of the orthobunyavirus tripodal spike and the structural changes induced by low pH and K+ during entry. S Hover, FW Charlton, J Hellert, JN Barr, J Mankouri, J Fontana. bioRxiv, https://doi.org/10.1101/2022.08.11.503604.

Keywords: cryo-electron tomography, subtomogram averaging, bunyavirus, glycoprotein, viral fusion

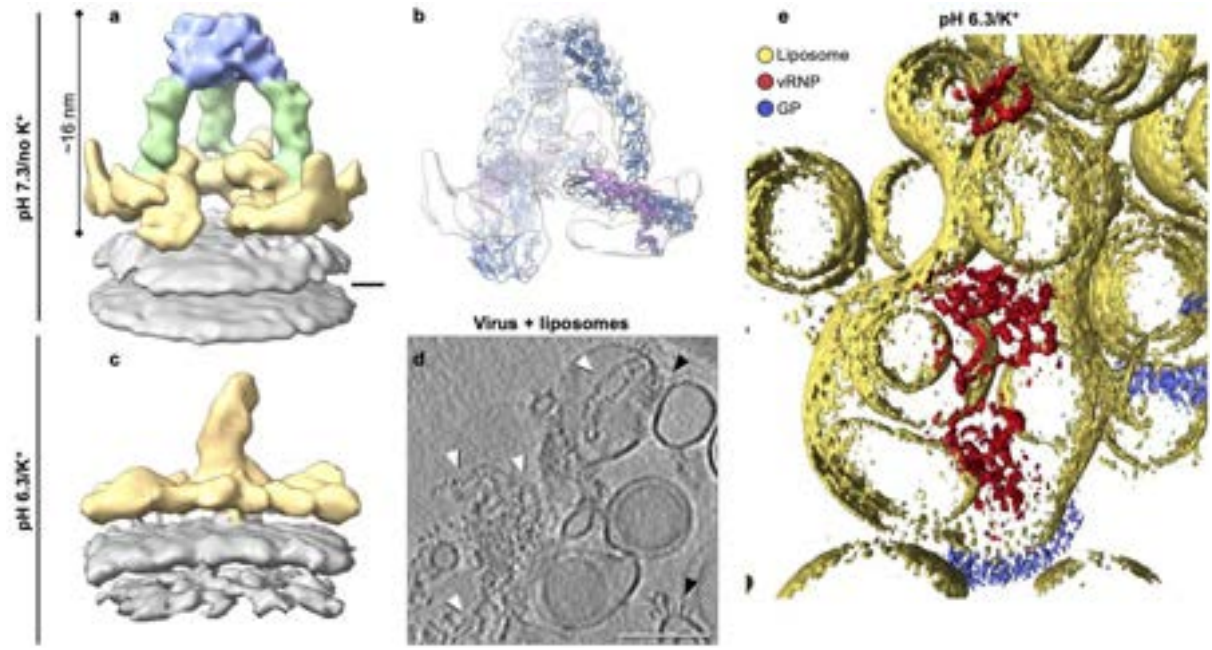
pH 7.3/no K+
pH 6.3/K+
~16 nm
a
b
c
d
e
pH 6.3/K+
Liposome
vRNP
GP
Virus + liposomes

CRYO-ELECTRON TOMOGRAPHY TO UNDERSTAND HOW EHD2 KEEPS CAVEOLAE IN PLACE

Elena Vazquez Sarandeses (Germany)[2]; Vasilii Mikirtumov (Germany)[2,3]; Mikhail Kudryashev (Germany)[1,2]; Oliver Daumke (Germany)[2,3]

1 - Institute of Medical Physics and Biophysics, Charité-Universitätsmedizin Berlin, Germany; 2 - Max-Delbrück-Center for Molecular Medicine, Structural Biology, Berlin, Germany; 3 - Freie Universität Berlin, Institute of Chemistry and Biochemistry, Berlin, Germany

Abstract

EHD2 is a dynamin-related ATPase which localizes to caveolae (1). These plasma membrane invaginations are involved in fatty acid uptake and act as nanodomains that buffer membrane plasticity in mechanical stress conditions (2). Several studies have shown that the deletion of EHD2 results in a higher number of detached caveolae from the plasma membrane and, consequently, in the release of their lipid content in the cell. In mice, this leads to larger and more abundant lipid droplets in cells and to white fat deposits around organs (3). It has been proposed that EHD2 plays an important role in stabilizing membrane curvature at the neck of caveolae, thereby regulating caveolae mobility and preventing abnormal lipid homeostasis (3).

It is known that EHD2 oligomerizes into ring-like structures upon recruitment to membranes (1). However, structural details about how EHD2 oligomerizes and binds to the lipid bilayer were missing. To address this question, we reconstituted EHD2 on liposomes. By using cryo-electron tomography (cryo-ET) and subtomogram averaging (StA), we obtained a map at an average resolution of 6.7Å. This has allowed us to describe the molecular interfaces that drive oligomerization, as well as how EHD2 binds to the lipid bilayer. We can observe that EHD2 forms oligomeric rings around lipid tubules which have the same diameter range as that of the caveolar neck. Moreover, oligomeric EHD2 can deform the membrane by generating negative curvature. Together with cryo-ET StA maps of EHD2 truncations, we can now better understand the role of each structural domain in guaranteeing the proper function of EHD2.

Furthermore, we have employed electron tomography of plastic-embedded cells to investigate the role of EHD2 assemblies within the cellular environment. Consistent with previous studies (3), we found an increased number of detached caveolae when EHD2 is not present. Interestingly, we can also observe that the caveolae which remain attached, have an altered neck morphology towards invagination. We are as well investigating this phenotype using cryo electron tomograms of whole cells. We expect that our combined approaches will provide a holistic understanding of the function of EHD2 at caveolae, where we believe it serves as a scaffold that generates the necessary membrane curvature for stability.

Acknowledgments

We thank Dr. Christoph Diebolder and Dr. Thiemo Sprink from the Core Facility for Cryo-Electron Microscopy in Berlin-Buch for cryo-ET data collection. We also thank Dr. Severine Kunz and Dr. Mara Rusu from the Electron Microscopy Facility at the MDC Berlin for plastic embedding and sectioning.

References

1. Daumke O., Lundmark R., Vallis Y., Martens S., Butler P. J. G., Mcmahon H. T. "Architectural and mechanistic insights into an EHD ATPase involved in membrane remodelling", *Nature*, vol. 449, 2007, doi: 10.1038/nature06173.

2. Echarri A. and Del Pozo M. A., "Caveolae - mechanosensitive membrane invaginations linked to actin filaments", *Journal of cell science,* vol. 128, 2015, doi:10.1242/jcs.153940.

3. Matthaeus C., Lahmann I., Kunz S., Jonas W., Melo AA., Lehmann M., Larsson E., Lundmark R., Kern M., Bluher M., Olschowski H., Kompa K., Brugger B., Muller D. N., Haucke V., Schurmann A., Birchmeier C., Daumke O., "EHD2-mediated restriction of caveolar dynamics regulates cellular fatty acid uptake", *Proc. Natl. Acad. Sci. U. S. A.*, vol. 117, 2020, doi:10.1073/pnas.1918415117.

Keywords: cryo-ET, cryo-EM, tomography, plasma membrane, subtomogram averaging

STRUCTURAL AND MOLECULAR INSIGHTS INTO DNA TRANSPOSITION

Mercedes Spínola Amilibia (Spain)[1]; Lidia Araújo Bazán (Spain)[1]; Álvaro De La Gándara (Spain)[1]; James M. Berger (United States of America)[2]; Ernesto Arias Palomo (Spain)[1]

1 - Department of Structural & Chemical Biology, Centro de Investigaciones Biológicas Margarita Salas, CSIC, 28040 Madrid, Spain; 2 - Department of Biophysics and Biophysical Chemistry, Johns Hopkins University School of Medicine, Baltimore, MD 21205, USA

Abstract

Transposons are ubiquitous, mobile DNAs that rely on dynamic nucleoprotein complexes to mediate transposition reactions (*a*). Transposases are ubiquitous enzymes that catalyze these DNA rearrangement events with broad impacts on gene expression, genome evolution, and the spread of drug-resistance in bacteria[1]. Here, we use biochemical and structural approaches to define the molecular determinants by which IstA, a canonical DDE transposase present in the widespread IS*21* family of transposons[2] (*b, c*), catalyzes efficient DNA transposition[3]. Solution studies show that IstA engages the transposon terminal sequences to form a high-molecular weight complex and promote DNA integration. A 3.4 Å resolution structure of the transposase bound to transposon ends corroborates our biochemical findings and reveals that IstA self-assembles into a highly intertwined tetramer that synapses two supercoiled terminal inverted repeats[3] (*d*). The three-dimensional organization of the IstA•DNA cleaved donor complex reveals remarkable similarities with retroviral integrases[4] and classic transposase systems, such as Tn7 and bacteriophage Mu, and provides insights into IS21 transposition.

Acknowledgments

The authors are grateful to María Cantero Gil for her work during initial IstA characterization, and to the EM platforms of the CIB Margarita Salas, CNB and IBMB (CSIC) for their assistance during grid screening and preparation. We also acknowledge Diamond for access and support of the Cryo-EM facilities at the UK national electron bio-imaging center (eBIC proposal BI26399, to E.A.-P.), funded by the Wellcome Trust, MRC, and BBSRC.

Funding: Access to eBIC was supported by Instruct-ERIC (PID 10284, to E.A.-P.) and initial data processing was supported by Instruct-ERIC (PID 12164, to E.A.-P.). This work was supported by grant GM071747 (to J.M.B.), grants PID2020-120275GB-I00 and BFU2017-89143-P funded by MCIN/AEI/10.13039/501100011033 and by "ERDF A way of making Europe" (to E.A.-P.), and grant PRE2018-086026 funded by MCIN/AEI/ 10.13039/501100011033 and by "ESF Investing in your future" (to E.A.- P. and A.G.).

References

1. Babakhani, S. & Oloomi, M. Transposons: the agents of antibiotic resistance in bacteria. *J. Basic Microbiol*. 58, 905 –917 (2018).
2. Berger, B. & Haas, D. Transposase and cointegrase: specialized transposition proteins of the bacterial insertion sequence IS *21* and related elements. *Cell. Mol. Life Sci*. 58, 403 –419 (2001).
3. IS*21* family transposase cleaved donor complex traps two right-handed superhelical crossings. *Nature Commun*. 2023 Apr 22;14(1):2335. DOI: 10.1038/s41467-023-38071-x.
4. Montaño, S. P. & Rice, P. A. Moving DNA around: DNA transposition and retroviral integration. *Curr. Opin. Struct. Biol*. 21, 370 –378 (2011).

Keywords: DNA Transposition, Transposase, Cleaved donor complex, DDE domain, IS21, IstA, Insertion sequence, DNA Binding Protein

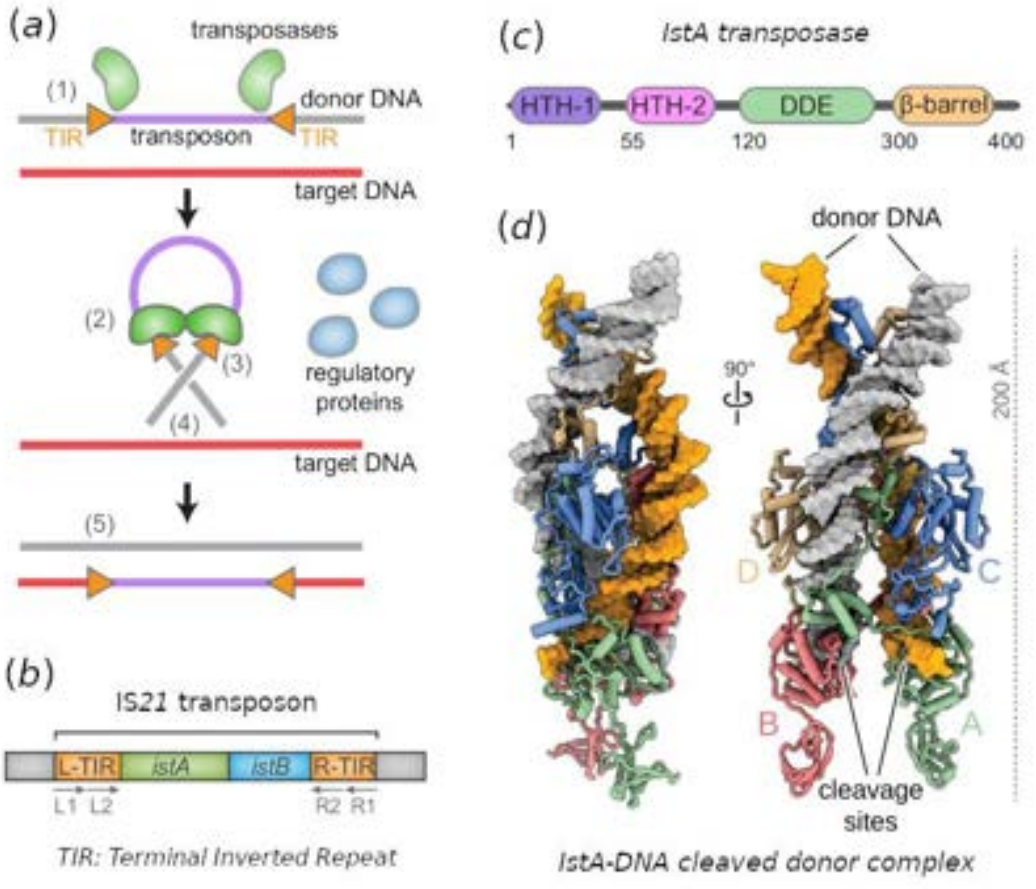

CRYO-EM GUIDED DEVELOPMENT OF ANTIVIRAL COMPOUNDS FOR CHEMICAL CONTROL OF FLEXIBLE FILAMENTOUS PLANT VIRUSES

Fernando Lamas López (Spain)[1]; Mikel Valle (Spain)[1]

1 - CIC-BIOGUNE

Abstract

One of the biggest inconveniences that we find when it comes to farming are the different infections that can damage our crops, if we look at their economic interest [1,2], a group of viruses, the filamentous viruses (alphaflexiviridae, betaflexiviridae, potyviridae y closteroviridae), the most widespread and studied, are of special importance, being examples of emerging filamentous viruses diseases that have caused great economic loss Potato Virus Y (PVY) and Potato Virus X (PVX) which ones co-infection produce a severe disease in potato crops all around the world [3].

The main objective from our proposal is to find one or several potential compounds that serve as controllers of filamentous viruses. All compounds were generated to interact with the well conserved RNA-binding site of this viruses [4]. For the selection of the candidate compound NMR and in silico docking of ligands experiments will carried out, and we will describe the interaction of the selected compounds with the viral protein by Cryo-EM.

For describing the interaction between a proposed ligand and the viral protein, in this case we use PVY, ultimately the model virus of the family. Initially, the characterization was achieved from the use of PVY VLPs [5], but as it is well defined, the absence of RNA meant that the VLPs were not as stable [6]. To achieve a stable interaction platform, we proposed the elimination of the interaction domain between the defined rings of the VLP, hypothesizing the formation of new structures formed by the capsid protein.

Our results show the formation of a novel structure of the PVY VLPs (Reconstruction Resolution achieved of 2.9Å by Cryo-EM) that could be used as a model of interaction with the ligands tested. On the other hand, the screening of ligands by NMR has been positive for some of the proposed. Ongoing perspective is the reconstruction by single particle of the interaction between this new structure and the NMR screening of the interaction of PVY VLPs new structure-ligands.

References

1. Mumford R. et al., 2016 The role and challenges of new diagnostic technology in plant biosecurity
2. Scholthof et al., 2011 Top 10 plant viruses in molecular plant pathology. Mol Plant Pathol. 2011 Dec;12(9):938-54.
3. Karasev and Gray, 2013 Continuous and emerging challenges of Potato virus Y in potato.
4. Miguel Zamora et al, 2017 Potyvirus virion structure shows conserved protein fold and RNA binding site in ssRNA viruses
5. Kežar, Andreja et al, 2019 Structural basis for the multitasking nature of the potato virus Y coat protein
6. Rebeca Cuesta et al 2019 Structure of Turnip mosaic virus and its viral-like particles

Keywords: Cryo-EM, Plant viruses, Flexible Viruses, VLPs

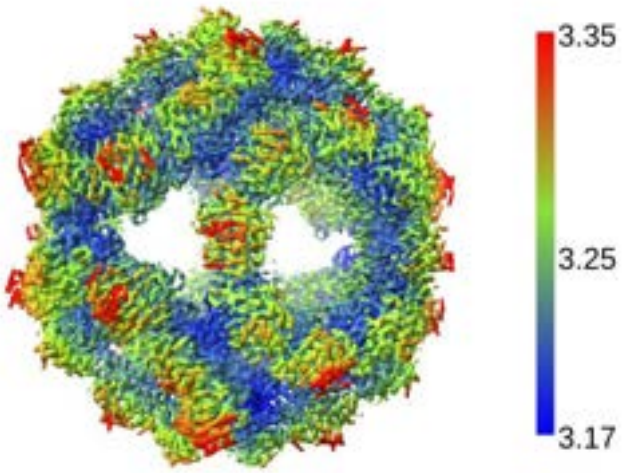

STRUCTURAL BASIS FOR THE ASSEMBLY OF SINGLE AND DOUBLE RING COMPLEXES IN HUMAN MITOCHONDRIAL HSP60-HSP10 CHAPERONIN

Jorge P. López-Alonso (Spain)[1,4]; Igor Tascón (Spain)[1,2]; Yoel Shkolnisky (Israel)[3]; Jesús Vílchez-García (Spain)[1]; Yacob Gómez-Llorente (United States of America)[5]; Radhika Malik (United States of America)[5]; Joel A. Hirsch (Israel)[6]; Fady Jebara (Israel)[6]; Malay Patra (Israel)[6]; Abdussalam Azem (Israel)[6]; David Gil-Cartón (Spain)[1,2,4]; Iban Ubarretxena-Belandia (Spain)[1,2,4]

1 - Instituto Biofisika (UPV/EHU, CSIC); 2 - IKERBASQUE, Basque Foundation for Science; 3 - Department of Applied Mathematics, School of Mathematical Sciences, Tel-Aviv University; 4 - Basque Resource for Electron Microscopy; 5 - Department of Pharmacological Sciences, Icahn School of Medicine at Mount Sinai; 6 - Department of Biochemistry and Molecular Biology, School of Neurobiology, Biochemistry and Biophysics, The George S. Wise Faculty of Life Sciences, Tel-Aviv University

Abstract

The ATP-driven human mitochondrial mHsp60 group I chaperonin assists protein folding through single- and double-ring pathways. Here, we present near-atomic resolution cryo-EM structures of mHsp60 in the absence of nucleotide, bound to ATP, and bound to both ATP and co-chaperonin mHsp10. ATP binding to single-ring apo $mHsp60_7$ triggers conformational changes in the intermediate and apical domains of each subunit that result in a highly dynamic apical region within a ring. Large inter-subunit rearrangements shift the equilibrium towards double-ring $mHsp60_{14}$ formation. Binding of heptameric mHsp10 to single- and double-ring complexes leads to further elevation and rotation of the apical domains to form half-football $mHsp60_7$-$mHsp10_7$ and football $mHsp60_{14}$-$(mHsp10_7)_2$ assemblies with one and two folding cages, respectively. The specificity of mHsp60 for mHsp10 can be explained by the presence of unique polar contacts not found in the bacterial relative GroEL-GroES. Consistent with the absence of negative inter-ring ATP-binding cooperativity, the complexes maintain strict nucleotide symmetry throughout their assembly. The cryo-EM structures provide a basis to understand the transitions from substrate-protein binding to substrate-protein folding conformations in the single- and double-ring reaction pathways of a chaperonin responsible for human mitochondrial proteome homeostasis.

Biological sciences/Structural biology/Electron microscopy/Cryoelectron microscopy Biological sciences/Biochemistry/Protein folding/Chaperones

Keywords: cryo-EM, chaperons, protein folding, structural biology

CRYO-ELECTRON TOMOGRAPHY OF PESTIVIRUS

Ane Martinez-Castillo (Spain)[1]; Diego Charro (Spain)[1]; Susanne Koethe (Germany)[2]; Isaac Santos-Perez (Spain)[1]; Mikel Azkargorta (Spain)[1]; Daniel Castano-Diez (Spain)[3]; Ander Vidaurrazaga (Spain)[1]; Kyle Dent (United Kingdom)[4]; Martin M Walsh (United Kingdom)[4]; Felix Elortza (Spain)[1]; Martin M Beer (Germany)[2]; Nicola Ga Abrescia (Spain)[1]

1 - CIC bioGUNE; 2 - Friedrich-Loeffler-Institut; 3 - Instituto Biofisika CSIC-UPV/EHU; 4 - Diamond Light Source

Abstract

Pleomorphic *Pestivirus* Bovine Viral Diahrrea Virus (BVDV) infects cattle, alpacas, deer, sheep and goats. The virus is considered as one of the most costly bovine viral diseases inflicting a severe burden to livestock welfare. Control of the disease relies on modified live and killed vaccine when prevention programs are in place. Three BVDV glycoproteins E^{rns}, E1 and E2 compose the viral envelope and are responsible for viral entry and infection. In addition, E2 represents the primary target of neutralizing antibodies. Despite the crystal structures of the corresponding ectodomains being available [1-3], the overall 3D architecture and organisation of glycoproteins on the viral lipid bilayer, remain elusive as well as the mechanism of antibody recognition [4].

Using cryo-electron tomography and sub-tomogram averaging we present the binding pose of monoclonal mAb against E^{rns} onto the virion and provide fundamental aspects of BVDV assembly.

Acknowledgments

We thank the EM platform team at CIC bioGUNE for infrastructural support and local contacts at eBIC-Diamond Light Source (UK) and at NeCEN (Netherlands), respectively, for help during tomographic data collection. We are grateful to Iker Arriaga for computing technical advice on Alphafold runs. We also acknowledge Diamond Light Source for access and support of the Cryo-EM facilities at the UK national eBIC, (proposals EM17171 and BI23872), funded by the Wellcome Trust, MRC and BBSRC.

References

[1] T. Krey et al. Structure 20, 862-873 (2012).
[2] K. El Omari et al. Cell Reports 3, 30–35 (2013).
[3] Y. Li et al. PNAS 110, 6805–6810 (2013).
[4] N. Callens et al. PLoS Pathog 12(3):e1005476 (2016).

Keywords: cryo-ET, structural virology, combined methods

A GENERAL FORMALISM FOR AVERAGING METHODS APPLIED TO CRYO-EM AND CRYO-ET RECONSTRUCTIONS

Hemant. D. Tagare (United States of America)[2]; Jose Maria Carazo (Spain)[1]; Carlos Oscar Sorzano (Spain)[1]; Jose Luis Vilas (Spain)[1]

1 - Spanish Research Council; 2 - Yale University

Abstract

One of the main targets of cryo-electron microscopy (cryo-EM) is the elucidation of the three-dimensional structure of macromolecular complexes. The acquired images have a poor Signal-to-Noise ratio[1], and the visualization of structure is almost impossible without image processing. Single Particle Analysis (SPA) and Subtomogram averaging (STA) undertake this task in a very different manner. However, both share the averaging of images at different steps of the workflow. Averaging is used in movie alignment, 2D classification, 3D reconstruction, and Subtomogram Averaging [1,2]. Averaging increases the signal to noise ratio (SNR), enhancing the signal hidden in noise. It is well known that some images present more quality than others, subtomograms in (STA) and particles in (SPA) are two examples. The use of a standard average is suboptimal for these cases, and a weighted approach seems a better estimator. In this communication, we propose a general framework for averaging which provides better estimators. Our theory is based on an optimization problem that attempts to optimize the weights that minimize the distance between the set of images and a target. The solution of this problem is extremely expensive in computational terms. We suggest the use of an aggregation function to solve this problem. Aggregation functions work as a consensus, they take different metrics and provide an estimator of the input measurements. In our applications we choose as the aggregation function [3] a product of two metrics: A real space correlation and phase correlation in Fourier Space. The results provide a significant enhancement in the quality of the weighted average, and remove outliers. As a use case, we show its performance in STA and 2D classification

Acknowledgments

Instruct Image Processing Center (I2PC), the European Strategic Infrastructure Project (ESFRI), Comunidad Autónoma de Madrid, European Union, Horizon2020. European Commision-NextGenerationEU, CSIC´s Global Health Platform (PTI Salud Global)

References

[1]J.L. Vilas et. al Emerging Themes in CryoEM-Single Particle Analysis Image Processing, Chemical Reviews 122, 17, 13915–13951 (2022)
[2] P. Navarro, et. al, Quantitative Cryo-Electron Tomography, Frontiers in Molecular Biosciences, 9, (2022)
[3] Giancarlo Lucca, Aggregation and pre-aggregation functions in fuzzy rule-based classification systems. Universidad Pública de Navarra (2018)

Keywords: subtomogram averaging, single particle analysis, electron microscopy, Image processing

TOWARDS THE CRYOEM STRUCTURE OF A YEAST METABOLON THAT REGULATES ARGININE BIOSYNTHESIS

Clara Marco-Marín (Spain)[1,2]; María Luísa López-Redondo (Spain)[1]; Nadine Gougeard (Spain)[1,2]; Sergio De Cima (Spain)[1]; Carolina Espinosa (Spain)[1]; José Luis Llácer (Spain)[1,2]; Vicente Rubio (Spain)[1,2]

1 - Instituto de Biomedicina de Valencia (IBV-CSIC).; 2 - Centro de Investigación Biomédica en Red en Enfermedades Raras (CIBERER).

Abstract

In yeasts, arginine is made from N-acetylglutamate (NAG) by a cyclic pathway in which NAG is regenerated by transacetylation from acetylornithine to glutamate. This cycle needs priming with NAG made from glutamate and acetyl-CoA by NAG synthase (yNAGS), an anaplerotic enzyme in yeast. Unlike yNAGK, which exists by itself, yNAGS only exists as a part of a hybrid metabolon with yNAGK. yNAGS and yNAGK are homologous enzymes composed of N-terminal AAK (catalytic in NAGK) and C-terminal GNAT/DUF619 (catalytic in NAGS) domains. Both yNAGS and yNAGK activities are feed-back inhibited by arginine. We (De Cima, PLoS One 2012) determined the structure of yNAGK, a homotetrameric dimer of dimers in which four AAK domains form a quadrangular four-tile layer flanked by two pairs of GNAT domains as end-globules. We now analysed the yNAGK-yNAGS metabolon (up to 2.7 Å resolution) by cryoEM. It is an octamer formed by two identical yNAGK-like tetramers, each one having 1NAGS:3NAGK stoichiometry, where a yNAGS subunit replaces one yNAGK subunit. The yNAGS chain is 107-residue longer than yNAGK due to insertions and differences in length of secondary structure elements. This creates asymmetry in each hybrid tetramer, with projection of enlarged protruding antiparallel adjacent alpha helices from the AAK domain of the yNAGS subunit. These helices are topped by a 2.5-turn helix connector that is inserted between the two N-terminal alpha helices of a yNAGK subunit in the other tetramer. These interactions are crucial for linking both tetramers into a closed octamer by these two bridges (one stemming from each tetramer towards the other). The octamer, in addition to stabilizing yNAGS perhaps by protecting this connector from cleavage if it were exposed, might promote channeling of de novo made NAG between yNAGS and yNAGK. The 1:3 stoichiometry appears limited by intrinsic factors (possibly stability or steric clash reasons). The fact that in the yeast cell in exponential growth there are about tenfold more chains of yNAGK than of yNAGS suggests that in vivo there are four tetramers of pure yNAGK per each octameric metabolon particle. We obtained structures with and without arginine and showed conformational changes in the octamer triggered by this effector, found binding only to yNAGK, suggesting transmission of the allosteric signal from yNAGK to yNAGS.

Acknowledgments

Supported by grants CIVP20A6610 (to VR) from the Fundación Ramón Areces and PID2020-116880GB-I00 from MICIN (to JLLlácer).

References

de Cima S, Gil-Ortiz F, Crabeel M, Fita I and Rubio V. (2012). Insight on an arginine synthesis metabolon from the tetrameric structure of yeast acetylglutamate kinase. PLoS One. 7:e34734.

Keywords: NAGK, NAGS, metabolon, yeast, arginine biosynthesis, cryoEM

STRUCTURAL BASIS OF TY1 INTEGRASE TETHERING TO RNA POLYMERASE III FOR TARGETED RETROTRANSPOSON INTEGRATION

Phong Q. Nguyen (Spain)[1]; Sonia Huecas (Spain)[1]; Amna Asif-Laidin (France)[2]; Adrián Plaza-Pegueroles (Spain)[1]; Beatrice Capuzzi (France)[2]; Chrsitine Conesa (France)[3]; Joël Acker (France)[3]; Juan Reguera (France)[4]; Pascale Lesage (France)[2]; Carlos Fernández-Tornero (Spain)[1]

1 - CIB Margarita Salas, CSIC; 2 - Université Paris Cité, IRSL; 3 - Université Paris-Saclay, CEA; 4 - AFMB, Inserm

Abstract

The yeast Ty1 retrotransposon integrates upstream of genes transcribed by RNA polymerase III (Pol III). Specificity of integration is mediated by an interaction between the Ty1 integrase (IN1) and Pol III, currently uncharacterized at the atomic level. We report cryo-EM structures of Pol III in complex with IN1, revealing a 16-residue segment at the IN1 C-terminus that contacts Pol III subunits AC40 and AC19, an interaction that we validate by in vivo mutational analysis. Binding to IN1 associates with allosteric changes in Pol III that may affect its transcriptional activity. The C-terminal domain of subunit C11, involved in RNA cleavage, inserts into the Pol III funnel pore, providing evidence for a two-metal mechanism during RNA cleavage. Additionally, ordering next to C11 of an N-terminal portion from subunit C53 may explain the connection between these subunits during termination and reinitiation. Deletion of the C53 N-terminal region leads to reduced chromatin association of Pol III and IN1, and a major fall in Ty1 integration events. Our data support a model in which IN1 binding induces a Pol III configuration that may favor its retention on chromatin, thereby improving the likelihood of Ty1 integration.

References

Nguyen PQ, Huecas S, Asif-Laidin A, Plaza-Pegueroles A, Capuzzi B, Palmic N, Conesa C, Acker J, Reguera J, Lesage P, Fernández-Tornero C. (2023) Structural basis of Ty1 integrase tethering to RNA polymerase III for targeted retrotransposon integration. Nat Commun. 14(1):1729. doi: 10.1038/s41467-023-37109-4.

Keywords: Retrotransposon, Transcription, RNA polymerase, cryo-EM

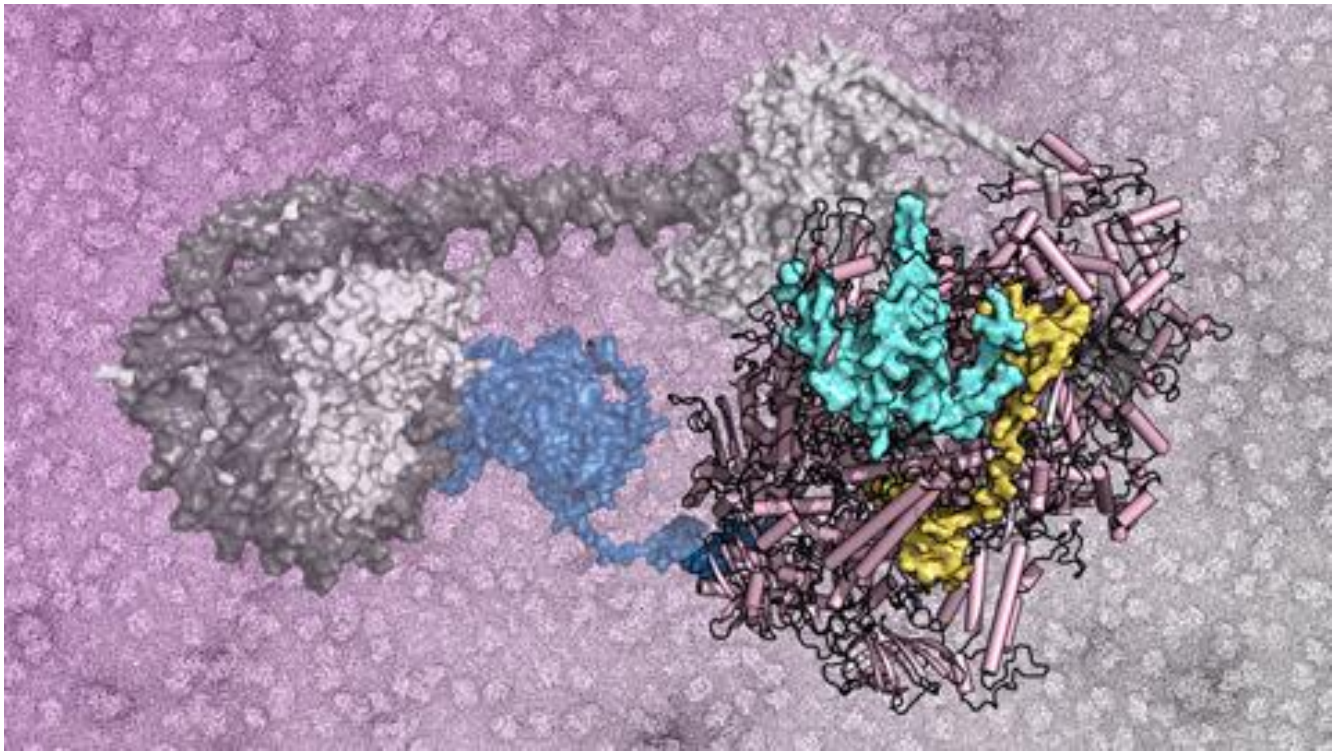

CRYO-EM STRUCTURE OF YADONUSHI AND YADOKARI VIRUSES

Guy Novoa (Spain)[2]; Nobuhiro Suzuki (Japan)[1]; José R. Castón (Spain)[2]

1 - University of Okayama; 2 - Centro Nacional de Biotecnología - CSIC

Abstract

Many fungal hosts are infected simultaneously by ssRNA, dsRNA and ssDNA viruses of different families. In the fungus *Rosellinia necatrix*, the (+) ssRNA capsidless Yadokari virus 1 (YkV1) hijacks the capsid protein (CP) of the dsRNA Yadonushi virus 1 (YnV1) to encapsidate its genome and RdRp. Whereas YnV1 is similar to totiviruses, YkV1 is close to caliciviruses and mimics the typical dsRNA virus life cycle. The mechanism by which YnV1 CP recognizes and encapsidates these two different cargos is yet to be understood. We report the 3D structure by single-particle cryo-EM of YnV1/YkV1. Purified YnV1 and YkV1 particles were visualized in a Titan Krios 300 kV cryo-electron microscope, and we merged 727,000 particles to calculate a 2.63 Å resolution map. The ~540 Å-diameter T=1 capsid shows 12 outwardly protruding decamers at the pentameric positions. The asymmetric unit is a CP homodimer (A- and B-subunits), which has been traced covering ~97% of the 1023 residues to build an atomic model de novo. Monomer A and B represent a case of structural polymorphism, in which the main difference is the presence of a long α-helix in monomer A, which reduces the diameter of the pores present in the 5-fold axes cavities, possibly playing a role in the exit of mRNA transcripts. Overlaying YnV1 CP on other dsRNA mycoviruses including ScV L-A, Penicillium chrysogenum virus and Rosellinia necatrix quadrivirus 1, as well as on the CP of a non-fungal totivirus such as Omono River Virus, that infects *Culex* mosquitos, highlighted the same conserved motif, formed by 8 α-helices and 5 β-strands, and the presence of conserved 'hot spots', in which structural and functional variations are introduced by the insertion of distinct segments. A preliminary reconstruction of the asymmetric genome has been calculated using a symmetry relaxation approach. The results indicate the presence of two types of genome organization: one with loosely packed dsRNA filaments arranged in a single-spooled organization in concentric layers of well-resolved dsRNA filaments, with a diameter of ~20 Å and intra and inter-strand spacings of ~35 Å; and the other with noisy filaments lacking the single-spooled organization. The relationship between these two different types of genome organization remains unclear.

Acknowledgments

We thank the Cryo-EM CNB-CSIC facility (Madrid), for help with cryo-EM data acquisition. This work was supported by grants from the Spanish Ministry of Science and Innovation (PID2020-113287RB-I00) and the Comunidad Autónoma de Madrid (P2018/NMT-4389) to JRC.

References

[1] Zhang et al. *Nat Microbiol*. **2015.** 1, 15001.

[2] Das et al. *J. Virol*. **2021**. 95, e0046721.

Keywords: Cryo-EM, Virus, Genome, Structure, Single-particle

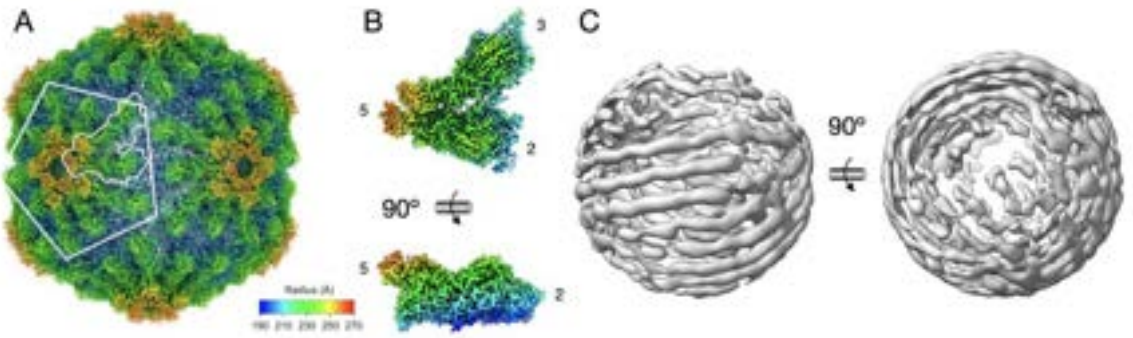

Figure 1. 3D cryo-EM structure of YnV1/YkV1. (A) Near-atomic structure of YnV1 capsid (boundaries for two CPs are outlined in white). (B) YnV1 asymmetric subunit. Position of 5-, 3- and 2-fold symmetry axes are indicated. (C) 3D reconstruction of multiple dsRNA layers showing one class of well-resolved filaments of YnV1/YkV1.

ORGANIZATION OF GENOMIC DSRNA AND THE RNA POLYMERASE INSIDE THE CAPSID OF THE L-A VIRUS OF SACCHAROMYCES CEREVISIAE

Juan M. Martínez-Romero (Spain)[1]; David Gil-Cantero (Spain)[1]; José R. Castón (Spain)[1]

1 - Centro Nacional de Biotecnología (CNB-CSIC)

Abstract

While the organization of nucleic acids and associated viral polymerases within capsids have been extensively studied in dsRNA viruses of higher eukaryotes such as reoviruses, which have highly packed genomes (~40 bp/100nm³) and 10-12 RNA polymerases [1,2], dsRNA mycoviruses contain a much lower dsRNA density (~20 bp/100nm³) and 1-2 copies of RNA polymerase [3,4]. Our goal is to develop computational approaches to determine the genome and the RNA polymerase organization inside the mycovirus L-A of the yeast *Saccharomyces cerevisiae* (ScV-L-A). The 4.6 kbp dsRNA genome encodes a capsid protein (Gag, 680 residues, 76 kDa) and an RNA polymerase (Pol, 868 residues, 94 kDa) as a Gag-Pol fusion protein (~170 kDa). In ScV-L-A assembly, Gag-Pol is thought to bind genomic RNA via its Pol moiety whereas the Gag domain primes the polymerization of Gag subunits.

We have calculated the 3D map of ScV-L-A at 2.52 Å of resolution. The ScV-LA capsid has a T=1 architecture made of 60 Gag homodimers. Additionally, the organization of the packaged genome inside the capsid have been determined by using a symmetry relaxation approach. The dsRNA is organized as three concentric layers of filaments with a single-spooled organization. These filaments have a diameter of ~20 Å and exhibit a strand-to-strand distance (both intra- and inter-layer) of ~35 Å, consistent with a single molecule of loosely packed dsRNA genome. In some regions, these filaments were resolved as an A-type dsRNA. Preliminary analysis solves two Pol copies in the oposite poles of the capsid, close to the five-fold axes, with a well-defined hand-shaped structure. Together, these results suggest that Pol functions as a coil shaft that is bound covalently to the inner capsid surfaces.

Acknowledgments

We thank the Cryo-EM CNB-CSIC facility (Madrid), for help with cryo-EM data acquisition. This work was supported by grants from the Spanish Ministry of Science and Innovation (PID2020-113287RB-I00) and the Comunidad Autónoma de Madrid (P2018/NMT-4389) to JRC.

References

1. Ding K, Celma CC, Zhang X, et al. In situ structures of rotavirus polymerase in action and mechanism of mRNA transcription and release. *Nat Commun*. 2019;10(1):1-9. doi:10.1038/s41467-019-10236-7

2. He Y, Shivakoti S, Ding K, Cui Y, Roy P, Zhou ZH. In situ structures of RNA-dependent RNA polymerase inside bluetongue virus before and after uncoating. *Proc Natl Acad Sci U S A*. 2019;116(33):16535-16540. doi:10.1073/pnas.1905849116

3. Castón JR, Trus BL, Booy FP, Wickner RB, Wall JS, Steven AC. Structure of L-A virus: A specialized compartment for the transcription and replication of double-stranded RNA. *J Cell Biol*. 1997;138(5):975-985. doi:10.1083/jcb.138.5.975

4. Mata CP, Rodríguez JM, Suzuki N, Castón JR. Structure and assembly of double-stranded RNA mycoviruses. *Adv Virus Res*. 2020;108:213-247. doi:10.1016/bs.aivir.2020.08.001

Keywords: Cryo-EM, dsRNA, ScV-L-A, RNA polymerase, Capsid

STRUCTURAL BASIS OF NEAR COGNATE CODON DISCRIMINATION BY THE EUKARYOTIC TRANSLATION INITIATION COMPLEX

Laura Villamayor-Belinchón (Spain)[2]; Prafful Sharma (India)[1]; Borja Sáez (Spain)[2]; Maria Luisa López-Redondo (Spain)[2]; Laura Flores (Spain)[2]; Carolina Espinosa (Spain)[2]; Monica Escamilla (Spain)[2]; Tanweer Hussain (India)[1]; José Luis Llácer (Spain)[2]

1 - Indian Institute of Science; 2 - Instituto de Biomedicina de Valencia (IBV-CSIC)

Abstract

Eukaryotic translation initiation is a multistep process in which a dozen of initiation factors (eIFs) and methionyl initiator tRNA (Met-tRNAi) associate with the 40S ribosomal subunit to form a 43S pre-initiation complex (PIC). Then this 43S PIC attaches to the capped 5' end of the mRNA and scans the 5´ untranslated region (5' UTR) in the 5**'** -to-3**'** direction for an AUG nucleotide triplet start codon using complementarity with the anticodon of Met-tRNAi in the 40S P site (1,2). Recognition of a suitable start codon (usually AUG in a good Kozak context) is followed by a major conformational change in the PIC to a scanning arrested closed (P_{IN}) complex in which Met-tRNAi is more tightly bound, eIF1 dissociates and is replaced by the N-terminal domain of eIF5 and the codon:anticodon duplex is stabilized by the N-terminal tail (NTT) of eIF1A (3,4). Translation initiation ends with dissociation of all eIFs and 60S subunit joining to produce an 80S initiation complex ready to enter the elongation cycle of protein synthesis (1,2).

In contrast to the strictness of A-site decoding during the elongation phase of translation, decoding at the P-site during initiation is more error-prone and indeed, many eukaryotic genes contain upstream open reading frames where AUG codons can be skipped when they are flanked by unfavorable sequences. At the same time, non-AUG triplets (which differ by in one base from AUG) can be selected if they are in good flanking regions, albeit less efficiently (5,6).

We aim to use cryoelectron microscopy to understand, at a structural level, how the various eIFs, structural elements of tRNAi and rRNA and protein components of the 40S contribute to the stringency of codon discrimination. We have produced all eIFs, 40S ribosomes, a near-cognate (AUC) capped mRNA and Met-tRNAi from *Saccharomyces cerevisiae*, and then *in vitro* reconstituted the 48S PIC and placed it in cryo-EM grids. A large dataset of more than 11.000 images and extensive 3D classifications using masks have been necessary to isolate several distinct and well defined maps of yeast 48S PICs in P_{IN}-like conformations at high resolutions (from 3.35 to 4.7Å-resolution). These complexes show in detail the geometry of a near-cognate codon: anticodon duplex with a mismatch in the third position of the codon and the role of eIF1, eIF5 and the eIF1A NTT in the discrimination of that third nucleotide of the mRNA initiation codon.

Acknowledgments

Supported by grants PID2020-116880GB-I00 from Spanish MICIN to JLL and IA/ I/ 17/ 2/ 503313 from Wellcome Trust/ DBT India Alliance to TH.

References

1- Hinnebusch,A.G. Structural Insights into the mechanism of scanning and start codon recognition in eukaryotic translation initiation. Trends Biochem. Sci. 42, 589–611. (2017)

2- Aylett,C.H. and Ban,N. Eukaryotic aspects of translation initiation brought into focus. *Philos. Trans. R. Soc. Lond. B Biol. Sci.*, 372, 20160186. (2017).

3- Llácer,J.L., Hussain,T., Saini,A.K., Nanda,J.S., Kaur,S., Gordiyenko,Y., Kumar,R., Hinnebusch,A.G., Lorsch,J.R. and Ramakrishnan,V. Translational initiation factor eIF5 replaces eIF1 on the 40S ribosomal subunit to promote start-codon recognition. *eLife*, 7, e39273. (2018)

4- Llácer JL, Hussain T, Dong J, Villamayor L, Gordiyenko Y, Hinnebusch AG. Large-scale movement of eIF3 domains during translation initiation modulate start codon selection. *Nucleic Acids Res*., 49, 11491. (2021).

5- Hinnebusch AG, Ivanov IP, Sonenberg N. Translational control by 5′-untranslated regions of eukaryotic mRNAs. *Science*352, 1413 (2016).

6 - Andreev DE, Loughran G, Fedorova AD, Mikhaylova MS, Shatsky IN, Baranov PV. Non-AUG translation initiation in mammals. *Genome Biology* 23, 111. (2022)

Keywords: 40S ribosome, eIFs, single particle, cryoEM, translation initiation complex, yeast

IMPROVING CRYO-EM SAMPLE PREPARATION

Rafael Fernandez-Leiro (Spain)[1]; Samuel Miguez-Amil (Spain)[1]; Ester Casajús-Pelegay (Spain)[1]; Araceli Grande-García (Spain)[1]; Maria Moreno-Morcillo (Spain)[1]

1 - CNIO

Abstract

Thanks to the continuous hardware and software improvements, the Cryo-EM revolution has achieved unprecedented results, with recent cryoEM reconstructions reaching atomic resolution. Still, important bottlenecks during sample preparation prevent the structural characterization of many important samples. Here we present some of our efforts to improve reproducibility and quality of cryo-EM sample preparation, and new advances on our plunger prototype that enables the implementation of time-resolved experiments.

Keywords: cryoEM, Plunger, Sample preparation

THE CRYOEM CNB-CSIC FACILITY: UNLOCKING DISCOVERIES IN STRUCTURAL BIOLOGY

Francisco Javier Chichón (Spain)[1]; Rocio Arranz (Spain)[1]; Noelia Zamarreño (Spain)[1]; Jose Javier Conesa (Spain)[1]; David Delgado (Spain)[1]; Javier Collado (Spain)[1]; Teresa Bueno (Spain)[1]

1 - CryoEM CSIC Facility (CNB)

Abstract

The CryoEM CNB-CSIC Facility: Unlocking Discoveries in Structural Biology

Located within the esteemed National Centre for Biotechnology in Madrid, the CryoEM CNB-CSIC facility plays a pivotal role as part of the INSTRUCT Node Spain. Collaborating closely with the Instruct Image Processing Centre (I2PC), our facility is proud to be included in the renowned Instruct-ERIC and iNEXT-discovery programs for infrastructures. We provide European researchers with exceptional access to advanced cryoelectron microscopy (cryoEM) infrastructure.

At our facility, we warmly welcome both seasoned experts and aspiring scientists, offering a unique opportunity to submit samples for meticulous cryoEM sample characterization and engage in high-resolution single-particle analysis (SPA) data acquisition. In line with our dedication to innovation, we have expanded our services to include cryo-electron tomography (ET), correlative microscopy (CLEM), and microdiffraction for molecules and small crystal proteins.

Join us at the CryoEM CNB-CSIC facility as we embark on an exciting journey, unraveling the secrets of structural biology and uncovering groundbreaking discoveries.

Acknowledgments
We acknowledge CNB-CSIC facility in the context of the CRIOMECORR project (ESFRI-2019-01-CSIC-16). Financial support also provided by European EC Horizon2020 iNEXT (Project 653706), Instruct-ERIC Projects"

Keywords: CryoEM, Tomography, Correlative Microscopy, CLEM, microED, iNEXT, INSTRUCT

MACROMOLECULAR COMPLEXES IN MTDNA REPLICATION PROCESSES: MOLECULAR AND STRUCTURAL MECHANISMS BY CRYO-EM

Samuel Míguez Amil (Spain)[1]; Araceli Grande Garcia (Spain)[1]; Emma Arean Ulloa (Spain)[1]; Rafael Fernandez Leiro (Spain)[1]

1 - Centro Nacional de Investigaciones Oncológicas (CNIO)

Abstract

Mutations in proteins that regulate mitochondrial DNA (mtDNA) replication can cause various diseases, including cancer and neurodegenerative disorders. The **Polymerase Gamma (Polγ)** protein is responsible for mtDNA replication, in which more than 200 mutations has been described to be linked to mitochondrial diseases. Polγ is the only replicative polymerase in mitochondria and has the ability to synthesize and proofread DNA, as well as displace complementary DNA strands to synthesize new DNA molecules. Despite of the available biochemical and structural information, how Polγ coordinates these activities is not known.

To address this, we used a range of biochemical and biophysical techniques to study Polγ at a molecular level. Our Cryo-EM models of Polγ in different states and bound to different DNA substrates allowed us to describe how exonuclease and strand displacement activities are performed, and to identify key regions and residues involved in these functions. Furthermore, we have investigated the mechanistic details of disease-causing mutations in Polγ. Our findings provide a more complete understanding of Polγ's complex functions and shed light on the molecular basis of mitochondrial diseases.

Keywords: cryoem, DNA replication, mitochondria, polymerase, helicase, polymerase gamma

EM01-CRYO-TEM: A NEW CRYO-ELECTRON MICROSCOPY PLATFORM AT ALBA

Pablo Guerra (Spain)[1]

1 - Spanish National Research Council

Abstract

The recent development of transmission electron microscopy has opened the door to data acquisition at atomic resolution and, consequently, to a new dimension in the research of high resolution molecular structures, both from biological and materials samples. However, the general situation of the advanced electron microscopy in Catalonia has not allowed the development of this technique. While other regions in Spain have made a strong commitment to equip themselves with state-of-the-art equipment (acquiring microscopes with acceleration voltages of 200 kV and 300 kV and powerful electron detectors), in Catalonia we are far behind with these kind of infrastructures. This situation has finally changed thanks to the installation of a new Thermofisher Glacios 200kV TEM located in the JEMCA (Joint Electron Microscopy Center at Alba), in the ALBA synchrotron. This new infrastructure, devoted to high-end transmission electron microscopy analyses, emerged thanks to the collaboration between several local and national institutions.

The IBMB-CSIC Cryo-electron Microscope Platform possess a specialized cryo-electron microscope for structural biology applications, equipped with an automated sample load system and a last generation direct electron detector. The platform will give access to state-of-the-art cryo-EM equipment for structure determination projects using the latest technology and methods. Glacios 200kV transmission electron microscope with extreme field emission gun (X-FEG) optics, equipped with a cryogenic sample manipulator robot for up to 12 grids and with the last generation of direct electron detector, a Falcon 4 that can take up to 400 movies per hour. Its high level of automation and user guidance of experimental settings enable scientists to efficiently unravel protein structures in 3D, as well as understand their functional context in the biological cell.

This equipment will be used mainly to obtain structural information of proteins and macromolecular complexes at atomic resolutions, in order to determine their three-dimensional atomic structure. This information is essential to determine how a protein is capable of carrying out its function at atomic level and the first step in the design of drugs and other molecules of interest in medicine and biotechnology.

Keywords: Glacios, Falcon 4, EER, platform

UNVEILING THE NATURE OF CELLULAR NANO-COMPARTMENTS – ELECTRON-DENSE GRANULES BY CRYO-STEM

André G. Gouveia (Portugal)[1]; Sara T. Silva (Portugal)[1]; Dean O. Ranmar (Israel)[2]; Ofra Golani (Israel)[2]; Sharon G. Wolf (Israel)[2]; Michael Elbaum (Israel)[2]; Célia V. Romão (Portugal)[1]

1 - ITQB-NOVA Universidade Nova de Lisboa; 2 - Weizmann Institute of Science

Abstract

Polyphosphate-like granules (pPLGs) are found in all domains of life and play a role in a wide diversity of functions from energy storage to stress resistance [1]. *Deinococcus radiodurans* is the model organism of radiation resistance and contains pPLGs in its native phenotype [2,3]. Increasing concentrations of salt (NaCl) promotes an evident multicellular morphotype in which cell separation is lower and clusters of cells are linked together by their septum region [4]. Here we investigate the pPLGs composition in two distinct morphotypes (in the presence and absence of NaCl) by applying Cryo-STEM-EDX. High-resolution cellular mapping revealed a wide heterogeneity of pPLGs and distribution within the *D. radiodurans* population. *D*. *radiodurans* pPLGs are able to incorporate and store, sodium, potassium, calcium, and magnesium. Moreover, the elemental composition of these subcellular structures is directly linked to environmental composition. Most cations incorporated in pPLGs granules are involved in stress resistance and are essential for the function of several enzymes (e.g. DNA repair system). In conclusion, our results suggest a certain level of cell specialization within the community where some cells could be prone to metal accumulation to allow the community to cope with environmental shifts.

Acknowledgments

We thank for the financial support by the Portuguese Fundação para a Ciência e Tecnologia (FCT), grants PTDC/BIA-BQM/31317/2017, Project MOSTMICRO-ITQB with references UIDB/04612/2020 and UIDP/04612/2020, and LS4FUTURE Associated Laboratory (LA/P/0087/2020). This project has received funding from the European Union's Horizon 2020 research and innovation program under grant agreement No. 857203. We also like to thank INSTRUCT-ERIC, access proposal, PID19879 "Unveiling the nature of cellular nano-compartments – electron-dense granules by cryo-STEM", Weizmann Institute Electron Microscopy Unit. André G. Gouveia is recipient of FCT grant SFRH/BD/06723/2020.

References

[1] Kornberg, A. (1999). Inorganic Polyphosphate: A Molecule of Many Functions. In: Schröder, H.C., Müller, W.E.G. (eds) Inorganic Polyphosphates. Progress in Molecular and Subcellular Biology, vol 23. Springer, Berlin, Heidelberg. doi: https://doi.org/10.1007/978-3-642-58444-2_1

[2] Thornley, M. J., Horne, R. W., and Glauert, A. M. (1965). The fine structure of micrococcus radiodurans. *Arch. Mikrobiol.* 51, 267–289. doi: 10.1007/BF00408143.

[3] Liu, F., Li, N., and Zhang, Y. (2023). The radioresistant and survival mechanisms of Deinococcus radiodurans. *Radiat. Med. Prot.* doi: 10.1016/J.RADMP.2023.03.001.

[4] Chou, F. I., and Tan, S. T. (1991). Salt-mediated multicell formation in Deinococcus radiodurans. *J. Bacteriol.* 173, 3184–3190. doi: 10.1128/jb.173.10.3184-3190.1991.

Keywords: Polyphosphate granules, Metal homeostasis, Deinococcus radiodurans, Cryo-STEM

THE HIGH RESOLUTION CRYOEM STRUCTURE OF DPS2 REVEALS THE STRUCTURAL LOCATION OF THE N-TERMINAL EXTENSIONS

Bruno Salgueiro (Portugal)[1]; Marcos Gragera (Spain)[2]; Ausra Domaska (Finland)[3]; André Gouveia (Portugal)[1]; Sara Silva (Portugal)[1]; Carlos Oscar Sorzano (Spain)[2]; José Maria Carazo (Spain)[2]; Sarah Butcher (Finland)[3]; Célia Romão (Portugal)[1]

1 - ITQB NOVA; 2 - CNB-CSIC; 3 - University of Helsinki

Abstract

DNA-binding proteins under starvation conditions (Dps) have been identified in several prokaryotic organisms. Their in-vitro function has been mainly attributed to DNA protection and/or metal homeostasis, however the in vivo function has not been fully stablished, in fact their function may differ from organism and/or response to different environments. We have been studied both Dps (Dps1 and Dps2) from the radiation resistant bacteria Deinococcus radiodurans [1-5]. These proteins share the same overall structure as the other Dps family members, as hollow spheres composed by twelve subunits [1,2]. However, both of these proteins contain longer and flexible N-terminals [3]. Our data, suggests that in vivo conditions, Dps2 is associated with the membrane, it is quite interesting that this protein is unique within the Dps family members since it contains a signal peptide [4,5]. Under stress conditions, Dps2 is cleaved from the membrane, and the cytosol is proposed to function as metal storage compartments for Mn or Fe. Under in vitro conditions we have observed the interaction of Dps2 and DNA, the protein is able to bind and protect the DNA, but is quite interesting that the interaction is conformational-specific for the type of DNA, being only specific for the supercolided DNA conformation [3,4] . However, in case of the truncated version in which the protein lacks the N-terminal, the protein can bind to different types of DNA, suggesting that the N-terminal is involved on selecting the DNA-type. Therefore, we have pursued our studies, aiming to determine the high resolution structure of the Dps2 using CryoEM, and also in complex with the DNA. We currently have a full dataset collected at ESRF in the CryoEM-300kV Titan Krios, the grids were prepared using the VitroJet system, and a first initial processing indicate the presence of two populations, one corresponding to the Dps2 only sphere and the second population that may correspond to two Dps2 hollow spheres in interaction with the DNA. Thus, the main objective of the current proposal is to process the data of the individual Dps2 in order to obtain the high resolution model (ca. 2 Å) and to process the data of the double-sphere in order to obtain a 3D model of the Dps2-DNA.

Acknowledgments

This study was financially supported by the Portuguese Fundação para a Ciência e Tecnologia (FCT), grants PTDC/BIA-BQM/31317/2017, Project MOSTMICRO-ITQB with references UIDB/04612/2020 and UIDP/04612/2020, LS4FUTURE Associated Laboratory (LA/P/0087/2020) and Instruct Access Proposals: 25373, 12696. This project has received funding from the European Union's Horizon 2020 research and innovation program under grant agreement No. 857203. Moreover, we acknowledge the Iberian ESRF BAG to access the CM01 beamline at ESRF.

References

1. Romao et al (2006) *JBIC*, 11, 891.
2. Cuypers et al., (2007) *JMB*, 371, 787.
3. Santos et al (2017) *JMB*, 249, 667
4. Santos et al (2015) *FEBS J*, 282, 4307.
5. Santos et al (2019) *Scient Rep,* 9, 17217.

Keywords: Dps, DNA, Deinococcus radiodurans

STRUCTURAL AND FUNCTIONAL INSIGHTS INTO DISSIMILATORY SULFATE REDUCTION - THE CRYO-EM STRUCTURES OF THE DSRMKJOP AND QRCABCD MEMBRANE COMPLEXES

Jose Artur Brito (Portugal)[1]; Max Yin (Portugal)[2]; Ana Barbosa (Portugal)[1]; Sofia Venceslau (Portugal)[1]; Raquel Bernardino (Portugal)[1]; Margarida Archer (Portugal)[1]; Bonnie Murphy (Portugal)[2]; Ines Pereira (Portugal)[1]

1 - ITQB NOVA; 2 - Max Planck Institute of Biophysics

Abstract

Dissimilatory sulfate reduction (DSR) is a dominant microbial process in anoxic environments, especially in marine sediments, estimated to be responsible for up to 30% of total organic carbon remineralization [1]. Syntrophic communities of sulfate-reducing bacteria with anaerobic methane oxidizing archaea (ANME) play an important role in reducing emissions of the harmful greenhouse gas methane. Microbial hydrogen sulfide (H_2S) production is a serious problem in the petroleum industry, causing oil souring and corrosion of pipelines leading to important losses (*ca*. $90 billion globally). Additionally, H_2S poses a significant health and safety risk for workers as it represents the second most frequent gas-related fatality in workplaces, after carbon monoxide, an issue covered by the air quality guidelines of WHO.

In addition to the major role played by sulfate-reducing organisms (SRO) in global sulfur and carbon cycles [2], these organisms are also common members of the human gut microbiota where H_2S production has been associated with inflammatory bowel diseases and cancer [3,4]. Studying the mechanisms of H_2S synthesis, its regulation and distribution is important to further understand a critical pathway in various pathologies directly related to H_2S metabolism. Dysfunctional human H_2S metabolism has been increasingly shown to be associated with several pathologies, ranging from cardiovascular (atherosclerosis), to neurodegenerative diseases, to diabetes and cancer. Indeed, in several cancer types (colorectal, ovarian, prostate, breast, among others), increased H_2S production was shown to occur with an impact on tumor angiogenesis and progression.

Despite the widespread occurrence of DSR, there is still a limited understanding of the molecular basis of this respiratory process due to the unusual DSR mechanism and proteins involved. We have been working to elucidate this process and made important contributions by isolating and characterizing several proteins involved in DSR, including the respiratory membrane complexes DsrMKJOP [5,6] and QrcABCD [7,8] from *Archaeoglobus fulgidus* and *Desulfovibrio vulgaris* Hildenborough, respectively.

Herein we will present the cryo-EM structures of these two complexes to 1.9 Å resolution. These structures are decisive to understand sulfur-based respiration, which is crucial to understand SRO physiology. Moreover, these structures provide novel insights into the development of specific SRO inhibitors.

References

[1] Bowles *et al.* (2014). *Science* 344, 889-891 (2014)
[2] Rabus *et al*. (2015). *Adv. Microb. Physiol.* 66, 55-321
[3] Carbonero F, Benefiel AC, and Gaskins HR (2012). *Nat Rev Gastroent Hepat* 504-518
[4] Rey FE *et al*. (2013). *PNAS* 110, 13582-13587
[5] Pires RH *et al*. (2006). *Biochemistry* 45(1), 249-62
[6] Grein F, Pereira IA, Dahl C (2010). J Bacteriol 192(24), 6369-77
[7] Venceslau S.S., Lino R.R., and Pereira I.A.C. (2010). *J Biol Chem* 285, 22774-22783
[8] Venceslau S. S., Matos D. & Pereira I. A. C. (2011). *FEBS Letters* 585, 2177-2181

Keywords: Sulfate reducing organisms, Sulfite reduction, Membrane protein complexes, Cryo-EM

CRYOEM STRUCTURE OF A CLASS F FLAVODIIRON PROTEIN FROM CLOSTRIDIUM DIFFICILE, REVEALS THE INTERACTION BETWEEN THE FOUR REDOX CENTERS

Marcos Gragera (Spain)[2]; Maria Martins (Portugal)[1]; Alessandro Grinzato (France)[3]; Mikel Iceta (Spain)[2]; Carlos Oscar Sorzano (Spain)[2]; José Maria Carazo (Spain)[2]; Filipe Folgosa (Portugal)[1]; Miguel Teixeira (Portugal)[1]; Célia Romão (Portugal)[1]; Bruno Alexandre Dos Anjos Salgueiro (Portugal)[1]

1 - ITQB-NOVA; 2 - CNB-CSIC; 3 - ESRF

Abstract

The presence of considerable amounts of oxygen in the atmosphere forced modifications in the cellular metabolism of organisms [1]. To overcome this problem, organisms have found ways to convert both reactive oxygen (ROS) and NO (RNS) species through enzymatic systems into non-toxic species. One of the family members are the Flavodiiron (FDP) proteins, and the common aspects of these enzymes is the presence of Fe centers responsible for the conversion of these species to harmless molecules in organisms.

FDPs are soluble enzymes, characterized with the minimal functional unit, the presence of a two-domain core, known as FDP core: a metallo-β-lactamase-like domain, with a diiron catalytic center, followed by a flavodoxin-like domain, containing a flavin mononucleotide (FMN)[2]. This protein is a prototype of modular enzymes that may harbor up to three additional domains, with putative extra redox centers for example rubredoxins, flavins, Fe/S clusters, besides the two common core domains[2].

Clostridium difficile is an important pathogen in human health, and as part of its ROS/RNS detoxification system contains two FDP proteins. One of those is a multidomain Class F FDP composed by four domains: the minimal FDP functional core and two extra redox domains, rubredoxin and reductase domains.

The aim of this study was to determine the first structure of a multidomain Class F FDP protein by Cryo-EM Single Particle Analysis. We have collected a dataset in the 300 kV Titan Krios at CM01- ESRF. The structure obtained revealed for the first time the electron transfer mechanism between the four domains.

Acknowledgments

This study was financially supported by the Portuguese Fundação para a Ciência e Tecnologia (FCT), Project MOSTMICRO-ITQB with references UIDB/04612/2020 and UIDP/04612/2020, and LS4FUTURE Associated Laboratory (LA/P/0087/2020). BAS is recipient of FCT grant Doctorates 4 covid-19 2020.08066.BD and CVR is recipient of FCT Institutional CEEC. For the Instruct Access Proposal 20983, the ImPAct project has received funding from the European Union's Horizon 2020 research and innovation program under grant agreement No. 857203. *the European Synchrotron Radiation Facility (ESRF)* SOS Proposal MX2383

References

[1] Romão, C. V., Vicente, J., Borges, P., Frazão, C., Teixeira, M. The dual fucntion of flavodiiron proteins: oxygen and/or nitric oxide reductase, J Biol Inorg Chem, 2016, 21:39-52

[2] Folgosa, F., Martins M. C. and Teixeira M. The multidomain flavodiiron protein from *Clostridium difficile* 630 is an NADH: oxygen oxidoreductase, Scientific Reports, 2018, 8:10164

Keywords: Flavodiiron protein; redox centers; CryoEM structure

VISUALIZING THE PROTEIN CORONA FORMATION OF VIRUS-LIKE MESOPOROUS SILICA NANOPARTICLES FOR DRUG DELIVERY

Ieva Ragaisyte (United Kingdom)[1]; Alexandra Porter (United Kingdom)[1]; Alessandra Pinna (United Kingdom)[1,2,3]

1 - Imperial College London; 2 - Francis Crick Institute; 3 - University of Surrey

Abstract

Neurological conditions affect 1 in 6 people worldwide, and present great challenges in their treatment.[1] The issue of drug delivery to the brain is two-fold: first, the drugs much reach the brain through blood, and second, they must pass the blood-brain barrier (BBB). Poorly water-soluble drugs often require delivery agents to improve treatment efficacy. Mesoporous silica nanoparticles have been investigated as drug delivery agents for treatments of a wide array of diseases due to their tunable pore size and morphology, high loading capacity, and biocompatibility.[2] Virus-like particles offer an additional advantage to traditional spherical particles due their favourable interactions with the body, including longer circulation time in the blood and distinct mechanisms for entering the cells.[3]

Upon entering the body, the fate of nanoparticles is largely determined by the composition and thickness of the protein corona that forms almost immediately after the particles enter the bloodstream. In addition to coating the surface of the particles, the proteins may also cause agglomeration.[4] It is therefore important to study effect of the morphology and design of nanoparticles on the protein corona formation.

In this study, the protein corona formation of virus-like mesoporous silica nanoparticles with two different lengths of spikes was compared to spherical particles of comparable size. Bovine serum albumin (BSA) was used as model protein due to its' abundance in the blood (50% of serum protein) and similarity to human serum albumin. Fetal bovine serum (FBS) was also used to simulate a more complex biological environment. Uranyl acetate-stained particle-protein solutions were imaged using transmission electron microscopy (TEM) (**Figure 1**, A-C). Cryo-TEM was used to image the particle-protein solutions in near-native state. In addition to microscopy techniques, dynamic light scattering (DLS) and small-angle X-ray scattering (SAXS) were used to distinguish corona formation from particle agglomeration at different protein concentrations (**Figure 1**, D). It was shown that the presence as well as length of spikes on the particles have an influence on protein corona formation, which in turn affects the metabolic rate and distribution of these particles in the body.

References

1. The Neurological Alliance. *Neuro Numbers 2019*. 2019. Available from: https://www.neural.org.uk/assets/pdfs/neuro-numbers-2019.pdf

2. Manzano M, Vallet-Regí M. Mesoporous Silica Nanoparticles for Drug Delivery. *Advanced Functional Materials.* 2020; 30(2): 1902634. Available from: doi.org/10.1002/adfm.201902634.

3. Wang W, Wang P, Tang X, Elzatahry AA, Wang S, Al-Dahyan D, et al. Facile Synthesis of Uniform Virus-like Mesoporous Silica Nanoparticles for Enhanced Cellular Internalization. *ACS Central Science.* 2017; 3(8): 839-846. Available from: doi.org/10.1021/acscentsci.7b00257.
4. Galdino FE, Picco AS, Capeletti LB, Bettini J, Cardoso MB. Inside the Protein Corona: From Binding Parameters to Unstained Hard and Soft Coronas Visualization. *Nano Lett.* 2021; 21(19): 8250-8257. Available from: doi.org/10.1021/acs.nanolett.1c02416.

Keywords: mesoporous silica, nanoparticles, nanomedicine, drug delivery, protein corona

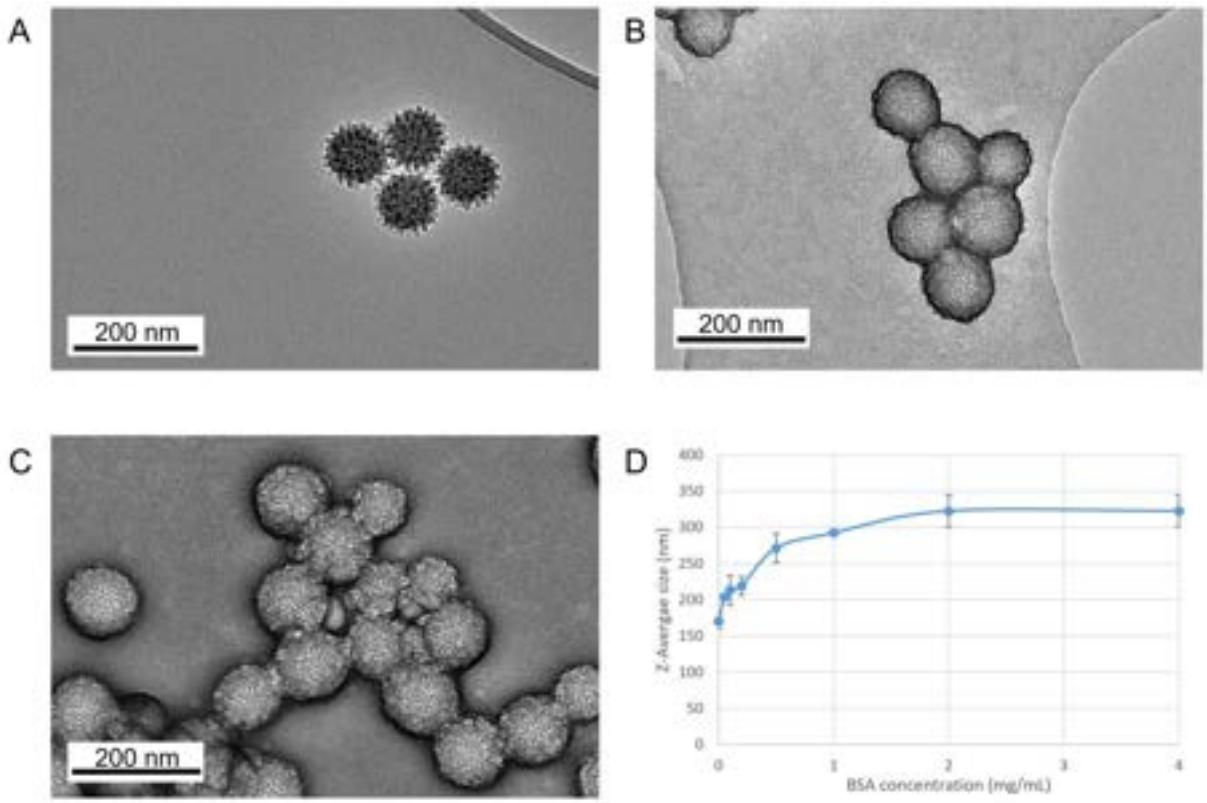

Figure 1. Transmission electron micrographs of virus-like mesoporous silica particles: A – naked particles, B – particles with BSA corona stained with uranyl acetate, C – particles with FBS stained with uranyl acetate; D – DLS data of Z-average size of particle-protein complexes at different BSA concentrations.

STRUCTURAL CHARACTERIZATION OF THE INFECTIOUS BURSAL DISEASE VIRUS RNA POLYMERASE BY CRYO-ELECTRON MICROSCOPY

José María Fernández-Palacios (Spain)[1]; José R. Castón (Spain)[1]; Javier M. Rodríguez (Spain)[1]

1 - Centro Nacional de Biotecnología, CSIC

Abstract

Infectious bursal disease virus (IBDV) is a non-enveloped dsRNA virus that causes Gumboro disease in chickens, which results in high mortality rates and imposes major economic losses to the poultry industry. Unlike other dsRNA viruses, IBDV is characterized by a single-shelled T = 13 capsid, and its genome is organized as ribonucleoprotein complexes (RNPs), in which the dsRNA is bound to VP3, the nucleocapsid protein, and VP1, the RNA polymerase. RNPs are the functional platform for RNA synthesis[1].

VP1 is a 100 kDa protein that initiates RNA synthesis through protein priming, covalently attaching itself to the 5' ends of the viral genome[2]. Together with VP3, it also participates in the initiation of viral protein translation through an unknown mechanism[3]. Using cryo-electron microscopy (cryo-EM) techniques, we aim to gain insights into the architecture and function of VP1, both *ex vivo* and *in situ* (in the context of the virion), to better understand its role in the viral replication process.

Recombinant his-tagged VP1 was expressed and purified from insect cells. After optimization of the vitrification conditions, a dataset of ~12 million particles was acquired using a Titan Krios microscope. Following iterative rounds of 2D and 3D classification, ~2 million particles were selected and we calculated the VP1 structure at 2.7 Å resolution. Residues spanning positions 21 to 797 were traced out of a total of 890. In comparison with the previous X-ray VP1 atomic structure, four alpha helices at the C-terminal region were absent in our structure. This missing region was nevertheless resolved at lower resolution after using the 3D variability analysis protocol (Cryosparc), including a set of 500k images (~4% of the particles). Our studies suggest that this region is highly flexible and could play a role in the regulation of the VP1 activity.

Finally, we have also purified intact IBDV virions and RNPs, and conducted pulldown experiments to purify the VP1-VP3 complex. Cryo-EM studies on these samples are currently in progress.

Acknowledgments

We thank the Cryo-EM CNB-CSIC facility (Madrid), for help with cryo-EM data acquisition. This work was supported by grants from the Spanish Ministry of Science and Innovation (PID2020-113287RB-I00) and the Comunidad Autónoma de Madrid (P2018/NMT-4389) to JRC.

References

1. Luque, D. *et al.* Infectious Bursal Disease Virus: Ribonucleoprotein Complexes of a Double-Stranded RNA Virus. *J Mol Biol* **386**, 891–901 (2009).
2. Pan, J., Vakharia, V. N. & Tao, Y. J. The structure of a birnavirus polymerase reveals a distinct active site topology. *Proc Natl Acad Sci U S A* **104**, 7385–7390 (2007).
3. Ye, C. *et al.* VP1 and VP3 Are Required and Sufficient for Translation Initiation of Uncapped Infectious Bursal Disease Virus Genomic Double-Stranded RNA. *J Virol* **92**, e01345-17 (2018)

Keywords: Cryo-EM, virus, polymerase, RNA

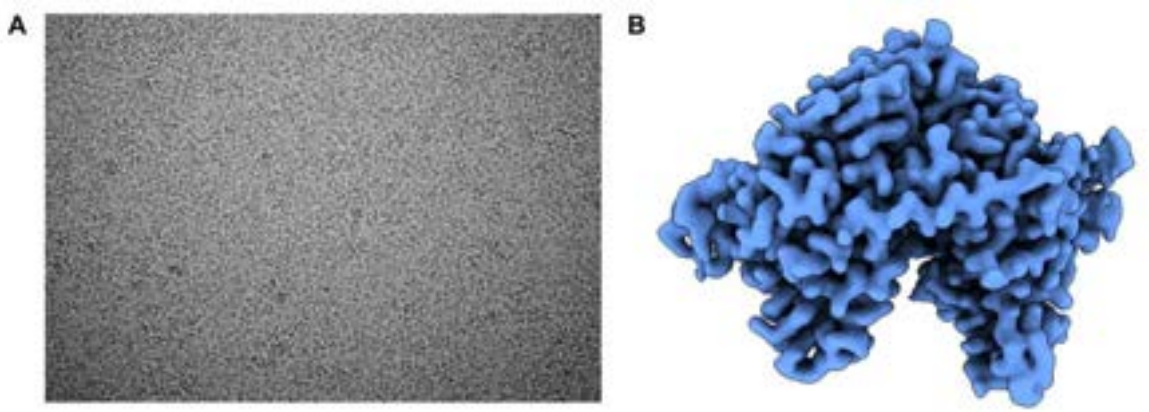

Figure 1. A: Representative micrograph taken at -2.2 µm defocus. **B:** VP1 model reconstructed at 2.7 Å resolution.

TRIGGERING LIGHT-REACTIONS AND CONFORMATIONAL CHANGES OF PHOTOSENSITIVE PROTEINS: IMPROVING OUR UNDERSTANDING OF PHOTOSYSTEM II MECHANISMS

André Graça (Sweden)[1]; Wolfgang Schröder (Sweden)[1]

1 - Umeå University;

Abstract

Biological water oxidation sustains life on Earth, it is the starting point of photosynthesis, and has become the blueprint for scalable artificial devices for solar-driven water splitting and oxygen production. In biological systems, this set of reactions is performed by the enzyme Photosystem II (PSII). Recent developments in cryo-EM are close to unlock the possibility to study this phenomenon, so far only feasible to study at x-ray free electron lasers (XFELs) 1-3. High-resolution structures with minimal radiation damage (zero-dose extrapolation) need to be obtained to understand the chemistry behind the biological water oxidation mechanism 4. Zero-dose extrapolation hight-resolution reconstructions were only recently demonstrated for a handful of protein complexes 5-6. Furthermore, the mechanism of water oxidation is a multi-step reaction driven by multiple flashes of light, therefore a discrete light intensity and a fine time resolution need to be achieved before it's possible to obtain the structure of intermediates of the biological water oxidation cycle. We propose the development of a new class of plunge freezing devices coupled with a programable light source for flash illumination of PSII and other photosensitive proteins with reactions whose lifetime are in the timescale of hundreds of milliseconds. We urge the manufacturers of plunge freezing devices to provide a communication port and open-source code in their instruments so that external devices can be easily coupled and synchronized. In theory, an automated flash illumination protocol, coordinated with the on grid plunge freezing procedure, occurring at constant 4 ºC, has the potential to turnover PSII and other protein systems, or activate caged compounds, for instance. Once these points can be addressed, we may get structural information of various intermediate states of metalloenzyme reactions, or protein conformation exchange dynamics, from diverse biological systems, that have been impossible to capture using x-ray diffraction methods.

References

1. X. Wei et al., Nature. 534, 69–74 (2016).
2. X. Su et al., Science (1979). 357, 815–820 (2017).
3. A. T. Graça, M. Hall, K. Persson, W. P. Schröder, Sci Rep. 11, 15534 (2021).
4. K. Kato et al., Communications Biology. 4, 1–11 (2021).
5. K. Naydenova et al., Science. 370,223-226 (2020).
6. Pu Qian et al., Sci. Adv. 8, 3139 (2022).

DEALING WITH A MULTI-PATHWAY ENZYMATIC REACTION BY CRYOEM

Jorge López-Alonso (Spain)[1]; Melisa Lazaro (Spain)[1]; David Gil-Cartón (Spain)[2]; Philip Choi (United States of America)[3]; Liang Tong (United States of America)[3]; Mikel Valle (Spain)[1]

1 - CIC bioGUNE, Basque Research & Technology Alliance (BRTA); 2 - Basque Resource for Electron Microscopy, Instituto Biofisika; 3 - Department of Biological Sciences, Columbia University, New York

Abstract

The number of structures of biomolecules determined by single particle cryo-electron microscopy (cryo-EM) is increasing exponentially in recent years. Cryo-EM maps also serve to identify multiple conformational states of complexes and their subunits. The question is how far cryoEM can go in deciphering the functional structures of oligomeric complexes involved in multi-pathway reactions. In this work we have explored by cryo-EM the functional space for such type of oligomers for the case of a biotin-dependent carboxylase, pyruvate carboxylase (PC).

Biotin-dependent carboxylases are metabolic enzymes that catalyze the transfer of carboxyl groups to different substrates. In order to complete the reaction, the biotin co-factor must access the biotin carboxylase (BC) domain where it becomes carboxylated using MgATP and bicarbonate. The carboxylated biotin is then translocated to the carboxyl transferase (CT) domain where the carboxyl group is transferred to the specific substrate. The biotin prosthetic group is attached to the biotin-carboxyl carrier protein (BCCP) domain that couples both reactions by traveling long distances between catalytic centers.

In this work, we have studied the structure of *Lactococcus lactis* PC (LlPC) during catalysis in the presence of positive allosteric regulator acetyl-CoA. Using cryo-EM and unsupervised classification techniques, we have determined conformations related to PC enzymatic activity. Our approach analyzes the structural landscape of PC tetramers during catalytic reactions with turnover of substrates and co-factors added in molar excess at the beginning of the sample preparation.

We have resolved several catalytic states of LlPC (at 2-3 Å resolution) and the motions that LlPC tetramers undergo during catalysis. By crossing these analyses, we conclude that the BCCP domain with the flexible linker can move between active sites driven by the affinity of carboxylated or non-carboxylated biotin and the readiness of the catalytic regions to accept it. The movement of the BCCP domain is not tightly coupled to the conformational changes of the tetramer, but the motions of the oligomer can facilitate its access to the active sites, and allosteric regulators modulate the landscape of these motions, that is, they narrow the conformational space which in turn conditions the functional space of the enzyme.

Acknowledgments

We acknowledge Diamond Light Source for cryoEM data collection under proposals EM-15997 and BI-22006. This study was supported by grants from the HFSP (RGP0062), and from the Spanish Ministerio de Ciencia e Innovación (PGC2018-098996-B-100) to MV, and grants from the NIGMS (R35GM118093) and the NIAID (R01AI116669) to LT.

References

Lopez-Alonso JP, Lazaro M, Gil-Carton D, Choi PH, Dodu A, Tong L, Valle M (2022) CryoEM structural exploration of catalytically active enzyme pyruvate carboxylase. Nat Commun 13, 7009 (2022). https://doi.org/10.1038/s41467-022-34543-8

Keywords: CryoEM, Enzyme, Multi-pathway

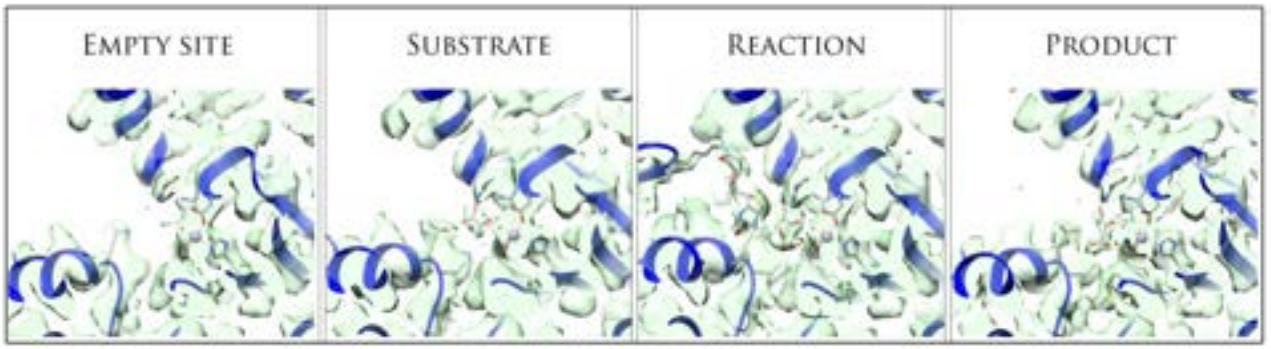

ARCHITECTURE OF THE ESCPE-1 MEMBRANE COAT

Aitor Hierro (Spain)[1]

1 - CIC bioGUNE

Abstract

Recycling of membrane proteins enables the reuse of receptors, ion channels and transporters. A key component of the recycling machinery is the endosomal sorting complex for promoting exit 1 (ESCPE-1), which rescues transmembrane proteins from the endolysosomal pathway for transport to the trans-Golgi network and the plasma membrane. This rescue entails the formation of recycling tubules through ESCPE-1 recruitment, cargo capture, coat assembly and membrane sculpting. Our results show that ESCPE-1 has a single-layer coat organization and suggests how synergistic interactions between ESCPE-1 protomers, phosphoinositides and cargo molecules result in a global arrangement of amphipathic helices to drive tubule formation. These findings define a key process of tubule-based endosomal sorting.

Acknowledgments

This work was funded by MCIN/AEI/10.13039/501100011033 (PID2020-119132GB-I00, CEX2021-001136-S). This study made use of the Diamond Light Source proposal MX20113, ALBA synchrotron beamline BL13-XALOC, the cryo-EM facilities at the UK Electron Bio-Imaging Centre, and the Midlands Regional Cryo-EM Facility at the Leicester Institute of Structural and Chemical Biology (LISCB).

References

Architecture of the ESCPE-1 membrane coat. Lopez-Robles C, Scaramuzza S, Astorga-Simon EN, Ishida M, Williamso CD, Baños-Mateos S, Gil-Carton D, Romero-Durana M, Vidaurrazaga A, Fernandez-Recio J, Rojas AL, Bonifacino JS, Castaño-Díez D, Hierro A. **Nat Struct Mol Biol.** (in press).

Keywords: Cryo-electron tomography; X-ray crystallography; Endosome; Membrane trafficking

HIGH RESOLUTION STRUCTURE OF RNA POLYMERASE III

Adrián Plaza (Spain)[1]; Sonia Huecas (Spain)[1]; Carlos Fernández Tornero (Spain)[1]

1 - Margarita Salas Center for Biological Research

Abstract

RNA polymerase III is one of the three types of RNA polymerases found in eukaryotic cells. It catalyzes the synthesis of RNA using a DNA template. Specifically, it transcribes transfer RNA, 5S ribosomal RNA, and several small nuclear RNAs. We formed a complex of *Saccharomyces cerevisiae* RNA polymerase III with a transcription DNA-RNA bubble and make cryo-EM grids.

We collected data in the Electron-event representation [1] format that records individual electron detection events instead of storing movies as a series of image frames, and used employed an upsampling factor of 2 in the single-particle image processing. After using multiple picking strategies as well as several rounds of both 2D and 3D classification we gathered a large set of very similar particles. Applying aberration correction protocols allowed us to push the resolution further. We obtained a map of the RNA polymerase III-DNA complex at an overall resolution of 1.9 Å. We achieved a very good angular distribution of particles, partially due to the addition of CHAPSO [2] detergent in the grid preparation stage.

There are only a dozen structures below 2 Å in the PDB for proteins lacking symmetry. This extraordinary resolution for this protein enables us to better define the amino acid residues, such as the holes in aromatic rings, and observe water molecules interacting with the protein. Furthermore, we are able to correctly model the catalytic magnesium octahedral coordination by one of the two available carboxylic acid moieties for each of the three conserved aspartic acid residues in the active site, the 3' end of the RNA, and two water molecules.

Acknowledgments

We are very grateful to the Electron Bio-Imaging Centre at Diamond Light Source for granting us access to the latest technological advancements in cryo-electron microscopy, such as the Selectris X imaging filter and the Falcon 4i electron detector, which allow improved contrast and enhanced image quality.

Acknowledgement to the microscopy facility of the Margarita Salas Center for Biological Research.

References

Guo H. et al. Electron-event representation data enable efficient cryoEM file storage with full preservation of spatial and temporal resolution. IUCrJ 7, 860–869 (2020)

Chen J, Noble AJ, Kang JY, Darst SA. Eliminating effects of particle adsorption to the air/water interface in single-particle cryo-electron microscopy: bacterial RNA polymerase and CHAPSO. J. Struct. Biol. X, 1:100005 (2019)

Keywords: CryoEM, structure. transcription, RNA polymerase

STRUCTURAL INSIGHTS INTO THE DIVERSITY OF PHOTOSYNTHETIC MEMBRANE PROTEINS BY CRYO-ELECTRON MICROSCOPY.

Dmitry Semchonok (Germany)[1,2,3]

1 - Martin-Luther-Universität Halle-Wittenberg; 2 - University of Tennessee, Knoxville; 3 - ITQB NOVA, Lisbon

Abstract

The recent resolution revolution in cryo-electron microscopy (cryo-EM) opens new perspectives in studying a wide range of protein complexes. Nowadays cryo-EM technique is able to provide structural information to reveal and explore the complex functional processes underlying nature.

Photosynthesis is a global process, including harvesting and converting light into chemical energy. Photosynthetic pigment-protein complexes drive the first steps of photosynthesis. They consist of antenna subunits and reaction centres, with the former responsible for light absorption and transport and the latter for light-induced charge separation and subsequent energy (electron) transfer. In my study, I present cryo-EM structures of various photosynthetic organisms from across the phylogenetic tree of life, highlighting the extreme architectural diversity of endogenous photosynthetic complexes. The resolution achieved allows us to decipher stoichiometries, subunit proximity, interfaces, and the localization of reaction centres and antennae.

Our work reveals the structural basis of a distinct adaptation strategy to different environmental conditions, reflected in the composition and reorganisation of key photosynthetic membrane proteins. This study demonstrates the logic behind the adaptability and efficient energy transfer mechanisms in ecosystems created by nature.

Acknowledgments

The work mentioned in the presentation was done in close collaboration with Dr Colette Jungas, Dr Marina Siponen, Dr Roman Kouril, Dr Monika Opatíková, Dr David Kopečný, Dr Panagiotis Kastritis, Dr Albert Guskov, Dr Barry D Bruce

References

1. Croce, Roberta, Rienk van Grondelle, Herbert van Amerongen, and Ivo van Stokkum, eds. “Organization of Photosynthetic Membrane Proteins into Supercomplexes.” In *Light Harvesting in Photosynthesis*, 1st ed., 207–17. Boca Raton : Taylor & Francis/CRC Press, 2017. | Series: Foundations of biochemistry and biophysics: CRC Press, 2018. https://doi.org/10.1201/9781351242899-10.

2. Gardiner, Alastair T., Tu C. Nguyen-Phan, and Richard J. Cogdell. “A Comparative Look at Structural Variation among RC–LH1 ‘Core’ Complexes Present in Anoxygenic Phototrophic Bacteria.”

Photosynthesis Research 145, no. 2 (August 2020): 83–96. https://doi.org/10.1007/s11120-020-00758-3.

3. Kouřil, Roman, Lukáš Nosek, Monika Opatíková, Rameez Arshad, Dmitry A. Semchonok, Ivo Chamrád, René Lenobel, Egbert J. Boekema, and Petr Ilík. "Unique Organization of Photosystem II Supercomplexes and Megacomplexes in Norway Spruce." *The Plant Journal* 104, no. 1 (September 2020): 215–25. https://doi.org/10.1111/tpj.14918.

4. Kühlbrandt, Werner. "The Resolution Revolution." *Science* 343, no. 6178 (March 28, 2014): 1443–44. https://doi.org/10.1126/science.1251652.

5. Semchonok, Dmitry A., Jyotirmoy Mondal, Connor J. Cooper, Katrina Schlum, Meng Li, Muhamed Amin, Carlos O.S. Sorzano, et al. "Cryo-EM Structure of a Tetrameric Photosystem I from Chroococcidiopsis TS-821, a Thermophilic, Unicellular, Non-Heterocyst-Forming Cyanobacterium." *Plant Communications* 3, no. 1 (January 2022): 100248. https://doi.org/10.1016/j.xplc.2021.100248.

6. Semchonok, Dmitry A., Marina I. Siponen, Christian Tüting, Quentin Charras, Fotis L. Kyrilis, Farzad Hamdi, Yashar Sadian, Colette Jungas, and Panagiotis L. Kastritis. "Cryo-EM Structure of the *Rhodobaca Bogoriensis* RC-LH1-PufX Dimeric Complex at 2.9 Å." Preprint. Biophysics, February 26, 2022. https://doi.org/10.1101/2022.02.25.481955.

Keywords: Photosynthesis, Photosystems, membrane proteins, cryo-electron microscopy

CRYOEM PLATFORM AT CIC BIOGUNE

Adriana Rojas Cardona (Spain)[1]; Isaac Santos (Spain)[1]; Idoia Iturriuoz (Spain)[1]; Diego Charro (Spain)[1]

1 - CIC bioGUNE

Abstract

The resolution revolution in cryoEM has expanded the number of researchers interested in this technique. However, for many scientists, the difficulties in sample preparation and/or sample screening remain a bottleneck for integrating this technique into their research questions. In CIC bioGUNE, we offer a service that focuses on these two aspects in an individualized approach than combines vitrification and screening in our JEOL2200. Using serialEM we can automatically collect up to 150 images/hour that are processed on-the-fly with cryosparc, providing a 2D classification to evaluate the grid's quality. Once the samples are in optimal conditions for high-end data acquisition, grids are clipped in house and delivered to the appropriate facility for remote data collection. We also offer quality control of different nanocarriers, and exosomes based on various parameters like sample integrity and/or size distribution.

Our service also includes quality control of AAVs used in Gene Therapy, for which we perform an analysis of ratios of empty versus filled viruses estimated by 2D and 3D classification. Statistical analysis is performed aiming at a minimum of 10000 particles per sample.

Keywords: CryoEM, CryoTEM, sample preparation, nano carries, exosomes, AAVs

MEMBRANE REMODELLING ON LIPID NANOTUBES OBSERVED BY CRYO ELECTRON MICROSCOPY

Isaac Santos Pérez (Spain)[1]; Anna Shnyrova (Spain)[2]; Isaac Pérez Jover (Spain)[2]

1 - Center for Cooperative Research in Biosciences (CIC bioGUNE); 2 - Biofisika Institute

Abstract

Lipid nanotubes (NTs) are extensively used as an in vitro system to study membrane remodeling by proteins using fluorescence microscopy. Two general type of NTs may be distinguished in these experiments: a) NTs performed by applying a reservoir membrane. In this case, the protein of interest is added to the NT a posteriori allowing to assess its sensing of membrane curvature. b) NTs formed by spontaneous tubulation of the flat reservoir by the protein. Here, the propensity of the protein of interest to induce membrane curvature can be measured. Importantly, both actions are not necessarily related. Interestingly, while membrane tubulation can be easily translated to cryo-EM, there is no equivalent method to create preformed NTs for cryo-EM. Here, we present a new microfluidics-based method enabling the rapid formation of a high number of free-standing lipid NTs of controlled geometry on the microscopy grid. To assay the performance of this new protocol, we observed how Dyn2 remodel NTs. Our results show several examples of membrane constriction and tethering events on the generated NTs, pointing towards the existence of non-canonical functions of Dyn2. Therefore, this method can be used to adapt the formation of such a widespread tool as lipid NTs for cryo-EM observations.

References

1- Electron Microscopy and Crystallography, Center for Cooperative Research in Biosciences (CIC bioGUNE), Bizkaia Science and Technology Park Bld 800, 48160-Derio, Bizkaia, Spain.

2- Biofisika Institute (CSIC, UPV/EHU) and Department of Biochemistry and Molecular Biology, University of the Basque Country, Leioa, Spain.

Keywords: dynamin, nanotubes, microfluidics, cryo-EM

SCNODES – A TOOLKIT FOR CORRELATED SUPER-RESOLUTION FLUORESCENCE & CRYO-ELECTRON MICROSCOPY

Mart G. F. Last (Netherlands)[1]; Lenard M. Voortman (Netherlands)[1]; Thomas H. Sharp (Netherlands)[1]

1 - Leiden University Medical Centre

Abstract

By combining cryo-super-resolution light imaging and cryo electron tomography, highly specific labelling and high resolution are integrated into a single in situ imaging technique. Correlating these modalities provides numerous benefits for in situ structural biology, including identifiying rare proteins and complexes or transient events, accurately targeted tomogram acquisition, and identification of biomolecules found within tomograms. The development of this correlated light and electron microscopy technique, called 'SR-cryoCLEM', requires improvements in software, hardware, cryocompatible photoswitchable fluorescent proteins, and sample preparation. Our lab is addressing all of these areas, and in this talk I will focus on our recent developments in a complete correlative microscopy processing toolkit called scNodes, which integrates super-resolution fluorescence data processing, correlation of light and electron microscopy datasets, tomogram segmentation, and particle picking, all into one freely available toolkit.

Keywords: cryoET, tomography, single molecule localization, super-resolution, CLEM, cryoCLEM

ADVANCES IN THE STUDY OF EXTRACELLULAR VESICLES SECRETED BY LEGIONELLA PNEUMOPHILA USING CRYO ELECTRON MICROSCOPY

Olena Mayboroda (France)[1]; Tobias Sahr (France)[1]; Carmen Buchrieser (France)[1]

1 - Institut Pasteur, Université Paris Cité, CNRS UMR 6047, Biologie des Bactéries Intracellulaires, Département de Microbiologie, F-75015 Paris, France

Abstract

Extracellular vesicles (EVs) are defined as membrane-enclosed structures released during the lifespan of most cells in all domains of life on earth, including eukaryotes, bacteria, and archaea [1,2]. This process is conserved throughout evolution from bacteria to humans and plants. Most of the EVs are described as spherical structures, however they can adopt a more tubular shape, probably deriving from so-called nanotubes. They are involved in component exchange between cells and organisms, like proteins, mRNAs, miRNAs, lipids, and metabolites, and as signaling vesicles in normal homeostatic or in pathological processes [3–5].

Recently we have shown that the bacterial pathogen *Legionella pneumophila*, subverts host cell signaling pathways via EVs (Lp-EVs) [6,7] and that it releases EVs *in vitro* and *in cellulo* during infection of the human U2OS cell line, human THP-1 monocytic cells, and human monocyte-derived macrophages (hMDMs). These *Lp*-EVs contain bacterial RNAs that are transported into the host cell where they downregulate IRAK1 and RIG-I, most likely by mimicking eukaryotic miRNAs [8].

The main goal of our project is to get a better understanding of the *Lp*-EVs structure and the mechanism of RNA loading and release that is important for host-pathogen communication and trans-kingdom signaling. Some of *Lp*-EV features, like size, morphology, concentration, origin, and molecular composition, can be characterized using Cryo Electron Microscopy (Cryo EM). Here we used Cryo-EM and 3D tomographic data collection for spatial visualization and show first results obtained in imaging and reconstruction of single *Lp*-EVs.

Another important part of our research line is the study of *Lp*-EV release inside the host cell. Combining Cryo CLEM, Cryo FIB and Cryo Tomography techniques we aim to get a better understanding of the cells infected with *L. pneumophila* and study the pathway of EV formation and role during infection *in cellulo*.

Acknowledgments

Work is financed by the grant n° ANR 20 CE15 0021 01 BIOEV

References

1. van Niel, G., D'Angelo, G. & Raposo, G. Shedding light on the cell biology of extracellular vesicles. *Nat. Rev. Mol. Cell Biol.* **19**, 213–228 (2018).

2. Kim, J. H., Lee, J., Park, J. & Gho, Y. S. Gram-negative and Gram-positive bacterial extracellular vesicles. *Semin. Cell Dev. Biol.* **40**, 97–104 (2015).

3. Lee, H.-J. Microbe-Host Communication by Small RNAs in Extracellular Vesicles: Vehicles for Transkingdom RNA Transportation. *Int. J. Mol. Sci.* **20**, E1487 (2019).

4. Lécrivain, A.-L. & Beckmann, B. M. Bacterial RNA in extracellular vesicles: A new regulator of host-pathogen interactions? *Biochim. Biophys. Acta BBA - Gene Regul. Mech.* **1863**, 194519 (2020).

5. Kulp, A. & Kuehn, M. J. Biological Functions and Biogenesis of Secreted Bacterial Outer Membrane Vesicles. *Annu. Rev. Microbiol.* **64**, 163–184 (2010).

6. Mondino, S. *et al.* Legionnaires' Disease: State of the Art Knowledge of Pathogenesis Mechanisms of *Legionella*. *Annu. Rev. Pathol. Mech. Dis.* **15**, 439–466 (2020).

7. *Legionella: Methods and Protocols*. vol. 954 (Humana Press, 2013).

8. Sahr, T. *et al.* Translocated Legionella pneumophila small RNAs mimic eukaryotic microRNAs targeting the host immune response. *Nat. Commun.* **13**, 762 (2022).

Keywords: Legionella pneumophila, Extracellular vesicles, Cryo CLEM, Cryo FIB, Cryo ET, in cellulo imaging

UNCOVERING THE MOLECULAR ARCHITECTURE OF THE SKIN WITH CRYO-ELECTRON TOMOGRAPHY

Florian Schur (Austria)[1]; Francisco Figueiredo (Austria)[1]; Bettina Zens (Austria)[1]; Ingrid De Vries (Austria)[1]

1 - Institute of Science and Technology Austria (ISTA), Klosterneuburg, Austria

Abstract

The skin is the largest organ of the human body. It has a variety of functions, including protection (against physical and chemical influences, or pathogens), thermoregulation, sensory functions and endocrine and exocrine processes such as vitamin D synthesis (Menon, 2002; Yousef et al., 2023). Skin is organized in three different layers, the epidermis, dermis and hypodermis, all three of which have a different anatomy and function (Yousef et al., 2023). The epidermis itself is also composed of several layers divided from the inside to the outside into the stratum basale, stratum spinosum, stratum granulosum, stratum lucidum and finally the stratum corneum. These layers illustrate the various stages of keratinocyte differentiation (Eckhart et al., 2013), which is the process by which the basal layer proliferates and produces new cells that will differentiate towards the skin's surface (Eckhart et al., 2013).

The majority of studies on skin architecture/morphology found in literature used mainly histology and conventional electron microscopy methods. These methods compromise structure details, due to the use of chemical fixatives and metal contrasting agents, among other compounds (Koster et al., 1997; Marko et al., 2007). As a result of the processing methods, these approaches do not preserve the native state of the tissue.

In this project we use cryo-focused ion beam scanning electron microscopy (FIB-SEM) lift-out milling and cryo-electron tomography of natively preserved skin tissue to obtain insights into the ultrastructural organization of the epidermis. Our initial results reveal new insights into the architecture of the outermost skin layers, specifically their cytoskeletal organization and lipid layer organization to provide strength and separation between different cell layers, respectively.

References

Eckhart, L., Lippens, S., Tschachler, E., Declercq, W., 2013. Cell death by cornification. Biochim. Biophys. Acta BBA - Mol. Cell Res. 1833, 3471–3480. https://doi.org/10.1016/j.bbamcr.2013.06.010

Koster, A.J., Grimm, R., Typke, D., Hegerl, R., Stoschek, A., Walz, J., Baumeister, W., 1997. Perspectives of Molecular and Cellular Electron Tomography. J. Struct. Biol. 120, 276–308. https://doi.org/10.1006/jsbi.1997.3933

Marko, M., Hsieh, C., Schalek, R., Frank, J., Mannella, C., 2007. Focused-ion-beam thinning of frozen-hydrated biological specimens for cryo-electron microscopy. Nat. Methods 4, 215–217. https://doi.org/10.1038/nmeth1014

Menon, G.K., 2002. New insights into skin structure: scratching the surface. Adv. Drug Deliv. Rev., Human skin: the Medium of Touch 54, S3–S17. https://doi.org/10.1016/S0169-409X(02)00121-7

Yousef, H., Alhajj, M., Sharma, S., 2023. Anatomy, Skin (Integument), Epidermis, in: StatPearls. StatPearls Publishing, Treasure Island (FL).

POSTERS - CRYO-EM

THE EFFECT OF HIGH LIGHT ON PHOTOSYSTEM II STRUCTURE

André T. Graça[1], Jack A. Forsman[1], Wolfgang P. Schröder[1]

1 - Kemiskt Biologiskt Centrum, Umeå Universitet, Sweden

Abstract

High light is known to be very damaging to Photosystem II.[1] As a result photosynthetic organisms have developed photoprotective mechanisms to prevent PS II from damaging itself during high light conditions such as cyclic electron transfer[2], non-photochemical quenching[3] and bicarbonate dissociation[4]. In many cases, these photoprotective mechanisms have been characterized biochemically, by observing changes in PS II activity. However, structural studies observing the ways in which the PS II structure adapts to high light conditions are lacking. Here we compare PS II structures from *Arabidopsis thaliana* in dark adapted state and following 30 seconds exposure of high light (2000 µE). The structures for the dark-adapted state (2.95 Å resolution) and high light state (3.03 Å resolution) were calculated from cryo-electron micrographs of solubilized Photosystem II isolated from *Arabidopsis* BBY membranes using sucrose gradients. Interestingly, there does not appear to be many obvious changes in the PS II structure before or after the high light treatment. In particular the bicarbonate bound to the non-heme iron is predicted to dissociate in high light, however, our structure shows an unambiguous density at the position of the bicarbonate. The similarity of the dark-adapted and high-light structures suggest that the implementation of photoprotective mechanisms may require additional accessory proteins which are not present in isolated PS II samples. In addition to being the first Photosystem II high light structure, the control Photosystem II structure represents the first fully intact (including extrinsic proteins) cryo-EM structure of Photosystem II from the model organism *Arabidopsis thaliana*.

References

1. P. Pospisil. *Front. Plant. Sci.*, 2016, *7*, 1950.
2. G. Ananyev, C. Gates, A. Kaplan *et al. BBA-bioenergetics.*, 2017, *1858*, 873-883.
3. G. Lambrev, Y. Miloslavina, P. Jahns *et al. BBA-bioenergetics.*, 2012, *1817*, 760-769.
4. K. Brinkert, S. De Causmaecker, A. Krieger-Liszkay *et al. PNAS.*, 2016, *113*, 12144-12149.

MICRO ELECTRON DIFFRACTION AT THE CNB-CSIC CRYOEM FACILITY: WORKFLOW AUTOMATIZATION

Javier Collado (Spain)[1]; César Santiago (Spain)[1]; José María Valpuesta (Spain)[1]; Rocío Arranz (Spain)[1]

1 - Macromolecular Structures Department, National Center for Biotechnology. CNB-CSIC. Madrid, Spain

Abstract

Micro-electron diffraction[1] is an electron microscopy technique used to determine the atomic structure of crystallized molecules. It has revolutionized both structural biology and chemistry by enabling the analysis of macromolecules and small molecule compounds, particularly when X-ray diffraction experiments are impractical due to the small crystal size.

Since the technique has been implemented in our facility, we have provided numerous services to different users, demonstrating the robustness of our workflow for resolving small molecule and macromolecule structures. Currently, our focus is on automating sample collection and processing. The SerialEM software has significantly automated the crystal collection process by utilizing scripts, exponentially increasing the number of crystals collected per session.

To optimize data processing, we are actively incorporating the AutoMicroED[2] workflow. This integration will not only yield significant time savings in data processing but also in data collection. With AutoMicroED, we can determine in real-time whether we have collected enough data for structure resolution, allowing us to proceed efficiently to the next sample.

In conclusion, our ongoing integration of the AutoMicroED workflow holds great potential for substantial time savings in both data processing and collection. This advancement will enhance overall productivity and workflow efficiency, further establishing micro-electron diffraction as a powerful technique for atomic structure determination.

References

1) Nannenga, B., Shi, D., Leslie, A. et al. High-resolution structure determination by continuous-rotation data collection in MicroED. Nat Methods 11, 927–930 (2014). https://doi.org/10.1038/nmeth.3043

2) Samantha M. Powell, Irina V. Novikova, Doo Nam Kim, James E. Evans bioRxiv 2021.12.13.472146; doi: https://doi.org/10.1101/2021.12.13.472146

Keywords: MicroED, CryoEM, Diffraction

EXPRESSION AND PURIFICATION OF RECOMBINANT HUMAN CHAPERONIN CONTAINING TCP-1 (CCT) FOR STRUCTURAL STUDIES.

Carmen Majano López De Madrid (Spain)[1]; Jorge Cuellar (Spain)[1]; Javier María Rodriguez Martinez (Spain)[1]; Sergio Pipaon (Spain)[1]; Jose María Valpuesta (Spain)[1]

1 - Centro Nacional de Biotecnología (Spain, CSIC)

Abstract

The eukaryotic chaperonin CCT (chaperonin-containing TCP-1) is a key player in cellular homeostasis since it assists the folding of 10% of cytosolic proteins and its malfunction is linked to cancer and neurodegenerative diseases. CCT is the most complex of all chaperonins with each of its two rings composed of eight paralogous subunits. Unraveling the mechanism of action and forces taking place upon its action depends on the heterologous overproduction of this protein, which is a considerable technical challenge due to its intricate multimeric nature.[1]

To understand how this chaperonin can interact with and fold such variety of substrates and cofactors, we can combine cryo-electron microscopy (cryoEM) with single molecule techniques, such as optical tweezers and single-molecule. This will undoubtedly contribute to understand how CCT works and how to deal with malfunctions that can lead to cell dysregulation.

With this aim, we have optimized the heterologous production and purification of human CCT by introducing specific recombinant tags. The eight different CCT subunits have been cloned and expressed using the Multibac modification of the Bac-to-Bac baculoviral expression system, in which insect cells are infected with recombinant baculoviruses expressing all the subunits[2]. Different baculoviruses have been constructed with the subunits containing purification tags (His tag in subunit 1, CBP-Strep-his tag in subunit 3) as well as other tags for single molecule experiments in the equatorial regions of subunits 1 and 7. These tags are Ppant sequences for AcpS and Sfp enzimes[3], and DogTag and SpyTag for their corresponding catchers.[4]

We succeeded at purifying the human CCT, and using mass spectrometry we identified all subunits with a good q-value (<0,01). The sample was vitrified on grids and images were recorded with a Titan Krios electron microscope. The final 3D reconstruction reached 4.0 Å resolution after postprocessing. The reconstruction shows human CCT in an open conformation very similar to that described by Cuéllar et al 2019. The docking of this structure (PDB 6QB8) into our final map is almost perfect in the equatorial domains and very good in the intermediate and the apical domains, which allowed us to unambiguously assign the different subunits of the chaperonin. Although the overall resolution is around 4.0 Å, the resolution was not isotropic along the map with equatorial domains yielding higher resolution than the flexible apical domain.

Acknowledgments

This research was supported by the grant PID2019-105872GB-I00/AEI/10.13039/ 501100011033 from the Spanish Ministry of Science and Innovation (JMV)

References

1.- Bueno-Carrasco, M. T., & Cuéllar, J. (2018). Mechanism and Function of the Eukaryotic Chaperonin CCT. eLS, 1–9. https://doi.org/10.1002/9780470015902.a0028208

2.- Noad, R. J., Stewart, M., Boyce, M., Celma, C. C., Willison, K. R., & Roy, P. (2009). Multigene expression of protein complexes by iterative modification of genomic Bacmid DNA. *BMC Molecular Biology*, *10*(1), 87. https://doi.org/10.1186/1471-2199-10-87

3.- Zhou Z, Cironi P, Lin AJ, Xu Y, Hrvatin S, Golan DE, Silver PA, Walsh CT, Yin J. Genetically encoded short peptide tags for orthogonal protein labeling by Sfp and AcpS phosphopantetheinyl transferases. *ACS Chem Biol*. 2007 May 22;2(5):337-46. https://doi.org/10.1021/cb700054k.

4.- Keeble, A. H., Yadav, V. K., Ferla, M. P., Bauer, C. C., Chuntharpursat-Bon, E., Huang, J., Bon, R. S., & Howarth, M. (2022). DogCatcher allows loop-friendly protein-protein ligation. Cell chemical biology, 29(2), 339–350.e10. https://doi.org/10.1016/j.chembiol.2021.07.005

Keywords: Molecular chaperones, human CCT, Chaperonin, Baculovirus expression system, recombinant protein, tagging strategies, Cryo-EM

BIOCHEMICAL AND STRUCTURAL CHARACTERIZATION OF HSP60 CHAPERONES OBTAINED THROUGH ANCESTRAL SEQUENCE RECONSTRUCTION

Rita Severino (Spain)[1]; Jorge Cuéllar (Spain)[2]; Moisés Maestro-López (Spain)[2]; Victor Parro (Spain)[1]; José María Valpuesta (Spain)[2]

1 - Centro de Astrobiología (CAB, INTA-CSIC); 2 - National Center for Biotechnology (CNB-CSIC)

Abstract

Ancestral sequence reconstruction (ASR) allows the reconstruction of ancestral protein sequences extending back to 4 Ga (*1*). Their expression and study is used for the characterization of paleoenvironments (*2*), as scaffolds for protein engineering (*3*) and, in our case, as proxies for biomarker discovery in astrobiology (*4*), as they are regularly detected in environments of astrobiological interest (*4*, *5*).

HSP60 chaperones (or chaperonins) are the most ancient members of the molecular chaperone family; they are ubiquitous proteins with origins dating back to the last universal common ancestor (*6*). They are classified into three evolutionary classes: Group I (GroEL, found in bacteria and eukaryotic organelles), Group II (thermosome, found in archaea and eukaryotic cytoplasm), and Group III (thermosome-like, found in bacteria) (*6*). They are multi-subunit assemblies (14 or more subunits) organized in two rings that facilitate protein folding in basal conditions and promote protein refolding during stress (*7*).

In this work, we obtained the ancestral sequences for the three HSP60 groups. We cloned and purified several of the ancestral chaperonins. Despite having up to 40% sequence divergence from modern sequences, these proteins assembled into multimeric structures, similarly to existing models. ATPase activity and protein client assays were used to characterize their functional properties. To gain further insight into the characterization of the ancestral chaperonins, the purified oligomers were structurally characterized using cryoelectron microscopy (cryoEM). The maps obtained, when compared to published structures of modern chaperonins, allow us to gain insight into the structural as well as the properties and probable biochemical differences, of modern and ancestral proteins.

Acknowledgments

This research was supported by the grant PID2019-105872GB-I00/AEI/10.13039/ 501100011033 (JMV) and by grants PID2021-126746NB-I00 and RTI2018-094368-B-I00 (VP) from the Spanish Ministry of Science and Innovation. R.S. is funded by a Ph.D. fellowship from INTA and by the fellowship “Ford-Apadriña la Ciencia”.

References

[1] R. Merkl, R. Sterner (2016), *Biol. Chem.* 397, 1–21. [2] A. K. Garcia, B. Kaçar (2019), *Free Radic. Biol. Med.* 140, 260–269. [3] V. A. Risso, J. M. Sanchez-Ruiz (2017) in *Directed Enzyme Evolution: Advances and Applications,* 229–255. [4] R. Severino et al. (2023), *Anal. Chem.* 95, 5323–5330. [5] M. Á. Fernández-Martínez et al. (2019) *Front. Microbiol.* 10:1641. [6] M. E. Rebeaud et al. (2021) *Proc. Natl. Acad. Sci. U. S. A.* 118 (21). [7] M. G. Bigotti et al. (2005) *Top. Curr. Genet.* 16, 251–283.

Keywords: Astrobiology, Ancestral Sequence Reconstruction, HSP60 chaperones, Cryo-EM

BIOCHEMICAL AND STRUCTURAL CHARACTERIZATION OF A NUCLEOTIDE DEPENDENT TRANSPOSON

Lidia Araujo-Bazan (Spain)[1]; Mercedes Spínola-Amilibia (Spain)[1]; Álvaro De La Gándara (Spain)[1]; James M. Berger (United States of America)[2]; Ernesto Arias-Palomo (Spain)[1]

1 - Centro de Investigaciones Biológicas Margarita Salas CIB-CSIC; 2 - Johns Hopkins University School of Medicine

Abstract

Transposon are discrete segments of DNA that can move between genomic locations. DNA transposons vary in size but all of them encode at least one enzyme called transposase which recognizes the transposon ends and catalyzes DNA cleavage and joining reaction required for their movement. Some transposons additionally encode accessory proteins that regulate the transposition reaction and may carry genetic cargos such as antibiotic resistance genes. The IS*21* family of transposons is found in most bacterial phyla, including numerous clinical and multidrug-resistant strains. It consists of a single operon with two terminal inverted repeats and two open reading frames: the transposase, IstA; and a regulatory factor member of the AAA+ family of ATPases, IstB. We have used biochemical and structural approaches to provide insights into IS21 transposition.

Our biochemical data reveal that IstA requires the presence of two complete direct repeats to perform the integration reaction and it does not show a strong preference for either of the transposon ends (left or right). The cryo-EM structure shows that IstA self-assembles into a tetramer that engages two transposon DNA ends around a local two-fold symmetry axis. The DDE motifs of the catalytic monomers are proximal to the signature 3' CA dinucleotide at the end of the donor DNAs, correctly positioned to perform a transposition reaction. Mutation of amino acids implicated in the stablilization of the transposon end and catalysis result in an almost complete abrogation of the integration activity. Additionally, mutants of residues of IstA implicated in the specific recognition of the donor DNA have also a significant effect on integration activity.

Our in vitro data also show that IstA stimulates IstB ATPase acivity and that this regulatory factor is essential to promote efficient strand transfer. A cryo-EM structure shows that IstB forms a clamshell-shaped pentamer of dimers through ATP-dependent AAA+ interactions. The relevance of these contacts is supported by the reduced levels of activity shown by a panel of ATP deficient mutants. In addition, the presence of non-hydrolyzable analogs has pronounced effect on DNA integration further highlighting the critical role of the nucleotide in IS21 transposition.

Acknowledgments

This work was supported by grant GM071747 (to J.M.B.), grants PID2020-120275GB-I00 and BFU2017-89143-P funded by MCIN/AEI/10.13039/501100011033 and by "ERDF A way of making Europe" (to E.A.-P.), and grant PRE2018-086026 funded by MCIN/AEI/10.13039/501100011033 and by "ESF Investing in your future" (to E.A.-P. and A.G.).

References

- IS21 family transposase cleaved donor complex traps two right-handed superhelical crossings. Nature Commun. 2023 Apr 22;14(1):2335. DOI: 10.1038/s41467-023-38071-x.

- An atypical AAA+ ATPase assembly controls efficient transposition through DNA remodeling and transposase recruitment. Cell. 2015 Aug 13; 162(4): 860–871. DOI: 10.1016/j.cell.2015.07.037.

- Moving DNA around: DNA transposition and retroviral integration. Curr. Opin. Struct. Biol. 2011 Jun;21(3):370-8. DOI: 10.1016/j.sbi.2011.03.004.

Keywords: Transposon, Cryo-EM

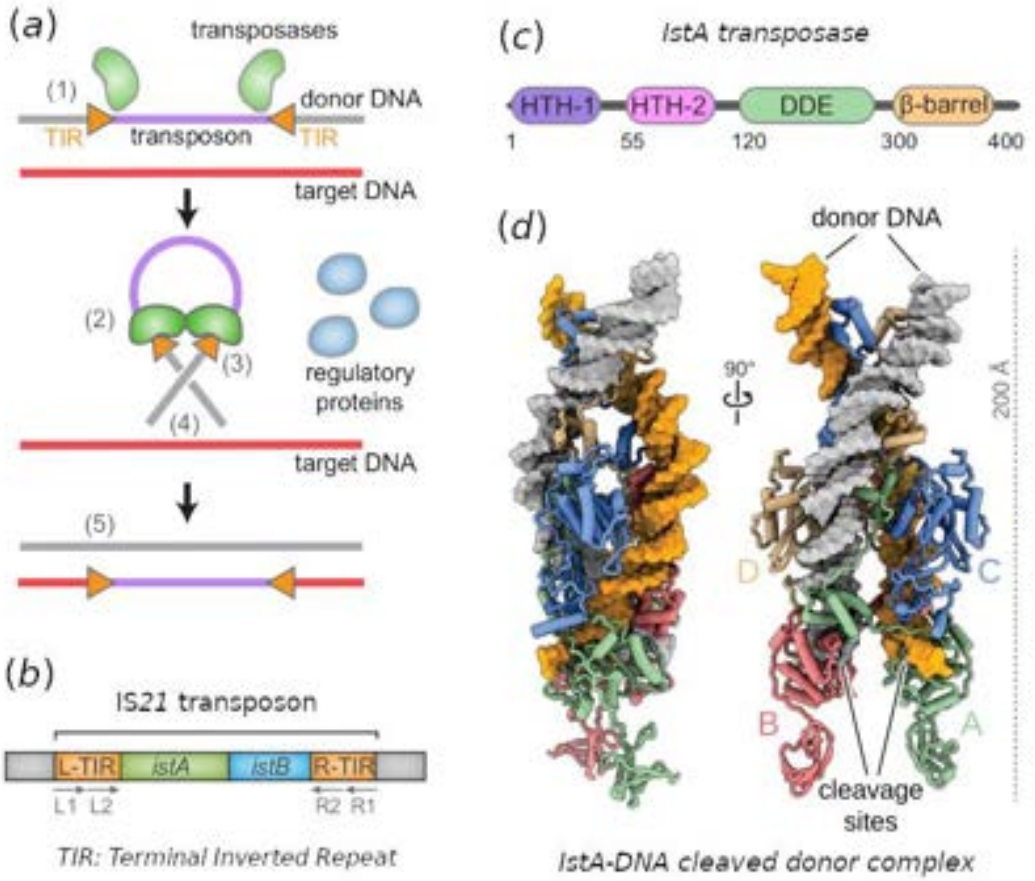

STRUCTURAL INSIGHTS ON THE ARABIDOPSIS THALIANA R2T COMPLEX

Andrés López-Perrote (Spain)[1]; Alberto Palacios-Abella (Spain)[2]; Jasminka Boskovic (Spain)[1]; Johanne Lecoq (Spain)[1]; David Alabadí (Spain)[2]; Oscar Llorca (Spain)[1]

1 - Spanish National Cancer Research Center (CNIO); 2 - Instituto de Biología Molecular y Celular de Plantas

Abstract

The R2TP (Rvb1-Rvb2-Tah1-Pih1) complex is a specialized HSP90 co-chaperone that provides specificity for a subset of clients, including mTOR and ATM kinases, RNA polymerase II or box C/D small nucleolar ribonucleoproteins (snoRNP), among others (1). In addition, adaptor subunits such as the TELO2–TTI1–TTI2 (TTT) complex or the URI1 Prefoldin-like complex assist R2TP during the assembly and maturation of certain clients (2). R2TP, as the core of this co-chaperone machinery, is essential and evolutionarily conserved across species from yeast to metazoan. Recent findings suggest the coexistence of non-canonical R2TP complexes, containing the Rvb1/Rvb2 (RUVBL1/RUVBL2 in mammals) subunits and either Tah1 (RPAP3) or Pih1 (PIH1D1), assembling the so-called R2T and R2P complexes, respectively (3). Similar to higher eukaryotes, plant R2TP is essential for protein homeostasis. Interestingly, vascular plants such as *Arabidopsis thaliana* do not have a PIH1D1 homologous gene, and the RPAP3 subunit is a simpler version of the human protein. Thus, a reduced version of the complex containing only RUVBL1-RUVBL2 and RPAP3 (R2T) is found in this model organism. Here we analyze the architecture of the *Arabidopsis thaliana* R2T (AtR2T) complex using high resolution cryo-electron microscopy (cryo-EM). In contrast with yeast and human R2TP homologues, AtR2T is assembled as a dodecameric RUVBL1-RUVBL2 platform to which RPAP3 is bound. Preliminary structural models show two molecules of RPAP3 interacting with a RUVBL1-RUVBL2 dodecamer, one to each hexameric ring. These findings could highlight new mechanistic insights about the chaperone activities of R2TP.

References

1. Kakihara, Houry. The R2TP complex: discovery and functions. *Biochim Biophys Acta Mol Cell Res*, 1823 (2012).

2. Houry, Bertrand, Coulombe. The PAQosome, an R2TP-based chaperone for quaternary structure formation. *Trends Biochem Sci*, 43 (2018).

3. Seraphim et al. Assembly principles of the human R2TP chaperone complex reveal the presence of R2T and R2P complexes. *Structure*, 30 (2022).

Keywords: cryo-EM, chaperone, R2TP, Arabidopsis thaliana

A QUICK LOOK AT THE CIB-CSIC TALOS L120C G2 CRYO-ELECTRON MICROSCOPE

Rafael Nuñez-Ramirez (Spain)[1]; Begoña Pau (Spain)[1]; Fernando Escolar (Spain)[1]; Ernesto Arias-Palomo (Spain)[1]

1 - Centro de Investigaciones Biologicas Margaritas Salas. CSIC.

Abstract

The electron microscopy facility (EMF) at the Centro de Investigaciones Biológicas Margarita Salas (CIB-CSIC) provides technical support to research groups interested in ultra-structural analysis and cryo electron microscopy of biological samples. The EMF is equipped with all the necessary tools and equipment to process and analyze different kinds of organs, tissues, cells, and biological samples.

Recently, the EMF has acquired a Talos L120C G2 cryo electron microscope, which is equipped with a 16-megapixel Ceta-F camera. This microscope features a robust vacuum system with large Ion Getter Pumps (IGP) that enable rapid sample exchanges using the standard side-entry mechanism. In addition, the multi-specimen Gatan cryo holder significantly speeds up sample checking and vitrification optimization.

Furthermore, in line with others TEM systems, the Talos L120C G2 offers enhanced automation of column alignments and data collection, improving productivity and efficiency in the analysis of the ultrastructure of biological tissues and macromolecular complexes.

The MAPS software allows the automatic acquisition of an overview of the sample, simplifying the visualization of sections of resin-embedded cells and tissues, and facilitating navigation through the specimen. The TOMO software allows the acquisition of three-dimensional information of the sections, providing insight into the identification of structural cell compartments and visual segmentation of different structures within the cell. Finally, the EPU software enables the automation of data collection for single particle analysis during cryo-electron microscopy experiments. The image processing of these data, although limited in resolution, could be crucial in the design of sample vitrification strategies to avoid problematic issues such as preferential view or structural heterogeneity.

Therefore, the addition of the Talos L120C G2 cryo electron microscope has enabled the EMF to offer advanced services in the ultra-structural analysis of biological samples. This new microscope, which is open to all academic and industry users, promises to further benefit the structural studies of a wide range of researchers interested in both cellular and structural biology.

Keywords: Facility, single particles, ultrastructure, Talos

STUDY OF ALLOSTERIC EFFECT OF COMPOUNDS BOUND TO THE HYDROPHOBIC POCKET OF THE RBD DOMAIN IN THE SPIKE PROTEIN OF SARS-COV-2 BY CRYO-EM

Aileen Santini Santiago (Spain)[1]

1 - CIC bioGUNE

Abstract

The receptor-binding domain (RBD) is a key component of the SARS-CoV-2 spike glycoprotein (S) and is responsible for binding to the cellular receptor angiotensin-converting enzyme 2 (ACE2), this interaction is the first step in the infection cycle of the virus that causes COVID-19 disease. Therefore, the RBD binding site where ACE2 interacts is an ideal target to block infectivity. To this end, significant progress has been made in the development of therapies that block the S glycoprotein binding to the cellular receptor ACE2 through the use of specific monoclonal antibodies, recombinant soluble ACE2, or fusion inhibitors that specifically target the S glycoprotein of SARS-CoV-2. However, studies on potential existing drugs targeting the ACE2 binding site on the RBD of the S glycoprotein and their mode of interaction at structural level still unknown. Therefore, structural studies by cryo-electron microscopy (cryo-EM) and molecular dynamics simulations are the fastest way to identify a suitable existing compound that binds to the RBD binding site and that could function as a potential inhibitor between the RBD of the SARS-CoV-2 S glycoprotein and the cellular receptor ACE2.

Structurally, the S glycoprotein exhibits two conformational states in the RBD: the open state and the closed state. In the open state, the RBD is outstretched and accessible for ACE2 binding; while in the closed state it does not. Recently, a hydrophobic binding pocket (HP) within the RBD has been discovered, and that this pocket is very well conserved within the genus of beta-coronaviruses (β-CoVs) that infect humans: SARS-CoV, MERS-CoV, SARS-CoV-2 and its variants. The discovery shows that the binding pocket primarily attracts essential free fatty acids such as linoleic acid (LA) and helps stabilize the S glycoprotein in its closed state by forming salt bridges with neighboring RBDs in the trimer. This has led to postulate that this HP in the RBD is an allosteric site that can block the closed state of the trimer and thus prevent the entrance of the virus into the host cell. In this study, we will test the allosteric nature of the HP within the RBD in trimers from β-CoVs. Candidate compounds after in silico docking will be tested for their binding to RBDs and for their effect in the conformational landscape of S trimers.

References

Benton, D.J., Wrobel, A.G., Xu, P., Roustan, C., Martin, S.R., Rosenthal, P., Skehel, J.J., and Gamblin, S.J. (2020). Receptor binding and priming of the spike protein of SARS-CoV-2 for membrane fusion. Nature 588, 327-330.

Brotzakis, Z.F., Lohr, T., and Vendruscolo, M. (2021). Determination of intermediate state structures in the opening pathway of SARS-CoV-2 spike using cryo-electron microscopy. Chem. Sci., 2021, 12, 9168.

Creutznacher, R., Maass, T., Veselkova, B., Ssebyatika, G., Krey, T., Empting, M., Tautz, N., Frank, M., Kolbel, K., Uetrecht, C., and Peters, T. (2022). NMR experiments provide insights into ligand-binding to the SARS-CoV-2 spike protein receptor-binding domain. J. Am. Chem. Soc. https://doi.org/10.1021/jacs.2c05603.

Day, C.J., Bailly, B., Guillon, P., Dirr, L., Jen, F.E-C., Spillings, B.L., Mak, J., von Itzstein, M., Haselhorst, T., and Jennings, M.P. (2021). Multidisciplinary approaches identify compounds that bind to human ACE2 or SARS-CoV-2 spike protein as candidates to block SARS-CoV-2-ACE2 receptor interactions. mBio 12:e03681-20. https://doi.org/10.1128/mBio.03681-20.

Farouk, A.E., Baig, M.H., Khan, M.I., Park, T., Alotaibi, S.S., and Dong, J.J. (2021). Screening of inhibitors against SARS-CoV-2 spike protein and their capability to block the viral entry mechanism: a viroinformatics study. Saudi Journal of Biological Sciences 28 (2021), 3262-3269.

Yan, W., Zheng, Y., Zeng, X., He, B., and Cheng, W. (2022). Structural biology of SARS-CoV-2: open the door for novel therapies. Sig Transduct Target Ther 7, 26 (2022). https://doi.org/10.1038/s41392-022-00884-5.

Shoemark, D.K., Colenso, C.K., Toelzer, C., Gupta, K., Sessions, R.B., Davidson, A.D., Berger, I., Schaffitzel, C., Spencer, J., and Mulholland, A.J. (2021). Molecular simulations suggest vitamins, retinoids and steroids as ligands of the free fatty acid pocket of the SARS-CoV-2 spike protein. Angew. Chem. Int. Ed. 2021, 60, 7098-7110.

Sztain, T., Ahn, S.H., Bogetti, A.T., Casalino, L., Goldsmith, J.A., Seitz, E., McCool, R.S., Kearns, F.L., Acosta-Reyes, F., Maji, S., et al. (2021). A glycan gate controls opening of the SARS-CoV-2 spike protein. Nature Chemistry, vol 13, 963-968. https://doi.org/10.1038/s41557-021-00758-3.

Toelzer, C., Gupta, K., Yadav, S.K.N., Borucu, U., Davidson, A.D., Williamson, M.K., Shoemark, D.K., Garzoni, F., Staufer, O., Milligan, R., et al. (2020). Free fatty acid binding pocket in the locked structure of SARS-CoV-2 spike protein. Science 370, 725-730.

Toelzer, C., Gupta, K., Yadav, S.K.N., Hodgson, L., Williamson, M.K., Buzas, D., Borucu, U., Powers, K., Stenner, R., Vasileiou, K., et al. (2022). The free fatty acid-binding pocket is a conserved hallmark in pathogenic b-coronavirus spike proteins from SARS-CoV to Omicron. bioRxiv 2022.04.22.489083; doi: http://doi.org/10.1101/2022.04.22.489083.

Keywords: SARS-CoV-2, cryo-EM, Compounds, Spike Protein

STRUCTURE DETERMINATION OF TRANSLATION INITIATION COMPLEXES BY SINGLE PARTICLE CRYOEM

Marisa Lopez Redondo (Spain)[1]; Maria Pilar Hernandez (Spain)[1]; Laura Flores (Spain)[1]; Alicia Forcada (Spain)[1]; Carolina Espinosa (Spain)[1]; Borja Saez (Spain)[1]; Laura Villamayor-Belinchon (Spain)[1]; Jose Luis Llacer (Spain)[1]

1 - Instituto de Biomedicina de Valencia - CSIC -

Abstract

Resistance to antibiotics by pathogenic bacteria will be an increasing problem for the next decades and ribosomes are the target for approximately 50% of the current known antibiotics (1). Hence, studying at molecular level biological processes like translation initiation can provide us with rational strategies for targeting specific complexes, especially if we are able to find the differences (and similarities) between eukaryotic and prokaryotic translation initiation.

Here our main goal is to study certain aspects of bacterial translation initiation by *in vitro* assembling a complex including the bacterial 30S subunit, initiation factor 1 (IF1), different IF2 variants, IF3, acylated tRNA, and a natural mRNA (that also include some non-canonical nucleotides). Although there is already previous structural work on this particular topic (2, 3, 4, 5), there are still many unknowns since in previous complexes occupancy and resolution for IF2 was very low and synthetic and sequence optimized mRNAs were used for structure determination.

A second goal we are interested in is to get the first structure of a Cyanobacterial ribosome from *Synechococcus elongatus* PCC 7942, bound to a ribosome late-maturation protein called EndgA. Cyanobacteria exhibit a great adaptability to changing environmental conditions through changes in gene expression. Numerous genome expression analyses have been carried out in these organisms, especially in the model Synechocystis sp. PCC 6803 (hereafter Synechocystis). Most of these studies are related to the transcriptional response to different environmental changes (6). However, far fewer studies address the structural studies of ribosomes in cyanobacteria. There is ever-increasing evidence that numerous protein factors interact with the ribosome to regulate protein synthesis and modulate the expression profile of the cell in response to different environmental stresses (7). In this context, EngA is an essential GTPase involved in the maturation of the ribosomal subunit 50S (8-10). This study aims to advance in the knowledge of how EngA is bound to the ribosome through the first structure of a ribosome from a cianobacteria.

Acknowledgments

Supported by grant PID2020-116880GB-I00 from MICIN (to JLLlácer).
CSIC cryoelectron microscopy (CryoEM) facility of the Centro Nacional de Biotecnología (CNB)
IBMB-CSIC CryoEM Platform

References

1- Wilson DN. Ribosome-targeting antibiotics and mechanisms of bacterial resistance. *Nat Rev Microbiol* 12, 35 (2014)

2 - Hussain T, Llácer JL, Wimberly B, Kieft JS & Ramakrishnan V. Large-Scale Movements of IF3 and tRNA during Bacterial Translation Initiation. *Cell* 167, 133. (2016)

3 – Rodnina MV. Translation in Prokaryotes. *Cold Spring Harb Perspect Biol*. 10, a032664. (2018).

4- Kaledhonkar, S., Fu, Z., Caban, K. *et al.* Late steps in bacterial translation initiation visualized using time-resolved cryo-EM. *Nature* 570, 400 (2019)

5- Jorge P. López-Alonso, Attilio Fabbretti, Tatsuya Kaminishi, Idoia Iturrioz, Letizia Brandi, David Gil-Carton, Claudio O. Gualerzi, Paola Fucini, Sean R. Connell, Structure of a 30S pre-initiation complex stalled by GE81112 reveals structural parallels in bacterial and eukaryotic protein synthesis initiation pathways, *Nucleic Acids Research*, 45, 2179 (2017).

6 - Hernandez-Prieto MA, Semeniuk TA, Giner-Lamia J, Futschik ME. The Transcriptional Landscape of the Photosynthetic Model Cyanobacterium Synechocystis sp. PCC6803. *Sci Rep*. 6, 22168 (2016).

7 -Starosta AL, Lassak J, Jung K, Wilson DN. The bacterial translation stress response. FEMS microbiology reviews. 38, 1172 (2014)

8- Hwang J, Inouye M. The tandem GTPase, Der, is essential for the biogenesis of 50S ribosomal subunits in Escherichia coli. *Mol Microbiol*. 61:1660.(2006)

9- Amrita Bharat, Eric D. Brown, Phenotypic investigations of the depletion of EngA in *Escherichia coli* are consistent with a role in ribosome biogenesis, *FEMS Microbiology Letters* 353, 26 (2014).

10- Young Jeon, Chang Sook Ahn, Hyun Ju Jung, Hunseung Kang, Guen Tae Park, Yeonhee Choi, Jihwan Hwang, Hyun-Sook Pai, DER containing two consecutive GTP-binding domains plays an essential role in chloroplast ribosomal RNA processing and ribosome biogenesis in higher plants, *Journal of Experimental Botany* 65, 117 (2014).

Keywords: Ribosome; eIFs; single particle; cryoEM; translation initiation complex; IFs; cyanobacteria

CRYOCORRELATIVE LIGHT ELECTRON MICROSCOPY PLATFORM AT THE SPANISH NATIONAL CENTRE FOR BIOTECHNOLOGY IN MADRID

David Delgado Gestoso (Spain)[1]; José Javier Conesa (Spain)[1]; Jonathan Gabriel Piccirillo (Spain)[1]; Noelia Zamarreño (Spain)[1]; Francisco Javier Chichón (Spain)[1]; M. Teresa Bueno-Carrasco (Spain)[1]; José Javier Collado-Ávila (Spain)[1]; Blanca Soler Palacios (Spain)[1]; Mario Mellado (Spain)[1]; José M Valpuesta (Spain)[1]; Rocío Delgado Gestoso (Spain)[1]

1 - Spanish National Centre for Biotechnology

Abstract

The CryoEM CNB-CSIC facility located in Madrid houses an advanced cryocorrelative imaging platform that integrates visible light and electron microscopy. This platform is open to the entire structural biology community for a variety of applications.

We have implemented a cryocorrelative workflow which starts with sample vitrification. Vitrification approach is determined by the thickness of the specimen. High-pressure freezing on planchettes is preferred for thicker samples such as tissues (up to 200 µm thickness). On the other hand, plunge freezing is used for cells attached to EM grids or purified samples. In addition, we have successfully implemented the waffle method for vitrification of cellular samples on EM grids by high-pressure freezing.

In our workflow, vitrified specimens are tagged or labelled with fluorophores to determine the three-dimensional location of events of interest and to gain functional information. Regions of interest are located and imaged using a cryoconfocal visible light microscopy (ZEISS LSM 900 with an AiryScan2 detector). Once cryofluorescence information is collected, samples are transferred to a cryofocused-ion-beam scanning electron microscope (cryoFIBSEM) (Zeiss Crossbeam 550 equipped with a Leica cryo stage) in which using the information obtained by cryovisible light microscopy, serial section volume imaging and lamellae preparation are performed. The facility is equipped with a 300 kV microscope for cryoelectron tomography (cryoET) data acquisition (JEOL CryoARM 300) on the generated lamellae.

Acknowledgments

Fondo Europeo de Desarrollo Regional (FEDER), Consejo Superior de Investigaciones Científicas (CSIC), Centro Nacional de Biotecnología (CNB), Ministerio de Ciencia e Innovación (Gobierno de España), CRIOMECORR, Cryo-EM CSIC

Keywords: Cryofocused-ion-beam scanning electron microscopy, cryocorrelative light-electron microscopy, vitrification, tomography, native state, structural biology

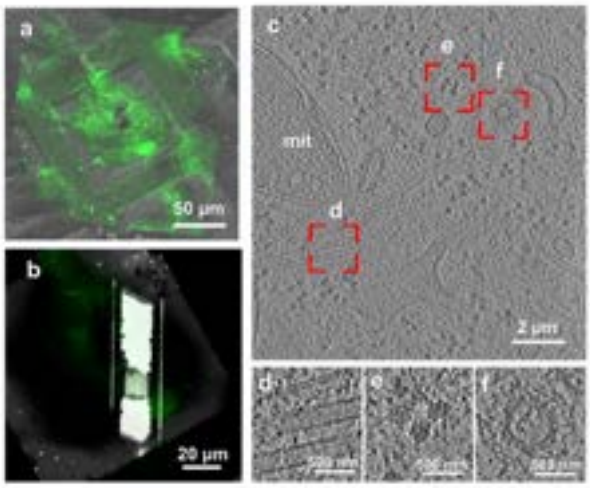

Figure 1. Correlative 3D cryolight electron microscopy (CLEM) of Jurkat cells expressing GFP-EB3 protein constitutively. (a) Overlay of bright field (grey) and maximum intensity projection of cryo-confocal microscopy stack of images of a cell attached to finder TEM grid. (b) CryoTEM image of a lamellae in the area shown in (a). (c) Cryoelectron tomogram section selected based on the confocal imaging information; mit, mitochondrion. (d-f), higher detail of the areas squared in (c); (d) microtubules; (e) ribosomes and (f) coated vesicle.

THE BASQUE RESOURCE FOR ELECTRON MICROSCOPY

Jorge P. López-Alonso (Spain)[1,2]; Kristina Barragán Sanz (Spain)[1,2]; Izaro Rodríguez-Renovales (Spain)[1,2]; Andrés Jiménez (Spain)[1,2]; David Gil-Cartón (Spain)[1,2,3]; Iban Ubarretxena-Belandia (Spain)[1,2,3]

1 - Instituto Biofisika (UPV/EHU, CSIC); 2 - Basque Resource for Electron Microscopy; 3 - Ikerbasque, Basque Foundation for Science

Abstract

The number of structures of biomolecules determined by single particle cryo-electron microscopy (cryo-EM) is increasing exponentially in recent years[1]. The improvements in the hardware of microscopes and the software used for data analysis have resulted in more detailed maps that frequently arrive to the atomic-level resolution. The Basque Resource for Electron Microscopy (BREM) provides access to high-end instrumentation and expertise in high-resolution cryo-EM to national and international researchers, from academia and industry. BREM is equipped with a ThermoFisher Krios G4 transmission electron microscope, paired with Gatan's BioContinuum Imaging Filter and a K3 direct electron detector. The system also includes a phase plate, a second Falcon III direct electron detector and Ceta-D CMOS camera. In addition, the facility contains the equipment for sample preparation: an ELMO glow discharger for TEM grids, a Leica EM GP2 single-side blotting automated plunge freezer, a ThermoFisher Vitrobot Mark IV double-side blotting automated plunge freezer and a Leica EM ICE automated high pressure freezer. BREM offers on-the-fly processing to analyze the quality of the data on real time using a processing server with 8 GPUs, a hot storage server with 130 TB SSD and a warm storage server with 500 TB HDD.

BREM has highly qualified staff to operate the facility and assist users with three-dimensional structure determination using all major cryo-EM techniques available for structural biology.

References

1. Callaway, E. *Nature*, **2020**, *578*, 201.

IMPLEMENTATION OF A WORKFLOW FOR THE STRUCTURAL CHARACTERIZATION OF HER2 BY SUBTOMOGRAM AVERAGING

Patricia Losana (Spain)[1]; Ana Cuervo (Spain)[1]; Chungyang Wang (Switzerland)[2]; Jose Javier Conesa (Spain)[1]; Andreas Plückthun (Switzerland)[2]; Ohad Medalia (Switzerland)[2]; Carlos Oscar Sorzano (Spain)[1]; Jose Maria Carazo (Spain)[1]

1 - National Center for Biotechnology (CNB-CSIC), Madrid, Spain; 2 - Biochemistry department, University of Zurich, Zurich, Switzerland

Abstract

Members of the Epithelial Growth Factors Receptor Family (EGFRs) influence cell growth and proliferation, and are key in all phases of tumor progression. Hence, in this work we are using this receptor family as a model to develop a subtomogram averaging image processing workflow, to solve its structure in a close to native environment. Vesicles from SKBR3 cancer cells, enriched with HER2 membrane receptors (~170 kDa) were used to acquire cryo-electron tomography (cryo-ET) data. The heterogeneity of the vesicle membrane protein content together with the small size of the target receptor, settles this image processing on the limit of the nowadays tomography tools, making it mandatory to push the different existing methods to their maximal capabilities. We used PySeg software [1] to perform a vectorial picking on CTF-corrected tomograms [2,3]. A combination of exhaustive 2D procedures using PySeg, and 3D classification and alignments implemented in RELION4 [4]; were used to try to identify HER2 protein on the membrane surface. The implementation of this new workflow into Scipion3 [5], will facilitate the use of the different softwares in a single platform, allowing in a near future to push image processing to a higher resolution.

Acknowledgments

The authors acknowledge the economical support from MICIN to the Instruct Image Processing Center (I2PC) as part of the Spanish participation in Instruct-ERIC, the European Strategic Infrastructure Project (ESFRI) in the area of Structural Biology (Grant PID2019-104757RB-I00 funded by MCIN/AEI/10.13039/501100011033/). The authors also acknowledge Horizon 2020 through grant HighResCells (ERC - 2018 - SyG, Proposal: 810057).

References

[1] Martinez-Sanchez A, et al. Nat Methods. 2020;17:209-216.
[2] Xiong Q, et al. J Struct Biol. 2009;168(3):378-387.
[3] Grant et al., eLife, 2018; e35383
[4] Zivanov J, et al. BioRxiv 2022
[5] Jiménez de la Morena J, et al. Struct Biol. 2022;214:107872.

Keywords: CryoET, Subtomogram Averaging, Membrane protein, Membrane receptor

STRUCTURAL AND MOLECULAR CHARACTERIZATION OF CST BINDING TO DNA SUBSTRATES

Nayim González Rodríguez (Spain)[1]; Javier Coloma (Spain)[1]; Oscar Llorca (Spain)[1]

1 - CNIO

Abstract

The CTC1-STN1-TEN1 (CST) complex is a critical mediator of both telomeric and genome-wide replication. It binds the ssDNA overhangs at telomeres, recruiting the Polymerase α-Primase to replicate the chromosomic 5' ends[1–3]. During genome-wide replication, it acts upon foci of replication stress, mainly G-rich sequences, preventing or restarting stalled replication forks [4,5] and by helping to repair double-stranded DNA breaks[6,7].

While many of the mutations in CST that result in genetic disorders, such as the Coat Plus Syndrome and Dyskeratosis Congenita, have been explained by recent structures of CST and some of its interaction partners, many others remain unclear[8,9]. Only the interaction with telomeric ssDNA substrates has been structurally characterized, although it is well established that CST interacts with other types of substrates both during telomere and genome-wide replication. We propose that alterations in the molecular mechanism behind these interactions are responsible for the aberrant function of CST in some of these genetic disorders. I will present our ongoing efforts and challenges towards using single-particle cryoEM to characterise the interactions between CST and several DNA substrates and our preliminary conclusions.

References

1. Feng, X. *et al.* CTC1-STN1 terminates telomerase while STN1-TEN1 enables C-strand synthesis during telomere replication in colon cancer cells. *Nat. Commun.* **9**, 1–12 (2018).

2. Lue, N. F., Chan, J., Wright, W. E. & Hurwitz, J. The CDC13-STN1-TEN1 complex stimulates Pol α activity by promoting RNA priming and primase-to-polymerase switch. *Nat. Commun.* **5**, 1–11 (2014).

3. Lim, C. J. & Cech, T. R. Shaping human telomeres: from shelterin and CST complexes to telomeric chromatin organization. *Nat. Rev. Mol. Cell Biol.* 1–16 (2021) doi:10.1038/s41580-021-00328-y.

4. Lyu, X. *et al.* Human CST complex protects stalled replication forks by directly blocking MRE11 degradation of nascent-strand DNA. *EMBO J.* (2020) doi:10.15252/embj.2019103654.

5. Stewart, J. A. *et al.* Human CST promotes telomere duplex replication and general replication restart after fork stalling. *EMBO J.* **31**, 3537–3549 (2012).

6. Mirman, Z. *et al.* 53BP1–RIF1–shieldin counteracts DSB resection through CST- and Polα-dependent fill-in. *Nature* **560**, 112–116 (2018).

7. Mirman, Z., Sasi, N. K., King, A., Chapman, J. R. & de Lange, T. 53BP1–shieldin-dependent DSB processing in BRCA1-deficient cells requires CST–Polα–primase fill-in synthesis. *Nat. Cell Biol. 2022* **24**, 51–61 (2022).

8. Cai, S. W. *et al.* Cryo-EM structure of the human CST–Polα/primase complex in a recruitment state. *Nat. Struct. Mol. Biol.* 1–7 (2022) doi:10.1038/s41594-022-00766-y.

9. Lim, C. J. *et al.* The structure of human CST reveals a decameric assembly bound to telomeric DNA. *Science* **368**, 1081–1085 (2020).

Keywords: cryoEM, SPA, telomere, CST, DNA

STRUCTURAL AND FUNCTIONAL CHARACTERIZATION BY CRYO-EM OF A NOVEL MONOCLONAL ANTIBODY WITH PAN-NEUTRALIZING SARS-COV-2 ACTIVITY INCLUDING BQ.1.1 VARIANT

Andrea Modrego Guillén (Spain)[3]; Leire De Campos-Mata (Spain)[1]; Benjamin Trinité (Spain)[2]; Diego Carlero (Spain)[3]; César Santiago (Spain)[3]; María Teresa Bueno (Spain)[3]; Jaime Martín-Benito (Spain)[3]; Carlo Carolis (Spain)[4]; Julia Blanco (Spain)[2]; Giuliana Magri (Spain)[1]; Rocío Arranz (Spain)[3]

1 - Institut Hospital del Mar d'Investigacions Mèdiques; 2 - IrsiCaixa AIDS Research Institute; 3 - Centro Nacional de Biotecnología; 4 - Centre for Genomic Regulation

Abstract

During previous COVID-19 waves, therapeutic administration of monoclonal antibodies (mAbs) has been highly effective in preventing COVID-19-related hospitalization and death. However, there are currently no approved therapeutic mAbs capable of neutralizing the new variant BQ.1.1. In this multidisciplinary work, we characterize, from a functional and structural point of view, 17T2, a new mAb with high and exceptionally broad neutralization activity against pre-Omicron and Omicron SARS-CoV-2 variants, including the highly immune evasive variants BA.5 and BQ.1.1.

Cryo-electron microscopy (cryo-EM) analysis showed that 17T2 binds the Omicron BA.1 spike protein with the three RBD domains in "up" position and recognizes a large epitope overlapping with the receptor binding motif. According to its type of interaction, 17T2 is considered a class 1 antibody, as it binds to the left shoulder-neck region of the RBD. A comparison with a structurally similar neutralizing mAb (S2E12) was carried out to understand the differences in the neutralizing activity against newest Omicron sublineages which led to the detection of point mutations in key residues that may lead to a higher interaction with the RBD, emphasizing a salt bridge between the CDR 3 of 17T2 heavy chain and the RBD that stabilizes the complex.

Altogether, the results highlight the impact of small and unique structural antibody changes, in both the heavy and the light chains, on neutralizing performance. As a result, 17T2 mAb could be considered a potential candidate for future therapeutic and prophylactic interventions.

References

[1] – L. De Campos-Mata, B.Trinité, A. Modrego, BioRxiv (2023) https://doi.org/10.1101/2023.01.20.524748

Keywords: SARS-CoV-2, Neutralizing antibody, Virology, Spike, Cryo-EM

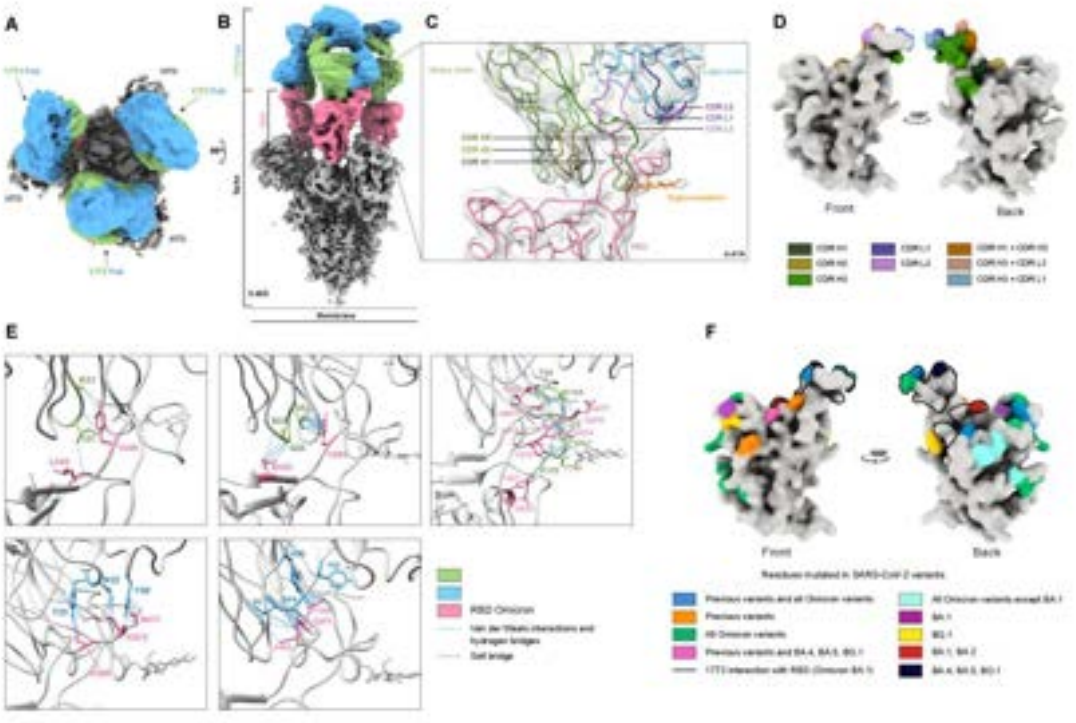
A
B
C
D
Front
Back
E
F
Front
Back

TARGETING AND CHARACTERIZATION OF CELLULAR ENVIRONMENTS BY CRYO-LIGHT ASSISTED CRYO-ELECTRON TOMOGRAPHY

Javier Fernandez Collado (Spain)[1]; Francisco Benitez Fuente (Spain)[2]; Duy Trong Vien Diep (Vietnam)[3]; Naama Zung (Israel)[4]; Jenny Prisca Keller (France)[1]; Miguel Angel Botella Mesa (Spain)[2]; Maria Bohnert (Germany)[3]; Maya Schuldiner (Israel)[4]; Ruben Fernandez Busnadiego (Spain)[1]

1 - Institute of Neuropathology, University Medical Center Göttingen, Göttingen, Germany.; 2 - Instituto de Hortofruticultura Subtropical y Mediterranea “La Mayora”, Universidad de Malaga-Consejo Superior de Investigaciones Cientificas (IHSM-UMA-CSIC), Universidad de Malaga, Malaga, Spain; 3 - Institute of Cell Dynamics and Imaging, University of Münster, Münster, Germany; 4 - Department of Molecular Genetics, Weizmann Institute of Science, Rehovot, Israel

Abstract

Cryo-electron tomography (Cryo-ET) allows the imaging of cellular compartments in a frozen-hydrated state that preserves molecules in close-to-native conditions. The ability to image cellular components while preserving their ultrastructure creates new opportunities to study their interactions with their molecular environment.

Membrane Contact Sites (MCSs) are a prime candidate for Cryo-ET. The function of these microdomains is heavily influenced by their morphology and the proteins at the cleft between them, which requires these features to be imaged in as close to physiological conditions as possible. Abundant MCSs like those between the endoplasmic reticulum (ER) and the plasma membrane in yeast can be found efficiently without the need for targeting, but more rare or short-lived contacts such as between ER and mitochondria or lipid droplets and vacuole can be challenging to find.

Some of the limitations of Cryo-ET when imaging infrequent cellular structures is that it remains a relatively low-throughput technique, and the identity of the feature of interest remains hidden until some form of tagging is employed. The integration of Cryo-light microscopy in our workflow has allowed us to actively target features of interest during sample thinning and later during tomography, drastically improving the output and reproducibility of our tomographic data.

By employing a combined approach of Cryo-ET assisted by Cryo-light microscopy we are able to reliably find and identify specific MCSs and other cellular components, while at the same time preserving the information of their cellular context.

Acknowledgments

Dr. Tat Cheng

Keywords: Cryo-EM, Cryo-light, Membrane Contact Sites

CRYOEM OF THE RUVBL1-RUVBL2 ATPASE IN COMPLEX WITH A SMALL COMPOUND

Jasminka Boskovic (Spain)[1]; Oscar Llorca (Spain)[1]; Carmen Garcia-Martin (Spain)[1]; Andres Lopez-Perrote (Spain)[1]

1 - Spanish National Cancer Center

Abstract

RUVBL1 and RUVBL2 are two highly conserved AAA+ ATPases that form a complex involved in diverse cellular processes, such as chromatin remodeling, DNA repair or regulation of gene expression. An overexpression of this RUVBL1-RUVBL2 has been reported in many cancer types, like gastric, breast or liver, and this demands to explore them as a therapeutic target (1, 2). RUVBL1 and RUVBL2 assemble hetero-hexameric oligomers that are scaffolding subunits of several macromolecular complexes, and ATP binding and/or hydrolysis has been described as essential for most of their functions (3). However, the molecular mechanism driven by the ATPase activity of RUVBL1-RUVBL2 is still poorly understood.

Several compounds and small molecules have been recently described to specifically interact with RUVBL1-RUVBL2 to inhibit its ATPase activity, showing potential against cancer (4, 5, 6). Here, we investigate the potential of cryo-electron microscopy (cryo-EM) to identify some of these small compounds in complex with RUVBL1-RUVBL2. We have cryo-EM sample preparation and preliminary single particle image processing of the complex shows some interesting features when compared with a compound-free sample, that might provide some light about the inhibition mechanism.

References

(1) The Role of Hsp90-R2TP in Macromolecular Complex Assembly and Stabilization. Lynham, J. and W. A. Houry. 2022. Biomolecules 12(8).

(2) RUVBL1–RUVBL2 AAA-ATPase: a versatile scaffold for multiple complexes and functions. Dauden M.I., Lopez-Perrote, A. Llorca, O. 2021 Current Opinion in Structural Biology 67:78–85.

(3) RUVBL1/RUVBL2 ATPase activity drives PAQosome maturation, DNA replication and radioresistance in lung cancer. Yenerall P, Das AK, Wang S, Kollipara RK, Li LS, Villalobos P., Flaming J, Lin YF, Huffman K, Timmons BC et al. 2020 Cell Chem Biol, 27:105-121.e14.

(4) Chemical perturbations revealthat RUVBL2 regulates the circadian phase in mammals. Ju D, Zhang W, Yan J, Zhao H, Li W, Wang J, Liao M, Xu Z, Wang Z, Zhou G et al.: Sci Transl Med 2020, 12:1-12.

(5) CB-6644 is a selective inhibitor of the RUVBL1/2 complex with anticancer activity. V. A. Assimon, Y. Tang, et al. 2019 ACS Chemical Biology 14 (2), 236-244.

(6) Sorafenib as an inhibitor of ruvbl2. Nano N, Ugwu F, Seraphim TV, Li T, Azer G, Isaac M, Prakesch M., Barbosa L., Ramos C., Datti A. et al. 2020 Biomolecules, 10:1-15.

Keywords: cryo-EM, ATPase

EXPLORING STRUCTURAL FLEXIBILITY AND CLASSIFICATION METHODS FOR IDENTIFYING INTERMEDIATE STATES OF HEPATIC ABCB TRANSPORTERS

Patricia Losana (Spain)[1]; David Herreros (Spain)[1]; Kamil Nosol (Switzerland)[2]; Carlos Oscar Sorzano (Spain)[3]; Julia Kowal (Switzerland)[2]; Kaspar P. Locher (Switzerland)[2]; Ana Cuervo (Spain)[1]; José María Carazo (Spain)[1]

1 - Centro Nacional de Biotecnología, CSIC, Campus de Cantoblanco. Madrid. Spain; 2 - Biochemistry department, ETH, Zurich, Switzerland.; 3 - PI

Abstract

Cryo-EM advances in Single Particle Analysis focuses nowadays in the study of the diverse conformations of the macromolecules beyond traditional 3D classification. Continuous flexibility methods, such as cryoDRGN or Zernike3D [1, 2], allow to study intermediate states as well as transitions between them, characterizing the full structural spectrum. In this work we have combined flexibility methods, together with static classification consensus strategies, to study the conformational landscape of ABCB4. This receptor is an ATP-binding cassette transporter expressed in hepatocytes that plays a crucial role in the formation of bile by translocating phosphatidylcholine (PC) into canaliculi [3]. While previous studies [4] have provided valuable insights into the structural basis of PC translocation, the precise transition mechanism between discrete conformations remains elusive. Although further characterization is needed to fully understand the mechanism of PC translocation, preliminary studies using these developing flexibility analysis tools [1,5] revealed what might be possible new intermediate states.

Acknowledgments

The authors acknowledge “Comunidad Autónoma de Madrid” (Grant: S2022/BMD-7232) and European Union (EU) and Horizon 2020 through grant HighResCells (ERC - 2018 - SyG, Proposal: 810057).

References

[1] Herreros D, Lederman RR, Krieger JM, Jiménez-Moreno A, Martínez M, Myška D, Strelak D, Filipovic J, Sorzano COS, Carazo JM. Estimating conformational landscapes from Cryo-EM particles by 3D Zernike polynomials. Nat Commun. 2023; 14:154.

[2] Zhong, E.D., Bepler, T., Berger, B. et al. CryoDRGN: reconstruction of heterogeneous cryo-EM structures using neural networks. Nat Methods 18, 176–185 (2021).

[3] Olsen JA, Alam A, Kowal J, Stieger B, Locher KP. Structure of the human lipid exporter ABCB4 in a lipid environment. Nat Struct Mol Biol. 2020; 27:62-70.

[4] Nosol K, Bang-Sørensen R, Irobalieva RN, Erramilli SK, Stieger B, Kossiakoff AA, Locher KP. Structures of ABCB4 provide insight into phosphatidylcholine translocation. Proc Natl Acad Sci U S A. 2021; 118:e2106702118.

[5] Jiménez de la Morena J, Conesa P, Fonseca YC, de Isidro-Gómez FP, Herreros D, Fernández-Giménez E, Strelak D, Moebel E, Buchholz TO, Jug F, Martinez-Sanchez A, Harastani M, Jonic S, Conesa JJ, Cuervo A, Losana P, Sánchez I, Iceta M, Del Cano L, Gragera M, Melero R, Sharov G, Castaño-Díez D, Koster A, Piccirillo JG, Vilas JL, Otón J, Marabini R, Sorzano COS, Carazo JM. J Struct Biol. 2022; 214:107872.

Keywords: Membrane Protein, Flexibility methods, Single Particle Analysis

MOLECULAR ARCHITECTURE AND OLIGOMERIZATION OF C. GLABRATA CDC13 DICTATES ITS TELOMERIC DNA UNFOLDING ACTIVITY

Javier Coloma (Spain)[1]; Nayim Gonzalez-Rodriguez (Spain)[1]; Francisco A. Balaguer (Spain)[2]; Karolina Gmurczyk (Spain)[2]; Clara Aicart-Ramos (Spain)[2]; Oscar M. Nuero (Spain)[3]; Juan Roman Luque-Ortega (Spain)[3]; Neal F. Lue (United States of America)[4]; Fernando Moreno-Herreros (Spain)[2]; Oscar Llorca (Spain)[5]

1 - CNIO; 2 - CNB; 3 - CIB; 4 - Weill Cornell Medicine; 5 - CNO

Abstract

The CST complex, composed of Cdc13, Stn1 and Ten1 in yeast, mediates thereplication and stability of telomeric DNA. While Stn1 and Ten1 are very well conserved across species, Cdc13 does not resemble its mammalian counterpart CTC1 either in sequence or domain organization, and Cdc13 but not CTC1 displays functions independently of the rest of CST. Whereas the structures of human CTC1 and CST have been determined, the molecular organization of yeast Cdc13 remains poorly understood. We have dissected the molecular architecture of Candida glabrata Cdc13and showed how each of its OB folds contributes to its self-association and binding to telomeric DNA sequences. Using a combination of biochemical and biophysical tools, we concluded that Cdc13 forms dimers through the interaction between OB-fold 2 (OB2) domains. Dimerization stimulates binding of OB3 to telomeric sequences, resulting in the unfolding of ssDNA secondary structure. Once bound to DNA, Cdc13 prevents the refolding of ssDNA by mechanisms that involve oligomerization of Cdc13. Furthermore,we showed that Cdc13 and CST form higher-order complexes via oligomerizationthrough OB1. Our results reveal the molecular organization of C. glabrata Cdc13, how this regulates DNA binding, and suggest that the distinct architectures of yeast Cdc13 may share common principles.

References

Coloma J, Gonzalez-Rodriguez N, Balaguer FA, Gmurczyk K, Aicart-Ramos C, Nuero ÓM, Luque-Ortega JR, Calugaru K, Lue NF, Moreno-Herrero F, Llorca O. Molecular architecture and oligomerization of Candida glabrata Cdc13 underpin its telomeric DNA-binding and unfolding activity. Nucleic Acids Res. 2023 Jan 25;51(2):668-686. doi: 10.1093/nar/gkac1261. PMID: 36629261; PMCID: PMC9881146.

Keywords: Telomere replication, CST complex

STRUCTURAL CHARACTERIZATION OF SHELTERIN COMPLEX

María Moreno Morcillo (Spain)[1]; Raquel Cuesta Ramos (Spain)[1]; Araceli Grande (Spain)[1]; María Gonzalez Corpas (Spain)[1]; Ester Casajus Pelegay (Spain)[1]; Rafael Fernández Leiro (Spain)[1]

1 - CNIO

Abstract

Telomeres are nucleoprotein structures that cap the end of linear chromosomes to protect them from inappropriate activation of the DNA damage response pathways. The Shelterin complex is a six-protein complex -TRF1, TRF2, RAP1, TIN2, TPP1, POT1- located at telomeres that confers telomere protection and length regulation (1,2). Misregulation of this complex is associated with many human diseases including premature aging syndromes, telomerase-associated disorders, and cancer (3,4). Despite its relevance, the structural and mechanistic information about human shelterin components is limited (5, 6).

In our group, we are trying to get insights on how shelterin orchestrates all these different processes that take place in telomeres, which are also tightly regulated. To achieve this aim, we use cryo-electron microscopy, among other techniques, to reveal some details about the dynamics of the complex and its organization at telomeres. After a though process of sample optimization, we are reconstituting all possible shelterin subcomplexes combinations in vitro to understand its different biological function and how they are regulated to fulfil its mission within cells at the right time.

References

1. Lange, Titia de. 2005. “Shelterin: The Protein Complex That Shapes and Safeguards Human Telomeres.” *Genes & Development* 19 (18): 2100–2110.
2. Lin, Chih-Yi Gabriela, Anna Christina Näger, Thomas Lunardi, Aleksandra Vančevska, Gérald Lossaint, and Joachim Lingner. 2021. “The Human Telomeric Proteome during Telomere Replication.” *Nucleic Acids Research*, November. https://doi.org/10.1093/nar/gkab1015.
3. Maciejowski, John, and Titia de Lange. 2017. “Telomeres in Cancer: Tumour Suppression and Genome Instability.” *Nature Reviews. Molecular Cell Biology* 18 (3): 175–86.
4. Donate, Luis E., and Maria A. Blasco. 2011. “Telomeres in Cancer and Ageing.” *Philosophical Transactions of the Royal Society of London. Series B, Biological Sciences* 366 (1561): 76–84.
5. Smith, Eric M., Devon F. Pendlebury, and Jayakrishnan Nandakumar. 2020. “Structural Biology of Telomeres and Telomerase.” *Cellular and Molecular Life Sciences: CMLS* 77 (1): 61–79.
6. Nguyen, Thi Hoang Duong. 2021. “Structural Biology of Human Telomerase: Progress and Prospects.” *Biochemical Society Transactions*, October. https://doi.org/10.1042/BST20200042.

Keywords: Telomeres, Shelterin, Cryo-EM

MECHANISMS FOR UNCOATING OF HUMAN PICOBIRNAVIRUS PARTICLES

María J Rodríguez-Espinosa (Spain)[1]; Javier M Rodríguez (Spain)[1]; Pedro J De Pablo (Spain)[2]; Jose R Caston (Spain)[1]

1 - Spanish National Center for Biotechnology; 2 - Autonomous University of Madrid

Abstract

High resolution cryo-electron microscopy (cryo-EM) structures of viruses qualitatively indicate the interaction degree between the genome and coat proteins (CPs), but lack the direct evaluation of its effects on the virus capsid. Here we study the mechanical and chemical uncoating of three variants of the human picobirnavirus (hPBV) virus-like particles (VLPs) which differ in the N-terminal of their CPs.

We used Atomic Force Microscopy (AFM) to induce and monitor mechanical disassembly of individual hPBV particles. Critical indentation experiments show that whereas lacking-RNA particles allowed a fast tip indentation after breakage, loaded-RNA particles showed a slower tip penetration after being fractured. Mechanical fatigue experiments confirm the interaction between RNA and the N-terminal capsid protein. The increased length of the CP N-terminal makes the hPBV VLPs to crumble slower than wild type N-terminal, indicating an enhanced RNA cargo retention.

In addition, we induced chemical disassembly of hPBV VLPs. An *in vitro* assembly/disassembly system shows the influence of salt, pH and RNA. The disassembly reaction after increasing the pH results in CP dimers and tetramers, but it is irreversible, possibly due to RNA degradation. However, the disassembly is reversible with increased pH and salt. Size exclusion chromatography and dynamic light scattering analysis show that the size of the disassembled particles is similar to that of the VLPs. Although these VLPs might not be completely disassembled, biochemical analysis shows that they release part of their genome. However, negative staining in transmission electron microscopy shows that CP dimers and tetramers are the major resulting disassembly products. The structure of these partially disassembled particles has been solved by cryo-EM without imposing icosahedral symmetry. Preliminary results indicate that, maintaining the structural integrity of the capsid, some CP dimers are detached and the genome can exit through the newly formed holes.

Acknowledgments

We thank the Cryo-EM CNB-CSIC facility (Madrid), for help with cryo-EM data acquisition. This work was supported by grants from the Spanish Ministry of Science and Innovation (PID2020-113287RB-I00) and the Comunidad Autónoma de Madrid (P2018/NMT-4389) to JRC.

References

[1] Ortega-Esteban et al. Journal of Virology, 94(24), e01542-20 (2020).
[2] De Pablo et al. Applied Physics Letters, 73(22), 3300-3302 (1998).
[3] Horcas et al. Review of Scientific Instruments, 78(1), 013705 (2007).
[4] Martín-González et al, 11(2), 021025 (2021).

Keywords: virus, structure, genome, afm, cryo-EM

STRUCTURAL AND FUNCTIONAL CHARACTERIZATION OF MYCOBACTERIUM ARABINOFURANOSYLTRANSFERASE D (AFTD), A NEW POTENTIAL DRUG TARGET AGAINST TUBERCULOSIS DISEASE

Vanessa Tavares Almeida (Portugal)[1]; Bárbara Rodrigues (Portugal)[1]; José Rodrigues (Portugal)[1]; Allen Zinkle (United States of America)[2]; Yaqi Liu (United States of America)[2]; José Alves De Brito (Portugal)[1]; Federico Issoglio (Portugal)[1]; Filippo Mancia (United States of America)[2]; Margarida Archer (Portugal)[1]

1 - ITQB NOVA; 2 - Columbia University

Abstract

Tuberculosis (TB) is one of the leading causes of death worldwide and is a disease caused by the infection of Mycobacterium tuberculosis (Mtb). The emergence of multidrug resistant mycobacteria has prompted the need to better understand their resistance mechanisms and develop novel therapeutics (1). Arabinofuranosyltransferases (AraTs) are membrane enzymes involved in the biosynthesis of arabinan, an important component of the unique cell-envelope of Mtb. High virulence and resistance of Mtb to common antibiotics is related to the protective role of the mycobacterial cell wall, so these enzymes are attractive targets against TB (2-7). This family of proteins, essential for bacterial survival and growth, comprises Embs (EmbA-C), which are known targets for ethambutol, a first-line drug for TB treatment; and Afts (AftA-D), which represent new potential drug targets against TB. Here we present our advances in the characterization of the mycobacterium AftD protein. We used Cryo-EM for structural studies, NMR for activity assays, and structure-based virtual screening with a drug repurposing strategy to search for molecules with the potential to inhibit AftD.

Acknowledgments

This work was supported by Fundação para a Ciência e Tecnologia (FCT) I. P., Portugal, fellowships BD/06824/2021 (to V.T. Almeida), PD/BD/128261/2016 (to J. Rodrigues) and grants PTDC/BIA-BQM/30421/2017, PTDC/BIA-BQM/4056/2020 (to M.Archer, V.T.Almeida and J.Rodrigues). This project has received funding from EU H2020 grant agreements No 823780 (PROMETEUS).

References

1 - WHO, Advice on the use of point-of-care immunodiagnostic tests for COVID-19, WHO/2019-nCoV/Sci_Brief/POC_immunodiagnostics/2020.1;
2 - H.Škovierová, et al., Glycobiology, 2009, 19, 1235–1247;
3 - F. E. Umesiri, et al., Med. Res. Rev., 2010, 30, 290–326;
4 - C. E. Barry, Trends Microbiol., 2001, 9, 237–241;
5 - M. Jankute, et al., Annu. Rev. Microbiol., 2015, 69, 405–423;
6 - K. A. Abrahams and G. S. Besra, Parasitology, 2018, 145, 116–133;
7 - C. E. Barry, et al., Infect. Disord. Drug Targets, 2007, 7, 182–202;

Keywords: Tuberculosis, Arabinofuranosyltransferases, Mycobacterium, Cryo-EM, NMR, Computational Biology, Biochemistry, Structural Biology, Drug discovery

DEVELOPING WORKFLOWS FOR PROCESSING MEGAVOLUME SAMPLES FOR CRYOET

Katrina Gundlach (Netherlands)[1,2,3]; Ariane Briegel (Netherlands)[2,3]; Oda Schiøtz (Germany)[4]; Jürgen Plitzko (Germany)[4]

1 - Pacific Biosciences Research Center, University of Hawaii at Manoa, Honolulu, HI USA; 2 - Centre for Microbial Cell Biology, Leiden University, Leiden, The Netherlands; 3 - Department of Microbial Sciences, Institute of Biology, Leiden University, Leiden, The Netherlands; 4 - Research Group CryoEM Technology, Max Planck Institute of Biochemistry, Martinsried, Germany

Abstract

The field of cryo-EM offers the possibility to gain high-resolution structural information of biomolecules in their native state. Advances in sample thinning of cryo-EM samples allows the study of proteins inside intact cells using tomography, opening the door for 'visual proteomics'. However, thicker samples such as tissues or entire organisms are still largely unsuitable for cryo-electron tomography (cryoET) imaging methods. Therefore, significant efforts are directed toward improving large or megavolume sample preparation methods to enable cryoET of such complex samples. Here we present the initial stages of a novel workflow and optimization of sample preparation methods for larger symbiotic tissues. We focused on the binary association between the Hawaiian bobtail squid *Euprymna scolopes* and the luminous bacteria *Vibrio fischeri*. The Squid-Vibrio system has long been studied to understand host-symbiont interactions. Once the squids hatch, *Vibrio fischeri* in the seawater migrate toward and into the squid's internal light organ, where they colonize and maintain a light-producing population for the lifetime of the squid. Our goal is to study this bacterial-host interface using cryoET, at a resolution previously unattainable by conventional EM methods. We describe two new workflows to investigate this biological system. First, we present the application of custom designed nanobiopsy needles to collect tissue cores, which can be high pressure frozen. This system can accurately excise tissues in regions of interest, and cryo-electron microscopy of vitreous section (CEMOVIS) showed that samples are well vitrified. Secondly, we present a high-pressure freezing protocol for entire dissected symbiotic light organs. In a cryo-ultramicrotome, the light organ or biopsy needle is attached to EM support grids with cryo-glue, enabling downstream thinning and imaging methods, e.g., focused ion beam milling (FIB-SEM) and cryoET. Resulting samples were thinned by cryo FIB-SEM using a novel method called serial lift-out, and generated lamella were imaged using cryoET. Visible crystalline ice indicates that further HPF optimization is required for proper vitrification. Our initial findings suggest that nanobiopsy needles are a suitable tool to enable the application of cryo-EM imaging methods to previously inaccessible large-volume samples. Additionally, we show that megavolume (>700µm) complex samples are capable of being cryo-processed into lamella suitable for cryoET.

Acknowledgments

This work was supported by funding from the Gordon and Betty Moore Foundation (Symbiosis Model Systems, Grant #9328).

Keywords: Large volume samples, FIB-SEM, Symbiotic Interactions, Host-microbe interface

THE STRUCTURE OF THE GE81112 STALLED BACTERIAL PRE-INITIATION COMPLEX

Andreas Schedlbauer (Spain)[2]; Xu Han (Spain)[1]; Paola Fucini (Spain)[3]; Sean Connell (Spain)[1]

1 - Biocruces; 2 - CIC bioGUNE; 3 - PiE-UPV/EHU

Abstract

The initiation phase is the rate-limiting step of protein synthesis (translation) and is subject to fine-tuning via posttranscriptional regulatory mechanisms. As such, the initiation pathway is an important drug target (1). During initiation, the start site and the reading frame of the messenger RNA are selected by the small ribosomal subunit (30S) when the start codon, typically an AUG, is decoded in the P-site by the initiator tRNA in a process guided and controlled by three initiation factors. This process can be efficiently inhibited by GE81112, a natural antibiotic that is specific toward bacteria (2). GE81112 is a highly hydrophilic chlorine-containing, noncyclic, nonribosomal tetrapeptide constituted by four nonproteinogenic l-amino acids(2, 3). It is found in nature in three structural variants (A, B, and B1 with molecular masses of 643–658 Da) (2, 3). Previous biochemical and structural characterization of GE81112, indicates that the main mechanism of action of this antibiotic is to (1) prevent the initiator tRNA from binding correctly to the P-site and (2) block conformational rearrangements in initiation factor IF3, resulting in a unlocked 30S preIC state (4, 5). We have determined the binding site of GE81112 in the (preIC) at about 3.0 Å resolution. This binding site is remote from the binding site of the initiation factors, tRNA and mRNA suggesting that it acts allosterically to prevent the initiator tRNA from being locked into place. The binding mode is consistent with recent studies identifying the key pharmacophores of GE8112.

Acknowledgments

This work was supported by the MINECO contracts, PID2021-122705OB-I00. The authors acknowledge the support and the use of resources of Instruct, a Landmark ESFRI project (specifically Instruct Access Project PID: 1604-73), including the Netherlands Centre for Electron Nanoscopy (NeCEN, Leiden). We acknowledge Diamond for access and support of the Cryo-EM facilities at the UK national electron bio-imaging centre (eBIC), proposal EM17171-2, funded by the Wellcome Trust, MRC and BBSRC.

References

1. Brandi, L., Fabbretti, A., Milon,P., Carotti,M., Pon,C.L. and Gualerzi,C.O. (2007) Methods for identifying compounds that specifically target translation. Methods Enzym., 431, 229–267.

2. Brandi, L., Fabbretti, A., La Teana,A., Abbondi,M., Losi,D., Donadio,S. and Gualerzi,C.O. (2006) Specific, efficient, and selective inhibition of prokaryotic translation initiation by a novel peptide antibiotic. Proc. Natl. Acad. Sci. U. S. A., 103, 39–44.

3. Brandi,L., Lazzarini,A., Cavaletti,L., Abbondi,M., Corti,E., Ciciliato,I., Gastaldo,L., Marazzi,A., Feroggio,M., Fabbretti,A., et al. (2006) Novel Tetrapeptide Inhibitors of Bacterial Protein Synthesis Produced by a Streptomyces sp. Biochemistry, 45, 3692–3702.

4. Fabbretti,A., Schedlbauer,A., Brandi,L., Kaminishi,T., Giuliodori,A.M., Garofalo,R., Ochoa-Lizarralde,B., Takemoto,C., Yokoyama,S., Connell,S.R., et al. (2016) Inhibition of translation initiation complex formation by GE81112 unravels a 16S rRNA structural switch involved in P-site decoding. Proc. Natl. Acad. Sci. U. S. A., 113.

5. López-Alonso,J.P., Fabbretti,A., Kaminishi,T., Iturrioz,I., Brandi,L., Gil-Carton,D., Gualerzi,C.O., Fucini,P. and Connell,S.R. (2017) Structure of a 30S pre-initiation complex stalled by GE81112 reveals structural parallels in bacterial and eukaryotic protein synthesis initiation pathways. Nucleic Acids Res., 45.

Keywords: ribosome, initiation

CRYO-CLEM TO STUDY SARS-COV-2 ENTRY MECHANISMS

Johannes Groen (France)[1]; Anna Sartori-Rupp (France)[1]

1 - Institut Pasteur Paris

Abstract

The COVID-19 pandemic caused by SARS-CoV-2 has had a significant impact on the global population. Despite the development of vaccines, effective antiviral therapies for COVID-19 are still lacking, although treatments targeting SARS-CoV-2 entry into host cells are promising. The virus enters host cells through two pathways: the TMPRSS2-based pathway in which binding and fusion takes place at the cell-membrane level, and the endocytic pathway in which the virus is first internalized, and binding and fusion take place from within matured endo-lysosomes (Jackson et al. 2022; Zhang et al. 2022). Therefore, understanding these pathways is crucial for the development of effective treatments. Here, we aim to describe the endocytic entry pathway of SARS-CoV-2; to map it and to visualize the host reaction towards viral entry. To achieve this, we are utilizing a cryo-correlative light and electron microscopy (cryo-CLEM) approach (Klein et al., 2021). This approach is very powerful as viral entry is a rare event and being able to identify entry sites tremendously increases the probability of visualizing the event. In this scenario, fluorescence information can act as a guide to target cells that have been infected, and cryo electron tomography (cryo-ET) can provide the 3D information of the virus containing endo-lysosomes, and its cellular context (Mahamid et al., 2016). To this aim, Vero cells were cultivated on EM grids and infected with UV-inactivated viruses, which are able to enter the host, but lacks the ability to replicate (Loveday et al., 2021). Fourty minutes post infection the samples were plunge-frozen and cryo-fluorescence maps were acquired to localize the fluorescently labelled endo-lysosomes. Using a cryo-focused ion beam scanning electron microscope (cryo-FIB-SEM), 200 nm thin cryo-lamellae were cut in areas containing the endo-lysosomes (Marko et al., 2007). Although we could not use the 3D fluorescence information to target the vesicles specifically due to the diffraction-limited resolution in the axial direction, we were able to localize them in some of the prepared lamellae. Cryo-ET on these vesicles, followed by 3D reconstruction showed that these vesicles can contain multiple viruses, among other cellular components, suggesting a possible fusion mechanism of multiple individual virus-containing endocytic vesicles.

References

Jackson, C. B., et al. "Mechanisms of SARS-CoV-2 entry into cells." *Nature reviews Molecular cell biology* 23.1 (2022): 3-20.

Zhang, Y, Renhong Y, and Qiang Z. "ACE2, B0AT1, and SARS-CoV-2 spike protein: Structural and functional implications." *Current Opinion in Structural Biology* (2022): 102388.

Klein, S. et al. "Cryo-correlative light and electron microscopy workflow for cryo-focused ion beam milled adherent cells." *Methods in cell biology*. Vol. 162. Academic Press, 2021. 273-302.

Mahamid, J. et al. "Visualizing the molecular sociology at the HeLa cell nuclear periphery." *Science* 351.6276 (2016): 969-972

Marko, M. et al. "Focused-ion-beam thinning of frozen-hydrated biological specimens for cryo-electron microscopy." *Nature methods* 4.3 (2007): 215-217.

Loveday, E. K. et al. Effect of inactivation methods on sars-cov-2 virion protein and structure. Viruses 13, (2021)

Keywords: cryo-CLEM, cryo-EM, SARS-CoV-2, Host-Pathogen Interaction

ADVANCES IN THE STUDY OF EXTRACELLULAR VESICLES SECRETED BY LEGIONELLA PNEUMOPHILA USING CRYO ELECTRON MICROSCOPY

Olena Mayboroda (France)[1]; Tobias Sahr (France)[1]; Carmen Buchrieser (France)[1]

1 - Institut Pasteur, Université Paris Cité, CNRS UMR 6047, Biologie des Bactéries Intracellulaires, Département de Microbiologie, F-75015 Paris, France

Abstract

Extracellular vesicles (EVs) are defined as membrane-enclosed structures released during the lifespan of most cells in all domains of life on earth, including eukaryotes, bacteria, and archaea [1,2]. This process is conserved throughout evolution from bacteria to humans and plants. Most of the EVs are described as spherical structures, however they can adopt a more tubular shape, probably deriving from so-called nanotubes. They are involved in component exchange between cells and organisms, like proteins, mRNAs, miRNAs, lipids, and metabolites, and as signaling vesicles in normal homeostatic or in pathological processes [3–5].

Recently we have shown that the bacterial pathogen *Legionella pneumophila*, subverts host cell signaling pathways via EVs (Lp-EVs) [6,7] and that it releases EVs *in vitro* and *in cellulo* during infection of the human U2OS cell line, human THP-1 monocytic cells, and human monocyte-derived macrophages (hMDMs). These *Lp*-EVs contain bacterial RNAs that are transported into the host cell where they downregulate IRAK1 and RIG-I, most likely by mimicking eukaryotic miRNAs [8].

The main goal of our project is to get a better understanding of the *Lp*-EVs structure and the mechanism of RNA loading and release that is important for host-pathogen communication and trans-kingdom signaling. Some of *Lp*-EV features, like size, morphology, concentration, origin, and molecular composition, can be characterized using Cryo Electron Microscopy (Cryo EM). Here we used Cryo-EM and 3D tomographic data collection for spatial visualization and show first results obtained in imaging and reconstruction of single *Lp*-EVs.

Another important part of our research line is the study of *Lp*-EV release inside the host cell. Combining Cryo CLEM, Cryo FIB and Cryo Tomography techniques we aim to get a better understanding of the cells infected with *L. pneumophila* and study the pathway of EV formation and role during infection *in cellulo*.

Acknowledgments

Work is financed by the grant n° ANR 20 CE15 0021 01 BIOEV

References

1. van Niel, G., D'Angelo, G. & Raposo, G. Shedding light on the cell biology of extracellular vesicles. *Nat. Rev. Mol. Cell Biol.* **19**, 213–228 (2018).
2. Kim, J. H., Lee, J., Park, J. & Gho, Y. S. Gram-negative and Gram-positive bacterial extracellular vesicles. *Semin. Cell Dev. Biol.* **40**, 97–104 (2015).

3. Lee, H.-J. Microbe-Host Communication by Small RNAs in Extracellular Vesicles: Vehicles for Transkingdom RNA Transportation. *Int. J. Mol. Sci.* **20**, E1487 (2019).
4. Lécrivain, A.-L. & Beckmann, B. M. Bacterial RNA in extracellular vesicles: A new regulator of host-pathogen interactions? *Biochim. Biophys. Acta BBA - Gene Regul. Mech.* **1863**, 194519 (2020).
5. Kulp, A. & Kuehn, M. J. Biological Functions and Biogenesis of Secreted Bacterial Outer Membrane Vesicles. *Annu. Rev. Microbiol.* **64**, 163–184 (2010).
6. Mondino, S. *et al.* Legionnaires' Disease: State of the Art Knowledge of Pathogenesis Mechanisms of *Legionella*. *Annu. Rev. Pathol. Mech. Dis.* **15**, 439–466 (2020).
7. *Legionella: Methods and Protocols*. vol. 954 (Humana Press, 2013).
8. Sahr, T. *et al.* Translocated Legionella pneumophila small RNAs mimic eukaryotic microRNAs targeting the host immune response. *Nat. Commun.* **13**, 762 (2022).

Keywords: Legionella pneumophila, Extracellular vesicles, Cryo CLEM, Cryo FIB, Cryo ET, in cellulo imaging

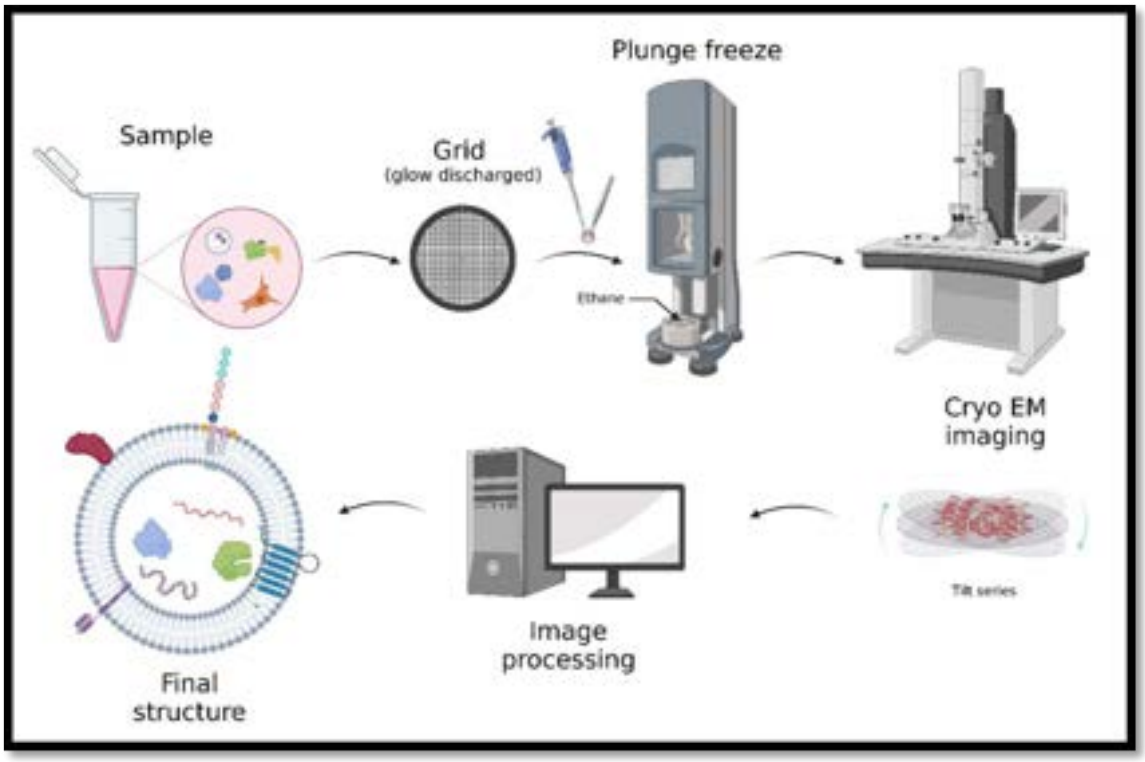

ARCHITECTURE OF THE ESCPE-1 MEMBRANE COAT

Carlos Lopez-Robles (Spain)[1]; Stefano Scaramuzza (Switzerland)[2]; Elsa N. Astorga-Simon (Spain)[1]; Morié Ishida (United States of America)[3]; Chad D. Williamson (United States of America)[3]; Soledad Baños-Mateos (Spain)[1]; David Gil-Carton (Spain)[4]; Miguel Romero (Spain)[5]; Ander Vidaurrazaga (Spain)[1]; Juan Fernandez-Recio (Spain)[5]; Adriana L. Rojas (Spain)[1]; Juan S. Bonifacino (United States of America)[3]; Daniel Castaño-Díez (Spain)[4]; Aitor Hierro (Spain)[1]

1 - CIC bioGUNE, Bizkaia Technology Park, 48160 Derio, Spain; 2 - BioEM Lab, Biozentrum, University of Basel, Basel, Switzerland; 3 - Neurosciences and Cellular and Structural Biology Division, Eunice Kennedy Shriver National Institute of Child Health and Human Development, National Institutes of Health, Bethesda, Maryland 20892, USA; 4 - Instituto Biofisika (UPV/EHU, CSIC), University of the Basque Country, 48940 Leioa, Spain; 5 - Barcelona Supercomputing Center (BSC), Barcelona, Spain

Abstract

Just as cargoes enter the endosomal network, various protein machineries contribute to their recycling by either bulk flow or selective processes. The SNX-BAR subfamily of sorting nexins, which contain a phox-homology (PX) domain and a Bin/Amphiphysin/Rvs (BAR) domain, play a central role as coat proteins in multiple endocitic retrograde/recycling pathways. Generation of tubular carriers by SNX-BAR proteins combines membrane association, cargo capture, coat assembly and lipid bilayer deformation mechanisms that remain unresolved. Using X-ray crystallography, cryo-electron tomography and cell-based analysis we reveal an unprecedented coat architecture for tubular-based cargo sorting mediated by the SNX1-SNX5 heterodimer.

Keywords: SNX1-SNX5, CI-MPR Recycling, CryoET

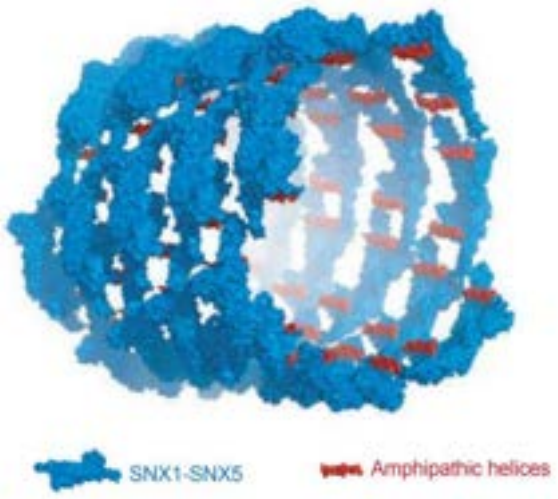

Figure1: 3D reconstruction of ESCPE-1 coat observed by cryoET. The SNX1-SNX5 atomic model has been fitted and symmetrized according to the arrangement calculated from the 3-start helix parameters. This tubular architecture is mediated by SNX1-SNX5 heterodimer in blue when CIMPR cargo needs to be recycled from endsomes. Amphipatic helices, colored in red, are responsible for the lateral expansion of lipids in the membrane vital for the tube formation.

STRUCTURAL CHARACTERISATION OF MITOCHONDRIA IN MICE AFFECTED BY COENZYME Q10 DEFICIENCY.

Isaac Santos Pérez (Spain)[1]; Juan Manuel Martinez Galvez (Spain)[2]; Adriana Lucely Rojas Cardona (Spain)[1]; Luis Carlos Lopez (Spain)[2]

1 - CIC bioGUNE; 2 - Universidad de Granada

Abstract

Primary mitochondrial diseases arise due to mutations in nuclear or mitochondrial genes, leading to impaired function of specific mitochondrial pathways. Coenzyme Q10 (CoQ10) is an electron carrier in the mitochondrial respiratory chain, and mutations in the genes involved in its biosynthesis give rise to primary CoQ10 deficiencies, a mitochondrial disease with heterogeneous clinical manifestation. In this work, we use the well-characterized Coq9 knockin R239X mouse model (CoQ9R239X), which manifests a severe encephalomyopathy. Since there is still no connection between mitochondrial structure and the loss of function in primary CoQ10 deficiencies, we explore by transmission electron microscopy the mitochondrial morphology in the brainstem of this mouse model. For that, mice neuronal tissues were embedded in resin and stained with uranyl acetate and Pb citrate to enhance membrane contrast, either for visualized mitochondrial shapes and sizes or an exhaustive visualization of mitochondrial cristae collected by 2D TEM and 3D electron tomography. The tissue blocks were sectioned by ultramicrotome in 70 nm and 150 nm thickness slices, which were mounted on copper grids for TEM visualization. For further robustness of the results, tissue blocks were sectioned at two different depths from the brains of healthy and affected mice at different time periods. This analysis allowed us to evaluate the number of cristae in each case and their volume and morphology. These results provide a better understanding of how the CoQ10 deficiency affects the mitochondrial morphology, resulting in a loss of its function, leading to the course of the disease.

Acknowledgments

MiTo Lab University of Granada, for the design and set-up of the study, involving mice that had been genetically engineered.

Servicio de Microscopía Electrónica del CBM (SME-CBM), for providing an integral service in the preparation and cutting of tissues for their visualization in TEM.Electron Microscopy

Platform at CIC bioGUNE for skillful support in sample visulization and processing of the collected images.

References

1. González-García P, Díaz-Casado ME, Hidalgo-Gutiérrez A, Jiménez-Sánchez L, Bakkali M, Barriocanal-Casado E, Escames G, Chiozzi RZ, Völlmy F, Zaal EA, Berkers CR, Heck AJR, López LC. The Q-junction and the inflammatory response are critical pathological and therapeutic factors in CoQ deficiency. Redox Biol. 2022 Jul 15;55:102403. doi: 10.1016/j.redox.2022.102403.

2. González-García P, Barriocanal-Casado E, Díaz-Casado ME, López-Herrador S, Hidalgo-Gutiérrez A, López LC.
Animal Models of Coenzyme Q Deficiency: Mechanistic and Translational Learnings. Antioxidants (Basel). 2021 Oct 26;10(11):1687. doi: 10.3390/antiox10111687.

3. Noh YH, Kim KY, Shim MS, Choi SH, Choi S, Ellisman MH, Weinreb RN, Perkins GA, Ju WK. Inhibition of oxidative stress by coenzyme Q10 increases mitochondrial mass and improves bioenergetic function in optic nerve head astrocytes. *Cell Death and Disease.* 2013;4(10):e820

Keywords: Mitochondria, CoQ, cristae, TEM Tomography, ROS

STRUCTURAL AND FUNCTIONAL INSIGHTS INTO HYDROGEN SULFIDE HOMEOSTASIS IN PATHOGENIC BACTERIA

Jose Artur Brito (Portugal)[1]; Sofia Costa (United States of America)[2]; Brenna Walsh (United States of America)[2]; David Giedroc (United States of America)[2]

1 - ITQB NOVA; 2 - Department of Molecular and Cellular Biochemistry, Indiana University

Abstract

Hydrogen sulfide is an ancient molecule present in Earth's primordial atmosphere and organisms from all Domains of Life soon evolved to utilize it in their physiology. However, H_2S can have either beneficial or toxic effects, depending on the concentration. Therefore, tight regulation of intracellular H_2S/H_2S-derived more oxidized reactive sulfur species (RSS) is paramount for survival of all organisms. In bacterial pathogens, H_2S/RSS is regarded as an important component in microbial defense mechanisms against oxidative and antibiotic stress.

The *cst* operon in *Staphylococcus aureus* encodes a nearly complete mitochondrial-like H_2S oxidation system. In addition, a *cst*-like operon has also been described in the human pathogen *E. faecalis*. Three enzymes encoded by these two operons include the coenzyme A persulfide reductase CoAPR, the multidomain persulfide dioxygenase-sulfurtransferase fusion protein CstB and the sulfide:quinone oxidoreductase SQR, which collectively protect the organism against H_2S and RSS toxicity.

Herein, we describe the X-ray crystallographic structures of full-length *Sa*CstB (native and single cysteine substitution mutants) and the CoA-bound crystal structure of *Ef*CoAPR. Companion cryo-EM data on these enzymes suggest a high mobility of the C-terminal rhodanese domains that may be important for catalysis. The structures of sulfite-bound mutant CstBs suggests a mechanism by which the C-terminal domain facilitates the concerted oxidation of a thiol persulfide (RSSH) to thiosulfate and thiol, without the release of the toxic sulfite intermediate.

These studies provide an enhanced understanding of the mechanisms of H_2S/RSS homeostasis encoded by the RSS-regulated *cst* operons in bacteria, putatively leading to the development of new antimicrobials to fight these human pathogens.

Keywords: hydrogen sulfide, sulfur-metabolising pathways, pathogenic bacteria, X-ray crystallography, cryo-EM

mfs2023

INL | Braga, Portugal

Powered by:

Sponsors: